

# DOCTORAL THESIS

## **Study on the thermal performance of lightweight wall using Phase-Change Material**

September 2023

**LIU ZUAN**

**2020DBB420**

The University of Kitakyushu

Faculty of Environmental Engineering

Department of Architecture

Bart Laboratory



## ACKNOWLEDGEMENTS

The three-year doctoral program has passed by in a flash. My study experience in Japan during these years has been very precious and unforgettable to me. Until this moment, when my doctoral dissertation was successfully completed, there is so much gratitude in my heart to express here.

Firstly, I would like to express my sincere respect and gratitude to my doctoral supervisor, Prof. Bart Dewancker. Although I could not return to campus at the beginning of the semester due to COVID-19, I always received your guidance through online meetings, and your practical academic advice and patient guidance helped me successfully complete my doctoral thesis. Secondly, I would also like to thank Prof. Gao Weijun and Prof. Fukuda for their academic guidance and care in my life. I appreciate Prof. Meng Xi from the iSMART at Qingdao University of Technology for your support of my academic research during the COVID-19 pandemic. Additionally, I would like to thank Dr. Zhang Tao for his assistance in my daily life after I arrived in Japan.

Meanwhile, I also want to thank Prof. Shiraishi, Prof. Hoki and Prof. Yamamoto for your valuable comments and suggestions on my doctoral thesis.

Furthermore, I would also like to express my gratitude to the teachers at the University of Kitakyushu International Student Support Center for your continuous help and care in my studies and daily life. At the same time, I want to thank my fellow colleagues from Bart Lab: Dr. Chen Shuo, Dr. Chen Shiyi, Dr. Wang Di, Dr. Wang Jinming, Dr. Dai Jialu, Dr. Mo Wensheng, Dr. Bao Xin, Dr. Wang Junru, Dr. Siswanti Zuraida, Dr. Athina Ardhyanto, Dr. Chen Chen, Dr. Huang Gonghu, Dr. Liu Yuanhao, Dr. Zhang Tianyang, Dr. Zeng Qian, Dr. Luo Yu, Dr. Wu Hao, M.s. Liu Tianyu, M.s. Li Yuting, and M.s. Satrio Agung Perwira. Thank you all for your help during my doctoral studies in Japan. Further, I want to thank my parents for their support in my studies, and for helping me to take care of my young son. I also thank my wife, Dr. Hou Jiawen, for her support, help, and companionship during my doctoral studies in Japan.

Finally, I would like to express my gratitude once again to the teachers, classmates, relatives, and friends who gave me help and support. Thank you all!



## ABSTRACT

Phase-change material (PCM) integrated into walls has been extensively studied and optimized, proving its effectiveness in thermal performance improvement of the wall. Among them, it can be drawn that the heat storage and release of PCM are affected by various factors, such as PCM thermo-physical parameters, application objects, installation locations, and climatic conditions, which are complex and non-linear. However, the current research mostly focuses on a specific factor, which makes the existing conclusions, rules, and interrelationships between the obtained influencing factors too absolute and flawed. Therefore, the typical unit lightweight walls (mainly thermal insulation materials) were taken as the research object to ascertain the basic scientific problem of the influence laws and suitability of different PCM thermo-physical parameters on the thermal performance of lightweight walls under different thermal boundaries through theoretical analysis, numerical simulation, and experiment. Meanwhile, evaluate the energy-saving potential (cooling and heating) of lightweight walls using PCM applied to buildings and determined economic feasibility in different climates/cities.

First of all, in Chapter 1, the effectiveness and difference of PCM application in different structural forms under different climatic conditions were obtained by reviewing the previous studies. Meanwhile, the thermo-physical parameters of PCM affecting its application effect were summarized. Eventually, the problems existing in the application of PCM in lightweight wall, the research contents, and the purposes of this paper were clarified.

Next, in Chapter 2, the mathematical heat transfer model of lightweight wall using PCM was established, and enthalpy method was used as solution method and validated by numerical simulation (CFD). Then, proposed the evaluation indexes for the effect of PCM on the thermal performance of lightweight wall.

Then, in Chapter 3, analyzed and evaluated comprehensively the influence rules of different PCM thermo-physical parameters (phase-transition temperature, location, thickness, latent heat, thermal conductivity, density, specific heat) on the thermal performance of lightweight wall by establishing four heat transfer model of lightweight wall using PCM.

In Chapter 4, assessed the influence laws and contribution efficiency of different PCM thermo-physical parameters on the thermal performance of lightweight walls with different thermal resistances ( $R_{wt}$ ) by establishing four heat transfer models of walls with different  $R_{wt}$ .

After that, in Chapter 5, the difference in the thermal environment around the external surface of the wall in different directions was tested and analyzed by manufacturing a small-scale lightweight building. Then, the influence laws and contribution efficiency of PCM thermo-physical parameters on the thermal performance of walls in different directions were

explored using the thermal environment in different directions as the thermal boundary conditions, and the suitable parameter values were obtained.

Subsequently, in Chapter 6, based on the above research results, four different kinds/configurations of lightweight walls were built, and the typical winter and summer climate characteristics were used as the thermal boundary conditions to discuss the influence laws and effectiveness of different kinds/configurations of PCM on the thermal performance of lightweight walls in summer and winter, and propose the suitable PCM configurations for both summer and winter.

Further on, in Chapter 7, the regulation ability of PCM on the thermal performance of lightweight walls and indoor thermal environments in different seasons (summer, transition season, and winter) under a natural environment (no mechanical equipment) was discussed by experimental measurements. Then, the energy-saving potential of the composite PCM in different seasons under natural conditions was calculated by theoretical equations.

Afterward, in Chapter 8, the energy-saving potential (cooling and heating) of lightweight walls using PCM applied to buildings was evaluated by using EnergyPlus, and economic feasibility (including payback period for different PCM amounts, and the maximum acceptable PCM cost price for different climates/cities based on a certain payback period) in different climates/cities was determined by static payback period (SPP).

Eventually, the main research results of this paper were summarized in Chapter 9.

Overall, this paper reveals the influence law of PCM thermo-physical parameters on the thermal performance of lightweight walls under different thermal boundaries and points out the optimal parameters and configurations of PCM for improving the thermal performance of lightweight buildings as well as the energy-saving benefits. The research results can provide a systematic evaluation method for effect of PCM applied to opaque envelopes under different thermal boundaries at the theoretical significance. Meanwhile, the research results can also provide reference for decision-makers to select suitable PCM products in lightweight wall or building in terms of energy-saving and economics, as well as provide data support for manufacturers to develop innovative energy-saving lightweight wall products using PCM.

**Keywords:** Lightweight wall; Phase-change material (PCM); Thermal performance; Different thermal boundaries; Effectiveness; Energy-saving;

# CONTENTS

<b>Chapter 1. Research on background, review and purpose .....</b>	<b>1-1</b>
1.1 Introduction.....	1-1
1.1.1 Research background .....	1-1
1.1.2 PCM characteristics and types.....	1-4
1.2 Literature review .....	1-7
1.2.1 Study on PCM integrated into different walls .....	1-7
1.2.2 Contribution benefits of PCM to building energy-saving under different climate characteristics .....	1-9
1.2.3 Study on suitable thermo-physical parameters of PCM .....	1-11
1.2.4 Summary of research status .....	1-16
1.3 Purpose and content overview of this study.....	1-18
References.....	1-23
<b>Chapter 2. Theoretical analysis of the causes of overheating in lightweight buildings and heat transfer processes in phase-change composite walls .....</b>	<b>2-1</b>
2.1 Introduction.....	2-1
2.2 Heat transfer analysis of lightweight building .....	2-1
2.2.1 Surface heat balance of lightweight envelope .....	2-1
2.2.2 Indoor air heat balance.....	2-6
2.2.3 Indoor thermal environment analysis of lightweight building .....	2-9
2.3 Heat transfer analysis of phase-change composite walls .....	2-10
2.3.1 Heat transfer characteristics of the building envelope (wall).....	2-10
2.3.2 Thermal characteristics of phase-change composite walls .....	2-13
2.3.3 Theoretical analysis of heat transfer of phase-change composite wall.....	2-14
2.3.4 Boundary condition setting.....	2-17
2.3.5 Model validation.....	2-18
2.3.6 Evaluation indexes .....	2-20
2.4 Summary .....	2-20
References.....	2-22
Nomenclature.....	2-25
<b>Chapter 3. Effect of PCM parameters on the thermal performance of lightweight wall .....</b>	<b>3-1</b>

3.1	Introduction.....	3-1
3.2	Methodology .....	3-3
3.2.1	Physical model description.....	3-3
3.2.2	Indoor and outdoor thermal boundary description.....	3-4
3.3	Selection of phase-transition temperature of PCM.....	3-4
3.4	Effects of other parameters of PCM.....	3-7
3.4.1	Effect of the PCM location.....	3-7
3.4.2	Effect of the PCM thickness.....	3-8
3.4.3	Effect of the PCM latent heat.....	3-10
3.4.4	Effect of the thermal conductivity coefficient of PCM.....	3-11
3.4.5	Effect of the PCM density.....	3-13
3.4.6	Effect of the PCM specific heat.....	3-14
3.5	Summary.....	3-15
	References.....	3-17
	Nomenclature.....	3-21

**Chapter 4. Influence of PCM parameters on the thermal performance of lightweight wall with different thermal resistances..... 4-1**

4.1	Introduction.....	4-1
4.2	Material and methods.....	4-4
4.2.1	Research flow.....	4-4
4.2.2	Physical model.....	4-4
4.2.3	Thermal boundaries.....	4-5
4.3	Effect and selection of PCM phase-transition temperatures.....	4-6
4.3.1	Effect of PCM phase-transition temperatures on the inner surface temperature of walls.....	4-6
4.3.2	The variation of liquid fraction under different phase-transition temperatures.....	4-8
4.4	Effect of other PCM parameters on evaluation indexes under different thermal resistance of original walls ( $R_{wt}$ ).....	4-9
4.4.1	Effect of the PCM location under different $R_{wt}$ .....	4-9
4.4.2	Effect of the PCM thickness under different $R_{wt}$ .....	4-11
4.4.3	Effect of the PCM latent heat under different $R_{wt}$ .....	4-13
4.4.4	Effect of the thermal conductivity coefficient of PCM under different $R_{wt}$ .....	4-15
4.5	Summary.....	4-17
	References.....	4-19
	Nomenclature.....	4-23

**Chapter 5. Thermal performance analysis of lightweight wall in different directions integrated with PCM..... 5-1**

5.1 Introduction.....	5-1
5.2 Physical model and thermal boundaries.....	5-3
5.2.1 Physical model description .....	5-3
5.2.2 Experimental system and indoor and outdoor thermal boundaries .....	5-4
5.2.3 Model validation.....	5-6
5.3 Selection of phase-transition temperature of PCM for walls in different directions.....	5-7
5.4 Effect of the other PCM parameters on the walls of different directions.....	5-10
5.4.1 Effect of the PCM location on the walls of different directions.....	5-10
5.4.2 Effect of the PCM thickness on the walls of different directions.....	5-12
5.4.3 Effect of the PCM latent heat on the walls of different directions .....	5-14
5.4.4 Effect of the thermal conductivity coefficient of PCM on the walls of different directions.....	5-16
5.5 Summary .....	5-18
References.....	5-20
Nomenclature.....	5-24

**Chapter 6. Effectiveness of different kinds/configurations of PCM for improving the thermal performance of lightweight wall in summer and winter ..... 6-1**

6.1 Introduction.....	6-1
6.2 Physical model and boundary conditions.....	6-4
6.2.1 Physical model.....	6-4
6.2.2 Boundary conditions .....	6-5
6.3 Utilization versus effectiveness of the PCM under different models.....	6-6
6.3.1 The variation of temperature and liquid fraction of PCM with different models .....	6-6
6.3.2 Effectiveness of different models .....	6-9
6.4 Utilization versus effectiveness of the PCM under different transition ranges.....	6-11
6.4.1 The variation of liquid fraction of PCM and inner surface temperature with different transition ranges .....	6-11
6.4.2 Effectiveness of different transition ranges of PCM .....	6-13
6.5 Effectiveness of the PCM under different thicknesses.....	6-14
6.6 Effectiveness of the PCM under different latent heats.....	6-17
6.7 Summary .....	6-19
References.....	6-21

Nomenclature.....	6-27
<b>Chapter 7. Effect of PCM on the thermal performance of lightweight wall and indoor thermal environment under natural conditions.....</b>	<b>7-1</b>
7.1 Introduction.....	7-1
7.2 Material and methods.....	7-2
7.2.1 Experimental system description.....	7-2
7.2.2 Experimental equipment and test methods .....	7-4
7.2.3 Evaluation indicators.....	7-5
7.3 Experimental result and analysis.....	7-5
7.3.1 Summer condition .....	7-5
7.3.2 Transitional season conditions.....	7-7
7.3.3 Winter conditions .....	7-9
7.3.4 Indoor temperature analysis.....	7-10
7.3.5 Energy saving potential analysis .....	7-13
7.4 Summary .....	7-14
References.....	7-16
Nomenclature.....	7-18
<b>Chapter 8. Impact and economic evaluation of the lightweight wall using PCM are used in building on reducing energy demands .....</b>	<b>8-1</b>
8.1 Introduction.....	8-1
8.2 Methodology .....	8-5
8.2.1 Climate zones division and representative cities.....	8-5
8.2.2 Physical model and boundary conditions .....	8-6
8.2.3 Orthogonal experiment .....	8-7
8.2.4 Numerical simulation.....	8-9
8.2.5 Model validation.....	8-11
8.3 Analysis of energy simulation results .....	8-13
8.3.1 Energy simulation results for reference building in different climates/cities .....	8-13
8.3.2 Energy simulation results for each typical city based on orthogonal experiment .....	8-14
8.4 Optimal level and influence degree of each factor (parameter/configuration) under different climates/cities.....	8-18
8.4.1 Suitability level of each factor.....	8-18
8.4.2 Influence degree of each factor .....	8-21

8.5 PCM optimal configuration and energy-saving evaluation based on orthogonal experiment .....	8-24
8.5.1 Energy-saving and suitability of different PCM configurations (single and double layer) .....	8-24
8.5.2 Energy-saving for different PCM amounts (thickness and utilization area)..	8-27
8.6 Economic analysis of energy-saving strategies.....	8-31
8.6.1 Payback period based on PCM cost price.....	8-31
8.6.2 Acceptable cost price for PCM based on payback period .....	8-34
8.7 Summary .....	8-36
Appendix.....	8-38
References.....	8-40
Nomenclature.....	8-49
<b>Chapter 9. Conclusions .....</b>	<b>9-1</b>
9.1 Conclusions.....	9-1



## ***Chapter 1. Research on background, review and purpose***

<i>1.1 Introduction.....</i>	<i>1-1</i>
<i>1.1.1 Research background.....</i>	<i>1-1</i>
<i>1.1.2 PCM characteristics and types.....</i>	<i>1-4</i>
<i>1.2 Literature review.....</i>	<i>1-7</i>
<i>1.2.1 Study on PCM integrated into different walls .....</i>	<i>1-7</i>
<i>1.2.2 Contribution benefits of PCM to building energy-saving under different climate characteristics .....</i>	<i>1-9</i>
<i>1.2.3 Study on suitable thermo-physical parameters of PCM .....</i>	<i>1-11</i>
<i>1.2.4 Summary of research status .....</i>	<i>1-16</i>
<i>1.3 Purpose and content overview of this study.....</i>	<i>1-18</i>
<i>References.....</i>	<i>1-23</i>



## **1.1 Introduction**

### **1.1.1 Research background**

Energy is essential for human survival and economic and social development. However, with the acceleration of industrialization and urbanization, higher energy consumption often follows. Currently, the majority of the world's energy is generated through burning non-renewable fossil fuels, leading to the emission of carbon dioxide and other greenhouse gases that exacerbate climate change. As a result, countries committed to addressing climate change following the 2015 Paris Climate Change Agreement by (a) reducing overall energy consumption through developing more energy-efficient products and processes, and (b) meeting a greater proportion of their total energy demand through renewable energy sources such as solar, wind, and tidal energy. In industrialized and highly urbanized societies, the three main sectors responsible for most of the energy consumption are industry (28.6%), transportation (29.1%), and construction (29.4%). In 2017, buildings (including public, residential, and commercial) accounted for nearly 30% of the world's total energy consumption [2]. The building and construction sector's total energy consumption has been increasing due to the rise in global construction and the greater use of high-energy equipment and materials. According to the International Energy Agency (IEA), the construction sector is responsible for 24% of the world's total CO<sub>2</sub> emissions and 40% of the total primary energy consumption [3,4]. This huge amount of energy consumption has led to an increase in hazardous gas emissions year by year as the industry grows and demand increases. In order to cope with climate change and reduce environmental pollution, practical solutions include the use of renewable energy, the development of energy-saving technologies, and the application of low-carbon emission processes. However, to successfully execute these programs, the building must be viewed as a substantial, untapped source of energy efficiency, and much can be done to develop its energy-saving potential, as reported by the International Energy Agency [2].

As a result, the thermal performance of the building envelope has a direct impact on the energy consumption ratio of a building since it determines the indoor thermal and cooling loads [5]. Today's ideal building should meet both high energy efficiency and low greenhouse gas emissions. Therefore, applying various energy-saving technologies to the building envelope is one of the important ways to save energy and reduce emissions. Heat, Ventilation, and Air Conditioning (HVAC) engineers have taken many measures to reduce the energy consumption of buildings, such as combining external walls, hydraulic systems, radiant heat regulation, and heat storage devices [6]. At the same time, many meaningful new building envelopes have also developed, such as passive solar walls [7], lightweight concrete envelopes [8], ventilated walls

[9,10], phase-change envelopes [11,12], radiant cooling coatings [13], and so on. These energy-saving technologies in three main ways: energy saving in the building envelope, energy saving in the heating system, and new energy development and utilization, thereby regulating indoor thermal comfort through the building envelope together with the important parts of the building while influencing building energy consumption to a large extent [14]. The building envelope accounts for approximately 50% of the heating and cooling load and 36% of the final global energy use of buildings, according to statistical data [15]. Therefore, enhancing the insulation and energy storage performance of the building envelope is of utmost importance to ensure indoor thermal comfort while reducing building energy consumption.

For buildings, the exterior envelope mainly includes exterior walls, roofs, floors, and exterior windows. However, according to the U.S. Department of Energy (as shown in Fig. 1-1), it can be shown that the opaque envelope is the largest contributor to envelope-related energy use, followed by air leakage (infiltration and exfiltration). Meanwhile, it can be seen that the building walls have the highest percentage of energy use compared to other opaque envelopes. The main reason is that the area of the wall can represent up to 80% or more of the area of the external surface exposed to outside air and solar radiation. On the other hand, walls are affected not only by air temperature but also by uneven solar radiation, which makes the external boundary conditions of walls more complex than those of roofs and floors, resulting in higher energy consumption. Therefore, it is necessary to first ascertain the thermal performance of the wall under different external thermal boundary conditions, on the basis of which improving the thermal performance of the wall can help to rapidly reduce the building energy consumption.

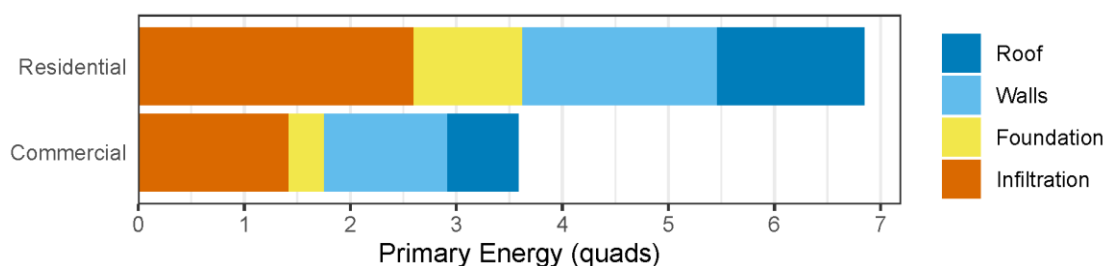


**Fig. 1-1. The breakdown of energy use by building envelope component in residential and commercial buildings during the heating and cooling seasons [16,17].**

Previously, the wall of the building was wide, which could store large amounts of sensible heat and then provide natural regulation in the indoor thermal environment by controlling temperature changes [18]. However, in modern buildings, the thermal mass of the walls has been reduced to save material, time and transportation costs. Ultimately, lightweight construction has gained explosive development in recent years due to its speed of construction, portability, low cost, and adaptability [19], but this has also led to a reduction in the heat

capacity of walls [20]. As a phenomenon, the internal surface of the envelope with low heat capacity often produces large temperature and heat flow fluctuations under the influence of outdoor temperature fluctuations, resulting in reduced indoor thermal comfort. Xu et al. [21] experimentally tested the indoor thermal environment of lightweight buildings in summer, and the results are shown in Fig. 1-2, where it was found that the maximum temperature difference between indoors and outdoors can reach 11°C in summer. Therefore, maintaining a high level of indoor thermal comfort in lightweight buildings often requires more use of air conditioning or heating equipment, which negatively affects building energy efficiency, so much so that the low heat capacity has become a common shortcoming for building envelopes with thermal insulation material (TIM) configurations [22].

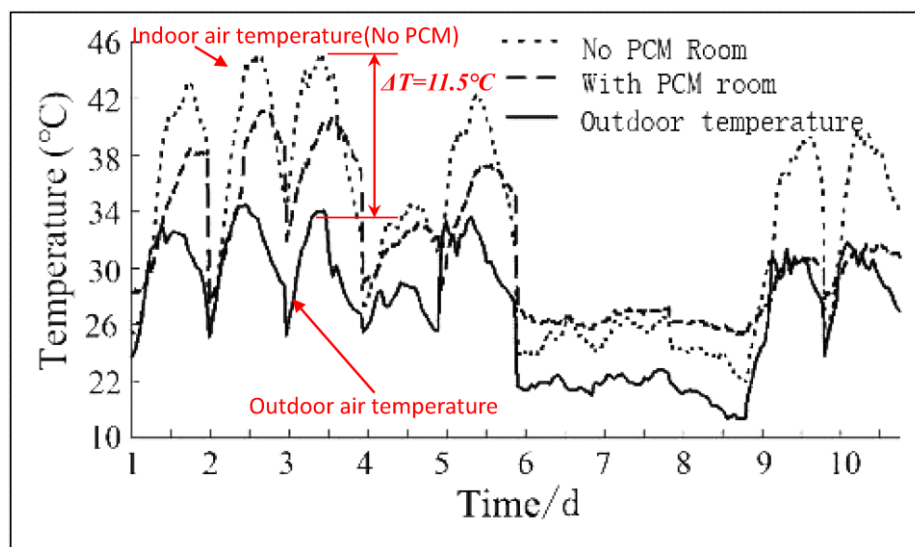


**Fig. 1-2. Indoor air temperature of lightweight building in summer [21].**

A new type of phase-change energy storage material (PCM) has been developed and applied to solve the problem of indoor thermal comfort and energy-saving in lightweight buildings. PCM is a class of materials that absorb and release large amounts of heat (i.e., latent heat) during melting and solidification, and its latent heat level is usually two orders of magnitude higher than that of ordinary building materials (i.e., concrete, gypsum or mortar). Therefore, high levels of heat capacity values are expected to be obtained if PCM is properly introduced, especially for light or thin building envelopes. Several researchers, including Liu et al. [23], De Gracia and Cabeza [24], Lecompte et al. [25], Lei et al. [26], Thiele et al. [27], Moreles et al. [28], Lee et al. [29], Ye et al. [30], and Halford et al. [31], have investigated the transient thermal performance of building envelopes integrated with PCM through experiments. The results demonstrate that the integration of PCM can significantly enhance the transient performance of the building envelope, as evidenced by the smooth fluctuations in room

temperature and the significant time-shift effects in inner surface heat flux. Further, previous studies suggest that the proper incorporation of PCM and thermal insulation materials (TIM) in building envelopes can achieve both high levels of fixed thermal performance (i.e., high thermal resistance) and transient thermal performance (i.e., stable fluctuation of indoor temperature). However, the critical and pressing issues that need to be solved include determining the optimal method for embedding PCM in envelopes based on common thermal insulation materials and accurately evaluating the thermal performance of building envelopes integrated with PCM.

### 1.1.2 PCM characteristics and types

Phase-change materials (PCM) are a material that absorbs and releases thermal energy by freezing and melting at a certain temperature. More precisely, PCMs are capable of storing and releasing heat energy by undergoing a transition from one state to another during the melting and freezing process. This property enables PCMs to release significant amounts of heat energy through either latent heat or crystallization during the condensation process, while absorbing an equivalent amount of heat from the surrounding environment when the material is melted as it changes from a solid to a liquid. As a result, PCMs can store and release thousands of thermal energy without altering their thermal properties. In heat storage, PCM technology is not only limited to sensible heat but can also utilize latent heat to enhance its heat storage capacity [32, 33]. The PCM transition cycle is depicted in Fig. 1-3 [34].

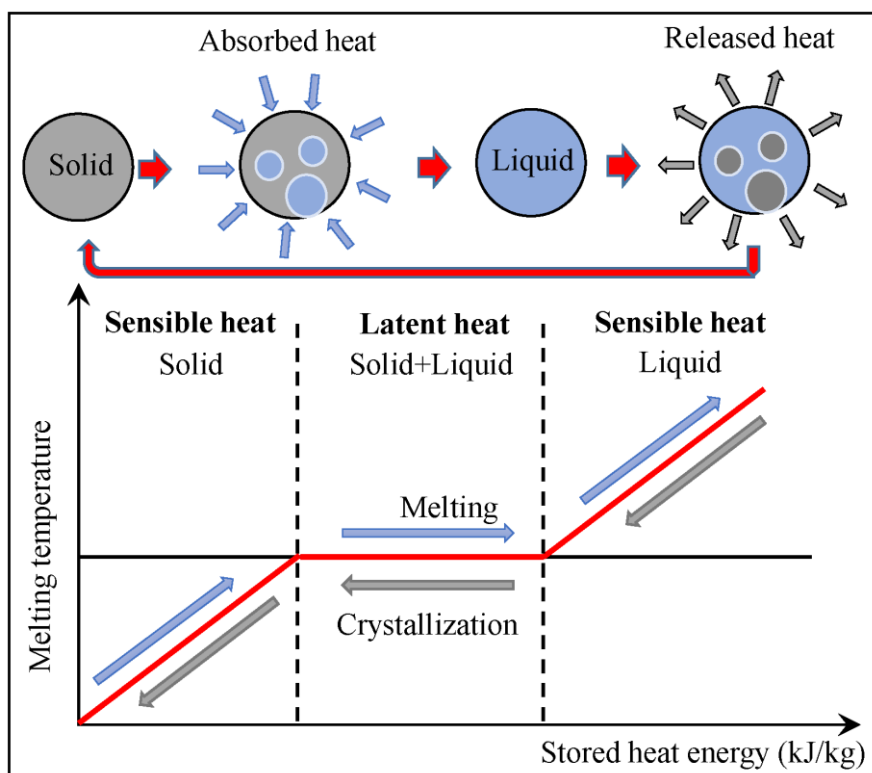
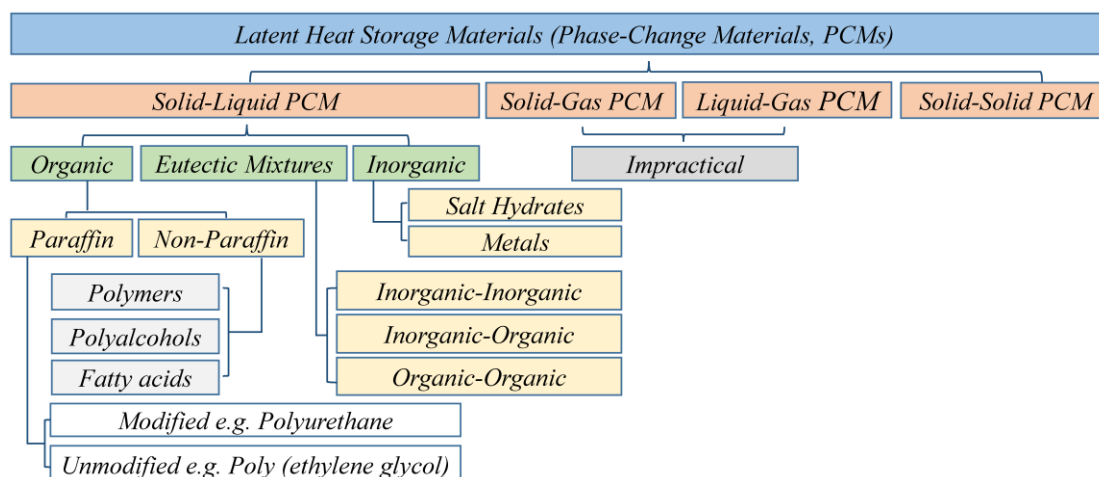


Fig. 1-3. Heat transition zones of PCM [34].

The excellent energy storage capabilities of PCM make it a popular choice for enhancing performance and safety in various applications. PCM is commonly used in building materials, electronic equipment, lithium-ion batteries, and solar systems due to its unique advantages, such as high energy density, abundant natural resources, and a wide temperature range [35, 36]. However, for most applications, PCMs with a narrow phase-transition temperature range, high latent heat, and strong chemical stability are preferred because they can store and release more energy in cycles. Additionally, phase change materials have a wide melting point range [37], which is why they are widely used in many different practical applications, including developing smart thermal micro-grids, portable thermal batteries, indoor thermal management systems, thermo-regulating textiles, warm supply thermal protection, solar-driven cookers, solar heating systems, water heaters, refrigerators, air-conditioning, cooling, enhancing thermal comfort in buildings, improving thermal performance of building materials, fabricating energy-saving equipment, healthcare, and food preservation [38-40]. Overall, in any application that relies on controlled and efficient thermal energy storage and release, PCM offers significant benefits by utilizing its melting and crystallization behavior. However, it is essential to select the phase-transition temperature (i.e., operating/working temperature) of the PCM for a given practical project in the temperature range of the given application. Otherwise, their performance will be no different from that of conventional sensible heat storage materials, and the latent heat action will not occur [41].

PCMs are widely used in latent heat thermal energy storage systems (LHTES) and can be classified into four states based on the phase-change mechanism and the phase-transition temperature [42]: solid-solid (S-S), solid-liquid (S-L), solid-gas (S-G) and (4) liquid-gas (L-G) (as shown in Fig. 1-4). Among them, solid-liquid PCMs are commonly used due to their compatibility with building materials. Other types of PCMs such as solid-gas and liquid-gas are not commonly used because they exhibit technical limitations such as large volume changes and high gas phase pressure during the phase transition process [43-45]. Therefore, it will not be discussed further. In addition, although there are various PCMs with different melting point ranges on the market, the most commonly used solid-liquid PCMs can be divided into three categories: organic, inorganic and eutectic mixtures. Solid-solid PCMs have been reported to have an advantage over solid-liquid PCMs as they allow for direct incorporation into building materials and components without the need for nano/microencapsulation technology [46], and this feature can lead to lower costs. However, although solid-solid PCMs are considered to have good compatibility with construction materials, so far, no studies have investigated this.



**Fig. 1-4. Classification of PCMs [42].**

Solid-liquid phase change materials (PCMs) are popularly used as effective thermal energy storage materials owing to their ability to store, absorb, or release large amounts of thermal energy through a phase change, while maintaining nearly constant temperature. Meanwhile, they undergo relatively small volume changes during phase changes compared to liquid-gas PCMs [47], and they have higher latent heat storage capacity than solid-solid PCMs. However, their practical usage is limited by their poor shape stability during phase change, which necessitates encapsulation techniques to maintain their original solid state, ultimately increasing the overall cost [47]. In addition, solid-liquid PCMs face other operational problems, such as super-cooling and corrosion [48]. By contrast, the characteristics of PCMs superior to other materials make these advantages and disadvantages of different PCMs lead to different processing, formulation, and ultimately meeting the requirements of use. The utilization of phase change materials (PCMs) in buildings can lead to a reduction in heating and cooling loads by decreasing heat transfer through the building envelope, while simultaneously maintaining indoor temperatures within the occupants' thermal comfort range by minimizing temperature fluctuations, especially for lightweight buildings, as illustrated in Fig. 1-5 [49]. The primary mechanism involves the PCM reaching its melting temperature during the day when the room temperature rises, and the chemical bonds in the material break, resulting in additional heat being absorbed by the material changing its state from solid to liquid [50]. Similarly, when the temperature drops below the freezing point of the PCM at night, the PCM releases energy and changes its state from a liquid to a solid [51]. Hence, if the melting and freezing temperatures are appropriately matched to the desired indoor comfort temperature, they can help decrease the heating and cooling loads by absorbing and releasing additional heat [50].

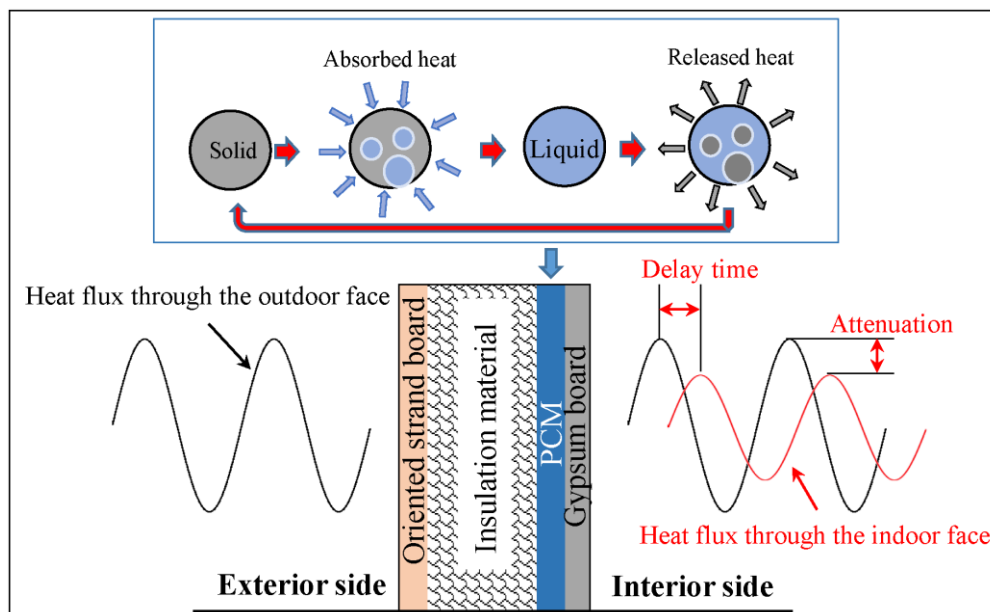


**Fig. 1-5. Schematic of the working principle and thermal inertia of PCM in walls [49].**

## 1.2 Literature review

### 1.2.1 Study on PCM integrated into different walls

PCMs have gained recognition as a promising energy storage material for energy-saving applications in buildings [52]. Researchers have integrated PCM with conventional building materials such as gypsum [53], brick [54], and concrete [55] to enhance the thermal performance of the materials. However, the factors affecting the energy performance of PCM composites for buildings include the phase-transition temperature, energy density, and shape of the enthalpy curve, as well as the climate zone [56]. Arivazhagan et al. [57] compared building blocks with integrated PCM (melting point of 30 °C) with normal building blocks in Chennai, India, and demonstrated that the maximum air temperature in the room decreased by 3 °C, and the temperature fluctuations weakened. Similarly, Cabeza et al. [58] prepared PCM energy storage concrete by blending concrete with PCM having a melting point of 26 °C, which showed better thermal conductivity compared to ordinary concrete and maintained the room temperature around 25 °C for a longer duration. Furthermore, Liu et al. [59] combined PCM (phase-change temperature of 44 °C) with foamed cement and concluded that a 30% PCM content offers the best thermal storage performance for climate regions with peak temperatures below 42.5 °C. Meng et al. [60] created PCM foamed cement using physical methods with PCM having a phase-change temperature of 32 °C and found that the PCM foamed cement roof could reduce the inner surface temperature by 2.9 °C. Shen et al. [61] produced PCM concrete thermal storage blocks by adsorbing paraffin wax on crushed lightweight shale ceramic particles at a melting temperature of 58.13 °C. The average specific heat capacity of PCM

concrete thermal storage blocks increased by 41.23% compared to that of ordinary concrete. Additionally, Mahdaoui et al. [62] observed that using PCM hollow blocks could stabilize and reduce indoor temperature fluctuations in extreme weather areas of Morocco. Frazzica et al. [63] developed composites by incorporating MEPCM into standard mortars and identified that the optimal melting temperature for the Sicilian climate was 27 °C. Al-Yasiri et al. [64] found through experimental studies that using PCM concrete blocks with a phase-change temperature of 44 °C can significantly enhance the thermal performance of concrete blocks in hot climates. In contrast, the optimal PCM melting point for buildings in mild climates (such as Fargo summer) was around 24 °C for improving indoor thermal comfort [65].

In addition, unlike concrete or mortar, gypsum board is an interior decoration material commonly used to retrofit existing buildings, and it has also been extensively studied to incorporate PCM into gypsum board so far. For instance, Lee et al. [66] found that the use of 10% shape-stabilized PCM in gypsum board reduced the cooling energy of a building by 3.4% in summer. Behzadi and Farid [67] demonstrated that a 13 mm thick gypsum board with 24-26% PCM had high thermal inertia, resulting in energy consumption reductions of 34.5% in summer and 21% in winter. Sharifi et al. [68] conducted numerical simulations and concluded that gypsum boards containing 50% PCM by volume could lower energy consumption for air conditioning in buildings by 39%, reducing heating demand by 59% and cooling demand by 31%. However, more research is necessary to evaluate the practicality and cost-effectiveness of adding large amounts of PCM to gypsum board. Wi et al. [69] injected PCM into a hollow gypsum board, which led to a 7.2 °C reduction in the peak temperature of the PCM gypsum board.

Meanwhile, in recent studies, researchers have explored the thermal performance of various walls integrated with phase change materials (PCM). Zhou et al. [70] conducted a comparison of the thermal behavior of shape-stabilized PCM, brick, foam concrete, and expanded polystyrene (EPS) at different outdoor temperatures based on an enthalpy method model. Results showed that shape-stabilized PCM had the best delay time and attenuation rate. Gao et al. [71] filled PCM in hollow bricks and found that the attenuation rate could be reduced from 13.07% to 0.92% -1.93%, and the delay time increased from 3.83 h to 8.83 h-9.83 h. At the same time, Jia et al. [72] found that combining both thermal insulation material (TIM) and PCM could comprehensively improve the thermal resistance and thermal inertia of hollow bricks. What's more, Li et al. [73] obtained through EnergyPlus simulation that integrating PCM in the ordinary foamed concrete wall could reduce the annual heating load by 4.74%. Liu et al. [74] observed that the delay time could be added to 6.86 hours and the attenuation rate decreased by 90.45%, and the peak heat flux ( $q_{peak}$ ) and average heat flux ( $q_{ave}$ ) reduced by

66.52% and 33.39%, respectively, for lightweight wall integrated with a suitable PCM compared to the reference wall (without PCM). Furthermore, to evaluate the thermal inertia of a lightweight wall integrated with PCM, Ling et al. [75] proposed a simplified method to calculate the PCM energy storage coefficient by dimensional analysis and numerical simulation. Based on this method, Sun et al. [76] derived that the thermal inertia index of lightweight walls could be improved by 60.3% with suitable PCM. In summary, the application of PCM in buildings has been widely studied, but the contribution efficiency of PCM integrated into different walls varies greatly. For this reason, Wu et al. [77] analyzed the effect of thermal properties of walls on the contribution efficiency of PCM layers. It was found that the thermal properties of the wall have a great influence on the contribution efficiency of the PCM layer. The higher the heat transfer coefficient or, the lower the thermal inertia, the better the operation of the phase-change thermal storage capacity.

### **1.2.2 Contribution benefits of PCM to building energy-saving under different climate characteristics**

In recent years, PCM has been used to improve the energy efficiency of building energy-saving and solar heating systems, which are recognized as the most practical ways to reduce fossil fuel consumption [78,79]. Many studies have been conducted on the application of PCM in buildings, demonstrating its effectiveness in reducing energy consumption. Among them, Shen and Liu [80] used EnergyPlus to investigate the energy-saving potential of integrating five PCM layers on the outer wall of a single-family house in a warm climate area (South Texas, USA). It was concluded that the reduction of heating demand was between 7.9% and 54.34%, while the cooling demand was between 1.2% and 7.2%. In the meantime, Mi et al. [81] examined the effect of PCM on the energy consumption of multi-story office buildings in different climate zones (Shenyang, Zhengzhou, Changsha, Kunming, and Hong Kong) in China and found that energy savings were more significant in hot summers and cold winter zones (Changsha). Alam et al. [82] compared the effects of PCM with different phase-transition temperature ranges in eight Australian cities and discovered that the effectiveness of PCM was highly dependent on the local weather, temperature range, PCM layer thickness, and surface area. Also, it was pointed out that PCM integration into buildings could provide 17-23% annual energy savings for houses in hot and humid cities such as Darwin. Besides, Lei et al. [83] evaluated the energy-saving potential of a single-zone building containing PCM in Singapore (tropical climate zone) and concluded that adding a PCM layer on the outside of the wall could reduce the annual cooling load by 26%. The authors also emphasized the importance of selecting a suitable PCM for this climate zone.

On the other hand, the use of phase change materials (PCM) has been investigated by several researchers for its energy-saving benefits in air conditioning and free-running buildings during hot seasons. Ascione et al. [84] found that the use of PCM with a melting temperature of 29 °C reduced the cooling demand by 7.2% in Ankara and less than 3% in Naples and Seville. In addition, the same quality of PCM extended the thermal comfort time by 15.4% and 22.9% in Seville and Naples, respectively. Similarly, Schossiga et al. [85] conducted an experiment in Germany that showed night ventilation with microcapsule PCM wallboard reduced the maximum inner surface temperature by 2 °C compared to a reference case without PCM, while extending the time of indoor temperature below 28 °C by 90%. As well, Aketouane et al. [86] carried out a numerical study on the energy-saving potential of PCM-filled bricks in six different climatic zones in Morocco. This study concluded that up to 40% energy saving could be achieved by determining the optimal phase-transition temperature of PCM. Ozyurt [87] found through DesignBuilder that placing PCM on the outer surface of walls could significantly contribute to energy savings in Izmir, especially during the cooling season. Imafidon et al. [88] pointed out that adding honeycomb PCM to the walls of a renovated building in Ottawa (Canada) could reduce the heat gained through the walls by 41%.

The effectiveness of PCM in improving the thermal performance of buildings conditions has been well documented under contemporary climatic. But beyond that, some studies have investigated the potential of PCM to affect buildings under future climate change. Firstly, Nurlybekova et al. [89] investigated the impact of PCM on building energy performance in different subtropical cities (Chengdu, Zhengzhou, Kathmandu, Hanoi, Lucknow, and Islamabad) under current and future climate conditions. The results revealed that optimal PCM usage could reduce the building's annual energy demand by 20%-37% under the current climate conditions and up to 16%-37% in the long term (by 2095), depending on the city. In another study, Ramakrishnan et al. [90] assessed the overheating risk of a building in Melbourne (Australia) for three periods (2009, 2030, and 2050) under a pessimistic climate change scenario. The authors found that combining PCM with a night ventilation strategy could reduce discomfort time by 65%, 48%, and 46% in 2009, 2030, and 2050, respectively. Recently, Adilkhanova et al. [91] analyzed the potential of PCM combined with natural ventilation strategies to enhance the summer thermal performance of lightweight buildings in Kazakhstan under future climate conditions (by 2095, high greenhouse gas emissions). The authors reported that the use of PCM with a high melting point was more effective in reducing discomfort time during the summer season. In summary, it is easy to conclude that the energy-saving contribution of PCM in buildings is highly correlated with the climatic conditions of its application, which further illustrates the importance of optimizing PCM applications for different climatic characteristics.

### 1.2.3 Study on suitable thermo-physical parameters of PCM

Recently, many scholars have studied the rules for the effective use of PCM in building envelopes and found that the thermal performance of walls integrated with PCM was affected by PCM thickness, latent heat, phase-transition temperature, thermal conductivity and location [92-101]. Selecting the appropriate thermo-physical parameters of PCM is crucial in order to meet the load demands of different buildings under varying climatic conditions [102]. Furthermore, the optimal application of PCM for thermal comfort requires a comprehensive analysis of indoor and outdoor temperature and climate conditions, with PCM parameters being optimized accordingly [103]. As a result, for PCM, the phase-transition temperature, latent heat, PCM thickness, thermal conductivity, and PCM arrangement (location) were usually considered in PCM parameter optimization. In the following, we will review the above PCM parameters to find the differences and insufficiencies in the optimization process of PCM applications.

#### (1) The phase-transition temperature of PCM

Recent studies have highlighted the significance of the phase-transition temperature of PCM in determining its effectiveness in building envelope applications. The phase-transition temperature should be carefully selected, as a high temperature can lead to a reduction in solar heat gain during the day, while a low temperature can result in poor indoor thermal comfort [102]. Therefore, it is crucial to determine the appropriate phase-transition temperature of the PCM based on the specific application requirements.

Numerous studies have investigated the optimal phase-transition temperature of PCM for effective use in building envelopes. Jin et al. [104] found that the optimal phase-transition temperature for heating and cooling storage in a double-layer PCM floor was 38 °C and 18 °C, respectively. Zhou et al. [105] studied the thermal performance of mixed PCM-reinforced gypsum and shape-stabilized PCM (SSPCM) in passive solar buildings in Beijing under winter conditions. The study found that the optimum phase-transition temperature of the composite PCM consisting of PCM-gypsum and SSPCM was 21 °C. Saffari et al. [106] demonstrated that phase-transition temperatures of 20 °C and 26 °C could significantly reduce energy consumption in air-conditioned residential buildings in different climates. Similarly, Alam M et al. [107] reported that the optimal phase-transition temperature for PCM roofs to regulate room temperature in Melbourne was 25 °C. However, Yan and Wang [108] suggested that the phase-transition temperature for PCM in the building envelope should be 2 °C higher than the minimum outdoor temperature in summer and preferably between 20 °C and 30 °C. In contrast, Sun et al. [109] studied the optimal phase-transition temperature of PCM in five typical cities

under five different climate zones of China and believed that the phase-transition temperature of PCM should be at least 3 °C higher than the average outdoor temperature. Furthermore, Liu et al. [110] determined that the optimal phase-transition temperature of PCM combined with night ventilation in office buildings during transitional and high-temperature seasons in 10 cities ranged from 23 °C to 29 °C. The determination of the optimal PCM phase-transition temperature varies depending on structural form and climatic conditions. Based on this, relevant studies have further explored to the effect of phase-transition temperature on heat flux of the exterior wall [111] and the energy-saving potential of new PCM wallboards [112]. Arguing that the phase change temperature depends on the season and the orientation of the wall, and the optimal phase-transition temperatures for external and internal walls mainly depend on outdoor and indoor air temperatures. Meanwhile, Neeper [113] proposed that the optimal phase-transition temperature for PCM exterior walls depends on the average indoor and outdoor temperatures and the thermal resistance of the original wall.

## **(2) The latent heat of PCM**

The amount of latent heat stored in PCM is an important factor influencing the thermal performance of PCM envelopes. Higher latent heat storage capacity leads to higher energy storage density during the quasi-isothermal process, which can potentially reduce indoor temperature fluctuations and improve thermal comfort [114]. Nevertheless, selecting the optimal amount of latent heat is subject to different opinions among scholars.

Kuznik et al. [115] studied the variation of heating demand with latent heat using a low-energy house and concluded that the optimal latent heat is 178 kJ/kg for a given condition. Xu et al. [116] suggested that practical applications of composite PCM floors should consider a balance between latent heat and thermal conductivity, and that the latent heat of the composite PCM floor should be greater than 120 kJ/kg to reduce indoor air temperature fluctuations. Zhou et al. [117] found that the latent heat should not be less than 90 kJ/kg for PCM to remain in the phase-change range for a long period. However, Liu et al. [118] found that the increase in latent heat is not proportional to its contribution efficiency by numerically simulating the thermal performance of PCM integrated into lightweight walls, and there exists a relatively suitable latent heat value of 125 kJ/kg. Sharma et al. [119] compared the effect of different latent heat of PCM installed in the roof on the indoor heat gain, and observed that the optimal latent heat for PCM should be within a reasonable range to improve its performance. Zhou et al. [120] evaluated the effectiveness of different latent heat of PCM set up in the internal and external walls on the inner surface temperature and daily stored heat. Concluding that a larger latent heat had a positive effect on diurnal heat storage when all PCMs could complete a phase-change

cycle in one day. Zhang et al. [102] also believed that the latent heat should be large enough to keep the indoor temperature in a comfortable range for a longer period [121].

### **(3) The thickness of PCM**

Selecting an appropriate phase change material (PCM) thickness is essential to achieve optimal thermal performance. The heat absorbed from the room can be significantly increased, and the heat released into the room can be reduced by selecting the appropriate PCM thickness in summer, which is the opposite conclusion in winter [122]. As a result, the thickness of the PCM must be optimized to obtain the best storage effect of the PCM during the day. Kuznik et al. [123] found that a 1 cm thickness of PCM was optimal by analyzing the effect of different PCM thicknesses on the daily internal and external temperature fluctuation for a lightweight building within a 24-hour temperature cycle. In contrast, Meng et al. [124] measured and simulated the effect of different PCM thicknesses on the indoor environment of a composite PCM room and found that 4 cm thick PCM was better in winter. However, the small size of the building and the limited simulation period of 24 hours may not reflect actual situations. For this reason, Ascione et al. [125] evaluated the effect of different PCM thicknesses on the performance of a typical large-scale building in Europe and noted that the cooling load decreased with increasing PCM thickness, and 30 mm thick PCM-gypsum achieved maximum energy savings. Chen et al. [126] concluded that the optimal PCM thickness was 30 mm with a latent heat of 60 kJ/kg by studying the effect of different PCM thicknesses and latent heat on the energy cost and energy-saving rate of indoor heating.

In addition, Xiao et al. [127] simulated the thermal insulation performance of SSPCM wallboards and studied the effect of PCM thickness on the performance in Beijing during summer. The authors suggested that the thickness of SSPCM wallboards should not exceed 20 mm for optimal performance. Silva et al. [128] conducted experimental tests and numerical simulations on building components containing PCM. They found that increasing the PCM thickness could reduce surface temperature fluctuations and increase the delay time, with a 25 mm PCM amplitude 22% lower than that of 19 mm PCM. Li et al. [129] investigated the influence of different PCMs on the thermal behavior of conventional walls in Iran and reported on the variation of inner surface temperature changes of RT-27 PCMs with thicknesses of 10 mm, 20 mm, and 40 mm. Their findings showed that energy storage of PCM was positively correlated with thickness. Increasing the thickness of PCM leads to a reduction in the heat passing the wall, but the reduction rate would be weakened as the thickness of the PCM was increased.

### **(4) The thermal conductivity**

Thermal conductivity is a crucial factor affecting the performance of phase change materials (PCM) in thermal energy storage systems. In particular, it plays a significant role in regulating the heat transfer rate and the phase-change process of the PCM. Various studies have explored the impact of thermal conductivity on the performance of PCM in different applications. For example, higher thermal conductivity in PCM can lead to faster melting or solidification, which is desirable in certain applications. However, it can also reduce the energy-saving effect of the system in some cases. The optimal range of thermal conductivity varies depending on the specific application and the envelope structure. Studies have found that lower thermal conductivity is preferred in multi-layer planar structures, while non-homogeneous materials require a higher range of thermal conductivity for optimal performance. Therefore, careful consideration of thermal conductivity is essential in the design and optimization of PCM-based thermal energy storage systems.

The rate of phase change in PCM wallboards (PCMW) is greatly influenced by the thermal conductivity of the PCM. In situations where PCM cannot completely solidify or melt for an extended period, its thermal conductivity is a crucial factor affecting the thermal resistance of the wallboard and directly impacting the heat flux of the structure [130]. As such, the thermal conductivity of PCM is a key parameter affecting the heat transfer rate of latent heat thermal storage systems (LHTES) [131,132]. To this end, Sari et al. [133] investigated the thermal conductivity and LHTES properties of a paraffin/expanded graphite composite PCM and found that increasing the thermal conductivity of PCM significantly reduced its melting time. Zhang et al. [121,134] simulated and analyzed the heat storage and nonlinear heat transfer characteristics of PCMW and discovered that the energy-saving effect of PCM was negatively correlated with its thermal conductivity. Zhang et al. [135] also discussed the critical values of thermo-physical parameters of the envelope by simulating a building in Beijing, finding that larger thermal conductivity of external thermal mass resulted in slower energy-saving increase, and the critical value for optimization of internal thermal mass was  $0.5 \text{ W}/(\text{m}\cdot\text{K})$ . Meanwhile, Zhou et al. [136] simulated the effect of combining SSPCM with a ventilation and cooling storage system and suggested that higher thermal conductivity led to better cooling. However, the effect became insignificant when thermal conductivity exceeded  $0.5 \text{ W}/(\text{m}\cdot\text{K})$ . Further studies [137-139] indicated that when the envelope is in a multi-layer planar structural mode, PCM with lower thermal conductivity can achieve more desirable thermal performance. In contrast, when the phase-change layer of the envelope was in the non-homogeneous material mode, namely, the distribution of PCM in the layer was not uniform but alternated with other materials (such as the hollow brick walls), the thermal conductivity of PCM was preferably in the range of  $0.2 \text{ W}/(\text{m}\cdot\text{K})$  and  $0.7 \text{ W}/(\text{m}\cdot\text{K})$ .

### (5) The arrangement of PCM

The placement of PCM within the wall is a crucial factor in managing and reducing heat transfer [140]. The arrangement of PCM in the building envelope is considered key to achieving optimal system performance [141]. Fachinotti [142] and Gounni et al. [143] suggest that higher thermal performance can be achieved when the PCM layer is located near the inner surface of the wall. Conversely, Lei et al. [144] used EnergyPlus to model a  $3 \times 3 \times 2.8$  m cube to study the energy-saving effect of building envelopes combined with PCM in tropical Singapore and found that PCM installed on the outer surface of the wall performed better. Lee et al. [145] evaluated the thermal performance of PCM in different locations within the walls in different orientations, finding that the best positions for thin PCM in south and west-facing walls were position-3 and position-2, respectively (see Fig. 1-6). Jin et al. [146] studied the thermal behavior of PCM at three different locations within the wall and reported that PCM arranged near the inner surface of the wall could reduce the peak heat flux of the wall by 11% compared to a wall without PCM, while the effect on the peak heat flux was minimal when it was located in the middle of the wall or near the outermost surface of the wall.

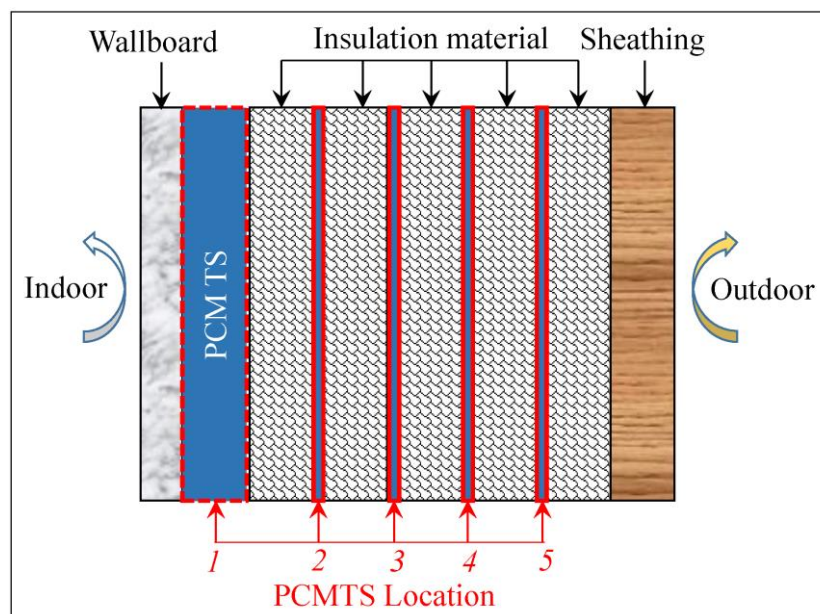


**Fig. 1-6. The schematic of the locations of the PCM thermal shields (PCMTS) [145].**

Moreover, the optimal location of PCM in the wall was studied by Jin et al. [146], who suggested that it should be placed at the farthest  $L/5$  from the heat source (as shown in Fig. 1-7) to achieve the best thermal performance. This conclusion was further supported by Jin et al. [147], who reported a 41% reduction in peak heat flux and an additional 2-hour delay time by placing PCM at this optimal location. Moreover, Jin et al. [148] investigated the impact of external climatic conditions and PCM thermal behavior on the placement of PCMs in the wall

and found that the optimal location shifted closer to the interior surface of the wall as the inner surface temperature increased. Izquierdo-Barrientos et al. [111] simulated the thermal performance of PCM in different locations of the wall during winter and summer and analyzed the heat gain of PCM in different orientations and locations. The results indicated that the location of PCM in the wall was primarily determined by the season, wall orientation, and building use. Additionally, another important result was found by Arnault et al. [149] that the establishment of the objective optimization function was very important in optimizing the PCM parameters in the building envelope, and it would directly affect the optimization results to some extent. Therefore, it also can be considered that the objective function (evaluation index) is also referred to as the optimization objective in the optimization process of the PCM envelope. Among them, the thermal performance of walls and energy saving of buildings are the most considered factors.

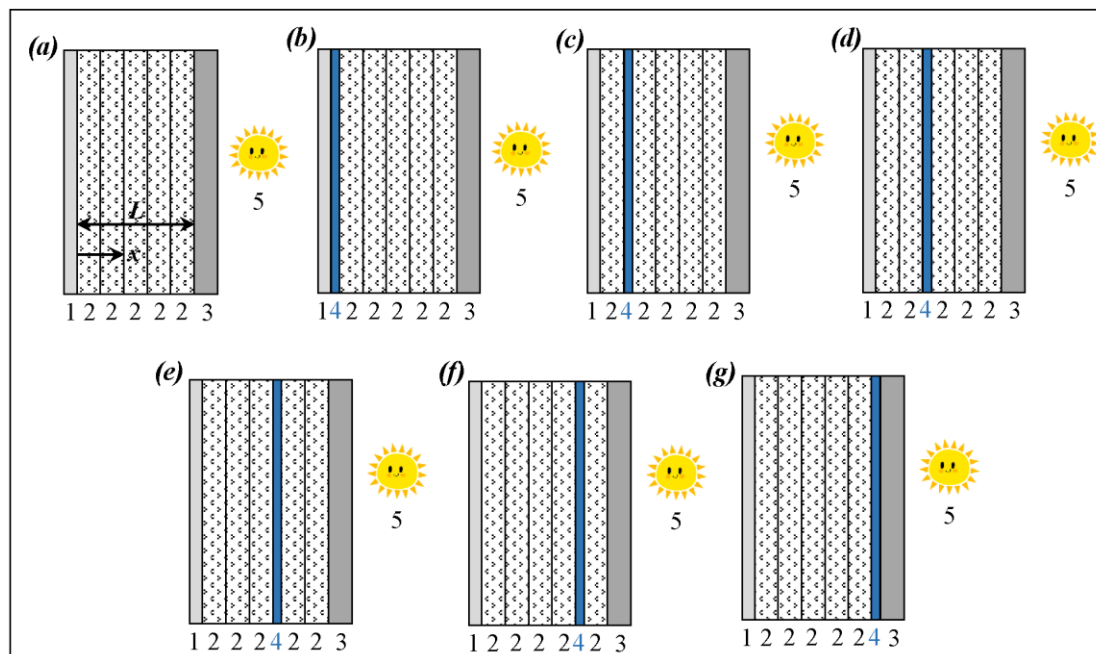


**Fig. 1-7. The schematic of wall construction. 1: gypsum wallboard, 2: insulating layer, 3: oriented strand board, 4: PCM thermal shields, 5: heat source [145].**

#### 1.2.4 Summary of research status

The aforementioned study achieved the improvement of material performance and indoor thermal comfort by adding PCM to traditional building materials [150]. However, the heat storage and release of PCM are affected by various factors such as PCM thermo-physical parameters, application object, installation location and climatic conditions, which are complex and non-linear. In addition, the composite PCM material has different adaptability to different climatic conditions, and the optimal phase-transition temperature of PCM depends on the

climatic characteristics [151]. Existing studies often discuss the application of PCM in a single climate zone. Therefore, selecting the appropriate PCM for buildings with different climatic characteristics remains a huge challenge. Meanwhile, current studies on suitable parameters for PCM have found that their suitable parameter values depend not only on climatic conditions but are also highly correlated with the building structure form and optimization objectives. Hence, the existing conclusions, rules, and interrelationships between the obtained influencing factors will likely be too absolute and flawed.

Furthermore, lightweight buildings are widely preferred for their good seismic performance, environmental protection, and short construction cycle. Nonetheless, lightweight buildings usually have larger indoor temperature fluctuations than conventional buildings due to the lower thermal mass. Larger temperature fluctuations not only affect indoor thermal comfort but also increase the air conditioning load. As innovative materials integrated into lightweight buildings, PCM can directly improve the thermal inertia of lightweight buildings. As a result, PCM integrated into lightweight buildings has been extensively studied and optimized, proving its effectiveness in reducing energy consumption and improving indoor thermal comfort. However, despite the fruitful research results accumulated by many scholars on the effective application of PCM, the following issues still need to be further explored:

- Most of the current research has focused on the energy-saving and indoor thermal comfort of existing PCM. The research on the heat transfer performance of PCM-integrated lightweight walls with different thermo-physical parameters is insufficient.
- PCM has a positive effect on improving the thermal performance of the wall, but most of the current research only optimizes the parameters for a particular structure. However, the thermal physical parameters of PCM suitable for different structural or thermal resistance walls are very different. Currently, the application research of PCM on different thermal resistance walls lacks systematicity, especially for lightweight buildings with different thermal insulation materials or forms.
- The storage and release of latent heat from PCM depend highly on the heat exchange between the wall surface and the ambient environment when PCM is integrated into a wall. Currently, most of the studies focus on improving the thermal performance of walls brought by PCM under fixed thermal boundary conditions. However, for actual buildings, the thermal environment (especially the solar radiation intensity) varies greatly between different wall orientations due to the shading effect of the building (or itself). Thus, it is more practical to explore the thermal performance of PCM integrated into walls with different orientations.
- The application effect of PCM is highly correlated with climatic conditions. Most current

studies have focused on a specific climate type or season. For PCM, the inherent phase-transition temperature may have satisfactory results in summer (winter) but may have unsatisfactory or negative results in winter (summer). Finding the best PCM kind and configuration to improve the thermal performance of buildings in different climates/seasons has not been well solved.

- The current research mostly focuses on optimizing the thermal performance of PCM integrated walls through numerical simulation under the air-conditioning environment. In contrast, the long-term comparative analysis of PCM for regulating the walls and indoor thermal environment in natural environments (without mechanical equipment intervention) is insufficient. At the same time, the numerical simulation is also ideal. So it is necessary for actual measurement and analysis under natural thermal environments for the application effect of PCM.
- There are climate differences in the energy-saving potential of PCM and suitable PCM parameters/configurations. Finding suitable PCM parameters/configurations for different climate zones are more conducive to maximizing PCM application benefits. However, the current studies on PCM parameters/configurations are limited to some of them. At the same time, the lack of the importance ranking of each parameter/configuration of PCM in energy saving potential reduces reference information when PCM is selected for use.
- The economics is an important consideration when PCM is selected for use. However, the PCM cost, energy-saving potential and energy price in different regions are the key factors affecting its application value. As a result, it is more important to discuss in-depth the suitability of PCM for different climatic conditions.

### **1.3 Purpose and content overview of this study**

Based on the above problems, the research aims of this paper are mainly **(1)** to ascertain the influence laws of PCM parameter on the thermal performance of lightweight wall under different thermal boundary conditions, and **(2)** to obtain the energy-saving potential (annual cooling and heating) of lightweight walls using PCM applied to buildings and determine economic feasibility in different climates/cities.

Therefore, this study systematically analyzes the influence laws and application effect of PCM thermo-physical parameters on the thermal performance of lightweight walls and the appropriate parameter values from the perspective of different thermal boundaries. Afterwards, the suitability, the influence degree and the selection priority for PCM parameters and configurations in the context of different climatic conditions and energy prices are proposed from the perspective of energy-saving. Meanwhile, the effect of different configurations (single

and double-PCM) and amounts (thickness and utilization area) of PCM on the energy-saving of lightweight buildings, payback period and economic applicability are evaluated.

The research results can provide a systematic evaluation method for effect of PCM applied to opaque envelopes under different thermal boundaries at the theoretical significance. Meanwhile, the research results can also provide reference for decision-makers to select suitable PCM products in lightweight wall or building in terms of energy-saving and economics, as well as provide data support for manufacturers to develop innovative energy-saving lightweight wall products using PCM.

The basic framework of this study is shown in Fig. 1-8. The specific research contents are described as follows:

**In Chapter 1, the research content and purpose of this paper are determined based on the research background and research status.**

Firstly, the current status of building energy consumption, energy-saving technologies, indoor thermal environment characteristics of lightweight buildings and PCM characteristics are introduced. Then, the effectiveness of PCM application in different structural forms is reviewed through a large number of previous studies, and the difference in the contribution benefits of PCM to reducing energy demand under different climatic conditions are obtained. Meanwhile, the thermo-physical parameters of PCM affecting its application effect and the appropriate values are summarized. Eventually, the problems existing in the application of PCM in buildings are deeply analyzed based on a large number of literature reviews, and the research contents and purposes of this paper are clarified.

**In Chapter 2, the heat transfer process of the envelope is analyzed, and the evaluation index of this study is proposed.**

Firstly, the causes of the indoor thermal environment of the building and the influence of PCM on the lightweight building are analyzed theoretically, and the mathematical model and solution method are established. Then, the evaluation index for improving the thermal performance of lightweight buildings is proposed.

**In Chapter 3, the influence rules of PCM thermo-physical parameters on the thermal performance of lightweight walls are systematically evaluated.**

Based on the existing PCM, the influence rules of PCM phase-transition temperature, PCM location, PCM thickness, PCM latent heat, PCM thermal conductivity, PCM density and PCM-specific heat on the thermal performance improvement of the lightweight wall are analyzed in this study one by one through the control variable method. Then, the relatively

suitable location in walls and thermal physical parameters of PCM are determined.

**In Chapter 4, the influence laws and contribution efficiency of different PCM thermo-physical parameters on the thermal performance of lightweight walls with different thermal resistance are assessed.**

Firstly, four lightweight walls with different thermal resistances are established based on the relevant standards and numerically verified in this study. Then, the variation law of PCM liquid fraction at different PCM locations for different thermal resistance walls is discussed, and the appropriate phase-transition temperature is determined. After that, the influence laws, contribution efficiency and suitable values of PCM thermo-physical parameters (thickness, latent heat, thermal conductivity) on the thermal performance improvement of different thermal resistance of the original wall are discussed.

**In Chapter 5, the difference, applicability and appropriate parameters for the application effect of PCM integrated into different directions of walls are determined.**

Firstly, the difference in the thermal environment around the external surface of the wall in different directions (orientation) was tested and analyzed by manufacturing a small-scale lightweight building. Then, the influence laws of PCM thermo-physical parameters on the thermal performance improvement of walls in different directions are explored using the thermal environment in different directions as the thermal boundary conditions, and the suitable parameter values are obtained. Finally, the contribution efficiency and applicability of PCM for the walls in different directions (orientation) are further evaluated based on the suitable parameters, and then the optimal choice is given for the PCM installation orientation.

**In Chapter 6, the effectiveness of different kinds/configurations of PCM on the thermal performance of lightweight walls in winter and summer are assessed, and suitable PCM kinds/configurations for both seasons are proposed.**

In this study, based on the above research results, four different kinds/configurations of lightweight walls are built, and the typical winter and summer climate characteristics are used as the thermal boundary conditions to discuss the application effects of different configurations of PCM (four models) in winter and summer, and then the optimized configuration of PCM suitable for both summer and winter is determined. After that, the influence laws and suitable values of different PCM thermo-physical parameters on the application effects for both summer and winter under the optimized configuration are further analyzed.

**In Chapter 7, the regulation ability of PCM on the thermal performance of lightweight walls and indoor thermal environments in different seasons under a natural environment (no mechanical equipment) is discussed by experimental measurements.**

Firstly, two test rooms of the same size (reference room and composite PCM room) are constructed in this study, and the effects of PCM on indoor temperature, wall surface temperature and heat flux (south-facing wall, for example) of lightweight buildings in different seasons (summer, transition season and winter) without mechanical equipment are compared through long time testing, based on this, the thermal regulation ability of PCM in different seasons is determined in different seasons. Finally, the energy-saving potential of the composite PCM in different seasons under natural conditions is calculated by theoretical equations. The research results provided the theoretical basis for the next step of energy-saving optimization of lightweight buildings for PCM under different climate characteristics.

**In Chapter 8, the parameters/configurations adaptability and economics of PCM integrated into lightweight buildings to reduce energy demands under different climates/cities are evaluated.**

Firstly, a typical lightweight building model is established in this study, and then some typical cities are selected under different climatic conditions (according to different climate zones) as the thermal boundary conditions. After that, the suitable PCM parameters/configurations for reducing the energy demand of lightweight buildings under different climatic conditions are evaluated using orthogonal experiments and EnergyPlus. Meanwhile, the influence degree and selection priority of each parameter/configuration of PCM is further determined. Subsequently, the suitability (energy-saving effect) of single and double-layer PCM configurations in different regions are assessed based on the optimal parameters/configurations. Further on, the energy-saving potential of different PCM thicknesses is analyzed. Eventually, the payback period for different PCM amounts (thickness and utilization area) are analyzed in the context of different energy prices (China-Japan comparison), and the maximum acceptable PCM cost price for different climates/cities is obtained based on a certain payback period.

**In Chapter 9, Conclusions.**

The main research findings of the each chapters are summarized.

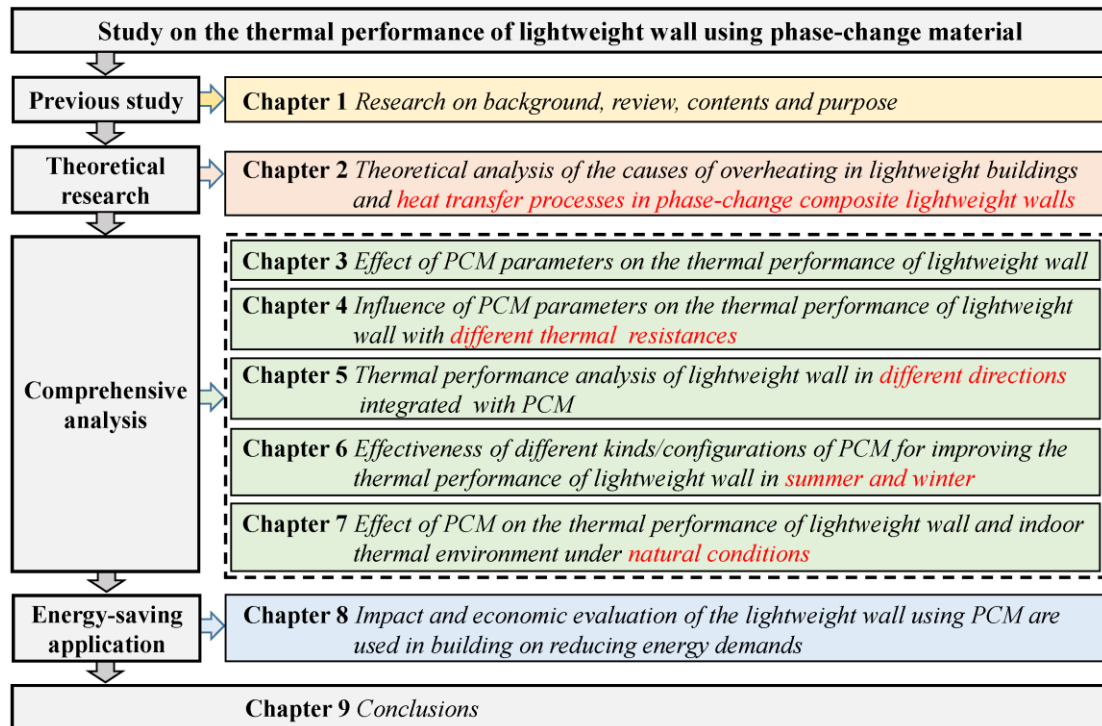


**Fig. 1-8. Research structure.**

**References**

- [1] United Nations Paris Climate Change. <https://unfccc.int/process-and-meetings/the-paris-agreement/the-paris-agreement>, 2022. (Accessed 28 October 2022).
- [2] IEA, Buildings: A source of enormous untapped efficiency potential. <https://www.iea.org/topics/buildings>, 2022. (Accessed 28 December 2022).
- [3] Q. Al-Yasiri, M. Szabó, Incorporation of phase change materials into building envelope for thermal comfort and energy saving: A comprehensive analysis, *Journal of Building engineering* 36 (2021) 102122.
- [4] IEA, CO<sub>2</sub> emissions-Global Energy Review 2021. <https://www.iea.org/reports/global-energy-review-2021/co2-emissions> (Accessed 2 July 2022).
- [5] S. B. Sadineni, S. Madala, R. F. Boehm, Passive building energy savings: A review of building envelope components, *Renewable and sustainable energy reviews* 15 (8) (2011) 3617-3631.
- [6] B. M. Santamaria, F.A. Gonzalo, B. Aguirregabiria, J. H. Ramos, Evaluation of Thermal Comfort and Energy Consumption of Water Flow Glazing as a Radiant Heating and Cooling System: A Case Study of an Office Space, *Sustainability* 12 (2020) 7596.
- [7] A. Abdeen, A. A. Serageldin, M. G. Ibrahim, A. El-Zafarany, S. Ookawara, R. Murata, Experimental, analytical, and numerical investigation into the feasibility of integrating a passive Trombe wall into a single room, *Applied Thermal Engineering* 154 (2019) 751-768.
- [8] E. Sassine, E. Kinab, Y. Cherif, E. Antczak, M. Nasrallah, Thermal performance of lightweight concrete applications in building envelopes in Lebanon, *Building Simulation* 14 (5) (2021) 1359-1375.
- [9] Z. Lin, Y. Song, Y. Chu, Summer performance of a naturally ventilated doubleskin facade with adjustable glazed louvers for building energy retrofitting, *Energy and Buildings* 267 (2022) 112163.
- [10] M. Ciampi, F. Leccese, G. Tuoni, Ventilated facades energy performance in summer cooling of buildings, *Solar Energy* 75 (6) (2003) 491-502.
- [11] A. de Gracia, J. Tarragona, A. Crespo, C. Fernández, Smart control of dynamic phase change material wall system, *Applied Thermal Engineering* 279 (2020) 115807.
- [12] L.V. Shilei, Z. Neng, F. Guohui, Impact of phase change wall room on indoor thermal environment in winter, *Energy and buildings* 38 (1) (2006) 18-24.
- [13] S. Ahmed, Z. Li, M.S. Javed, T. Ma, A review on the integration of radiative cooling and solar energy harvesting, *Materials Today Energy* 21 (2021) 100776.
- [14] Q. Li, Z. Ju, Z. Wang, L. Ma, W. Jiang, D. Li, J. Jia, Thermal performance and economy

- of PCM foamed cement walls for buildings in different climate zones, *Energy and Buildings* 277 (2022) 112470.
- [15] UN Environment Programme, 2019 Global Status Report for Buildings and Construction: Towards a Zero-Emission, Efficient and Resilient Buildings and Construction Sector, Available online: 2019, <https://www.unenvironment.org/resources/publication/2019-global-status-reportbuildings-and-construction-sector>.
- [16] U.S. Energy Information Administration. 2021. Annual Energy Outlook 2021. Washington, D.C. URL: <https://www.eia.gov/outlooks/aeo/>.
- [17] Langevin, Jared, Harris, Chioke B., and Reyna, Janet L. 2019. "Assessing the Potential to Reduce U.S. Building CO2 Emissions 80% by 2050." *Joule* 3 (10): 2403–2424.
- [18] M. Ostry, P. Charvat, Materials for Advanced Heat Storage in Buildings, *Procedia Engineering* 57 (2013) 837-843.
- [19] G. Maracchini, M. D’Orazio, Improving the livability of lightweight emergency architectures: A numerical investigation on a novel reinforced-EPS based construction system, *Building and Environment* 208 (2022) 108601.
- [20] V. V. Tyagi, S. C. Kaushik, S. K. Tyagi, T. Akiyama, Development of phase change materials based microencapsulated technology for buildings: A review. *Renewable and sustainable energy reviews* 15 (2011) 1373-1391.
- [21] L. Xu, H. Wang, Y. Gao, J. Wang, E. Long, R. Zhao, Study on performance of composite PCM (phase-change material)’s adjusting indoor thermal environment of light weight enclosure buildings, *Building Science* 29 (12) (2013) 45-49.
- [22] Y. Zhang, W. Jiang, J. Song, L. Xu, S. Li, L. Hu, A parametric model on thermal evaluation of building envelopes containing phase change material, *Applied Energy* 331 (2023) 120471.
- [23] Y. Liu, M. Wang, H. Cui, L. Yang, J. Liu, Micro-/macro-level optimization of phase change material panel in building envelope, *Energy* 195 (2020) 116932.
- [24] A. De Gracia, L. F. Cabeza, Phase change materials and thermal energy storage for buildings, *Energy and Buildings* 103 (2015) 414-419.
- [25] T. Lecompte, P. Le Bideau, P. Glouannec, D. Nortershauser, S. Le Masson, Mechanical and thermo-physical behaviour of concretes and mortars containing phase change material, *Energy and buildings* 94 (2015) 52-60.
- [26] J. Lei, J. Yang, E. H. Yang, Energy performance of building envelopes integrated with phase change materials for cooling load reduction in tropical Singapore, *Applied energy* 162 (2016) 207-217.
- [27] A. M. Thiele, G. Sant, L. Pilon, Diurnal thermal analysis of microencapsulated PCM-

- concrete composite walls, *Energy Conversion and Management* 93 (2015) 215-227.
- [28] E. Moreles, G. Huelsz, G. Barrios, Hysteresis effects on the thermal performance of building envelope PCM-walls, *Building Simulation*. Springer Berlin Heidelberg 11 (2018) 519-531.
- [29] K. O. Lee, M. A. Medina, X. Sun, X. Jin, Thermal performance of phase change materials (PCM)-enhanced cellulose insulation in passive solar residential building walls, *Solar Energy* 163 (2018) 113-121.
- [30] H. Ye, L. Long, H. Zhang, R. Zou, The performance evaluation of shape-stabilized phase change materials in building applications using energy saving index, *Applied energy* 113 (2014) 1118-1126.
- [31] C. K. Halford, R. F. Boehm, Modeling of phase change material peak load shifting, *Energy and Buildings* 39(3) (2007) 298-305.
- [32] H. Mehling, L. F. Cabeza, Heat and cold storage with PCM, *Heat and mass transfer* 2008 (2008) 11-55.
- [33] Q. Al-Yasiri, M. Szabó, Incorporation of phase change materials into building envelope for thermal comfort and energy saving: A comprehensive analysis, *Journal of Building engineering* 36 (2021) 102122.
- [34] M. Terhan, G. Ilgar, Investigation of used PCM-integrated into building exterior walls for energy savings and optimization of PCM melting temperatures, *Construction and Building Materials* 369 (2023) 130601.
- [35] J. Yang, G. Q. Qi, Y. Liu, R. Y. Bao, Z. Y. Liu, W. Yang, B. H. Xie, M. B. Yang, Hybrid graphene aerogels/phase change material composites: thermal conductivity, shape-stabilization and light-to-thermal energy storage. *Carbon* 100 (2016) 693-702.
- [36] M. Y. Abdelsalam, H. M. Teamah, M. F. Lightstone, J. S. Cotton, Hybrid thermal energy storage with phase change materials for solar domestic hot water applications: direct versus indirect heat exchange systems. *Renewable Energy* 147 (2020) 77-88.
- [37] S. N. Gunasekara, V. Martin, J. N. Chiu, Phase equilibrium in the design of phase change materials for thermal energy storage: state-of-the-art, *Renewable and Sustainable Energy Reviews* 73 (2017) 558-81.
- [38] A. Jamekhorshid, S. M. Sadrameli, M. Farid, A review of microencapsulation methods of phase change materials (PCMs) as a thermal energy storage (TES) medium, *Renewable and Sustainable Energy Reviews* 31 (2014) 531-42.
- [39] D. Q. Ng, Y. L. Tseng, Y. F. Shih, H. Y. Lian, Y. H. Yu, Synthesis of novel phase change material microcapsule and its application, *Polymer* 133 (2017) 250-62.
- [40] M. M. Umair, Y. Zhang, K. Iqbal, S. Zhang, B. Tang, Novel strategies and supporting

- materials applied to shapestabilize organic phase change materials for thermal energy storage – a review, *Applied energy* 235 (2019) 846-873.
- [41] C. Amaral, R. Vicente, P. Marques, A. Barros-Timmons, Phase change materials and carbon nanostructures for thermal energy storage: a literature review, *Renewable and Sustainable Energy Reviews* 79 (2017) 1212-1228.
- [42] A. Sivanathan, Q. Dou, Y. Wang, Y. Li, J. Corker, Y. Zhou, M. Fan, Phase change materials for building construction: An overview of nano-/micro-encapsulation, *Nanotechnology Reviews* 9(1) (2020) 896-921.
- [43] W. Su, J. Darkwa, G. Kokogiannakis, Review of solid–liquid phase change materials and their encapsulation technologies. *Renewable and Sustainable Energy Reviews* 48 (2015) 373-91.
- [44] H. Akeiber, P. Nejat, M. Z. A. Majid, M. A. Wahid, F. Jomehzadeh, I. Z. Famileh, J. K. Calautit, B. R. Hughes, S.A. Zaki, A review on phase change material (PCM) for sustainable passive cooling in building envelopes, *Renewable and Sustainable Energy Reviews* 60 (2016) 1470-1497.
- [45] M. A. Wahid, S. E. Hosseini, H. M. Hussien, H. J. Akeiber, S. N. Saud, An overview of phase change materials for construction architecture thermal management in hot and dry climate region, *Applied Thermal Engineering* 112 (2017) 1240-1259.
- [46] A. Fallahi, G. Guldentops, M. Tao, S. Granados-Focil, S. Van Dessel, Review on solid–solid phase change materials for thermal energy storage: Molecular structure and thermal properties, *Applied Thermal Engineering* 127 (2017) 1427-1441.
- [47] X. Huo, W. Li, Y. Wang, N. Han, J. Wang, N. Wang, X. Zhang, Chitosan composite microencapsulated comb-like polymeric phase change material via coacervation microencapsulation, *Carbohydrate polymers* 200 (2018) 602-610.
- [48] A. Bayon, M. Liu, D. Sergeev, M. Grigore, F. Bruno, M. Muller, Novel solid–solid phase-change cascade systems for high-temperature thermal energy storage, *Solar Energy* 177 (2019) 274-283.
- [49] O. J. Imafidon, D. S. K. Ting, Retrofitting buildings with phase change materials (PCM)–The effects of PCM location and climatic condition, *Building and Environment* [Online] (2023) 110224.
- [50] Z. A. Al-Absi, M. H. M. Isa,; M. Ismail, Phase Change Materials (PCMs) and Their Optimum Position in Building Walls, *Sustainability* 12(4) (2020) 1294.
- [51] A. Madad, T. Mouhib, A. Mouhsen, Phase Change Materials for Building Applications: A Thorough Review and New Perspectives, *Buildings* 8(5) (2018) 63.
- [52] D. Li, Y. Zheng, C. Liu, G. Wu, Numerical analysis on thermal performance of roof

- contained PCM of a single residential building, *Energy conversion and management* 100 (2015) 147-156.
- [53] M. Lachheb, Z. Younsi, H. Naji, M. Karkri, S. Ben Nasrallah, Thermal behavior of a hybrid PCM/plaster: A numerical and experimental investigation, *Applied Thermal Engineering* 111 (2017) 49-59.
- [54] A. Castell, M. M. Faridb, Experimental validation of a methodology to assess PCM effectiveness in cooling building envelopes passively, *Energy and Buildings* 81 (2014) 59-71.
- [55] A. Eddhahak-Ouni, S. Drissi, J. Colin, J. Neji, S. Care, Experimental and multiscale analysis of the thermal properties of Portland cement concretes embedded with Microencapsulated Phase Change Materials (PCMs), *Applied Thermal Engineering* 64 (2014) 32-39.
- [56] G. Paranjothi, A. Odukomaiya, S. Cui, A. Bulk, Evaluation of Phase Change Plaster/Paste Composites for Building Envelopes, *Energy and Buildings* 253 (2021) 111372.
- [57] R. Arivazhagan, S. Arun Prakash, P. Kumaran, S. Sankar, G. B. Loganathan, A. Arivarasan, Performance analysis of concrete block integrated with PCM for thermal management, *Materials Today: Proceedings* 22 (2020) 370-374.
- [58] L. F. Cabeza, C. Castell ón, M. Nogu é, M. Medrano, R. Leppers, O. Zubillaga, Use of microencapsulated PCM in concrete walls for energy savings, *Energy and Buildings* 39 (2007) 113-119.
- [59] L. Liu, J. Chen, Y. Qu, T. Xu, H. Wu, G. Huang, X. Zhou, L. Yang, A foamed cement blocks with paraffin/expanded graphite composite phase change solar thermal absorption material, *Solar Energy Materials and Solar Cells* 200 (2019) 110038.
- [60] E. Meng, J. Yang, B. Zhou, C. Wang, J. Li, Preparation and thermal performance of phase change material (PCM) foamed cement used for the roof, *Journal of Building Engineering* 53 (2022) 104579.
- [61] Y. Shen, S.i Liu, C. Zeng, Y. Zhang, Y. Li, X. Han, L. Yang, X. Yang, Experimental thermal study of a new PCM-concrete thermal storage block (PCM-CTSB), *Construction and Building Materials* 293 (2021) 123540.
- [62] M. Mustapha, H. Said, A.M. Abdelouahad, K. Tarik, E.R. Tarik, J. Abdelmajid, A. Mohammed, Building bricks with phase change material (PCM): Thermal performances, *Construction and Building Materials* 269 (2020) 121315.
- [63] A. Frazzica, B. Vincenza, P. Valeria, L. R. Davide, G. Francesco, C. Luigi, P. Edoardo, Thermal performance of hybrid cement mortar-PCMs for warm climates application, *Solar Energy Materials and Solar Cells* 193 (2019) 270-280.

- [64] Q. Al-Yasiri, M. Szabo, Effect of encapsulation area on the thermal performance of PCM incorporated concrete bricks: A case study under Iraq summer conditions, *Case Studies in Construction Materials* 15 (2021) e00686.
- [65] M. Li, Q. Cao, H. Pan, X. Wang, Z. Lin, Effect of melting point on thermodynamics of thin PCM reinforced residential frame walls in different climate zones, *Applied Thermal Engineering* 188 (2021) 116615.
- [66] J. Lee, S. Wi, B. Y. Yun, S. Yang, J. H. Park, S. Kim, Development and evaluation of gypsum/shape-stabilization phase change materials using large-capacity vacuum impregnator for thermal energy storage, *Applied Energy* 241 (2019) 278-290.
- [67] S. Behzadi, M. M. Farid, Energy storage for efficient energy utilization in buildings, in: *International High Performance Buildings Conference*, Purdue University, West Lafayette, Indiana, USA, 2010.
- [68] N. P. Sharifi, A. A. N. Shaikh, A. R. Sakulich, Application of phase change materials in gypsum boards to meet building energy conservation goals, *Energy and buildings* 138 (2017) 455-467.
- [69] S. Wi, J. H. Park, Y. U. Kim, S. Yang, S. Kim, Thermal, hygric, and environmental performance evaluation of thermal insulation materials for their sustainable utilization in buildings, *Environmental Pollution* 272 (2021) 116033
- [70] G. Zhou, Y. Yang, X. Wang, J. Cheng, Thermal characteristics of shape-stabilized phase change material wallboard with periodical outside temperature waves, *Applied Energy* 87(8) (2010) 2666-2672.
- [71] Y. Gao, F. He, X. Meng, Z. Wang, W. Gao, Thermal behavior analysis of hollow bricks filled with phase-change material (PCM), *Journal of Building Engineering* 31 (2020) 101447.
- [72] C. Jia, X. Geng, F. Liu, Y. Gao, Thermal behavior improvement of hollow sintered bricks integrated with both thermal insulation material (TIM) and Phase-Change Material (PCM), *Case Studies in Thermal Engineering* 25 (2021) 100938.
- [73] Y. Li, E. Long, L. Zhang, X. Dong, S. Wang, Energy-saving potential of intermittent heating system: influence of composite phase change wall and optimization strategy, *Energy Exploration & Exploitation* 39(1) (2021) 426-443.
- [74] Z. Liu, J. Hou, X. Meng, B.J. Dewancker, A numerical study on the effect of phase-change material (PCM) parameters on the thermal performance of lightweight building walls, *Case Studies in Construction Materials* 15 (2021) e00758.
- [75] H. Ling, C. Chen, H. Qin, S. Wei, J. Lin, N. Li, M. Zhang, N. Yu, Y. Li, Indicators evaluating thermal inertia performance of envelopes with phase change material, *Energy*

- and Buildings 122 (2016) 175-184.
- [76] X. Sun, J. Jovanovic, Y. Zhang, S. Fan, Y. Chu, Y. Mo, S. Liao, Use of encapsulated phase change materials in lightweight building walls for annual thermal regulation, *Energy* 180 (2019) 858-872.
- [77] Q. Wu, J. Wang, X. Meng, Influence of wall thermal performance on the contribution efficiency of the Phase-Change Material (PCM) layer, *Case Studies in Thermal Engineering* 28 (2021) 101398.
- [78] K. Saafi, N. Daouas, Energy and cost efficiency of phase change materials integrated in building envelopes under Tunisia Mediterranean climate, *Energy* 187 (2019) 115987.
- [79] C. Fabiani, C. Piselli, A.L. Pisello, Thermo-optic durability of cool roof membranes: effect of shape stabilized phase change material inclusion on building energy efficiency, *Energy and Buildings* 207 (2020) 109592
- [80] H. Shen, X. Liu, Energy savings potential of phase change material integrated building envelope in South Texas, *International High Performance Buildings Conference* 223 (2016)
- [81] X. Mi, R. Liu, H. Cui, S.A. Memon, F. Xing, Y. Lo, Energy and economic analysis of building integrated with PCM in different cities of China, *Applied Energy* 175 (2016) 324-336.
- [82] M. Alam, H. Jamil, J. Sanjayan, J. Wilson, Energy saving potential of phase change materials in major Australian cities, *Energy and Buildings* 78 (2014) 192-201.
- [83] J. Lei, J. Yang, E. Yang, Energy performance of building envelopes integrated with phase change materials for cooling load reduction in tropical Singapore, *Applied Energy* 162 (2015) 207-217.
- [84] F. Ascione, N. Bianco, R.F.De Masi, F. de' Rossi, G.P. Vanoli, Energy refurbishment of existing buildings through the use of phase change materials: energy savings and indoor comfort in the cooling season, *Applied Energy* 113 (2014) 990-1007.
- [85] P. Schossig, H.M. Henning, S. Gschwander, T. Haussmann, Micro-encapsulated phase-change materials integrated into construction materials, *Solar energy materials and solar cells* 89(2-3) (2005) 297-306.
- [86] Z. Aketouane, M. Malha, D. Bruneau, A. Bah, B. Michel, M. Asbik, O. Ansari, Energy savings potential by integrating Phase Change Material into hollow bricks: The case of Moroccan buildings, *Building Simulation* 11 (2018) 1109-1122.
- [87] E. E. Ozyurt, The evaluation of solar radiation contribution on the use of phase change materials in the exterior walls regarding building energy efficiency: example of Izmir, Turkey, Istanbul Technical University, Istanbul, Turkey, 2019. Master's Thesis.
- [88] O.J. Imafidon, D.S.-K. Ting, Energy consumption of a building with phase change

- material walls – the effect of phase change material properties, *Journal of Energy Storage* 52 (2022) 105080.
- [89] G. Nurlybekova, S.A. Memon, I. Adilkhanova, Quantitative evaluation of the thermal and energy performance of the PCM integrated building in the subtropical climate zone for current and future climate scenario, *Energy* 219 (2021) 119587.
- [90] S. Ramakrishnan, X. Wang, J. Sanjayan, J. Wilson, Thermal performance of buildings integrated with phase change materials to reduce heat stress risks during extreme heatwave events, *Applied Energy* 194 (2017) 410-421.
- [91] I. Adilkhanova, S.A. Memon, J. Kim, A. Sheriyev, A novel approach to investigate the thermal comfort of the lightweight relocatable building integrated with PCM in different climates of Kazakhstan during summertime, *Energy* 217 (2021) 119390.
- [92] X. Jin, M. A. Medina, X. Zhang, On the importance of the location of PCMs in building walls for enhanced thermal performance, *Applied Energy* 106 (2013) 72-78.
- [93] X. Jin, M. A. Medina, X. Zhang, Numerical analysis for the optimal location of a thin PCM layer in frame walls, *Applied Thermal Engineering* 103 (2016) 1057-1063.
- [94] X. Jin, D. Shi, M. A. Medina, X. Shi, X. Zhou, X. Zhang, Optimal location of PCM layer in building walls under Nanjing (China) weather conditions[J]. *Journal of Thermal Analysis and Calorimetry* 129 (2017) 1767-1778.
- [95] P. C. Tabares-Velasco, C. Christensen, M. Bianchi, Verification and validation of EnergyPlus phase change material model for opaque wall assemblies, *Building and Environment* 54 (2012)186-196.
- [96] E. Meng, H. Yu, G. Zhan, Y. He, Experimental and numerical study of the thermal performance of a new type of phase change material room, *Energy conversion and management* 74 (2013) 386-394.
- [97] Y. Cascone, A. Capozzoli, M. Perino. Optimisation analysis of PCM-enhanced opaque building envelope components for the energy retrofitting of office buildings in Mediterranean climates, *Applied Energy* 211 (2018) 929-953.
- [98] R.A. Kishore, M. V. A. Bianchi, C. Booten, J. Vidal, R. Jackson, Optimizing PCM-integrated walls for potential energy savings in U.S. *Energy and Buildings* 226 (2020) 110355.
- [99] R.A. Kishore, M. V. A. Bianchi, C. Booten, J. Vidal, R. Jackson, Parametric and sensitivity analysis of a PCM-integrated wall for optimal thermal load modulation in lightweight buildings, *Applied Thermal Engineering* 187 (2021) 116568.
- [100] D. Mazzeo, G. Oliveti, N. Arcuri, Definition of a new set of parameters for the dynamic thermal characterization of PCM layers in the presence of one or more liquid-

- solid interfaces, *Energy and Buildings* 141 (2017) 379-396.
- [101] A Lagou, A Kylili, J Šadauskienė, P. A. Fokaides, Numerical investigation of phase change materials (PCM) optimal melting properties and position in building elements under diverse conditions, *Construction and Building Materials* 225 (2019) 452-464.
- [102] Y. P. Zhang, G. B. Zhou, K. P. Lin, Q. L. Zhang, H. F. Di, Application of latent heat thermal energy storage in buildings: state-of-the-art and outlook, *Building and Environment* 42 (2007) 2197-2209.
- [103] J. H. Park, J. Lee, S. Wi, S. Jeon, S. J. Chang, S. Kim, Optimization of phase change materials (PCMs) to improve energy performance within thermal comfort range in the South Korean climate, *Energy and Buildings* 185 (2018) 12-25.
- [104] X. Jin, X.S. Zhang, Thermal analysis of a double layer phase change material floor, *Applied Thermal Engineering* 31 (2011) 1576-1581.
- [105] G. B. Zhou, Y. P. Zhang, X. Wang, K. P. Lin, W. Xiao, An assessment of mixed type PCM-gypsum and shape-stabilized PCM plates in a building for passive solar heating, *Solar Energy* 81 (2007) 1351-1360.
- [106] M. Saffari, A. Gracia, C. Fernández, L.F. Cabeza, Simulation-based optimization of PCM melting temperature to improve the energy performance in buildings, *Applied Energy* 202 (2017) 420-434.
- [107] M. Alam, H. Jamil, J. Sanjayan, J. Wilson, Energy saving potential of phase change materials in major Australian cities, *Energy and Buildings* 78 (2014) 192-201.
- [108] Q. Y. Yan, W. Wang, An study on PCMs applied in the building envelope, *Materials review* 19 (2005) 102-105.
- [109] X. Q. Sun, Q. Zhang, M. A. Medina, K. O. Lee, Energy and economic analysis of a building enclosure outfitted with a phase change material board (PCMB), *Energy conversion and Management* 83 (2014) 73-78.
- [110] J. Liu, Y. Liu, L. Yang, T. Liu, C. Zhang, H. Dong, Climatic and seasonal suitability of phase change materials coupled with night ventilation for office buildings in Western China, *Renewable Energy* 147 (2020) 356-373.
- [111] M. A. Izquierdo-Barrientos, J. F. Belmonte, D. Rodríguez-Sánchez, A. E. Molina, J. A. Almendros-Ibáñez, A numerical study of external building walls containing phase change materials (PCM), *Applied Thermal Engineering* 47 (2012) 73-85.
- [112] N. Zhu, F.L. Liu, P.P. Liu, P.F. Hu, M.D. Wu, Energy saving potential of a novel phase change material wallboard in typical climate regions of China, *Energy and Buildings* 128 (2016) 360-369.
- [113] D. A. Neeper, Thermal dynamics of wallboard with latent heat storage, *Solar Energy* 68

- (2008) 393-403.
- [114] B. Eanest Jebasingh, A. Valan Arasu, A comprehensive review on latent heat and thermal conductivity of nanoparticle dispersed phase change material for low- temperature applications, *Energy Storage Materials* 24 (2020) 52-74.
- [115] F. Kuznik, J. B. A. Lopez, D. Baillis, K. Johannes, Phase change material wall optimization for heating using metamodeling, *Energy and Buildings* 106 (2005) 216-224.
- [116] X. Xu, Y. P. Zhang, K. P. Lin, H. F. Di, R. Yang, Modeling and simulation on the thermal performance of shape-stabilized phase change material floor used in passive solar buildings, *Energy and Buildings* 37 (2005) 1084-1091.
- [117] G. B. Zhou, Y. P. Zhang, K. P. Lin, W. Xiao, Thermal analysis of a direct-gain room with shape-stabilized PCM plates, *Renewable Energy* 33 (2008) 1228-1236.
- [118] Z. Liu, J. Hou, Y. Huang, J. Zhang, X. Meng, B. J. Dewancker, Influence of phase change material (PCM) parameters on the thermal performance of lightweight building walls with different thermal resistances, *Case Studies in Thermal Engineering* 31 (2022) 101844.
- [119] V. Sharma, A.C. Rai, Performance assessment of residential building envelopes enhanced with phase change materials, *Energy and Buildings* 208 (2020) 109664.
- [120] D. Zhou, G. S. F. Shire, Y. Tian, Parametric analysis of influencing factors in phase change material wallboard (PCMW), *Applied Energy* 119 (2014) 33-42.
- [121] Y. P. Zhang, K. P. Lin, Y. Jiang, G. B. Zhou, Thermal storage and nonlinear heat- transfer characteristics of PCM wallboard, *Energy and Buildings* 40 (2008) 1771-1779.
- [122] E. L. Meng, H. Yu, B. Zhou, Study of the thermal behavior of the composite phase change material (PCM) room in summer and winter, *Applied Thermal Engineering* 126 (2017) 212-225.
- [123] F. Kuznik, J. Virgone, J. Noel, Optimization of a phase change material wallboard for building use, *Applied Thermal Engineering* 28 (2008) 1291-1298.
- [124] E. L. Meng, H. Yu, G. Y. Zhan, Y. He, Experimental and numerical study of the thermal performance of a new type of phase change material room, *Energy conversion and management* 74 (2013) 386-394.
- [125] F. Ascione, N. Bianco, R.F. De Masi, F. de' Rossi, G.P. Vanoli, Energy refurbishment of existing buildings through the use of phase change materials: energy savings and indoor comfort in the cooling season, *Applied Energy* 113 (2014) 990-1007.
- [126] C. Chen, H. F. Guo, Y. N. Liu, H. L. Yue, C. D. Wang, A new kind of phase change material (PCM) for energy-storing wallboard, *Energy and Buildings* 40 (2008) 882-890.
- [127] W. Xiao, X. Wang, Y. P. Zhang, Thermal analysis of lightweight wall with shape-

- stabilized PCM panel for summer insulation, *J. Eng. Thermophys.* 30 (2009) 1561-1563.
- [128] T. Silva, R. Vicente, N. Soares, V. Ferreira, Experimental testing and numerical modelling of masonry wall solution with PCM incorporation: a passive construction solution, *Energy and Buildings* 49 (2012) 235-245.
- [129] Z.X. Li, A.A.A.A. Al-Rashed, M. Rostamzadeh, R. Kalbasi, A. Shahsavari, M. Afrand, Heat transfer reduction in buildings by embedding phase change material in multi-layer walls: effects of repositioning, thermophysical properties and thickness of PCM, *Energy Conversion and Management* 195 (2019) 43-56.
- [130] R. Cai, Z. Sun, H. Yu, E. Meng, J. Wang, M. Dai, Review on optimization of phase change parameters in phase change material building envelopes, *Journal of Building Engineering* 35 (2021) 101979.
- [131] A. Sari, Thermal energy storage characteristics of bentonite-based composite PCMs with enhanced thermal conductivity as novel thermal storage building materials, *Energy Conversion and Management* 117 (2016) 132-141.
- [132] B. X. Li, S. B. Nie, Y. G. Hao, T. X. Liu, J. B. Zhu, S. L. Yan, Stearic-acid/carbon-nanotube composites with tailored shape-stabilized phase transitions and light-heat conversion for thermal energy storage, *Energy Conversion and Management* 98 (2015) 314-321.
- [133] A. Sari, A. Karaipekli, Thermal conductivity and latent heat thermal energy storage characteristics of paraffin/expanded graphite composite as phase change material, *Applied Thermal Engineering* 27 (2007) 1271-1277.
- [134] J. Ding, Y. Zhang, X. Wang, K. Lin, R. Yang, Influence of additives on thermal conductivity of shape-stabilized phase change material, *International Solar Energy Conference* 47373 (2005) 823-832.
- [135] Y. P. Zhang, K. P. Lin, Q. L. Zhang, H. F. Di, Ideal thermophysical properties for free-cooling (or heating) buildings with constant thermal physical property material, *Energy and Buildings* 38 (2006) 1164-1170.
- [136] G. B. Zhou, Y. P. Yang, X. Wang, S. X. Zhou, Numerical analysis of effect of shape-stabilized phase change material plates in a building combined with night ventilation, *Applied Energy* 86 (2009) 52-59.
- [137] Y. Zhang, K. Du, J. He, L. Yang, Y. Li, S. Li, Impact factors analysis on the thermal performance of hollow block wall. *Energy and Buildings* 75 (2014) 330-341.
- [138] Y. Zhang, Impact of structural configuration on the thermal performance of PCM hollow block wall, *Science and Technology for the Built Environment* 24(9) (2018) 945-961.
- [139] Y. Zhang, Q. Wang, Impact of phase change material's thermal properties on the thermal

- performance of phase change material hollow block wall, *Heat Transfer Engineering* 40(19) (2019)1619–1632.
- [140] F. Kuznik, J. Virgone, Experimental assessment of a phase change material for wall building use, *Applied Energy* 86 (2009) 2038-2046.
- [141] X. Jin, M.A. Medina, X.S. Zhang, On the placement of a phase change material thermal shield within the cavity of buildings walls for heat transfer rate reduction, *Energy* 73 (2014) 780-786.
- [142] V. D Fachinotti, F. Bre, C. Mankel, E. A. B. Koenders, A. Caggiano, Optimization of Multilayered Walls for Building Envelopes Including PCM-Based Composites, *Materials* 13(12) (2020) 2787.
- [143] A. Gounni, M. E. I. Alami, The optimal allocation of the PCM within a composite wall for surface temperature and heat flux reduction: An experimental Approach, *Applied Thermal Engineering* 127 (2017) 1488-1494.
- [144] J. Lei, J. Yang, E. H. Yang, Energy performance of building envelopes integrated with phase change materials for cooling load reduction in tropical Singapore, *Applied Energy* 162 (2016) 207-217.
- [145] K.O. Lee, M.A. Medina, E. Raith, X.Q. Sun, Assessing the integration of a thin phase change material (PCM) layer in a residential building wall for heat transfer reduction and management, *Applied Energy* 137 (2015) 699-706.
- [146] X. Jin, M.A. Medina, X.S. Zhang, On the importance of the location of PCMs in building walls for enhanced thermal performance, *Applied Energy* 106 (2013) 72-78.
- [147] X. Jin, S. L. Zhang, X. D. Xu, X. S. Zhang, Effects of PCM state on its phase change performance and the thermal performance of building walls, *Building and Environment* 81 (2014) 334-339.
- [148] X. Jin, M. A. Medina, X. S. Zhang, Numerical analysis for the optimal location of a thin PCM layer in frame walls, *Applied Thermal Engineering* 103 (2016) 1057-1063.
- [149] A. Arnault, F. Mathieu-Potvin, L. Gosselin, Internal surfaces including phase change materials for passive optimal shift of solar heat gain, *International Journal of Thermal Sciences* 49(11) (2010) 2148-2156.
- [150] M. Li, A nano-graphite/paraffin phase change material with high thermal conductivity, *Applied Energy* 106 (2013) 25-30.
- [151] M. Arıcı, F. Bilgin, S. Niżetic', H. Karabay, PCM integrated to external building walls: An optimization study on maximum activation of latent heat, *Applied Thermal Engineering* 165 (2020) 114560.

**Chapter 2. Theoretical analysis of the causes of overheating in  
lightweight buildings and heat transfer processes in phase-change  
composite walls**

2.1	Introduction.....	2-1
2.2	Heat transfer analysis of lightweight building.....	2-1
2.2.1	Surface heat balance of lightweight envelope .....	2-1
2.2.2	Indoor air heat balance .....	2-6
2.2.3	Indoor thermal environment analysis of lightweight building.....	2-9
2.3	Heat transfer analysis of phase-change composite walls .....	2-10
2.3.1	Heat transfer characteristics of the building envelope (wall) .....	2-10
2.3.2	Thermal characteristics of phase-change composite walls .....	2-13
2.3.3	Theoretical analysis of heat transfer of phase-change composite wall .....	2-14
2.3.4	Boundary condition setting.....	2-17
2.3.5	Model validation.....	2-18
2.3.6	Evaluation indexes.....	2-20
2.4	Summary .....	2-20
	References.....	2-22
	Nomenclature.....	2-25



## **2.1 Introduction**

From the literature review in Chapter 1, it is found that the indoor thermal environment of lightweight buildings are usually bad, and their energy consumption is higher than that of traditional buildings to achieve a certain thermal comfort. Therefore, it is urgent to take effective measures to improve the indoor thermal environment of lightweight buildings and reduce their energy consumption. On the other hand, among the various measures introduced in the literature review to improve the indoor thermal environment of buildings, phase-change materials (PCM) have a better improvement effect on the indoor thermal environment of buildings, especially for lightweight buildings. As a result, the feasibility of this study to explore the effect of different PCM thermo-physical properties on improving the thermal performance of lightweight buildings is also proved. In view of the following evaluation of the influence law and application effect of the thermo-physical parameters of PCM on the thermal performance of lightweight building envelopes. This chapter will focus on the theoretical analysis of the causes of the indoor thermal environment of lightweight buildings and the influence of PCM on the indoor thermal environment of lightweight buildings, and carry out mathematical modelling, and then proposes the evaluation index to the influence of PCM on the thermal performance of lightweight buildings from the theoretical analysis.

## **2.2 Heat transfer analysis of lightweight building**

### **2.2.1 Surface heat balance of lightweight envelope**

The heat exchange on the surface of the lightweight building envelope is carried out in three ways: convection heat transfer, radiation heat transfer and heat conduction, as shown in Fig. 2-1. Among them, the radiation heat gain from the outer surface includes: solar radiation heat gain, atmospheric long-wave radiation heat gain, ground reflection radiation heat gain, and ground thermal radiation heat gain. Then, the outer surface of the envelope transfers heat to the inner surface by heat conduction. After that, the inner surface of the envelope then exchanges heat with the air inside the room by convection heat transfer. In the meantime, the air inside of the building envelope is also affected by long-wave radiation from the room surface, light sources, and solar radiation through the transparent envelope.

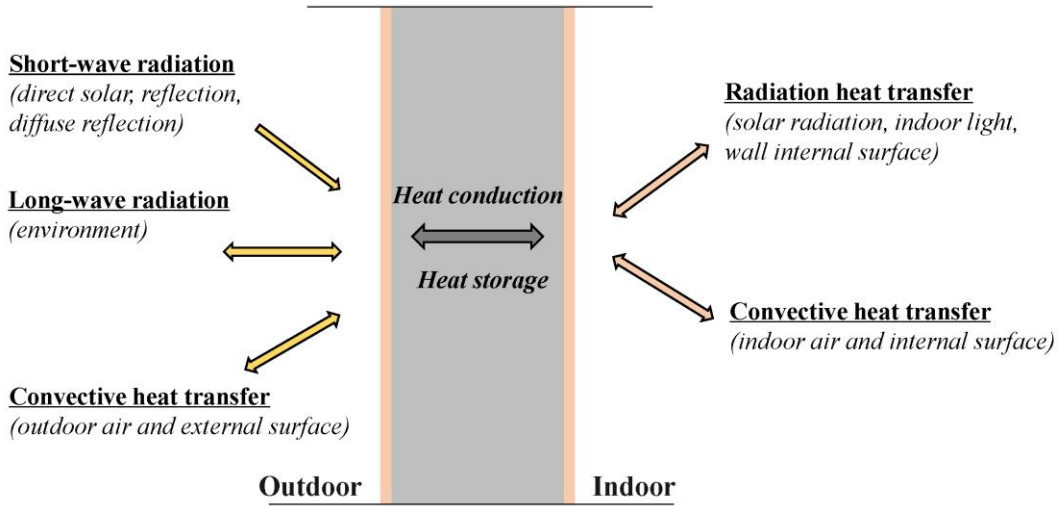


**Fig. 2-1. Heat exchange diagram of the walls.**

**(1) Lightweight building envelope outer surface heat balance**

The three parts of the heat exchange on the outer surface of the lightweight building envelope are radiation heat exchange, convection heat transfer and heat conduction. The radiation heat exchange includes solar radiation and long-wave radiation. In the case of no internal heat source, the heat exchange capacity on the outer surface of the building envelope within the  $\Delta\tau$  time interval is shown below:

$$Q(\Delta\tau) = (Q_{RO} + Q_{CO} + Q_{HCO}) \Delta\tau \quad (2-1)$$

Where  $Q_{RO}$  is the radiation heat transfer on the outer surface of the lightweight building envelope, W;  $Q_{CO}$  is the convective heat transfer of the outer surface of the lightweight building envelope, W;  $Q_{HCO}$  is the heat conduction from the outer surface to the inner surface of the building envelope, W.

In equation (2-1), the calculation formula of  $Q_{RO}$  is as follows:

$$Q_{RO} = Q_{SO} + Q_{AO} + Q_{GRO} + Q_{GHO} + Q_{BL} \quad (2-2)$$

Where  $Q_{SO}$  is the solar radiation heat gain from the outer surface of the light building envelope, W;  $Q_{AO}$  is the atmospheric long-wave radiation heat gain from the outer surface of the building envelope, W;  $Q_{GRO}$  is the ground reflected radiation heat gain from the outer surface of the building envelope, W;  $Q_{GHO}$  is the ground thermal radiation from the outer surface of the building envelope, W;  $Q_{BL}$  is the long-wave radiation heat from the outer surface of the lightweight building envelope and the surrounding buildings, W.

In equation (2-2), the calculation formula of  $Q_{SO}$  is as follows:

$$Q_{SO} = I_{D\theta} + I_{d\theta} \quad (2-3)$$

Where  $\theta$  is the inclination angle of the arbitrary surface;  $I_{D\theta}$  is the direct solar radiation received by the lightweight building envelope, W;  $I_{d\theta}$  is the sky scattered radiation received by the outer surface of the lightweight building envelope, W.

For a horizontal plane,  $\theta=0$ , its received direct solar radiation is:

$$I_{D\theta} = I_{DH} = I_{TN} \sin \gamma \quad (2-4)$$

For the vertical plane,  $\theta=90^\circ$ , its received direct solar radiation is:

$$I_{D\theta} = I_{DN} = I_{TN} \cos \gamma \cos \zeta \quad (2-5)$$

Based on the solar radiation, the sky scattered radiation can also be calculated as:

$$I_{d\theta} = I_{TH} - I_{DH} \quad (2-6)$$

Where  $I_{TH}$  and  $I_{TN}$  are horizontal, normal solar total radiation values, separately, W, which can be directly measured by the solar radiometer;  $\gamma$ ,  $\zeta$  are the solar altitude angle, and azimuth, respectively. The joint equations (2-3)-(2-6) can be obtained as follows.

The total solar radiation intensity in the horizontal plane is:

$$Q_{SO} = I_{DH} + I_{d\theta} = I_{TH} - I_{DH} + I_{TN} \sin \gamma \quad (2-7)$$

The total solar radiation intensity in the vertical plane is:

$$Q_{SO} = I_{DN} + I_{d\theta} = I_{TH} - I_{TN} \sin \gamma + I_{TN} \cos \gamma \cos \zeta \quad (2-8)$$

In addition, the calculation formula of  $Q_{AO}$  in equation (2-2) is as follows:

$$Q_{AO} = \alpha_{sd} I_{AO} \varphi_{AO} \quad (2-9)$$

Where  $\alpha_{sd}$  is the absorption rate of atmospheric long-wave radiation on the outer surface of lightweight building envelopes;  $I_{AO}$  is the atmospheric long-wave radiation received by the outer surface of the lightweight building envelope, W.

In equation (2-2), the calculation formula of  $Q_{GRO}$  is as follows:

$$Q_{GRO} = \alpha_{D\theta} I_{GR\theta} = \alpha_{D\theta} I_{G\theta} \left( 1 - \cos^2 \frac{\theta}{2} \right) \quad (2-10)$$

Where  $I_{GR\theta}$  is the ground reflected radiation received by the outer surface of the lightweight building envelope, W;  $I_{G\theta}$  is the solar radiation received by the ground, W.

In equation (2-2), the calculation formula of  $Q_{GHO}$  is as follows:

$$Q_{GHO} = C_b \varepsilon_o \left( \frac{T_G}{100} \right)^4 \varphi_G \quad (2-11)$$

Where  $C_b$  is the blackbody radiation constant;  $\varepsilon_o$  is the wall blackness;  $T_G$  is the ground temperature, K.

In equation (2-2), the calculation formula of  $Q_{BL}$  is as follows:

$$Q_{BL} = C_b \varepsilon_o \left[ (\phi_S + \phi_G \varepsilon_G) T_{wo}^4 - \phi_G \varepsilon_G T_G^4 - \phi_S T_S^4 \right] \quad (2-12)$$

Where  $\phi_S$ ,  $\phi_G$  are the angular coefficients of the outer surface of the lightweight building envelope facing the sky and the ground, respectively;  $\varepsilon_G$  is the ground blackness;  $T_S$  is the sky's effective temperature, K.

For the horizontal plane, the approximation values are taken as  $\phi_S = 1$ ,  $\phi_G = 0$ , then:

$$Q_{BL} = C_b \varepsilon_o \left[ T_{wo}^4 - T_S^4 \right] \quad (2-13)$$

For the vertical plane, the approximation value is taken as  $\phi_S + \phi_G = 0.5$ , then:

$$Q_{BL} = 0.5 C_b \varepsilon_o \left[ (1 + \varepsilon_G) T_{wo}^4 - \varepsilon_G q_{ARD} - \varepsilon_G T_G^4 \right] \quad (2-14)$$

Furthermore, according to the heat balance of the outer surface of the building envelope, the short-wave radiation, long-wave radiation, convective heat exchange and heat transfer to the inner surface by the outer surface of the lightweight envelope are in equilibrium, as shown in the following equation.

$$\begin{aligned} & (\alpha_{D\theta} I_{D\theta} + \alpha_{d\theta} I_{d\theta}) + \left[ \alpha_{sd} I_{AO} \varphi_{AO} + \alpha_{D\theta} I_{G\theta} \left( 1 - \cos^2 \frac{\theta}{2} \right) + C_b \varepsilon_o \left( \frac{T_G}{100} \right)^4 \varphi_G \right] \\ & + C_b \varepsilon_o \left[ (\phi_S + \phi_G \varepsilon_G) T_{wo}^4 - \phi_G \varepsilon_G T_G^4 - \phi_S T_S^4 \right] \\ & + h_{out} (T_{out} - T_{wo}) + \frac{T_{wo} - T_{wi}}{\sum \frac{\delta_i}{\lambda_i}} = 0 \end{aligned} \quad (2-15)$$

Where  $T_{out}$  is the outdoor air temperature, °C;  $T_{wi}$ ,  $T_{wo}$  are the inner and outer surface temperatures of the lightweight building envelope, respectively, °C;  $\delta_i$  is the thickness of the  $i^{\text{th}}$  layer material in the lightweight envelope, m;  $\lambda_i$  is the thermal conductivity of the  $i^{\text{th}}$  layer material, W/(m K).

## (2) Lightweight building envelope inner surface heat balance

The heat gain of the inner surface of the lightweight building envelope comes from four

sources, namely, the heat conduction from the outer surface to the inner surface, the short-wave radiation heat gain of the inner surface, the long-wave radiation heat gain, and the convection heat transfer between the inner surface and the indoor air. The equation is as follows:

$$Q_i(\Delta\tau) = (Q_{SI} + Q_{EI} + Q_{HCl} + Q_{CI})\Delta\tau \quad (2-16)$$

Where  $Q_{SI}$  is the short-wave radiation heat gain for the inner surface of the building envelope, W;  $Q_{EI}$  is the long-wave radiation heat gain from the inner surface of the building envelope, W;  $Q_{HCl}$  is the heat conduction from the outer surface to the inner surface of the building envelope, W;  $Q_{CI}$  is the convective heat transfer between the inner surface of the building envelope and the indoor air, W.

According to the literature, the heat gain from short-wave radiation received by the inner surface of the building envelope can be approximated as absorbed by the ground and the inner surface of the envelope, respectively, and the following equation can be obtained as follows:

$$Q_{SI} = 0.3 \frac{Q_{gt}}{\sum A_{wi}} + 0.7 \frac{Q_{gt}}{\sum A_{fi}} \quad (2-17)$$

Where  $Q_{gt}$  is the heat gain from solar radiation entering the room through the transparent envelope of the lightweight building, W;  $A_{wi}$ ,  $A_{fi}$  is the area of the interior walls and floors of the lightweight building, respectively, m<sup>2</sup>.

For a lightweight building in a steady state, the radiation heat gain through the transparent envelope into the room is shown in the following equation:

$$Q_{gt} = \sum C_g F_g (\alpha_{D\theta} I_{D\theta} + \alpha_{d\theta} I_{d\theta}) \left( \eta_g + \frac{h_{in}}{h_{out}} \rho_g \right) \quad (2-18)$$

Where  $C_g$  is the shading coefficient;  $F_g$  is the light-transmitting area of the transparent envelope, m<sup>2</sup>;  $\alpha_{d\theta}$  is the sky-scattered radiation absorption rate;  $I_{d\theta}$  is sky-scattered radiation, W/m<sup>2</sup>;  $\alpha_{D\theta}$  is the absorption rate of direct solar radiation;  $I_{D\theta}$  is the direct solar radiation, W/m<sup>2</sup>;  $\eta_g$  is the light-transmission coefficient of the transparent envelope;  $h_{in}$ ,  $h_{out}$  are the combined heat transfer coefficients of the inner and outer surfaces of the envelope, respectively, W/(m<sup>2</sup>·K);  $\rho_g$  is the absorption coefficient of the building envelopes.

Additionally, according to the heat balance of the inner surface of the lightweight building envelope, the radiation heat transfer and convection heat transfer of the inner surface, as well as the heat conduction to the inner surface by the outer surface of the building envelope are in

equilibrium. The heat balance equation of the inner surface is presented as follows.

$$h_{in}(T_{in} - T_{wi}) + \frac{T_{wo} - T_{wi}}{\sum \frac{\delta_i}{\lambda_i}} + 0.3 \frac{Q_{gt}}{\sum A_{wi}} + 0.7 \frac{Q_{gt}}{\sum A_{fi}} = 0 \quad (2-19)$$

Where,  $h_{in}$  is the combined heat transfer coefficients of the inner surfaces of the envelope,  $W/m^2 K$ ;  $T_{in}$  is the indoor air temperature of a lightweight building,  $^{\circ}C$ ;  $T_{wi}, T_{wo}$  are the inner and outer surface temperatures of the lightweight building envelope, respectively,  $^{\circ}C$ ;  $\delta_i$  is the thickness of the  $i^{th}$  layer material in the lightweight envelope, m;  $\lambda_i$  is the thermal conductivity of the  $i^{th}$  layer material,  $W/(m K)$ .

The expressions for the inner and outer surface temperature of the lightweight building envelope can be derived from the simultaneous equations (2-15) and (2-19) as equation (2-20):

$$T_{wi} = \frac{h_{in}T_{in} + 0.3 \frac{Q_{gt}}{\sum A_{wi}} + 0.7 \frac{Q_{gt}}{\sum A_{fi}} + \frac{T_{wo}}{\sum \frac{\delta_i}{\lambda_i}}}{h_{in} + \frac{1}{\sum \frac{\delta_i}{\lambda_i}}} \quad (2-20)$$

$$T_{wo} = \frac{h_{in}T_{in} + 0.3 \frac{Q_{gt}}{\sum A_{wi}} + 0.7 \frac{Q_{gt}}{\sum A_{fi}} + \alpha I + h_{out}T_{out}}{\left( h_{in} + \frac{1}{\sum \frac{\delta_i}{\lambda_i}} \right) h_{out}} \quad (2-21)$$

### 2.2.2 Indoor air heat balance

The heat exchange of building indoor air includes convection heat transfer, radiation heat transfer and air infiltration heat transfer, as depicted in Fig. 2-2. Among them, the radiation heat gain from the inner surface of the envelope includes: solar radiation heat gain through the transparent envelope and long-wave radiation heat gain from each wall surface. Moreover, another way of heat gain from the inner surface of the building envelope is through heat conduction to the inner surface, and then through convection heat transfer to exchange heat with the air in the room. At the same time, the indoor air is also directly exchanged with the outdoor air through infiltration.

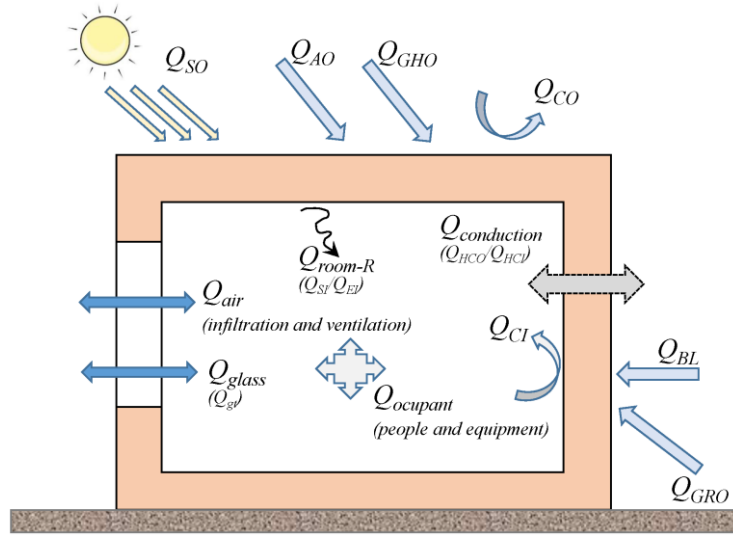


**Fig. 2-2. Building indoor air heat balance diagram.**

In order to comprehensively express the influence of the outdoor thermal environment on the indoor of the building, the comprehensive outdoor temperature ( $T_{sa}$ ) is introduced, which is the expression of the comprehensive effect of outdoor air and environmental radiation on the outer surface of the lightweight building envelope. On the basis of introducing the comprehensive outdoor temperature ( $T_{sa}$ ), the equation for the heat gain per unit area of the outer surface of the lightweight building envelope can be changed to:

$$Q_{RO} + Q_{CO} = h_{out} \left[ \left( \frac{\alpha_{D\theta} I_{D\theta} - Q_{lo}}{h_{out}} + T_{out} \right) - T_{wo} \right] = h_{out} (T_{sa} - T_{wo}) \quad (2-22)$$

Where  $h_{out}$  is the combined heat transfer coefficients of the outer surfaces of the building envelope,  $W/m^2 \cdot K$ ;  $[\text{W}/(\text{m}^2 \cdot \text{K})]$ ;  $\alpha_{D\theta}$  is the absorption rate of direct solar radiation;  $I_{D\theta}$  is the direct solar radiation,  $W/m^2$ ;  $Q_{lo}$  is the total long-wave radiation received by the outer surface of the building envelope,  $W/m^2$ ;  $T_{out}$  is the outdoor air temperature of the lightweight building,  $^{\circ}\text{C}$ ;  $T_{wo}$  is the outer surface temperature of the lightweight building envelope,  $^{\circ}\text{C}$ ;  $T_{sa}$  is the comprehensive outdoor air temperature of the lightweight building,  $^{\circ}\text{C}$ .

Besides, it should be stated that  $T_{sa}$  is the comprehensive result is based on the short-wave solar radiation, the total long-wave radiation received by the outer surface and the outdoor ambient temperature of the lightweight building. So, the  $T_{sa}$  can be obtained from equation (2-22) as follows:

$$T_{sa} = \frac{\alpha_{D\theta} I_{D\theta} - Q_{lo}}{h_{out}} + T_{out} \quad (2-23)$$

The heat gain of indoor air comes from the short-wave solar radiation through the

transparent envelope, air infiltration and heat conduction from the outer surface to the inner surface of the building envelope. Based on the expression of the comprehensive outdoor temperature in the heat balance of the envelope surface, the heat conduction of the envelope can be transformed into the expression of the comprehensive outdoor temperature, and then the comprehensive outdoor temperature can be linked with the indoor air heat balance to obtain the heat gain of indoor air in lightweight buildings under steady state, as in equation (2-24).

$$Q_t(\Delta\tau) = \sum C_g F_g (\alpha_{D\theta} I_{D\theta} + \alpha_{d\theta} I_{d\theta}) \left( \eta_g + \frac{h_{in}}{h_{out}} \rho_g \right) + \frac{n_a c_o \rho_o V_{room} (T_{out} - T_{in,\tau})}{3600} + \sum K_{to} F_{to} (T_{sa} - T_{in,\tau}) \quad (2-24)$$

Where  $n_a$  is the number of indoor air changes in lightweight buildings, 1/h;  $c_o$  is the specific heat capacity of the outdoor air of the lightweight building, kJ/kg K;  $\rho_o$  is the density of outdoor air in lightweight buildings, kg/m<sup>3</sup>;  $V_{room}$  is the room volume of a lightweight building, m<sup>3</sup>;  $T_{out}$  is the outdoor dry bulb temperature of the lightweight building, °C;  $T_{in,\tau}$  is the indoor air temperature of light building at time  $\tau$ , °C;  $K_{to}$  is the heat transfer coefficient of the lightweight building envelope, W/(m<sup>2</sup> K);  $F_{to}$  is the heat transfer area of the lightweight building envelope, m<sup>2</sup>.

In the time interval  $\Delta\tau=1h$ , the change of the indoor air temperature is  $T_{in,\tau} - T_{in,\tau-1}$ , then the heat gain of the indoor air in lightweight building at time  $\Delta\tau$  is as follows:

$$Q_t(\Delta\tau) = c_i \rho_i V_{room} (T_{in,\tau} - T_{in,\tau-1}) \quad (2-25)$$

Where  $c_i$  is the specific heat capacity of the indoor air of the lightweight building, kJ/kg K;  $\rho_i$  is the density of indoor air in lightweight buildings, kg/m<sup>3</sup>;  $T_{in,\tau-1}$  is the indoor air temperature of the lightweight building at the time  $\tau-1$ , °C.

Bringing (2-23) and (2-24) into (2-25) obtains the indoor air temperature of the lightweight building at the time  $\tau$ , as indicated by the following equation:

$$T_{in,\tau} = \frac{3600 \sum C_g F_g (\alpha_{D\theta} I_{D\theta} + \alpha_{d\theta} I_{d\theta}) \left( \eta_g + \frac{h_{in}}{h_{out}} \rho_g \right) + n_a c_o \rho_o V_{room} T_{out} + 3600 c_i \rho_i V_{room} T_{in,\tau-1}}{n_a c_o \rho_o V_{room} + 3600 c_i \rho_i V_{room} + 3600 \sum K_{to} F_{to}} \quad (2-26)$$

As a result, the inner and outer surfaces temperature of the lightweight building envelope can be obtained respectively, when the equation (2-26) is brought into the equations (2-20) and (2-21).

### 2.2.3 Indoor thermal environment analysis of lightweight building

The indoor air temperature of lightweight buildings (equation (2-26)) is further deformed to equation (2-27).

$$T_{in,\tau} = \frac{\sum C_g F_g (\alpha_{D\theta} I_{D\theta} + \alpha_{d\theta} I_{d\theta}) \left( \eta_g + \frac{h_{in}}{h_{out}} \rho_g \right)}{\frac{n_a c_o \rho_o V_{room}}{3600} + c_i \rho_i V_{room} + \sum K_{to} F_{to}} + \frac{\frac{n_a c_o \rho_o V_{room}}{3600}}{\frac{n_a c_o \rho_o V_{room}}{3600} + c_i \rho_i V_{room}} T_{out} + \frac{c_i \rho_i V_{room}}{\frac{n_a c_o \rho_o V_{room}}{3600} + c_i \rho_i V_{room} + \sum K_{to} F_{to}} T_{\tau-1} \quad (2-27)$$

Then, the difference between indoor and outdoor air temperature in lightweight buildings can be obtained as equation (2-28).

$$T_{in,\tau} - T_{out} = \frac{\sum C_g F_g (\alpha_{D\theta} I_{D\theta} + \alpha_{d\theta} I_{d\theta}) \left( \eta_g + \frac{h_{in}}{h_{out}} \rho_g \right)}{\frac{n_a c_o \rho_o V_{room}}{3600} + c_i \rho_i V_{room} + \sum K_{to} F_{to}} + \frac{c_i \rho_i V_{room}}{\frac{n_a c_o \rho_o V_{room}}{3600} + c_i \rho_i V_{room}} T_{in,\tau-1} - \frac{c_i \rho_i V_{room} + \sum K_{to} F_{to}}{\frac{n_a c_o \rho_o V_{room}}{3600} + c_i \rho_i V_{room} + \sum K_{to} F_{to}} T_{out} \quad (2-28)$$

Hence, the reason why the indoor air temperature appears much higher than the outdoor in lightweight buildings can be explained theoretically by equation (2-28). Namely, the difference between indoor and outdoor air temperature ( $T_{in,\tau} - T_{out}$ ) is directly related to the initial temperature ( $T_{\tau-1}$ ) of the lightweight building and is positively related to solar radiation, and is negatively correlated with outdoor air temperature and long-wave radiation. The following further discusses the theoretical basis for the phenomenon that the indoor air temperature is higher than the outdoor when the thermo-physical parameters of the building  $C_g$ ,  $F_g$ ,  $\alpha_{D\theta}$ ,  $\alpha_{d\theta}$ ,  $\eta_g$ ,  $h_{in}$ ,  $h_{out}$ ,  $c_o$ ,  $\rho_o$ ,  $V_{room}$ ,  $K_{to}$ ,  $F_{to}$  are the same.

When the sum of the initial indoor air temperature and the solar radiation entering the room through the transparent envelope is greater than the energy sum of the long-wave radiation entering the room and the outdoor air temperature in the same volume, that is:

$$\begin{aligned}
 & c_o \rho_o V_{room} T_{in, \tau} + 3600 \sum C_g F_g \left( \eta_g + \frac{h_{in}}{h_{out}} \rho_g \right) + 3600 \sum K_{to} F_{to} \frac{\alpha_{D\theta} I_{D\theta} + \alpha_{d\theta} I_{d\theta}}{h_{out}} \\
 & > 3600 \sum K_{to} F_{to} \frac{I}{h_{out}} Q_{BL} + n_a c_o \rho_o V_{room} T_{out}
 \end{aligned} \tag{2-29}$$

At this time,  $T_{in, \tau} - T_{out} > 0$ , namely, the indoor air temperature of the light building is higher than the outdoor air temperature at time  $\tau$ . When solar radiation is strong during the daytime, lightweight buildings are prone to the phenomenon that the indoor air temperature is much higher than the outdoor air temperature. Typically, the indoor-outdoor temperature difference ( $\Delta T$ ) in lightweight buildings is very large under strong solar radiation in summer, resulting in a poor indoor thermal environment in lightweight buildings.

## 2.3 Heat transfer analysis of phase-change composite walls

### 2.3.1 Heat transfer characteristics of the building envelope (wall)

Since the focus of this study is on the heat transfer characteristics of phase-change composite walls, only theoretical analysis of heat transfer characteristics of the non-transparent envelope (wall) is conducted in this part.

The change law of indoor and outdoor temperature affects the thermal insulation design of buildings. As the indoor and outdoor temperatures change, heat is constantly transferred in and out through the envelope. When the outdoor temperature is lower than the indoor temperature in winter, the heat will be absorbed by the wall surface and transferred from the building envelope to the outdoor and then released through the outer surface. In comparison, when the outdoor temperature is higher than the indoor temperature in summer, the heat transfer is the opposite of that in winter. The following selection of winter outdoor temperature is lower than the indoor temperature analysis. Strictly considered, each heat transfer process is from surface heat absorption to structural heat transfer and then to surface heat release (see Fig. 2-3 (a)), which is generally referred to as "surface heat transfer" [1]. In the process of surface heat transfer, there is both convection and heat conduction between the surface and the surrounding air, and radiation heat transfer between the surface and other surrounding surfaces. In addition, in the heat transfer process of the building wall, except for a few special structures, most of the buildings are flat-walled heat transfer. The heat transfer of a flat-wall is generally a three-dimensional heat transfer process, but because the width and height of the wall is much greater than the thickness of the wall, its heat transfer always occurs between the inner and outer surfaces, so the process of heat transfer through the flat wall can be considered as a one-dimensional heat transfer along the thickness direction.

Additionally, in the heat transfer process of the wall, due to the existence of some pores in the pores more or less in the interior of the general building materials, there is radiation and convection heat transfer in addition to heat conduction. However, due to the small proportion of convection and radiation heat transfer, only heat conduction through the wall is considered in the thermal calculation process.

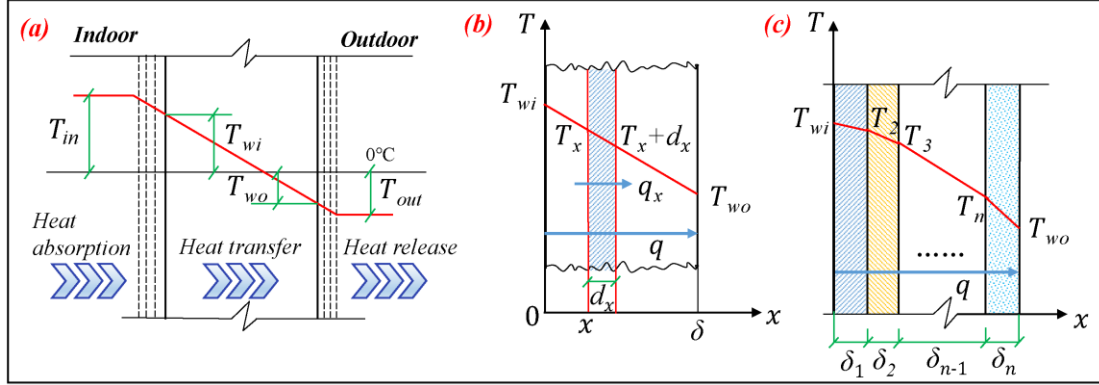


**Fig. 2-3. (a) Heat transfer process of the building envelope; (b) one-dimensional heat conduction model of the flat-wall; (c) multi-layer flat-wall heat conduction.**

The exterior envelope wall is generally composed of multiple layers of different materials, which can be regarded as a flat-wall heat conduction model consisting of multiple layers of materials in the calculation. To simplify the analysis process this paper takes a single-layer homogeneous flat wall as an example, and the heat transfer model is given in Fig. 2-3(b). Assuming that there is only heat transfer in the wall thickness ( $x$  direction), i.e., one-dimensional heat transfer. It is considered that only heat conduction is transferred in the flat wall, and the inner surface and outer surface temperatures of the wall are  $T_{wi}$  and  $T_{wo}$ , respectively, and  $T_{wi} > T_{wo}$ , then the heat flux intensity  $q_x$  ( $\text{W}/\text{m}^2$ ) through the unit cross-sectional area in the unit time is:

$$q_x = -\lambda \frac{\partial T_x}{\partial x} \quad (2-30)$$

The temperature gradient at each point is:

$$\frac{dT}{dx} = -\frac{T_{wi} - T_{wo}}{\delta} \quad (2-31)$$

Substituting equation (2-31) into (2-30), the heat flux intensity ( $q$ ) for a single homogeneous flat-wall at one-dimensional steady heat transfer is obtained:

$$q = -\frac{\lambda}{\delta} (T_{wi} - T_{wo}) = -\frac{T_{wi} - T_{wo}}{\frac{\delta}{\lambda}} \quad (2-32)$$

Equation (2-32) shows that the heat flux intensity through a flat-wall section during steady heat transfer is proportional to the thermal conductivity ( $\lambda$ ,  $\text{W}/(\text{m K})$ ) of the material and the

temperature difference between the inner and outer surfaces, and inversely proportional to the thickness of the material ( $\delta$ , m). Also,  $\delta/\lambda$  is defined as the resistance of heat transfer from the inner surface to the outer surface of the flat-wall, is also known as material thermal resistance  $R$ , ( $\text{m}^2 \text{ K})/\text{W}$ .

The heat conduction and thermal resistance of the flat-wall composed of multiple-layers material can be regarded as consisting of multiple single-layer flat-walls (as shown in Fig. 2-3(c)), and the heat flux intensity of each layer ( $q_1, q_2, \dots, q_n$ ) is calculated separately using equation (2-30). According to the steady-state heat transfer characteristics, the heat flux intensity of the flat wall is:  $q = q_\lambda = q_1 = q_2 = \dots = q_n$ , so as to obtain:

$$q_\lambda = \frac{T_{wi} - T_{wo}}{\frac{\delta_1}{\lambda_1} + \frac{\delta_2}{\lambda_2} + \dots + \frac{\delta_n}{\lambda_n}} = \frac{T_{wi} - T_{wo}}{R_1 + R_2 + \dots + R_n} \quad (2-33)$$

The total thermal resistance of multi-layer flat wall heat conduction is:

$$R = R_1 + R_2 + \dots + R_n \quad (2-34)$$

Considering that in the process of stable heat transfer of flat-wall, the inner surface gets heat under the combined action of convection heat transfer and radiation heat transfer, and the outer surface dissipates heat by convection and radiation, it is concluded that:

$$q = q_\lambda = q_{wi} = q_{wo} = \frac{T_{wi} - T_{wo}}{\frac{1}{h_{in}} + \sum \frac{\delta_i}{\lambda_i} + \frac{1}{h_{out}}} = \frac{T_{wi} - T_{wo}}{R_{in} + R + R_{out}} = K_0 (T_{wi} - T_{wo}) \quad (2-35)$$

$$K_0 = \frac{1}{R_0} = \frac{1}{\frac{1}{h_{in}} + \sum \frac{\delta_i}{\lambda_i} + \frac{1}{h_{out}}} = \frac{1}{R_{in} + R + R_{out}} \quad (2-36)$$

Where  $K_0$  is the heat transfer coefficient of the building envelope,  $\text{W}/(\text{m}^2 \text{ K})$ ;  $R_0$  is the heat transfer thermal resistance of the envelope,  $(\text{m}^2 \text{ K}) / \text{W}$ ;  $h_{in}$  and  $h_{out}$  are the heat transfer coefficient of the inner and outer surface of the walls,  $\text{W}/(\text{m}^2 \text{ K})$ ;  $T_{wi}$  and  $T_{wo}$  are the inner and outer surface temperatures of the walls,  $^\circ\text{C}$ ;  $\delta_i$  is the thickness of each material layer, m;  $\lambda_i$  is the thermal conductivity of each material layer,  $\text{W}/(\text{m K})$ .

The above result is analyzed only in winter when the outdoor temperature is lower than the indoor temperature. However, the heat transfer process is similar in summer and winter, it is not repeated here.

### 2.3.2 Thermal characteristics of phase-change composite walls

The main thermal parameters involved in the analysis of the thermal characteristics of the phase-change composite wall include thermal resistance, heat storage coefficient and thermal inertia, which can be obtained by calculation based on the thermo-physical parameters (density, specific heat, thermal conductivity) of each layer of the phase-change composite wall. The thermal resistance reflects the ability of the wall to prevent the heat flux from crossing, which is the most important index to evaluate the thermal insulation performance of the phase change composite wall. The calculation equations are shown in (2-33) and (2-34). The heat storage coefficient reflects the capacity of the wall to store heat. When the outdoor environment of the wall is in a non-steady state of cycle fluctuation, the wall material with a larger heat storage coefficient can effectively weaken the inner surface temperature fluctuation of the wall and reduce the heat exchange with the indoor air. Thermal inertia reflects the ability of a material to resist temperature changes, which is directly related to thermal resistance and heat storage coefficient. The heat storage coefficient and thermal inertia are calculated as demonstrated in equations (2-37) and (2-38).

$$S = \sqrt{\frac{2\pi\lambda c \rho}{3.6T}} \quad (2-37)$$

$$D = R \cdot S \quad (2-38)$$

Where  $S$  denotes the heat storage coefficient of the wall,  $W/(m^2 K)$ ;  $\lambda$  indicates the thermal conductivity of the material,  $W/(m K)$ ;  $c$  represents the specific heat capacity of the material,  $kJ/(kg K)$ ;  $\rho$  is the density of the material,  $kg/m^3$ ;  $T$  is the temperature wave period (h), generally taken as 24h; " $\pi$ " is the circumference rate, taken as 3.14;  $D$  is a thermal inertness of the wall (dimensionless);  $R$  is the thermal resistance of the wall,  $(m^2 K) / W$ .

For lightweight buildings, the indoor temperature is much higher than the outdoor temperature in summer, which is directly related to the thermal resistance and thermal inertia index of lightweight walls being too small. When the lightweight wall is integrated with PCM, the heat storage coefficient, thermal resistance and thermal inertia of the wall increase. As a result, in the summer daytime, the temperature rise of the inner surface of the phase-change composite wall decreases, then reducing the convective heat transfer between the inner surface of the wall and the indoor air and improving the indoor thermal environment of the lightweight building. In contrast, at night in summer, the inner surface temperature of the phase-change composite wall decreases without the influence of solar radiation. However, due to the large heat storage coefficient of the phase-change composite wall, when the inner surface temperature is reduced by 1 °C, the heat released into the lightweight building interior increases, which

leads to the negative effect of heating the interior of the lightweight building at night in summer after the composite PCM.

### 2.3.3 Theoretical analysis of heat transfer of phase-change composite wall

#### (1) Mathematical description

On the premise of ensuring the accuracy and reliability of simulation results, to simplify the complex heat transfer process between each layer, the following assumptions are proposed in this paper when building the analytical model, viz.:

- The heat is assumed to be transferred only in the thickness and height direction due to the heat transfer always occurs between the inner and outer surfaces, namely, two-dimensional heat transfer.
- The volume change during the melting process of PCM and the undercooling effect during the solidification process of PCM are ignored.
- Specific heat capacity and density of PCM do not change with temperature.
- The physical properties of other solid materials are constant.
- PCM in the phase-change layer is homogeneous and isotropic.
- The thermal contact resistance between layers is negligible.
- Liquid of PCM is Newton incompressible fluid and obeys Fourier heat conduction.

The heat transfer equilibrium equations of PCM and other solid materials are established by defining  $x$  and  $y$  as the thickness and height direction of the wall. The detailed mathematical expression of the two-dimensional governing equations of the melting behavior of the PCM is written as following [2-4]:

$$\frac{\partial u}{\partial x} + \frac{\partial v}{\partial y} = 0 \quad (2-39)$$

$$\frac{\partial u}{\partial t} + u \frac{\partial u}{\partial x} + v \frac{\partial u}{\partial y} = -\frac{1}{\rho} \frac{\partial P}{\partial x} + \frac{\mu}{\rho} \left( \frac{\partial^2 u}{\partial x^2} + \frac{\partial^2 u}{\partial y^2} \right) + S_u \quad (2-40)$$

$$\frac{\partial v}{\partial t} + u \frac{\partial v}{\partial x} + v \frac{\partial v}{\partial y} = -\frac{1}{\rho} \frac{\partial P}{\partial y} + \frac{\mu}{\rho} \left( \frac{\partial^2 v}{\partial x^2} + \frac{\partial^2 v}{\partial y^2} \right) + \omega g (T - T_{ref}) + S_v \quad (2-41)$$

$$S_u = \frac{1}{\rho} \frac{(1 - \beta)^2}{(\beta^3 + \zeta)} A_{mush} u \quad (2-42)$$

$$S_v = \frac{1}{\rho} \frac{(1 - \beta)^2}{(\beta^3 + \zeta)} A_{mush} v \quad (2-43)$$

Where  $u$  and  $v$  are velocity components in the  $x, y$  directions, m/s;  $t$  is the time, s;  $P$  is air pressure, Pa/s;  $\mu$  is the dynamic viscosity, (N s)/m<sup>2</sup>;  $\rho$  denotes the material density, kg/m<sup>3</sup>;  $T$  is the temperature, °C;  $T_{ref}$  is the reference temperature, °C;  $g, \omega$  are the gravitational acceleration, and the coefficient of thermal expansion, m/s<sup>2</sup> and 1/K respectively;  $\beta$  and  $A_{mush}$  are the PCM liquid fraction and the mushy constant, respectively. Among them, the  $A_{mush}$  is taken to be  $10^6$  in this study and the  $\zeta$  is taken to be  $10^{-3}$  to avoid division by zero as recommended by [2,5].

### (2) Three types of boundary conditions of heat transfer process

The initial conditions and three types of boundary conditions for the heat storage and release process of PCM are shown below. Among them, the first type of boundary conditions is the temperature field of the given phase-change interface; the second type of boundary is the heat flux density of the given phase-change interface; the third type of boundary is the heat transfer coefficient of the given phase-change interface.

Initial condition: given the initial value of the variable to be solved  $-T(x, y, t)|_{t=0} = T_i$

- Type I boundary: the temperature value on the given boundary  $T_i = T_0$
- Type II boundary: gradient value of temperature on a given boundary  $-k \frac{\partial T}{\partial n} = q_0$
- Type III boundary: given the function relationship between the boundary temperature gradient and the boundary temperature  $-k \frac{\partial T}{\partial n} = k(T_i - T_0)$

For the boundary conditions of the phase-change composite wall, the indoor temperature also changes periodically because the outdoor solar radiation and air temperature of the lightweight building show an unsteady periodic change. Therefore, in the unsteady heat transfer process of the phase-change composite wall, the outer surface of the building envelope and the outdoor air interface, and the inner surface and the indoor air interface are the first boundary conditions, that is, the given interface temperature. Meanwhile, the periodic fluctuations of the ambient air temperature at the interface can be simplified.

### (3) Heat transfer model

The exact analytical solutions of heat transfer problems are mainly focusing on one-dimensional infinite and semi-infinite regions with simple boundary and initial conditions and constant physical properties (or ordinary walls [6-9]). It is difficult to obtain analytical solutions for one-dimensional finite regions and multidimensional cases due to their inherent non-linear nature at moving interfaces [10]. While the multidimensional phase-transition problem under

complex conditions, the numerical solution is almost the only feasible method. Literature [11-13] considered the problem with convection to find the approximate solution of the Stefan problem in one or two-dimensional geometries using several numerical methods, that is, the movement of the fluid particles and their influence on the change of location of the interface. Currently, the numerical solution method mainly includes the interface tracking method [14] and the fixed-grid method [15]. Among them, the interface tracking method also includes the level set method [16], moving mesh method [17], volume of fluid method [18] and immersed boundary method [19]. But special interpolation and coordinate transformation are required in the above solution, and the methods are extremely complex. In contrast, the fixed-grid method does not require tracking the location of the solid-liquid two-phase interface and is solved as a whole, to the moving boundary problems with moving PCM is much easier and also produces desired accuracy. It mainly includes the effective heat capacity method [20,21] and the enthalpy method [22]. While the enthalpy method is one of the most popular methods to solve the solid-liquid phase-change problems, it can effectively deal with phase-change problems occurring in both cases at a fixed temperature and in a range of temperature [22,23]. Up to now, the enthalpy method has been widely applied for phase-change problems [24,25].

In this study, the PCM in lightweight building is considered as a whole due to the fact that it is no need to consider the variation interface of the solid-liquid phase. Therefore, to simplify the solution of PCM heat transfer and not explicitly track the solid-liquid interface, the enthalpy model [26-29] is used in this paper.

According to energy conservation laws, considering the difference in heat transfer between PCM and other materials, the energy conservation equations of OSB, Glass wool, and gypsum board are described as follows [30]:

$$\frac{\partial T_i}{\partial t} = \frac{\lambda_i}{\rho c_{p,i}} \left( \frac{\partial^2 T_i}{\partial x^2} + \frac{\partial^2 T_i}{\partial y^2} \right) \quad (2-44)$$

In addition, The effectiveness of the enthalpy method for solving phase-change problems (solid-liquid) in both a fixed or range of temperatures has been widely proved [22-24,26]. Its main idea is to establish a unified energy equation in the whole region (solid phase, liquid phase, and two-phase interface) by taking enthalpy and temperature together as the solved function, calculating the enthalpy distribution by numerical method, and then determining the two-phase interface [31]. The energy equation for the liquid and solid PCM are described by the following equation [2]:

$$\frac{\partial H_p}{\partial t} + u \frac{\partial H_p}{\partial x} + v \frac{\partial H_p}{\partial y} = \frac{\lambda_{p,l}}{\rho c_p} \left( \frac{\partial^2 H_p}{\partial x^2} + \frac{\partial^2 H_p}{\partial y^2} \right) \quad (2-45)$$

$$\frac{\partial H_p}{\partial t} = \frac{\lambda_{p,s}}{\rho c_p} \left( \frac{\partial^2 H_p}{\partial x^2} + \frac{\partial^2 H_p}{\partial y^2} \right) \quad (2-46)$$

The enthalpy value ( $H_p$ ) of the wall phase-change layer can be expressed as:

$$H_p = h_{ref} + \int_{T_0}^T c_p dT + \beta L_p \quad (2-47)$$

The liquid fraction ( $\beta$ ) is introduced as follow [26,28,32]:

$$\beta = \begin{cases} 0 & (T < T_s) \\ \frac{T - T_s}{T_l - T_s} & (T_s \leq T \leq T_l) \\ 1 & (T_l < T) \end{cases} \quad (2-48)$$

The thermal conductivity of PCM is assumed to change linearly with temperature in the phase changing state [26,32], so that the thermal conductivity of PCM is described as:

$$\lambda_p = \lambda_{p,s} + \beta (\lambda_{p,l} - \lambda_{p,s}) \quad (2-49)$$

For the interface between two layers of materials, its heat is kept conservative, as given by follow equation:

$$-\lambda_i \frac{\partial T_i}{\partial x} = -\lambda_j \frac{\partial T_j}{\partial x} \quad (2-50)$$

Where  $\lambda_{p,s}$  and  $\lambda_{p,l}$  are the solid and liquid thermal conductivity of PCM, respectively, [W/(m K)];  $c_p$  is the material specific heat, J/(kg·K);  $h_{ref}$  is the reference enthalpy at reference temperature  $T_{ref}$ ;  $L_p$  is the latent heat of PCM (kJ/kg);  $T_s$  and  $T_l$  are the PCM solidus and liquid temperature (°C).

### 2.3.4 Boundary condition setting

Considering the above factors, the composite wall of the building envelope realizes indoor-outdoor heat exchange through the inner and outer surfaces.

In the process of heat transfer along the wall thickness direction, a two-dimensional coordinate system is established at the coordinate origin in the thickness direction  $x$  (as shown in Fig. 2-2(b)), where the inner surface of the wall is set to  $x=0$  and the outer surface is set to  $x=\delta$ , and the bottom and top surfaces are set to  $y=0$  and  $y=h$ . As a result, on boundary conditions, the adiabatic boundaries were applied to the bottom and top surfaces ( $y=0$  and  $y=h$ ), while the convective heat transfer boundaries were adopted on inner and outer surfaces ( $x=0$  and  $x=\delta$ ) can be expressed by equations (2-51) and (2-52):

$$-\lambda \frac{\partial T}{\partial y} \Big|_{y=0} = 0, \quad y=0 \quad -\lambda \frac{\partial T}{\partial y} \Big|_{y=h} = 0, \quad y=h \quad (2-51)$$

$$\begin{aligned} -\lambda \frac{\partial T}{\partial x} \Big|_{x=0} &= h_{in} (T_{wi} - T_{in}) & x=0 \\ -\lambda \frac{\partial T}{\partial x} \Big|_{x=\delta} &= h_{out} (T_{out} - T_{wo}) + \alpha I & x=\delta \end{aligned} \quad (2-52)$$

Where  $T_{out}$  and  $T_{wo}$  are the temperature of outdoor air and outer surface, respectively, °C;  $T_{in}$  and  $T_{wi}$  are the temperature of indoor air and inner surface, respectively, °C;  $I$  is the solar radiation intensity, W/m<sup>2</sup>;  $\alpha$  is the solar radiation absorptivity of outer surface;  $h_{in}$  and  $h_{out}$  are the convective heat transfer coefficients of inner and outer surfaces, W/(m<sup>2</sup>·K).

### 2.3.5 Model validation

In this study, the series of above equations in sections are iteratively solved by the full implicit difference scheme, and the computational region is divided into uniform grids along the thickness direction of the wall. In addition, the second-order central difference is used to discrete the equation. The computational convergence is declared when the following criterion is satisfied:

$$\frac{\sum_i |T_i^{m+1} - T_i^m|}{\sum_i |T_i^{m+1}|} \leq 10^{-6} \quad (2-53)$$

The experimental results obtained by Kuznik, F and Virgone, J [33] on the dynamic thermal response of PCM integrated with the multi-layer lightweight wall are utilized to validate to ensure the accuracy and reliability of the numerical model. The experimental walls include 2mm aluminum, 60mm polyurethane foam, and 5mm PCM-2 from outside to inside. The thermophysical parameters are given in Table 2-1.

**Table 2-1 Thermo-physical parameters of wall materials [32,33].**

Material	$t_m$ (°C)	$L_p$ (kJ/kg)	$d$ (m)	$\lambda$ [W/(m K)], Solid (Liquid)	$c_p$ [J/(kg K)]	$\rho$ (kg/m <sup>3</sup> )
PCM-2	17.8- 22.3	72.4	0.005	0.18(0.22)	2400	900
Aluminum	-	-	0.002	230	8800	2700
Polyurethane foam	-	-	0.06	0.04	1210	35

During the experiment, the test wall was placed in a chamber with a sinusoidal temperature

variation of 15-30 °C. The test point was set at the center of the inner surface of the wall (sensor error is  $\pm 0.25$  °C), and the data were collected every 2 min by multiplexer-multimeter data acquisition. Fig. 2-4(a) shows the variation in air temperature with time. Fig. 2-4(b) compares the present numerical value with the experimental [33] and the numerical result from Zhang et al. [32], two metrics: root mean square error (RMSE) and coefficient of variation ( $CV_{(RMSE)}$ ) were employed [34,35] to ensure the validation accuracy. RMSE measures the average spread of errors which provides a measure for the model's dispersion [34,36],  $CV_{(RMSE)}$  is the coefficient of variation in RMSE, as expressed by equations (2-54) - (2-55), respectively, as follows:

$$RMSE = \sqrt{\frac{1}{n} \sum_{i=1}^n (M_i - S_i)^2} \quad (2-54)$$

$$CV_{(RMSE)} = \frac{RMSE}{M_i} \times 100\% \quad (2-55)$$

It is found by calculation that the RMSE and  $CV_{(RMSE)}$  of the present numerical results are 0.98°C and 4.32%, respectively, compared to experimental results[33], while the RMSE and  $CV_{(RMSE)}$  are only 0.28°C and 1.25% compared to the values of Zhang et al. [32]. These results meet the ASHRAE criterion of  $CV_{(RMSE)}$  less than 30% [37] and indicate that the numerical models can be used to solve the heat transfer problem of lightweight walls integrated with PCM in this paper.

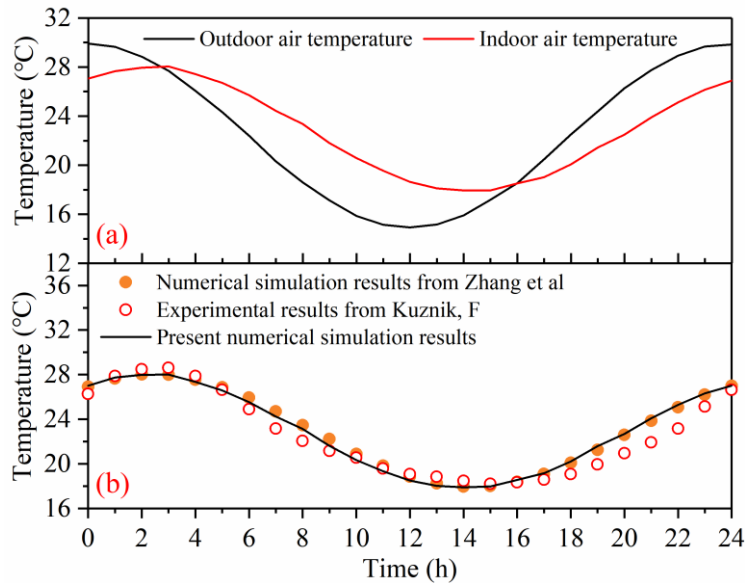


**Fig. 2-4. Comparison of the present numerical results with the experimental values [33] and other numerical values [32].**

### 2.3.6 Evaluation indexes

For the thermal performance of walls, the delay time ( $\varphi$ ) and attenuation rate ( $f$ ) of the inner surface temperature are two important factors affecting indoor comfort, and the peak heat flux ( $q_{peak}$ ) and average heat flux ( $q_{ave}$ ) of the inner surface are essential elements affecting the energy-saving [28,38]. Therefore, the above evaluation indexes are utilized to analyze the effect of different kinds/configurations of PCM on the thermal performance improvement of walls under different thermal boundaries in this study, as described in equations (2-56) - (2-59) [1,27,28,39]:

$$\varphi = t_{T_{wi,max}} - t_{T_{out,max}} \quad (2-56)$$

$$f = \frac{T_{wi,max} - T_{wi,min}}{T_{out,max} - T_{out,min}} \times 100\% \quad (2-57)$$

$$q_{peak} = q(t)_{max} \quad (2-58)$$

$$q_{ave} = \frac{\int_0^t q(t) dt}{t} \quad (2-59)$$

Where  $t_{T_{wi,max}}$  and  $t_{T_{out,max}}$  are the time appeared of maximum inner surface temperature and outdoor comprehensive temperature (solar-air), respectively, h;  $T_{wi,max}$  and  $T_{wi,min}$  are respectively the maximum and minimum values of inner surface temperatures, °C;  $T_{out,max}$  and  $T_{out,min}$  are respectively the maximum and minimum values of outer temperatures (solar-air), °C;  $q_{peak}$  and  $q_{ave}$  are the inner surface peak and average heat flux, W/m<sup>2</sup>, separately, where they are negative in summer (heat gain) and positive in winter (heat loss).

## 2.4 Summary

In this chapter, mathematical modelling and theoretical analysis of the causes of the indoor thermal environment of lightweight buildings and the heat transfer process to phase-change composite walls are carried out, and then evaluation indexes for the effect of PCM on the thermal performance of lightweight wall are proposed. The main conclusions are as follows.

(1) The difference between indoor and outdoor air temperature ( $T_{in,\tau} - T_{out}$ ) is directly related to the initial temperature ( $T_{\tau-1}$ ) of the lightweight building and is positively related to solar radiation, and is negatively correlated with outdoor air temperature and long-wave radiation.

(2) When the  $T_{in,\tau} - T_{out} > 0$ , lightweight buildings are prone to indoor temperatures much

higher than outdoor in summer, which is directly related to the thermal resistance and thermal inertia index of lightweight walls being too small. When solar radiation is strong during the daytime in summer, the indoor-outdoor temperature difference ( $\Delta T$ ) in lightweight buildings is very large, which leads to a poor indoor thermal environment in lightweight buildings.

(3) When the lightweight wall is integrated with PCM, the heat storage coefficient, thermal resistance and thermal inertia of the wall increase. As a result, in the summer daytime, the temperature rise of the inner surface of the phase-change composite wall decreases, then improving the indoor thermal environment of the lightweight building. In contrast, at night in summer, more heat is released into the room due to the large heat storage of phase-change composite walls, which leads to a negative impact on the room, but the opposite is in winter.

(4) The enthalpy method model is determined to be used to solve the heat storage and release process of the phase-change composite wall, and it is validated.

(5) The delay time ( $\varphi$ ) and attenuation rate ( $f$ ) of the inner surface temperature, and the peak heat flux ( $q_{peak}$ ) and average heat flux ( $q_{ave}$ ) of the inner surface are proposed to evaluate the thermal performance improvement of lightweight walls integrated with different PCM thermo-physical parameters.

## References

- [1] J.P. Liu, *Building Physics*, fourth ed., China Architecture & Building Press, 2009.
- [2] N. Elawady, M. Bekheit, A. A. Sultan, A. Radwan, Energy assessment of a roof-integrated phase change materials, long-term numerical analysis with experimental validation, *Applied Thermal Engineering* 202 (2022) 117773.
- [3] D. Pal, Y. K. Joshi, Melting in a side heated tall enclosure by a uniformly dissipating heat source, *International Journal of Heat and Mass Transfer* 44(2) (2001) 375-387.
- [4] M. Fadl, P. Eames, A numerical investigation into the heat transfer and melting process of lauric acid in a rectangular enclosure with three values of wall heat flux, *Energy Procedia* 158 (2019) 4502-4509.
- [5] M. Emam, S. Ookawara. Performance study and analysis of an inclined concentrated photovoltaic-phase change material system, *Solar Energy* 150 (2017) 229-245.
- [6] G. Koutsakis, G. F. Nellis, J. B. Gandhi, Surface temperature of a multi-layer thermal barrier coated wall subject to an unsteady heat flux, *International Journal of Heat and Mass Transfer* 155 (2020) 119645.
- [7] L. Mazarella, R. Scoccia, P. Colombo, M. Motta, Improvement to EN ISO 52016-1: 2017 hourly heat transfer through a wall assessment: the Italian National Annex, *Energy and Buildings* 210 (2020) 109758.
- [8] J. Duan, N. Li, J. Peng, C. Wang, Q. Liu, Full-response model of transient heat transfer of building walls using thermoelectric analogy method, *Journal of Building Engineering* 46 (2021) 103717.
- [9] W. Bi, Z. Yan, Z. Zhang, S. Yao, J. Zhang, X. Wang, Modeling and numerical simulation of heat and mass transfer in the cave wall of the Mogao Grottoes in China, *Building and Environment* 201 (2021) 108003.
- [10] S. Nandi, Y. Sanyasiraju, A second order accurate fixed-grid method for multi-dimensional Stefan problem with moving phase change materials, *Applied Mathematics and Computation* 416 (2022) 126719.
- [11] M. Turkyilmazoglu, Stefan problems for moving phase change materials and multiple solutions, *International Journal of Thermal Sciences* 126 (2018) 67-73.
- [12] A. K. Singh, A. Kumar, A Stefan problem with variable thermal coefficients and moving phase change material, *Journal of King Saud University-Science* 31(4) (2019) 1064-1069.
- [13] A. K. Singh, A. Kumar, Exact and approximate solutions of a phase change problem with moving phase change material and variable thermal coefficients, *Journal of King Saud University-Science* 31(4) (2019) 1318-1325.
- [14] M. Cutforth, P. T. Barton, N. Nikiforakis, An efficient moment-of-fluid interface tracking

- method, *Computers & Fluids* 224 (2021) 104964.
- [15] Y. Zhou, L. Xia, Exact solution for Stefan problem with general power-type latent heat using Kummer function, *International Journal of Heat & Mass Transfer* 84 (2015) 114-118.
- [16] J. Shaikh, A. Sharma, R. Bhardwaj, On sharp-interface level-set method for heat and/or mass transfer induced Stefan problem, *International Journal of Heat and Mass Transfer* 96 (2016) 458-473.
- [17] G. Beckett, J. A. Mackenzie, M. L. Robertson, A moving mesh finite element method for the solution of two-dimensional Stefan problems, *Journal of Computational Physics* 168(2) (2001) 500-518.
- [18] H. Zhao, J. Qi, H. Chen, Z. Tian, J. Sun, Z. Sun, A control volume method based interface movement equation for one-dimensional Stefan problem achieving mass conservation, *Journal of Materials Research and Technology* 9(6) (2020) 16107-16115.
- [19] G. Lupo, M. N. Ardekani, L. Brandt, An immersed boundary method for flows with evaporating droplets, *International Journal of Heat and Mass Transfer* 143 (2019) 118563.
- [20] Y. Li, J. Zhou, E. Long, X. Meng, Experimental study on thermal performance improvement of building envelopes by integrating with phase change material in an intermittently heated room, *Sustainable cities and society* 38 (2018) 607-615.
- [21] M. Iten, S. Liu, A. Shukla, Experimental validation of an air-PCM storage unit comparing the effective heat capacity and enthalpy methods through CFD simulations, *Energy* 155 (2018) 495-503.
- [22] M. Wu, L. Liu, J. Ding, An enthalpy method based on fixed-grid for quasi-steady modeling of solidification/melting processes of pure materials, *International Journal of Heat and Mass Transfer* 108 (2017) 1383-1392.
- [23] A. D. Brent, V. R. Voller, K. T. J. Reid, Enthalpy-porosity technique for modeling convection-diffusion phase change: application to the melting of a pure metal, *Numerical Heat Transfer, Part A Applications* 13(3) (1988) 297-318.
- [24] W. Ma, L. Zhao, G. Ding, Y. Yang, T. Lv, M. Wu, Numerical study of heat transfer during sapphire crystal growth by heat exchanger method, *International Journal of Heat and Mass Transfer* 72 (2014) 452-460.
- [25] Y. Li, E. Long, Z. Jin, J. Li, X. Meng, J. Zhou, L. Xu, D. Xiao, Heat storage and release characteristics of composite phase change wall under different intermittent heating conditions, *Science and Technology for the Built Environment*. 25(3) (2019) 336-345.
- [26] Z. Liu, J. Hou, D. Wei, X. Meng, B. J. Dewancker, Thermal performance analysis of lightweight building walls in different directions integrated with phase change materials (PCM), *Case Studies in Thermal Engineering* 40 (2022) 102526.

- [27] Z. Liu, J. Hou, Y. Huang, J. Zhang, X. Meng, B. J. Dewancker, Influence of phase change material (PCM) parameters on the thermal performance of lightweight building walls with different thermal resistances, *Case Studies in Thermal Engineering* 31 (2022) 101844.
- [28] Z. Liu, J. Hou, X. Meng, B. J. Dewancker, A numerical study on the effect of phase-change material (PCM) parameters on the thermal performance of lightweight building walls, *Case Studies in Construction Materials* 15 (2021) e00758.
- [29] W. Xu, Research and comparison on international building energy codes & standards, China Architecture & Building Press, Beijing, 2012, pp. 235-280.
- [30] Y. Gao, X. Meng, X. Shi, Z. Wang, E. Long, W. Gao, Optimization on non-transparent envelopes of the typical office rooms with air-conditioning under intermittent operation, *Solar Energy* 201 (2020) 798-809.
- [31] L. Min, C. Zhuang, H. Zhang, A. Deng, S. Li, Validity Analysis for Applying Enthalpy Method to Solve the Phase Change Heat Conduction Problem, *Journal of Logistical Engineering University* 27(3) (2011) 58-62.
- [32] C. Zhang, Y. Chen, L. Wu, M. Shi, Thermal response of brick wall filled with phase change materials (PCM) under fluctuating outdoor temperatures, *Energy and Buildings* 43(12) (2011) 3514-3520.
- [33] F. Kuznik, J. Virgone, Experimental Investigation of Wallboard Containing Phase Change Material: Data for Validation of Numerical Modeling, *Energy and Buildings* 41(5) (2009) 561-570.
- [34] C. Wang, S. Deng, J. Niu, E. Long, A numerical study on optimizing the designs of applying PCMs to a disaster-relief prefabricated temporary-house (PTH) to improve its summer daytime indoor thermal environment, *Energy* 181 (2019) 239-249.
- [35] C. Amaral, T. Silva, F. Mohseni, J. S. Amaral, V. S. Amaral, Experimental and numerical analysis of the thermal performance of polyurethane foams panels incorporating phase change material, *Energy* 216 (2021) 119213.
- [36] R. H. Inman, H. T. C. Pedro, C. F. M. Coimbra, Solar forecasting methods for renewable energy integration, *Progress in energy and combustion science* 39(6) (2013) 535-576.
- [37] ASHRAE, Guideline 14-2014: Measurement of Energy and Demand Savings, Atlanta, 2014, pp. 17-20.
- [38] Y. Gao, F. He, X. Meng, Z. Wang, M. Zhang, H. Yu, W. Gao, Thermal behavior analysis of hollow bricks filled with phase-change material (PCM), *Journal of Building Engineering* 31(2020) 101447.
- [39] Q. Wu, J. Wang, Influence of wall thermal performance on the contribution efficiency of the Phase-Change Material (PCM) layer, *Case Stud. Therm. Eng.* 28 (2021) 101398.

## Nomenclature

$t_m$	Phase-transition temperature, ( $^{\circ}\text{C}$ )
$L_p$	Phase change latent heat, (kJ/kg)
$d$	Material thickness, (m)
$\lambda$	Thermal conductivity, [W/(m K)],Solid (Liquid)
$c_p$	Specific heat, [J/(kg K)]
$\rho$	Density, (kg/m <sup>3</sup> )
$T_i$	Material temperature, ( $^{\circ}\text{C}$ )
$T_p$	PCM temperature, ( $^{\circ}\text{C}$ )
$\Delta T$	Phase-transition temperature ranges, ( $^{\circ}\text{C}$ )
$h_{in}$	Convective heat transfer coefficient of inner surface, [W/(m <sup>2</sup> ·K)]
$h_{out}$	Convective heat transfer coefficient of outer surface, [W/(m <sup>2</sup> ·K)]
$q_{peak}$	Inner surface peak heat flux, (W/m <sup>2</sup> )
$q_{ave}$	Inner surface average heat flux, (W/m <sup>2</sup> )
$H_p$	Enthalpy of PCM, (kJ/kg)
$M_t$	Measured temperatures at each hour, ( $^{\circ}\text{C}$ )
$S_t$	Simulated temperatures at each hour, ( $^{\circ}\text{C}$ )
$\overline{M}_t$	Average of the measured data values, ( $^{\circ}\text{C}$ )
$T$	Temperature, ( $^{\circ}\text{C}$ )
$t$	Time, (s)
$\alpha$	Solar radiation absorptivity of outer surface, -
$I$	Solar radiation intensity, (W/m <sup>2</sup> )
$\delta$	Wall thickness, (m)
$h$	Wall height, (m)
$\beta$	Liquid fraction, -
$\varphi$	Delay time, (h)
$f$	Attenuation rate, (%)
$m$	Internal iteration number, -
$n$	Total number of hours, $t$

## Subscripts

$x$	Wall thickness direction
$y$	Wall height direction
$i$	Representatives OSB, glass wool or gypsum board
$p$	Phase-change materials
$s$	Solid states

<i>l</i>	Liquid states
<i>0</i>	Initial value
<i>w,in</i>	Inner surfaces
<i>w,out</i>	Outer surfaces
<i>out</i>	Outdoor
<i>T,w,in,max</i>	Inner surface peak temperature
<i>T,out,max</i>	Outdoor air peak temperature

***Abbreviations***

PCM	Phase-Change Materials
OSB	Oriented Strand Board
TMY2	Typical Meteorological Year 2
RMSE	Root Mean Square Error
$CV_{(RMSE)}$	Coefficient of Variation of the Root Mean Square Error

**Chapter 3. Effect of PCM parameters on the thermal performance  
of lightweight wall**

3.1 Introduction.....	3-1
3.2 Methodology .....	3-3
3.2.1 Physical model description.....	3-3
3.2.2 Indoor and outdoor thermal boundary description .....	3-4
3.3 Selection of phase-transition temperature of PCM.....	3-4
3.4 Effects of other parameters of PCM .....	3-7
3.4.1 Effect of the PCM location.....	3-7
3.4.2 Effect of the PCM thickness.....	3-8
3.4.3 Effect of the PCM latent heat .....	3-10
3.4.4 Effect of the thermal conductivity coefficient of PCM.....	3-11
3.4.5 Effect of the PCM density .....	3-13
3.4.6 Effect of the PCM specific heat .....	3-14
3.5 Summary .....	3-15
References.....	3-17
Nomenclature.....	3-21



### 3.1 Introduction

Lightweight buildings are widely favored by people due to their better seismic resistance, environmental protection and short construction period. However, lightweight buildings usually have sizeable indoor temperature fluctuations due to lower thermal mass. Specifically, the delay and attenuation of solar radiation heat irradiated on the exterior wall in summer are not obvious, resulting in high indoor temperature. The measured results show that the indoor temperature of lightweight buildings can reach 42.5 °C in summer when the average daily outdoor temperature is about 31 °C [1]. Higher temperature fluctuation not only affects indoor thermal comfort but also increases air conditioning load. Therefore, phase-change materials (PCM) have become the focus of research to improve the low thermal inertia of lightweight buildings. Within a specific temperature range, PCM can change their physical state (solid-solid, solid-liquid) by using the temperature difference between environment and materials as the driving force to achieve thermal storage and release [2]. This characteristic is widely used in building envelopes, air conditioning and heating systems [3,4].

The application of PCM in building envelopes mainly includes directly soaking [5], blending [6], and figuration phase-change [7]. Kissock [8] and Feldman et al. [9] made phase-change wallboard by soaking and blending methods, respectively found that phase-change wallboard could significantly reduce indoor temperature fluctuations, improve comfort, reduce and transfer peak load, its thermal storage capacity was ten times higher than common wallboard. Kuznik and Virgone [10] and Xu et al. [11] installed shape-stabilized PCM in lightweight building walls (LBW) found that PCM could effectively control the fluctuation and the rise of indoor air temperature in summer. Further, considering the uncontrollability of experimental tests, Adilkhanova et al. [12-15] studied the effect of PCM applied to lightweight buildings based on different climatic conditions by numerical simulation (EnergyPlus). The studies found that PCM could effectively reduce indoor discomfort, but the energy-saving rate depended on climatic conditions and the thermal insulation characteristics of the envelope. In addition, Sarri et al. [16] found that PCM combined with shading equipment under natural conditions was more conducive to improving indoor thermal comfort hours, and its energy-saving potential can reach 44.13%~59.11%. Fateh et al. [17] studied the effects of solar radiation (solar radiation was regarded as the time-varying heat source at the boundary) and concluded that the appropriate PCM could save 75% of the heat load. For the study of thermal performance of walls, Zhou et al. [18] compared the thermal performance of shape-stabilized PCM, brick, foam concrete and expanded polystyrene (EPS) under outdoor periodic temperature based on the enthalpy method model. Their results showed that the delay time and attenuation coefficient of shape-stabilized PCM was the best.

For PCM, multiple parameters greatly affect the performance of PCM integrated LBW, including the PCM location, the phase-transition temperature, thickness, latent heat, density and thermal conductivity [19]. Some studies have also been carried out on PCM parameters to maximize the performance of PCM. Among them, Mohseni et al. [20] showed that the phase-transition temperature and thickness of PCM have optimal values by analyzing the energy consumption of residential buildings in Australia. Stovall [21], Neeper [22], and Fateh et al. [17] pointed out that PCM has the best performance when the phase-transition temperature is close to the internal temperature. Wang et al. [23] indicated that different room locations were suitable for different phase-transition temperatures. Moreover, different researchers have different views on the optimal location of PCM. Zwanzig et al. [24] presented the best location of PCM depends on the thermal resistance between the PCM layer and external boundary conditions. Yang et al. [25] obtained by experimental tests that setting PCM on the inner surface could reduce the temperature fluctuation by 32.4% compared with the outer surface, and the delay time was increased by 1.2h. Jin et al. [26,27] reported that the best PCM location was 1/5th of wall thickness from the inner surface. Fateh et al. [17,28] noted the optimal PCM location was near the middle of the wall. Jin et al. [29,30] suggested that the optimal location was affected by several parameters, including exterior and interior temperature conditions as well as PCM thermophysical properties like phase-transition temperature, thickness, latent heat and others.

By previous studies, it can be easily found that PCM plays a very positive role in improving the thermal performance of LBW, but its application effect depends not only on climatic conditions but also on PCM parameters [12-15,19,23,24,29,30]. Most of the researches were mainly focused on the energy-saving of existing PCM and indoor thermal comfort, and there were insufficient studies on the heat transfer performance of LBW based on PCM parameters. However, several PCM parameters have been studied mainly on the phase-transition temperature, location and thickness [17,20-31]. For PCM integrated LBW, PCM latent heat, density, thermal conductivity will also greatly affect the thermal performance of the wall. Zhou et al. [19] pointed out that there were relatively optimal values of PCM latent heat under a certain external heat disturbance. The thermal conductivity has little effect on the phase-transition keeping time ( $\psi$ ) but has a great effect on the decrement factor ( $f$ ). Kishiore et al. [32] showed that the PCM transition temperature is the strongest parameter affecting thermal load modulation, followed by PCM location and PCM thickness. PCM latent heat and density are next in the order of priority, specific heat and thermal conductivity showed no impact. As a result, previous studies have revealed the necessity to conduct a comprehensive analysis PCM parameters better to utilize the PCM. Meanwhile, although the effect of PCM parameters has

been studied previously [32], the application effect and optimization parameters of PCM in different climate zones are quite different. Therefore, A typical summer climate (TMY2) [33,34] in Fukuoka (Japan) was adopted as the thermal boundary and a typical two-dimensional LBW numerical model was built in this paper with the heat transfer process of melting-solidifying and validated. Based on this, the influence rules of each parameter on its thermal performance were analyzed in-depth, and the relative optimal value of each parameter was obtained. The research results can provide reference and data support for the application and preparation of PCM in local lightweight buildings.

### 3.2 Methodology

#### 3.2.1 Physical model description

Fig. 3-1 shows the schematic diagram of LBW. Among them, Model-0 is a reference wall (no PCM) with three layers, from outside to inside are exterior wallboard (12mm oriented strand board-OSB), insulation material (60mm glass wood) and interior wallboard (10mm gypsum board). On the basis of Model-0 (reference wall), Model-(1-3) places PCM in different locations of reference wall (outside, middle and inside of the insulation material) to study the dynamic thermal behavior of the wall to seek the best PCM phase change parameters and locations. Table 3-1 shows the relevant thermophysical parameters of wall materials.

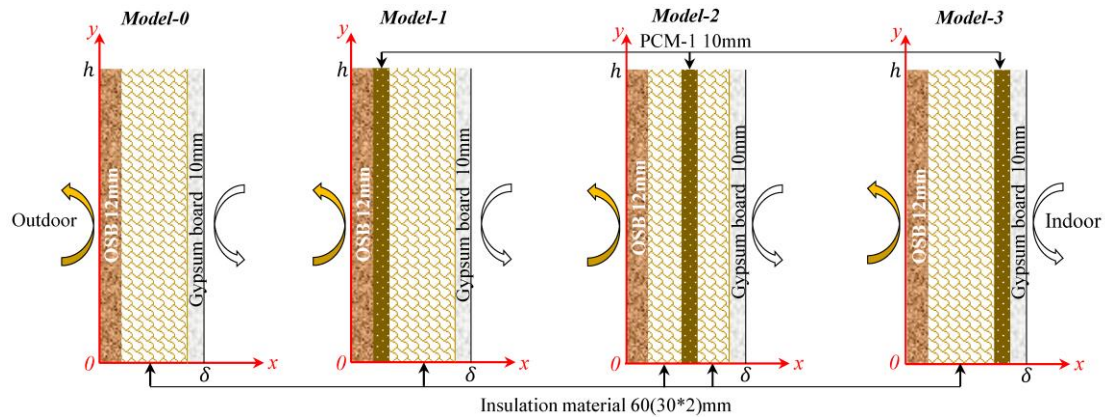


**Fig. 3-1. Schematic diagram of the two-dimensional geometric model of the LBW and the location of the PCM.**

**Table 3-1 Thermo-physical parameters of wall materials.**

Material	$t_m(^{\circ}\text{C})$	$L_p(\text{kJ/kg})$	$d_p(\text{mm})$	$\lambda[\text{W}/(\text{m K})]$ , Solid (Liquid)	$c_p[\text{J}/(\text{kg K})]$	$\rho(\text{kg}/\text{m}^3)$
PCM-1	18-28	216	10	0.5(0.25)	1785	1300
OSB	-	-	12	0.105	1400	593
Glass wool	-	-	60	0.035	1220	40
Gypsum board	-	-	10	0.33	1050	1050

### 3.2.2 Indoor and outdoor thermal boundary description

In this study, outdoor thermal boundary data were selected from July to August based on the typical summer climate (TMY2) [33,34] in Fukuoka (Japan). The TMY2 are datasets of hourly values of solar radiation and meteorological elements for a 1-year period and it was downloaded from the National Renewable Energy Laboratory [35]. The numerical simulation time is from July 1st to August 5th. However, in order to eliminate the difference between the initial temperature and the actual temperature, the data of 7 days were selected with higher relative temperatures from July 30th to August 5th for analysis. Fig. 3-2 shows the variation of outdoor air temperature and solar radiation intensity from July 30th to August 5th (7 consecutive days). In addition, for the indoor temperature, the relevant Japanese energy-saving norms (Criteria for Clients on the Rationalization of Energy Use for Houses, CCREUH) stipulate that the indoor set temperature of an air-conditioned room  $\leq 27^{\circ}\text{C}$  [36]. While some research [37] found that the comfortable temperature range needs to be from  $25^{\circ}\text{C}$  to  $28^{\circ}\text{C}$  when the PMV is between -0.5 and 0.5 in the air-conditioned room in summer. Therefore, considering energy-saving and human thermal comfort, the indoor air temperature maintains  $26^{\circ}\text{C}$ . Adiabatic boundaries were applied to the top and bottom surfaces of the numerical model, while the convective heat transfer coefficients  $h_{in}$  and  $h_{out}$  are  $8.7\text{W}/(\text{m}^2\cdot\text{K})$  and  $19\text{W}/(\text{m}^2\cdot\text{K})$ , respectively [38,39].

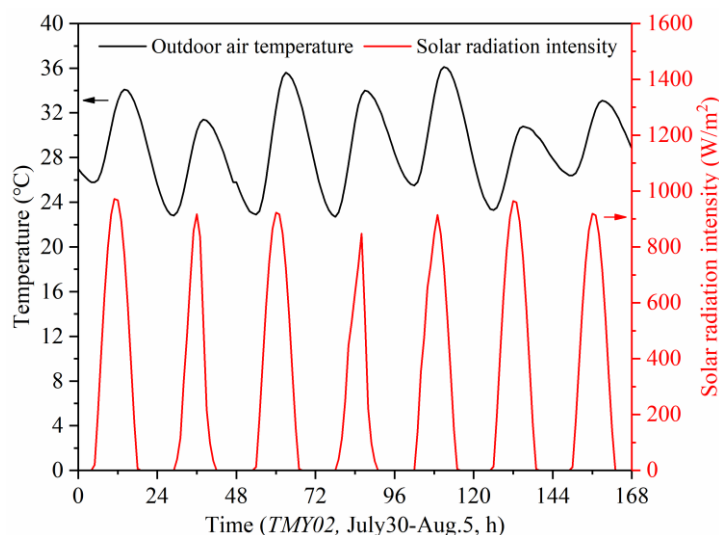


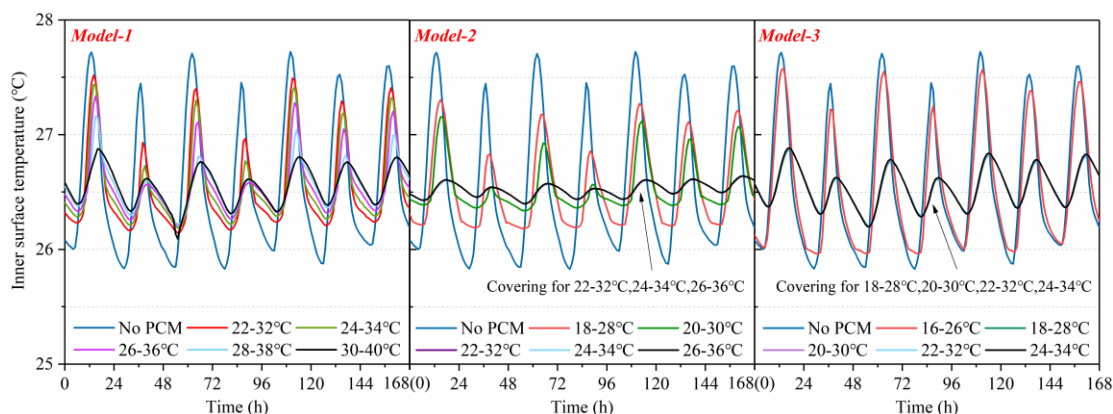
Fig. 3-2. Variation of outdoor air temperature and solar radiation intensity with time.

### 3.3 Selection of phase-transition temperature of PCM

The phase-transition temperature of PCM determines the degree of phase change. However, the degree has a significant impact on the thermal performance of the wall when PCM is integrated into building walls. The phase change will not occur or quickly complete

when the phase-transition temperature is lower or higher than the actual temperature range, but both whether and how much the phase change of PCM happens depends on the overlap ratio between its temperature fluctuation and its phase-transition temperature [49]. As a result, gaining a suitable phase-transition temperature is the primary task in this study.

Fig. 3-3 gives the variation of inner surface temperature with time under different phase-transition temperatures for different locations. It can be seen that there are large differences in the internal surface temperatures at different phase-transition temperatures no matter where the PCM is installed. When the PCM is close to the outer surface, the phase change occurs rapidly at a lower transition temperature due to its strong interaction with the outdoor temperature, which leads to the weakening of the thermal storage efficiency. This is also why the peak temperature of the inner surface occurs at different times under different phase-transition temperatures. Secondly, the fluctuation amplitude of inner surface temperature decreases gradually with the increase of phase-transition temperature, indicating that appropriate transition temperature can improve the thermal storage and release capacity of PCM. In addition, there are many overlapping curves for different phase-transition temperatures when the PCM is installed in the middle or inside, which main reason is that the actual temperature change of PCM is in the range of phase-transition temperature under the interaction of the outdoor and indoor temperature. It further illustrates that the optimal phase-transition temperature of PCM is determined by the actual temperature change. As a consequence, the suitable phase-transition temperatures are initially determined as 30-40°C for Model-1, 22-32°C, 24-34°C and 26-36°C for Model-2, 18-28°C, 20-30°C, 22-32°C and 24-34°C for Model-3.



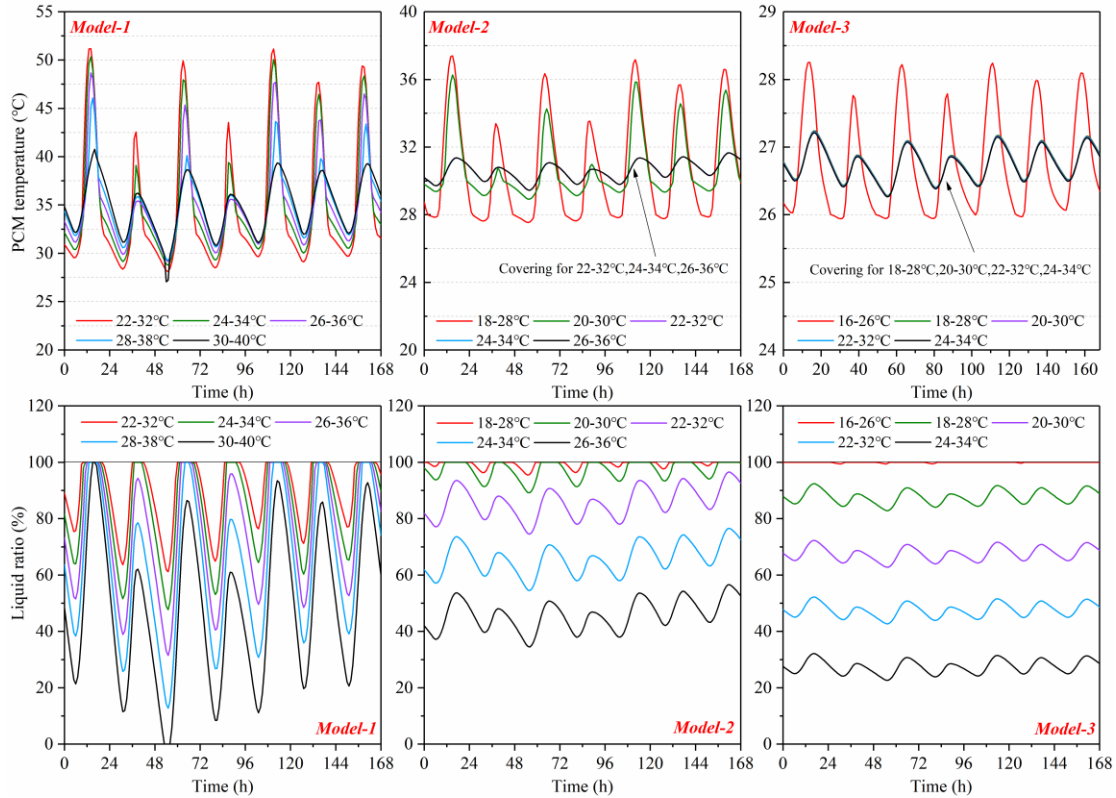
**Fig. 3-3. Variation of inner surface temperature with time under different phase-transition temperatures for Model 1-3.**

Fig. 3-4 depicts the variation of PCM temperature and liquid ratio with time under different phase-transition temperatures for different locations. It can be drawn that the actual temperatures of the PCM are all above 26 °C. The PCM is always in the liquid state only sensible heat reaction occurred when the phase-transition temperature is lower than 26 °C. Taking

model-1 as an example, it can be concluded that the temperature changes of the PCM within 27.04 °C-51.18 °C when the PCM is close to the outdoor side due to the high outdoor temperature. Furthermore, the PCM temperature is higher than 32 °C for 41% of the time when the phase-transition temperature is selected to be 22 °C-32 °C, during which the PCM is fully saturated with thermal storage and reaches a sensible heat state. Nevertheless, when the PCM temperature is reduced to 32 °C, then it begins to decrease slowly with the decrease of outdoor temperature due to the latent heat, and that the temperature will drop rapidly after the heat release is completed. The above phenomenon is mainly because the PCM has less thermal storage resulting in shorter phase change maintenance time.

Moreover, more importantly, the temperature variation of PCM gradually decreases and approaches the phase-transition temperature as phase-transition temperature rise. Such as, when the phase-transition temperature is defined as 30-40 °C, the PCM temperature fluctuates at 30.90 °C-38.39 °C. At this time, the phase-transition temperature completely covers the actual temperature change and the thermal performance of the PCM is better developed, which is also the reason why the temperature fluctuation curves overlap in Model-2 and Model-3.

Besides, it can be seen from the liquid ratio change of the PCM in Fig. 3-4 that the difference is huge at different phase-transition temperatures when the phase-transition temperature is relatively appropriate. Taking model-2 for example, when the suitable phase-transition temperature is chosen to be 22-32 °C, 24-34 °C and 26-36 °C, the liquid ratio fluctuates range (average value) in 74.49%-96.56% (85.78%), 54.45%-76.56% (65.77%) and 34.46%-56.57% (45.79%) respectively. It means that the liquid ratio will be larger as the actual temperature of PCM gets closer to the maximum value of phase-transition temperature. As a result, choosing the PCM with a low phase-transition temperature at a suitable temperature will exert higher thermal storage capacity for transitional seasons. The outdoor temperature selected during this study is the highest of the year, so the appropriate phase-transition temperatures are determined to be 30-40 °C, 22-32 °C and 18-28 °C for Model-1, Model-2 and Model-3, severally.



**Fig. 3-4. Variation of PCM temperature and liquid ratio with time under different phase-transition temperatures for Model 1-3.**

### 3.4 Effects of other parameters of PCM

#### 3.4.1 Effect of the PCM location

The different locations of PCM in the wall determine the degree of interaction with the indoor and outdoor environment [17]. But for the thermal performance analysis of the wall, the delay time ( $\varphi$ ) and attenuation rate ( $f$ ) of the inner surface temperature are two important factors affecting the indoor comfort, and the peak heat flux ( $q_{peak}$ ) and average heat flux ( $q_{ave}$ ) of the inner surface are essential elements affecting the energy-saving [40]. Based on this, Table 2 lists the indexes evaluating the thermal behavior of LBW under suitable phase-transition temperatures. Compared with Model-0 (no PCM), the peak temperature ( $T_{peak}$ ) decreases by about 1 °C at different PCM locations, and the average temperature ( $T_{ave}$ ) changes are slight. The  $\varphi$  is enhanced by 3.57h-4.4h from 0.86h, and the  $f$  is decreased by 72.78%-91.57% from 5.34%. It shows that the PCM has a potent inhibition on the fluctuation of the inner surface temperature at a suitable phase change temperature, but the thermal insulation is poor. Meanwhile, liken to Model-0 (no PCM), the  $q_{peak}$  is reduced by 7.32W/m<sup>2</sup>-8.78W/m<sup>2</sup> (reduction rate reach 52.81%-63.35%), while the  $q_{ave}$  is reduced only by 1.13W/m<sup>2</sup>-1.54W/m<sup>2</sup>, and the cumulative heat gain ( $Q_c$ ) is reduced by 3.45%-8.18%. The results show that the PCM can restrain the higher temperature but raise the lower temperature due to latent heat, which leads

to the energy-saving effect of higher temperature period is significant than other periods, while the total energy-saving effect is small. Furthermore, it finds that the difference in evaluation indexes of the three models are relatively small, but all evaluation indexes are the best for Model-2 by comparison. The results indicated that the PCM installed in the middle of the wall is better than the outside or inside at a suitable phase-transition temperature.

**Table 3-2 Thermal performance of LBW with different PCM location and suitable phase-transition temperatures**

Location ( $t_m$ , °C)	PCM		Inner surface temperature				Inner surface heat fluxes		
	$T_{PCM}$ (°C)	$\beta$ (%)	$T_{peak}$ (°C)	$T_{ave}$ (°C)	$\varphi$ (h)	$f$ (%)	$q_{peak}$ (W/m <sup>2</sup> )	$q_{ave}$ (W/m <sup>2</sup> )	$Q_c$ (W h/m <sup>2</sup> )
Model-0 (No PCM)	-	-	27.60	26.56	0.86	5.34	13.86	6.02	824.88
Model-1 (30-40)	30.90- 38.39	13.29- 83.01	26.75	26.55	4.43	1.37	6.48	4.71	796.43
Model-2 (22-32)	29.89- 31.19	78.86- 92.14	26.59	26.52	5.29	0.45	5.08	4.48	757.39
Model-3 (18-28)	26.43- 27.06	84.29- 90.09	26.76	26.54	4.57	1.40	6.54	4.70	794.58

### 3.4.2 Effect of the PCM thickness

The total thermal storage and release capacity of the wall is directly determined by the amount of PCM when other parameters are fixed. Based on the above analysis, PCM installed in the middle (Model-2) is studied on subsequent related issues in this paper. The phase-transition temperature is chosen to be 22-32 °C, and other parameters are set according to the basic value in table 1. Fig. 3-5 shows the thermal performance indexes in the inner surface with different thicknesses of PCM. As shown, the thickness not only affects the  $\varphi$  and  $f$  but also has a significant effect on the  $q$ . As shown in Fig. 3-5 (a), the  $\varphi$  presents an increasing linear trend with the increase of PCM thickness on the reference wall, the  $\varphi$  increases by 3.43h, 4.43h, 5.71h and 7.28h for each 5mm increase, respectively. However, the  $f$  gradually weakens when the thickness is added more than 10mm.

Furthermore, the  $q$  is presented in Fig. 3-5 (b). For each increase of 5mm on the basis of 0mm, the reduction rates of  $q_{peak}$  are 51.88%, 23.84%, 9.45% and 8.26%, respectively. The  $q_{ave}$  reduction rates are 22.26%, 4.27%, 5.80% and 6.63%, respectively. The above data can be concluded that the reduction rate of  $q_{peak}$  tends to be smooth gradually when the thickness is more than 10mm, while the increase of PCM thickness (more than 5mm) has little effect on the  $q_{ave}$ . This phenomenon is because thicker PCM provides a higher heat storage capacity per unit surface, which leads to a higher thermal regulation mechanism. However, the additional PCM

added only plays a certain role of thermal resistance for the relatively stable heat from the outside, and the total heat storage and release capacity are not fully utilized. This result is consistent with the literature [32], but the latter gives an increase in total heat flux with increasing thickness. This differentiation mainly from the thermal resistance of basic layer (no PCM) varies with the PCM thickness in [32], as a result, the above also further illustrates that the advantage of PCM is not thermal insulation but thermal adjustment. To sum up, if blindly increasing the thickness of PCM with the thermal resistance of the basic layer unchanged, although the purpose of energy-saving can be achieved, the energy-saving effect will gradually stabilize with the increase of thickness, and the cost of PCM will increase linearly. Therefore, the PCM thickness of 10mm is more suitable to achieve a better application effect. In this case, the  $\varphi$  is 5.29h (increased by 4.43h), the  $f$  is reduced from 5.34% (no PCM) to 0.45%, and the  $q_{peak}$  and  $q_{ave}$  are also reduced by 63.35% and 25.58%.

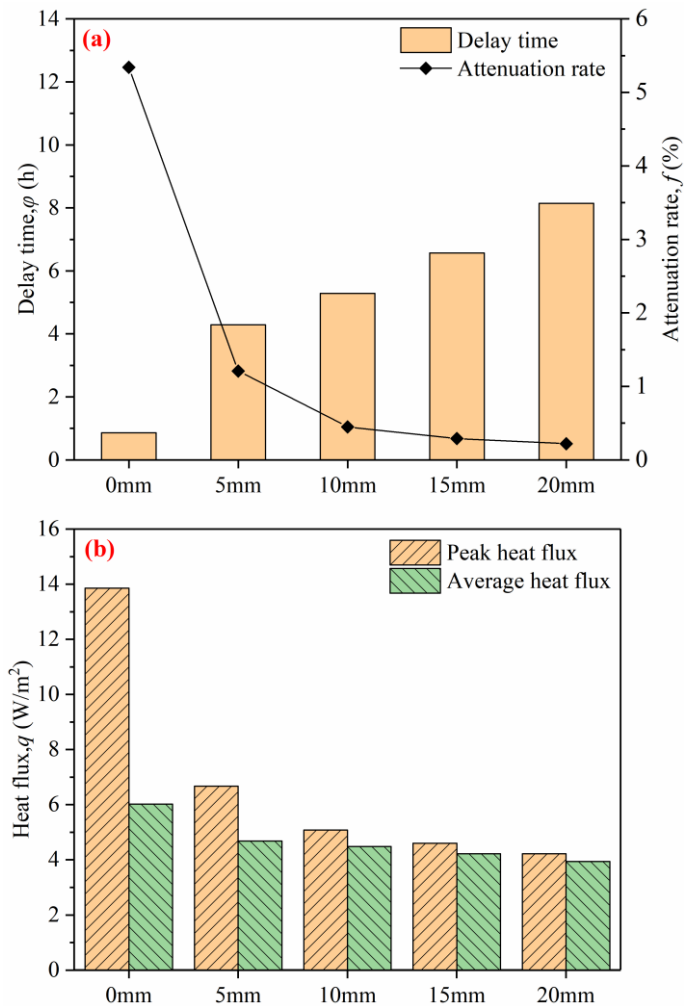


**Fig. 3-5. Variation of (a) Delay time and attenuation rate of inner surface temperature and (b) inner surface heat flux under different PCM thicknesses.**

### 3.4.3 Effect of the PCM latent heat

The thermal storage and release capacity of PCM is mainly measured by PCM latent heat at the appropriate phase-transition temperature. The use of PCM in buildings can effectively improve the thermal mass of the wall under a small mass, but the improvement effect is closely related to the latent heat of PCM. For this reason, seven groups of data are selected as the research indicators from 25kJ/kg to 325kJ/kg with an interval of 50kJ/kg, and other non-research parameters are set according to the basic values. Fig. 3-6 depicts the changes of various evaluation indicators under different phase change latent heats. As shown in Fig. 3-6(a), the larger the latent heat results longer  $\varphi$  and lower the  $f$ . When increasing from 25kJ/kg to 175kJ/kg, the  $\varphi$  increased by 2.28h-4.28h, and the  $f$  decreased from 5.34% to 0.54% (reduced by 89.89%) compared with the reference wall (no PCM). But from 175kJ/kg to 325kJ/kg, the  $\varphi$  only increased by 0.86h, and the  $f$  is only reduced from 0.54% to 0.29%. It shows that its benefit is relatively high when the latent heat is taken as 175kJ/kg and then continues to increase, the  $\varphi$  and  $f$  will be weakened.

From Fig.7(b) can be seen that the  $q_{peak}$  decreases gradually with the increase of latent heat. When the latent heat is increased from 25kJ/kg to 325kJ/kg, the  $q_{peak}$  can be reduced by 37.37%-66.52% compared with no PCM. However, it is obvious that the  $q_{peak}$  reduction rate has leveled off when the latent heat is higher than 175kJ/kg. This phenomenon has a similar conclusion to the increased PCM thickness, that is, its heat storage capacity is improved with the increase in latent heat, but beyond a certain value, its effect gets stable because of the limited outdoor heat. These results are quite different from the previous findings [32], where the effect tends to be relatively stable after latent heat exceeds 50 kJ/kg. It shows that different outdoor thermal boundaries and the thermal resistance of the basic layer (no PCM) can affect the contribution efficiency of PCM. Furthermore, the change range of different from the  $q_{peak}$ , the  $q_{ave}$  does not change much with the strengthening of phase change latent heat. This further illustrates that the PCM only adjusts the temperature fluctuation through its inherent thermal mass but does not weaken the heat transfer effect to a certain extent. A high thermal storage capacity and superior thermal regulation mechanism of the wall can bring certain energy-saving effects for the  $q$ , but its benefit can be ignored when the latent heat is higher than a specific value (175kJ/kg). The  $q_{peak}$  is only 0.7w/m<sup>2</sup> (13.33%) higher than the  $q_{ave}$  when the phase change latent heat is 175 kJ/kg, while compared with the reference wall (no PCM), the  $q_{peak}$  and  $q_{ave}$  are reduced by 62.12% and 24.41%, respectively.

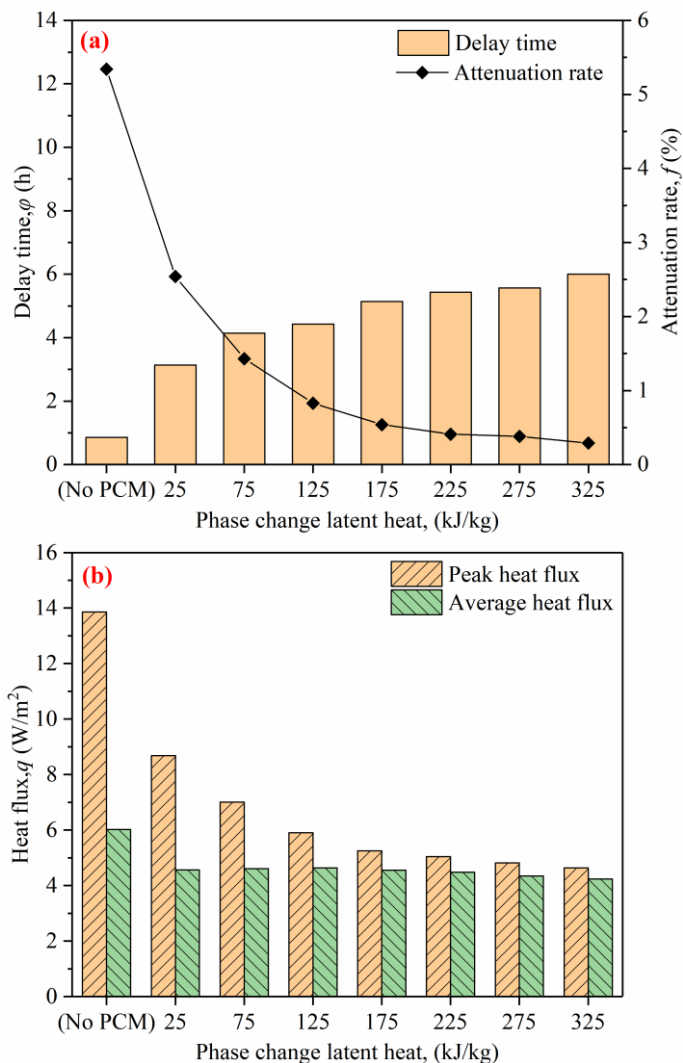


**Fig. 3-6. Variation of (a) Delay time and attenuation rate of inner surface temperature and (b) inner surface heat flux under different PCM latent heats.**

### 3.4.4 Effect of the thermal conductivity coefficient of PCM

The thermal conductivity coefficient affects the thermal insulation performance of the material, indoor comfort and energy consumption of the building. Thus, five groups of different thermal conductivity coefficient values [solid (liquid), W/(m K)] of PCM from minor to large are selected for analysis, and other parameters are set according to the basic value except for the above optimization parameters. As shown in Fig. 3-7 (a) indicates a change range of  $f$  is small only from 0.45% to 0.25% as the thermal conductivity coefficient is decreased from 0.75(0.375) to 0.05(0.025), but the  $\phi$  increases by 4.42h. The results are caused by a high total thermal resistance (due to low thermal conductivity coefficient) of the wall prevents the impact of outdoor temperature peak period on indoor temperature, and the thermal storage effect of PCM is also delayed. In the meantime, the reference wall is compared to suggest that the  $\phi$  enhances 4.43h-8.85h and the  $f$  reduces 91.57%-95.32% respectively. It can be clearly shown

that the phenomena are mainly caused by the PCM latent heat.

Meanwhile, reducing the thermal conductivity coefficient of PCM from 0.25(0.125) to 0.05(0.025), the effect on the  $\varphi$  and  $f$  is higher than that from 0.75(0.375) to 0.25(0.125). Similar conclusions are also drawn in Fig. 3-7 (b), that is, the influence degree on the  $q$  is more evident after reducing from 0.25(0.125) to 0.05(0.025). At the same time, it is worth noting that the  $q_{peak}$  and  $q_{ave}$  change less from 0.75 (0.375) to 0.05 (0.025) during the reduction of the thermal conductivity of the PCM, which is only 0.87 W/m<sup>2</sup> and 0.63 W/m<sup>2</sup>. It is mainly due to the thinness of the PCM (only 10mm), whose variation in thermal conductivity has a small effect on the total thermal resistance of the wall, which is consistent with the results of the literature [32,49]. In addition, when the smaller thermal conductivity coefficient is selected as 0.05 (0.025), compared with other values, the  $q_{peak}$  and  $q_{ave}$  are reduced by 8.87%-17.13% and 7.64%-14%. However, compared with the reference wall (no PCM), the  $q_{peak}$  and  $q_{ave}$  are reduced by 69.62% and 35.71%.

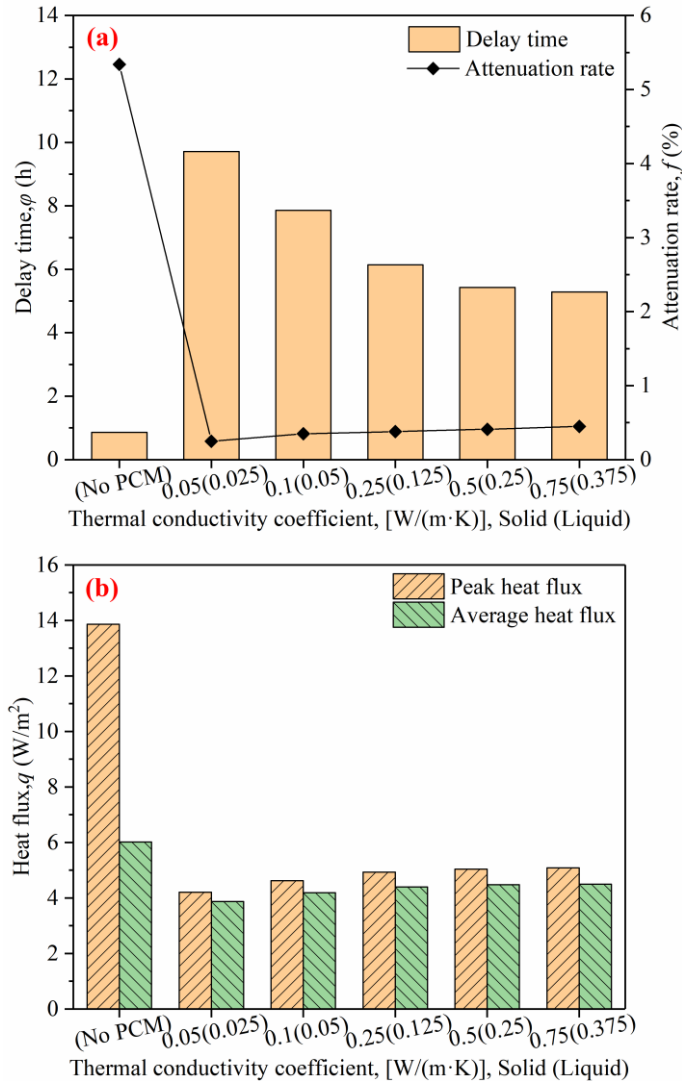


**Fig. 3-7. Variation of (a) Delay time and attenuation rate of inner surface temperature and (b) inner surface heat flux under different thermal conductivity coefficients of PCM.**

### 3.4.5 Effect of the PCM density

Based on the above-optimized parameters, the influence of PCM density on the thermal performance of the wall is further studied in this paper. From Fig. 3-8(a) can be concluded that the  $\varphi$  exhibits linear growth with the increase of density, conversely, the  $f$  tends to be reduced. Indicating that a higher density reduces the influence of outdoor temperature on the indoor due to the enhancement of thermal inertia of the wall. However, when the density is greater than  $1000 \text{ kg/m}^3$ , the impact on the  $f$  is minimal and tends to be smooth, although the  $\varphi$  is increased continuously. Increasing density from  $250 \text{ kg/m}^3$  to  $1000 \text{ kg/m}^3$ ,  $f$  lowered from 2.64% to 0.48%, while from  $1000 \text{ kg/m}^3$  by  $2000 \text{ kg/m}^3$ ,  $f$  decreased by only 0.29%. What's more, increasing the density positively affects reducing the  $q_{peak}$  and a little effect on  $q_{ave}$ , as observed in Fig. 3-8(b). With the increase of PCM density from  $250 \text{ kg/m}^3$  to  $1000 \text{ kg/m}^3$ , the reduction rate of  $q_{peak}$  increases by 27.13%, but it is only raised by 4.54% from  $1000 \text{ kg/m}^3$  to  $2000 \text{ kg/m}^3$ . It indicates that although increasing the density can improve the peak energy-saving rate, the effect is basically negligible when its value exceeds  $1000 \text{ kg/m}^3$ . At the same time, found by calculation that the  $Q_c$  changed little with adding density from  $250 \text{ kg/m}^3$  to  $1000 \text{ kg/m}^3$ , and then it only began to decline when it exceeds  $1000 \text{ kg/m}^3$ . This result can well explain that a lower material density cannot well boost the thermal inertia of the wall for the thinner PCM (only 10mm), and the thermal regulation effect mainly comes from the latent heat of PCM at low density. In conclusion, considering the characteristics of lightweight walls, selecting the PCM with a density of  $1000 \text{ kg/m}^3$  based on the above suitable analysis parameters can reduce the  $q_{peak}$  by 66.38%, the  $q_{ave}$  by 33.39% and the  $Q_c$  by 15.16% compared with the reference wall (no PCM).

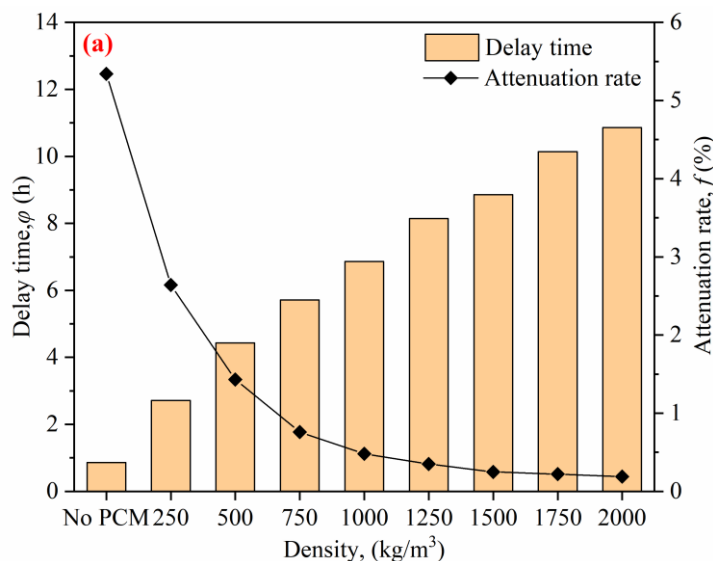


**Fig. 3-8. Variation of (a) Delay time and attenuation rate of inner surface temperature and (b) inner surface heat flux under different densities of PCM.**

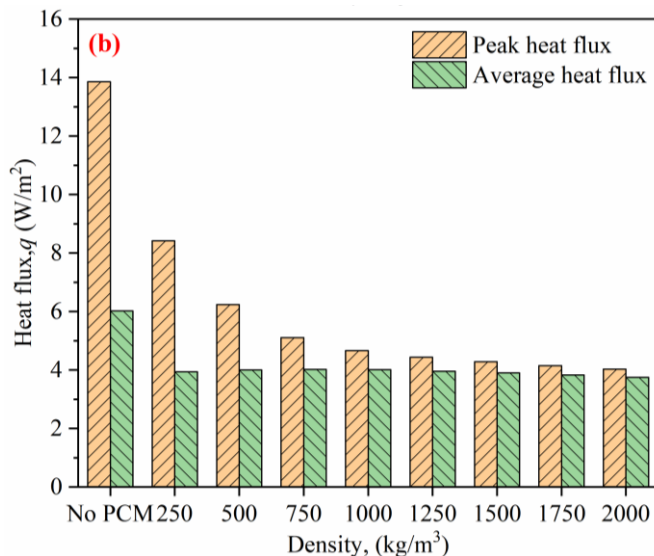


**Fig. 3-8. (Continued).**

### 3.4.6 Effect of the PCM specific heat

Fig. 3-9 demonstrates the thermal performance of the inner surface under different specific heat of PCM, and it is found that the change of specific heat does not have much effect on it. When the specific heat is increased from 500J/(kg K) to 2000J/(kg K), the  $\phi$  increased by only 0.43h, the  $f$  decreased from 0.54% to 0.51%, the  $q_{peak}$  is reduced only 0.11W/m<sup>2</sup>, the variation of  $q_{ave}$  approaches to 0%. The main reason is that the specific heat of PCM is very small compared with the latent heat (only about 0.5% of the latent heat). The equivalent specific heat resulting from the conversion of the latent heat is much larger than the specific heat of the PCM in the solid or liquid state, so that heat gain caused by the specific heat of PCM is negligible for the heat gain of PCM integrated wall. Meanwhile, the specific heat of PCM close to the basic value of 2000 is selected for analysis in this paper. Compared with the reference wall (no PCM) in the above PCM parameters are taken to the relative optimal value, the  $\phi$  is added to 6.86h, the  $f$  is cut down from 5.34% to 0.51%, and the  $q_{peak}$  and  $q_{ave}$  reduced by 66.52% and 33.39%. As a result shows that although the PCM is thinner (only 10mm), its high heat storage and release capacity after selecting appropriate PCM, which not only ensures the stability of indoor temperature but also be prominent in the energy-saving of light buildings.

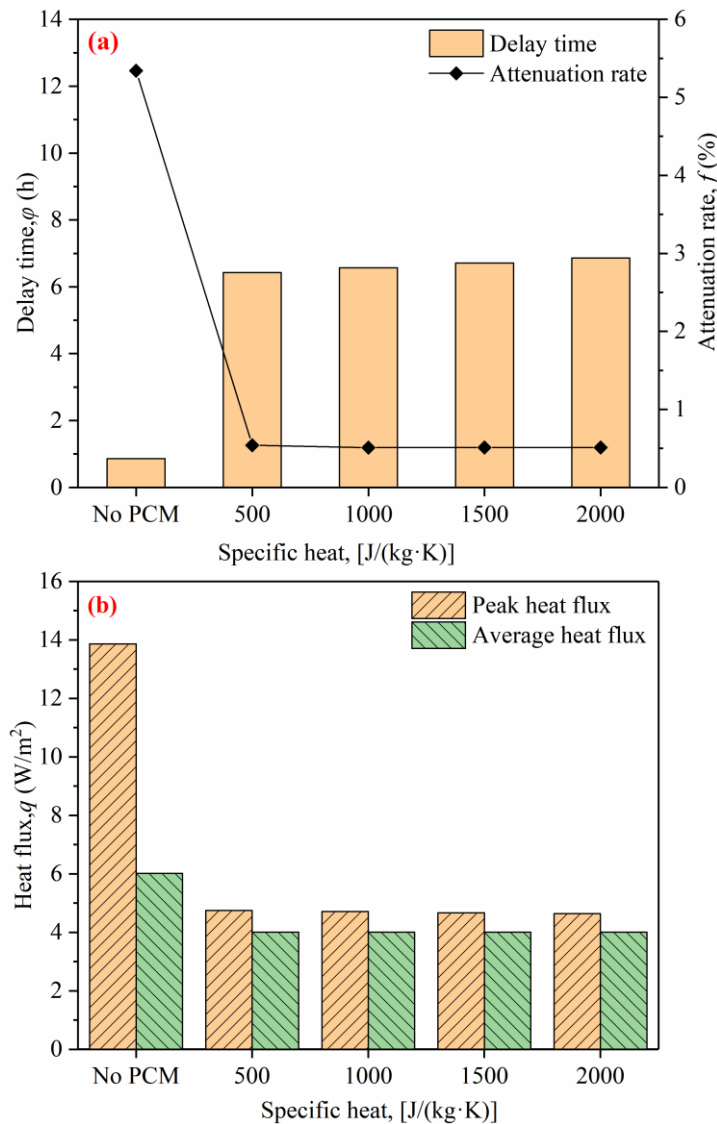


**Fig. 3-9. Variation of (a) Delay time and attenuation rate of inner surface temperature and (b) inner surface heat flux under different specific heats of PCM.**

### 3.5 Summary

Although PCM integrated wall was widely studied, previous studies mostly focused on indoor thermal environment and energy consumption. Few studies on the heat transfer performance of lightweight building walls (LBW) based on PCM parameters. Therefore, the effects law of different PCM parameters (location, transition temperature, thickness, latent heat, thermal conductivity, density, specific heat) on the thermal performance of LBW is roundly analyzed in this paper by numerical simulation. The main conclusions are gained as follows:

- PCM integrated into the LBW can significantly improve the thermal inertia and reduce the fluctuation of the inner surface temperature and peak heat flux ( $q_{peak}$ ) but has little effect on the average temperature ( $T_{ave}$ ), average heat flux ( $q_{ave}$ ), and cumulative heat gain ( $Q_c$ ).
- The suitable phase-transition temperature is also different when the PCM is installed in

different locations. PCM installed in the middle of the wall is better than the outside or inside at a suitable phase-transition temperature.

- The thickness, latent heat and density of PCM have a positive correlation with the delay time ( $\varphi$ ) and a negative correlation with the attenuation rate ( $f$ ) and  $q_{peak}$ . That is, as their value is increased, the  $\varphi$  is increased, the  $q_{peak}$  and  $f$  are reduced. However, the influence begins to be weakened when it exceeds a particular value and there are relatively optimal values for different parameters. What's more, the specific heat of PCM has basically no effect on thermal performance.
- Considering the cost and thermal performance, PCM-thickness should not exceed 10mm. In addition, the influence begins to weaken when the PCM-latent heat exceeds 175kJ/kg. The influence is more apparent when the thermal conductivity coefficient of PCM is less than 0.25 (0.125)W/(m K), and it can be ignored above this value. Furthermore, selecting the PCM with a density of 1000kg/m<sup>3</sup> is suitable considering the characteristics of lightweight walls.
- Under suitable PCM parameters compared to the reference wall (no PCM), the  $\varphi$  increases by 6.86h, the  $f$  decreases by 90.45%, the  $q_{peak}$ ,  $q_{ave}$  and  $Q_c$  reduced by 66.52%, 33.39% and 18.24%. Furthermore, the liquid ratio of PCM can reach 78.86%-92.14% at the appropriate phase-transition temperature (22-32°C), which is conducive to adjust different outdoor thermal environments.

## References

- [1] C. Wang, X. Huang, S. Deng S, E. Long, J. Niu, An experimental study on applying PCMs to disaster-relief prefabricated temporary houses for improving internal thermal environment in summer, *Energy and Buildings*. 179 (2018) 301-310.
- [2] X. Chen, J. Ren, Z. Xie, K. Dong, Temperature and Energy Consumption Simulation of Phase Change Materials Applied to Building Exterior Wall, *Building Energy Efficiency*. 45(4) (2017) 56-62.
- [3] V. V. Tyagi, D. Buddhi, PCM thermal storage in buildings: A state of art, *Renewable and Sustainable Energy Reviews*. 11(6) (2007) 1146-1166.
- [4] A. D. Gracia, L. F. Cabeza, Phase change materials and thermal energy storage for buildings, *Energy and buildings*. 103 (2015) 414-419.
- [5] Q. Yan, W. He, L. Yue, Experimental study on preparation of phase change energy storage building materials by direct immersion method, *New Building Materials*. 42(6) (2015) 78-80.
- [6] B. Xu, H. Ma, Z. Lu, Z. Li, Paraffin/expanded vermiculite composite phase change material as aggregate for developing lightweight thermal energy storage cement-based composites, *Applied Energy*. 160 (2015) 358-367.
- [7] C. Barreneche, L. Navarro, A. D. Gracia, A. Ines Fernandez, L. F. Cabeza, In situ thermal and acoustic performance and environmental impact of the introduction of a shape-stabilized PCM layer for building applications, *Renewable Energy*. 85 (2016) 281-286.
- [8] J. K. Kissock, J. M. Hannig, T. I. Whitney, M. L. Drake, Testing and simulation of phase change wallboard for thermal storage in buildings, *Solar Engineering*. (1998) 45-52.
- [9] D. Feldman, D. Banu, D. W. Hawes, Development and application of organic phase change mixtures in thermal storage gypsum wallboard, *Solar Energy Materials and Solar Cells*. 36(2) (1995) 147-157.
- [10] F. Kuznik, J. Virgone, Experimental assessment of a phase change material for wall building use, *Applied Energy*. 86(10) (2009) 2038-2046.
- [11] L. Xu, H. Wang, Y. Gao, J. Wang, E. Long, R. Zhao, Study on Performance of Composite PCM (Phase-change Material)'s Adjusting Indoor Thermal Environment of Light Weight Enclosure Buildings, *Building Science*. 29(12) (2013) 45-49,107.
- [12] I. Adilkhanova, S. A. Memon, J. Kim, A. Sheriyev, A novel approach to investigate the thermal comfort of the lightweight relocatable building integrated with PCM in different climates of Kazakhstan during summertime, *Energy*. 217 (2021) 119390.
- [13] P. Marin, M. Saffari, A. De Gracia, X. Zhu, M. M. Farid, L. F. Cabeza, S. Ushak, Energy savings due to the use of PCM for relocatable lightweight buildings passive heating and

- cooling in different weather conditions, *Energy and Buildings*. 129 (2016) 274-283.
- [14] Y. Hong, L. Long, H. Zhang, R. Zou, The performance evaluation of shape-stabilized phase change materials in building applications using energy saving index, *Applied energy*. 113 (2014) 1118-1126.
- [15] N. Soares, A. R. Gaspar, P. Santos, J. J. Costa, Multi-dimensional optimization of the incorporation of PCM-drywalls in lightweight steel-framed residential buildings in different climates, *Energy and buildings*. 70 (2014) 411-421.
- [16] A. Sarri, D. Bechki, H. Bouguettaia, S. Al-Saadi, M. M. Farid, Effect of using PCMs and shading devices on the thermal performance of buildings in different Algerian climates. A simulation-based optimization, *Solar Energy*. 217 (2021) 375-389.
- [17] A. Fateh, D. Borelli, F. Devia, H. Weinlader. Summer thermal performances of PCM-integrated insulation layers for light-weight building walls: effect of orientation and melting point temperature, *Thermal Science and Engineering Progress*. 6 (2018) 361-369.
- [18] G. Zhou, Y. Yang, X. Wang, J. Cheng, Thermal characteristics of shape-stabilized phase change material wallboard with periodical outside temperature waves, *Applied Energy*. 87(8) (2010) 2666-2672.
- [19] R. A. Kishore, M. V. Bianchi, C. Booten, J. Vidal, Parametric and sensitivity analysis of a PCM-integrated wall for optimal thermal load modulation in lightweight buildings, *Applied Thermal Engineering*. 187 (2021) 116568.
- [20] E. Mohseni, W. Tang, Parametric analysis and optimization of energy efficiency of a lightweight building integrated with different configurations and types of PCM, *Renewable Energy*. 168 (2021) 865-877.
- [21] T.K. Stovall, J.J. Tomlinson, What are the potential benefits of including latent storage in common wallboard?, *27th Intersociety Energy Conversion Engineering Conference*. 117 (1995) 1-1.
- [22] D. A. Neeper, Thermal dynamics of wallboard with latent heat storage, *Solar energy*. 68(5) (2000) 393-403.
- [23] H. Wang, W. Lu, Z. Wu, G. Zhang, Parametric analysis of applying PCM wallboards for energy saving in high-rise lightweight buildings in Shanghai, *Renewable Energy*. 145 (2020) 52-64.
- [24] S. D. Zwanzig, Y. Lian, E. G. Brehob, Numerical simulation of phase change material composite wallboard in a multi-layered building envelope, *Energy Conversion and Management*. 69 (2013) 27-40.
- [25] L. Yang, Y. Qiao, Y. Liu, X. Zhang, Z. Chen, J. Liu, A kind of PCMs-based lightweight wallboards: Artificial controlled condition experiments and thermal design method

- investigation, *Building and Environment*. 144 (2018) 194-207.
- [26] X. Jin, M. A. Medina, X. Zhang, On the importance of the location of PCMs in building walls for enhanced thermal performance, *Applied energy*. 106 (2013) 72-78.
- [27] X. Jin, S. Zhang, X. Xu, X. Zhang, Effects of PCM state on its phase change performance and the thermal performance of building walls, *Building and Environment*. 81 (2014) 334-339.
- [28] A. Fateh, F. Klinker, M. Bruetting, H. Weinlaeder, F. Devia, Numerical and experimental investigation of an insulation layer with phase change materials (PCMs), *Energy and Buildings*. 153 (2017) 231-240.
- [29] X. Jin, M. A. Medina, X. Zhang, Numerical analysis for the optimal location of a thin PCM layer in frame walls, *Applied Thermal Engineering*. 103 (2016) 1057-1063.
- [30] X. Jin, D. Shi, M. A. Medina, X. Shi, X. Zhou, X. Zhang, Optimal location of PCM layer in building walls under Nanjing (China) weather conditions, *Journal of Thermal Analysis and Calorimetry*. 129(3) (2017) 1767-1778.
- [31] R. A. Kishore, M. Bianchi, C. Booten, J. Vidal, R. Jackson, Optimizing PCM-integrated walls for potential energy savings in US. Buildings, *Energy and Buildings*, 226 (2020) 110355.
- [32] R. A. Kishore, M. Bianchi, C. Booten, J. Vidal, R. Jackson, Parametric and sensitivity analysis of a PCM-integrated wall for optimal thermal load modulation in lightweight buildings, *Applied Thermal Engineering*, 187 (2021) 116568.
- [33] B. Brury. Which weather data should you use for energy simulations of commercial buildings, In: *ASHRAE Trans*. 104(2) (1998) 499 -515.
- [34] B. S. Hua, S. Tian, W. Jing, Accuracy of TMY2 and stochastic climatic model, *Hv & Ac*. 34 (1) (2004) 5-7.
- [35] National Renewable Energy Laboratory. <https://nslrdb.nrel.gov>, 2021. (Accessed 6 March 2021).
- [36] W. Xu, Research and comparison on international building energy codes & standards, *China Architecture & Building Press*. (2012) 235-260.
- [37] R. Wang, H. Hu, C. Zhao, Y. Qiu, Study on Thermal Comfort of Indoor Environment about Typical Residential Air Conditioning Room, *Chinese Journal of Ergonomics*. 24 (6) (2018) 11-16.
- [38] J.P. Liu, *Building Physics Fourth Edition*, China Building Industry Press. (2009).
- [39] X. Meng, T. Luo, Y. Gao, L. Zhang, X. Huang, C. Hou, Q. Shen, E. Long, Comparative analysis on thermal performance of different wall insulation forms under the air-conditioning intermittent operation in summer, *Applied thermal engineering*. 130 (2018)

429-438.

- [40] Y. Gao, F. He, X. Meng, Z. Wang, W. Gao, Thermal behavior analysis of hollow bricks filled with phase-change material (PCM), *Journal of Building Engineering*. 31 (2020) 101447.

### Nomenclature

$t_m$	Phase-transition temperature, (°C)
$L_p$	Phase change latent heat, (kJ/kg)
$d_p$	Thickness, (mm)
$\lambda$	Thermal conductivity, [W/(m K)], Solid (Liquid)
$c_p$	Specific heat, [J/(kg K)]
$\rho$	Density, (kg/m <sup>3</sup> )
$T_i$	The material temperature, (°C)
$T_p$	The temperature of PCM, (°C)
$h_{in}$	Convective heat transfer coefficient of inner surface, [W/(m <sup>2</sup> ·K)]
$h_{out}$	Convective heat transfer coefficient of outer surface, [W/(m <sup>2</sup> ·K)]
$A_{w,in}$	Inner surface temperature amplitude, (°C)
$A_{out}$	Outdoor air temperature amplitude, (°C)
$Q_c$	Cumulative heat gain, (W h/m <sup>2</sup> )
$H_p$	The enthalpy of PCM, (kJ/kg)
$T$	Temperature, (°C)
$t$	Time, (s)
$\alpha$	Solar radiation absorptivity of outer surface, -
$q$	Inner surface heat flux, (W/m <sup>2</sup> )
$\mu$	Solar radiation intensity, (W/m <sup>2</sup> )
$\delta$	Wall thickness, (m)
$h$	Wall height, (m)
$\beta$	Liquid fraction, -
$\varphi$	Delay time, (h)
$f$	Attenuation rate, (%)
$m$	the internal iteration number, -

### Subscripts

$x$	Wall thickness direction
$y$	Wall height direction
$i$	Representatives OSB, Glass wool or Gypsum board
$p$	Phase-Change Materials
$s$	Solid states
$l$	Liquid states
$peak$	Peak value

*ave* Average value

***Abbreviations***

LBW Lightweight Building Walls  
PCM Phase-Change Materials  
OSB Oriented Strand Board  
TMY2 Typical Meteorological Year 2

**Chapter 4. Influence of PCM parameters on the thermal  
performance of lightweight wall with different thermal resistances**

4.1	Introduction.....	4-1
4.2	Material and methods .....	4-4
4.2.1	Research flow.....	4-4
4.2.2	Physical model.....	4-4
4.2.3	Thermal boundaries.....	4-5
4.3	Effect and selection of PCM phase-transition temperatures.....	4-6
4.3.1	Effect of PCM phase-transition temperatures on the inner surface temperature of walls .....	4-6
4.3.2	The variation of liquid fraction under different phase-transition temperatures ...	4-8
4.4	Effect of other PCM parameters on evaluation indexes under different thermal resistance of original walls ( $R_{wt}$ ) .....	4-9
4.4.1	Effect of the PCM location under different $R_{wt}$ .....	4-9
4.4.2	Effect of the PCM thickness under different $R_{wt}$ .....	4-11
4.4.3	Effect of the PCM latent heat under different $R_{wt}$ .....	4-13
4.4.4	Effect of the thermal conductivity coefficient of PCM under different $R_{wt}$ .....	4-15
4.5	Summary .....	4-17
	References.....	4-19
	Nomenclature.....	4-23



## 4.1 Introduction

In recent years, lightweight buildings have been widely developed due to their construction convenience and sustainability. Nevertheless, although lightweight buildings have higher thermal insulation performance, their thermal mass (i.e., thermal storage capacity) is lower, and the suppression of temperature fluctuations is poor compared to traditional buildings [1]. However, phase-change materials (PCM) as innovative materials, within a specific temperature range, can change their physical state (solid-solid, solid-liquid) by using the temperature difference between environment and materials as the driving force to store and release large amounts of heat in small volumes and have the advantages of small temperature change and high energy storage density[2]. A related study [3] was proved that a 25mm-thick PCM wall can store the equivalent thermal energy as a 420mm-thick concrete wall. Lightweight walls integrated with PCM can directly improve their thermal inertia, stabilize the indoor thermal environment, and improve building energy savings. Therefore, lightweight buildings combined with PCM have become widely studied. Soares et al. [4] investigated the performance of adding PCM to lightweight steel buildings in Europe and found that PCM can reduce the energy demand by about 10-60% in various climate zones. Lei et al. [5] showed that PCM can reduce the heat gain of the building envelopes by 21%-32% per year in Singapore. Long et al. [6] concluded that in humid subtropical climates, the annual energy consumption of lightweight buildings with integrated PCM can be reduced by 23.85%.

Moreover, for the study of thermal performance of different walls, Zhou et al. [7] compared the thermal performance of shape-stabilized PCM, brick, foam concrete and expanded polystyrene (EPS) under outdoor periodic temperature based on the enthalpy method model. Results showed that the delay time and attenuation rate of shape-stabilized PCM were the best. Gao et al. [8] filled PCM in hollow bricks and found that the results could reduce the attenuation rate from 13.07% to 0.92%-1.93% and increase the delay time from 3.83h to 8.83h-9.83h. While Jia et al. [9] revealed that Integrating both thermal insulation material and PCM could improve the thermal performance of hollow bricks comprehensively in the thermal resistance and thermal inertia. In addition, Li et al. [10] derived from EnergyPlus simulation-based analysis that integrating PCM in a normal foamed concrete wall could reduce the yearly heating energy consumption by 4.74%. Meanwhile, Liu et al. [11] found that for LBW integrated with suitable PCM, the delay time increased to 6.86h, the attenuation rate decreased by 90.45%, the peak heat flux ( $q_{peak}$ ) and average heat flux ( $q_{ave}$ ) were reduced by 66.52% and 33.39% compared with the reference wall (no PCM). Besides, to evaluate the thermal inertia of LBW integrated with PCM, Ling et al. [12] proposed a simplified method for calculating the

heat storage coefficient of PCM by dimensional analysis and numerical simulation. Based on this method, Sun et al. [13] concluded that the thermal inertia index of LBW could be improved by 60.3% when a suitable PCM was used. In summary, PCM has been widely studied for applications in buildings, but there are considerable differences in the contribution efficiency of PCM integrated into different walls. For this reason, Wu et al. [14] analyzed the effect of wall thermal performance on the contribution efficiency of the PCM layers by establishing a phase-change heat transfer model. The results found that the wall thermal performance had a large influence on the contribution efficiency of the PCM layer. The higher the heat transfer coefficient or the lower the thermal inertia, the better the phase-change thermal storage capacity operation.

In addition, related studies found that multiple parameters of the PCM greatly affected the performance of walls integrated with PCM [15,16]. Kishore et al. [17] revealed that the PCM transition temperature was the strongest parameter affecting thermal load modulation, followed by PCM location and PCM thickness. PCM latent heat and density were next in the order of priority, specific heat and thermal conductivity showed no impact. The results of Berardi [18] and Bimaganbetova et al. [19] showed that PCM with different melting temperatures had different contribution efficiency on reducing the cooling load. Neepser [20] studied the thermodynamic properties of PCM wallboard and concluded that the optimal phase-transition temperature depended on the average room temperature, outdoor temperature and thermal resistance of the original walls ( $R_{wt}$ ). The same conclusion was reached by Adilkhanova et al. [21]. Moreover, different researchers have further views on the optimal location of PCM. Wang et al. [22] experimentally concluded that optimizing the sequence of wall material layers (PCM layer, insulation layer, and structural layer) can reduce indoor air temperature fluctuations by 31%, with the best effect of PCM layer installed on the inner side. Al-mudhafar et al. [23] found by simulation (Fluent) that the installation of PCM with higher phase-transition temperature on the outside for concrete walls (200mm) could significantly reduce the peak internal surface temperature and peak heat gain. Instead, Tunçbilek et al. [24] argued that PCM close to the exterior could not save energy, suggesting locating the PCM layers close to the interior. Bhamare et al. [25] believed that for ceilings (concrete slab) PCM was best installed near the interior side (bottom). In addition, Gao et al. [8] discovered that the inner cavities were the better choice for hollow blocks to fill PCM. Liu et al. [11] concluded that the middle was the best PCM location for LBW.

Furthermore, Meng et al. [26] studied the effect of different PCM thicknesses on indoor thermal environments in winter and found that 30-40mm-thick PCM was the best. Xiao et al. [27] discussed the effect of PCM thickness on the thermal performance of shape-stabilized

PCM wallboard in Beijing in summer and pointed out that the thickness should not exceed 20mm. While Bohórquez-Órdenes et al. [28] concluded that different structures correspond to different PCM thicknesses, the ideal PCM layer thickness of the ceiling and walls was 4 and 8 mm, respectively. Secondly, the latent heat of PCM is a major factor affecting the thermal storage capacity of PCM after the thickness was determined. when the PCM was integrated into different walls, different researchers believe that the optimal latent heat value was 178 kJ/kg [29], 175 kJ/kg [11], 125 kJ/kg [8], 90 kJ/kg [7] and 50 kJ/kg [15], respectively, but the same conclusion was reached by them that the PCM contribution efficiency started diminishing when the latent heat exceeds a certain value (optimization). This further illustrates the importance of selecting appropriate PCM parameters for different envelope structures. Also, the thermal conductivity of PCM is another important factor affecting the thermal performance of the wall, which directly affects the phase-transformation rate of PCM [30, 31]. Zhang [32] and Zhou et al. [7] discovered by simulation that  $0.5\text{W}/(\text{m}\cdot\text{K})$  was the critical value, above which the effect was smaller. However, Liu et al. [11] pointed out that the influence was more apparent when the thermal conductivity coefficient of PCM was less than  $0.25\text{W}/(\text{m}\cdot\text{K})$  for LBW. Xie et al. [33] considered that the latent heat utilization of PCM was higher when its thermal conductivity was about  $0.6\text{W}/(\text{m}\cdot\text{K})$  for a wall [ $k = 0.58\text{W}/(\text{m}^2\cdot\text{K})$ ].

With the above review, PCM has a very positive effect on the improvement of the thermal performance of walls. Nevertheless, it can be obtained that the thermal performance of the original walls has a large impact on the contribution efficiency of the PCM layer [14] and the appropriate PCM parameters are also different for different walls. For LBW, although it has good thermal insulation (greater  $R_{wt}$ ), its thermal storage capacity is poor. Besides, different LBW have large differences in the  $R_{wt}$  due to different insulation materials, whereas the  $R_{wt}$  represents the ability of the envelope to resist heat transfer. When PCM is integrated into LBW, the different  $R_{wt}$  directly affects the heat absorption and release efficiency of the PCM and then affects the contribution efficiency of PCM to improve the thermal performance of LBW. However, current research on the building walls integrated PCM are mostly focusing on a fixed structure or thermal resistance, which makes the research conclusion of PCM applicable to LBW is greatly limited. Also, the contribution efficiency of PCM in optimizing the thermal performance of different building walls is not very clear, especially for LBW with low thermal inertia. Therefore, to find the suitable application of the PCM in LBW, a typical two-dimensional LBW of different  $R_{wt}$  models was built with the heat transfer process of melting-solidifying and validated in this paper, and the enthalpy model is used to explore the influence laws of PCM parameters on the thermal performance of LBW with different  $R_{wt}$ . The research conclusions are more informative for improving the indoor thermal environment and energy

saving of different types of lightweight buildings.

## 4.2 Material and methods

### 4.2.1 Research flow

In this paper, CFD numerical simulation method is used for the study. The relevant parameters (PCM parameters and thermal resistance of the original walls,  $R_{wt}$ ) are first determined. Meanwhile, to simulate the application of different PCM parameters on different  $R_{wt}$ , typical two-dimensional model of LBW with different  $R_{wt}$  are built with the heat transfer process of melting-solidifying and validated. Afterward, the appropriate phase-transition temperatures are analyzed in section 3.1 with different  $R_{wt}$  and PCM layer locations. Then, in section 3.2, the suitable PCM location and contribution efficiency with different  $R_{wt}$  are discussed under the suitable phase-transition temperature obtained by section 3.1 through the proposed evaluation index. Subsequently, to obtain the effect rules of PCM thickness for different  $R_{wt}$ , PCM thickness is analyzed at suitable phase-transition temperature and location in section 3.3. Further on, the effect of PCM latent heat is analyzed in section 3.4. Eventually, the effect and contribution efficiency of different PCM thermal conductivity with different  $R_{wt}$  are described in section 3.5 based on the above-optimized parameters. The whole research flow can be seen in Fig. 4-1.

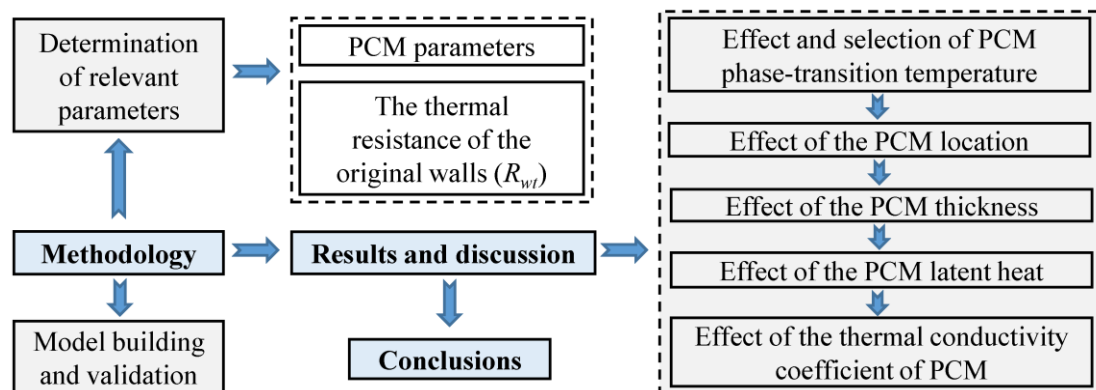


Fig. 4-1. Flow diagram of the study.

### 4.2.2 Physical model

To compare and analyze the effect of PCM parameters on the thermal performance of LBW with different  $R_{wt}$ , the physical model in Chapter 3 is used as the basis for a typical two-dimensional wall to be built, as shown in Fig. 4-2, and the thermo-physical parameters of wall materials are given in Table 4-1 [11,36,37]. On the basis of this, by changing the thermal conductivity of the insulation material,  $2.0(\text{m}^2 \text{ K})/\text{W}$  is taken as the minimum value, four levels are selected at an interval of  $1.0(\text{m}^2 \text{ K})/\text{W}$  as  $R_{wt}$  based on relevant energy-saving standards [34]

and it can be calculated by equation (1) [35]:

$$R_{wt} = \sum_{i=1}^n \frac{d_i}{\lambda_i} \quad (4-1)$$

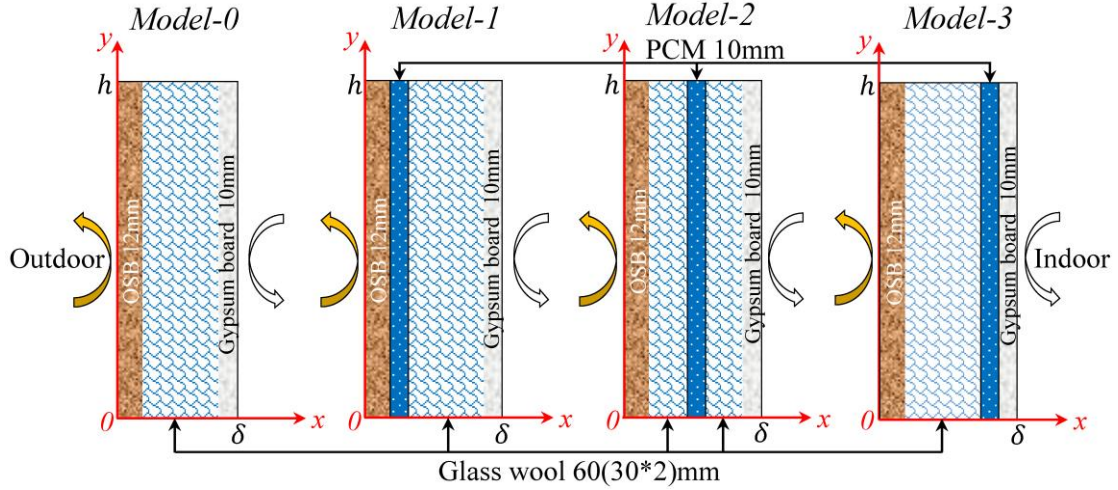


**Fig. 4-2. Schematic diagram of the two-dimensional geometric model of the LBW and the location of the PCM [11].**

**Table 4-1 Thermo-physical parameters of wall materials [11,36,37].**

Material	$t_m$ (°C)	$L_p$ (kJ/kg)	$d$ (m)	$\lambda$ [W/(m K)], Solid (Liquid)	$c_p$ [J/(kg K)]	$\rho$ (kg/m <sup>3</sup> )
PCM-1	18-28	216	0.01	0.5(0.25)	1785	1300
OSB	-	-	0.012	0.105	1400	593
Glass wool	-	-	30/60	0.035	1220	40
Gypsum board	-	-	0.01	0.33	1050	1050

### 4.2.3 Thermal boundaries

In order to explore the effects of PCM thermo-physical parameters on the different thermal resistances of the original walls ( $R_{wt}$ ) under the same thermal boundary conditions, this paper still uses the outdoor climatic conditions of Fukuoka summer from July-August in Chapter 3 (data from Typical Meteorological Year 2, TMY2 [38,39]) as the outdoor thermal boundary for numerical simulation analysis. In the meantime, to obtain the outdoor comprehensive temperature thermal boundary (solar- air,  $T_{sa}$ ), the solar radiation absorption coefficient ( $\alpha$ ) of the outer surface of the wall is taken as 0.48. Fig. 4-3 gives the variation of comprehensive temperature under outdoor air temperature and solar radiation intensity from July 30th to August 5th (7 consecutive days). In addition, the indoor air temperature still maintains 26 °C. Adiabatic boundaries were applied to the top and bottom surfaces of the numerical model, and the convective heat transfer coefficients of the inner surface ( $h_{in}$ ) and outer surface ( $h_{out}$ ) are

still  $8.7\text{W}/(\text{m}^2\cdot\text{K})$  and  $19\text{W}/(\text{m}^2\cdot\text{K})$  [9,40].

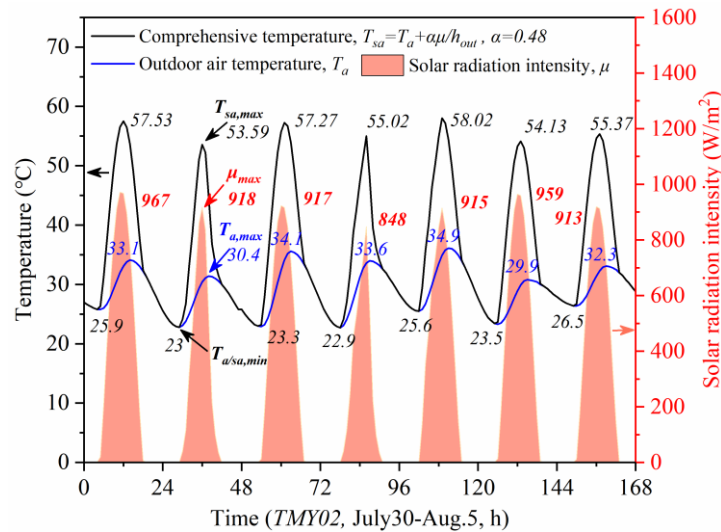


**Fig. 4-3. Variation of outdoor air temperature and solar radiation intensity with time [11,39,40].**

### 4.3 Effect and selection of PCM phase-transition temperatures

The phase-transition temperature of PCM determines the degree of phase-change, which in turn directly affects the heat absorption and release efficiency of the PCM. When the PCM is integrated into the Lightweight building walls (LBW), the thermal resistance of the original walls ( $R_{wt}$ ) and the phase-transition temperature are two important factors affecting the thermal performance of the walls under relatively stable outdoor thermal fluctuations. When the phase-transition temperature is lower or higher than the actual PCM temperature, the phase-change of PCM will not occur or rapidly occur and lead to its only thermal insulation. Moreover,  $R_{wt}$  also directly affects the heat absorption and heat release of the PCM when the phase-transition temperature is appropriate. Therefore, gaining a suitable phase-transition temperature is the primary task in this study.

#### 4.3.1 Effect of PCM phase-transition temperatures on the inner surface temperature of walls

Fig. 4-4 gives the effect of different phase-transition temperatures of PCM on the inner surface temperature at different locations and  $R_{wt}$ , which clearly shows that the fluctuation of the inner surface temperature varies widely for different phase-transition temperatures at the same location and  $R_{wt}$ . Taking Model-1 as an example, the fluctuation is gradually decreased with the phase-transition temperature raises, indicating that a suitable phase-transition temperature can obviously improve the total heat storage and release capacity of the LBW. Based on the suitable phase-transition temperature (30-40 °C), the fluctuation amplitude of the

inner surface temperature is reduced by 1.17 °C compared with that of the reference wall (1.57 °C) when the  $R_{wt}$  is 2.0(m<sup>2</sup> K)/W. However, when the  $R_{wt}$  is increased to 5.0(m<sup>2</sup> K)/W, the fluctuation amplitude only decreases from 0.64°C (reference wall) to 0.16°C. This result indicates that the effect of PCM is weakened as the  $R_{wt}$  is enhanced. The main reason for this phenomenon is that the higher  $R_{wt}$  suppresses the interference caused by outdoor temperature fluctuations. Meanwhile, the PCM is installed on the outer side, and its superior heat storage and release capability result in less temperature fluctuation on the outer surface, following the temperature transferred to the inner surface is further weakened due to the increased  $R_{wt}$ .

In addition, it can be seen that the curves of different phase-transition temperatures appear to overlap when the PCM installation location is shifted from the outside to the inside at the same  $R_{wt}$ . For Model-2 (middle), there are three curves (22-32 °C, 24-34 °C and 26-36 °C) that completely overlap, while the Model-3 (inside) overlap curves are 18-28 °C, 20-30 °C, 22-32 °C, 24-34 °C, respectively. This phenomenon is mainly caused by the actual temperature change of PCM is within the phase-transition temperature range during the interaction between indoor and outdoor, which further proves that the actual temperature change of the PCM layer determines the optimal phase-transition temperature. It is also observed that the suitable phase-transition temperature from Model-1 to Model-3 gradually descends, which indicates that the suitable phase-transition temperature is different for different PCM locations, the closer to the inside, its optimal value is also closer to the indoor temperature due to the stronger the PCM is affected by the indoor temperature under the  $R_{wt}$ . Moreover, the suitable phase-transition temperature (the number of overlapping curves) remains unchanged with the change of  $R_{wt}$  under the same PCM location, while the fluctuation of the inner surface temperature is significantly reduced, under the higher  $R_{wt}$ . It shows that the increase of  $R_{wt}$  does not affect the selection of the suitable phase-transition temperature, but it will reduce the contribution efficiency of PCM. As a consequence, the suitable phase-transition temperatures are initially determined as 30-40 °C for Model-1, 22-32 °C, 24-34 °C, and 26-36 °C for Model-2, 18-28 °C, 20-30 °C, 22-32 °C and 24-34 °C for Model-3.

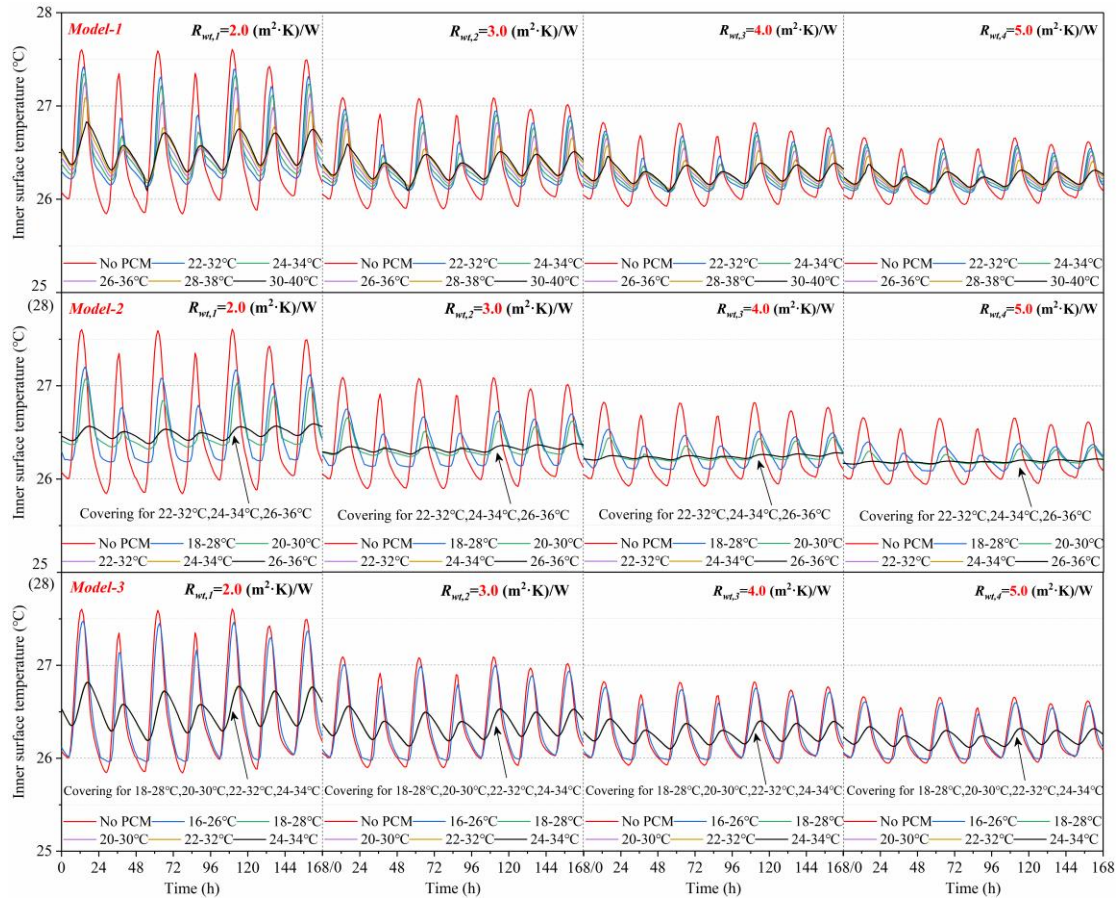


**Fig. 4-4. Variation of inner surface temperatures with time under different phase-transition temperatures and  $R_{wt}$  for Model 1-3.**

### 4.3.2 The variation of liquid fraction under different phase-transition temperatures

For the same PCM location, the PCM at different phase-transition temperatures has different degrees of phase-change. Taking Model-2 as an example, Fig. 4-5 depicts the variation of the liquid fraction (%) of PCM with time under different phase-transition temperatures. It can be drawn that the liquid fraction can reach 95.8%-100% (average value) when the phase-transition temperature is low (18-28 °C). While, the liquid fraction gradually decreased with the phase-transition temperature raises under a certain thermal resistance ( $R_{wt,1}$ ), the average liquid fraction is reduced from 99.49% to 45.90% by increasing the phase-transition temperatures from 18-28 °C to 26-36 °C. It shows that the PCM with lower phase-transition temperatures is basically in the liquid state under the action of higher indoor and outdoor temperatures, and its function is close to zero. This is why the above lower phase-transition temperature has a less inhibitory effect on the temperature fluctuation. So, selecting the appropriate phase-transition temperature can make the heat storage and release capacity of PCM play better. In addition, when the phase-transition temperatures are taken as 22-32 °C, 24-34 °C and 26-36 °C, respectively (initially determined optimal values), taking the  $R_{wt}$  as 2.0(m<sup>2</sup> K)/W can yield the

liquid fraction ranges (average value) of 79.54%-91.66% (85.93%), 59.50%-71.65% (65.91%) and 39.50%-51.66% (45.90%), respectively. As a result, the main reason is that when the phase-transition temperature is high, the actual temperature change of the PCM focuses on the low value of the phase-transition temperature ranges, and the parts above this value are basically no phase-change resulting in a lower liquid fraction. Therefore, choosing the PCM with a low phase-transition temperature at a suitable temperature will exert higher thermal storage capacity for transitional seasons.

Moreover, although the  $R_{wt}$  has less influence on the choice of phase-transition temperatures, the greater  $R_{wt}$ , the lower phase-change for PCM with the same phase-transition temperature. Reference to 22-32 °C, the liquid fraction decreased from 79.54%-91.66% (85.93%) to 78.96%-84.46% (81.84%) when the  $R_{wt}$  increased from 2.0(m<sup>2</sup> K)/W to 5.0(m<sup>2</sup> K)/W, and the fluctuation amplitude is reduced from 12.12% to 5.5%. It is suggested that the greater  $R_{wt}$ , the more stable liquid fraction within the proper phase-transition temperatures. The reason is that higher  $R_{wt}$  inhibits the heat transfer from outdoor to indoor, which makes the heat absorbed by the PCM tend to be relatively constant. Based on the above analysis, the suitable phase-transition temperatures for Model-1, Model-2 and Model-3 are finally determined to be 30-40 °C, 22-32 °C and 18-28 °C, respectively.

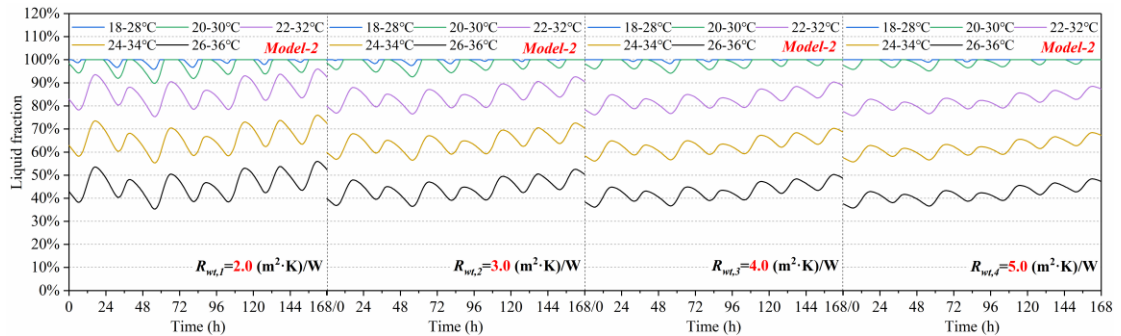


**Fig. 4-5. Variation of PCM liquid fraction with time under different phase-transition temperatures and  $R_{wt}$  for Model-2.**

#### 4.4 Effect of other PCM parameters on evaluation indexes under different thermal resistance of original walls ( $R_{wt}$ )

##### 4.4.1 Effect of the PCM location under different $R_{wt}$

The different locations of PCM in the wall determine the degree of its interaction with the indoor and outdoor environment [29]. For the thermal performance analysis of the wall, the delay time ( $\phi$ ) and attenuation rate ( $f$ ) of the inner surface temperature are two important factors affecting the indoor comfort, and the peak heat flux ( $q_{peak}$ ) and average heat flux ( $q_{ave}$ ) of the inner surface are essential elements affecting the energy-saving [8,11]. Therefore, based on the

above suitable phase-transition temperatures, the effects of different PCM locations on the thermal performance of the LBW with different  $R_{wt}$  are shown in Fig. 4-6 and it can be found that Model-1 and Model-3 have basically the same effect, all evaluation indexes are the best for Model-2 by comparison. This finding is quite different from previous studies [8,22,23,25], indicating that the suitable PCM location is strongly related to the building wall type. Compared with Model-0 (no PCM), the smaller the  $R_{wt}$ , the more significant the contribution of PCM, from Fig. 4-6(a) can be seen that the  $f$  is reduced by 4.64% for Model-2 when the  $R_{wt}$  is set to  $2.0(\text{m}^2 \text{ K})/\text{W}$ , and only 1.97% at the  $R_{wt}$  increased to  $5.0(\text{m}^2 \text{ K})/\text{W}$ . The reason for this phenomenon is that the effect of outdoor on the indoor will be suppressed with the increase of the  $R_{wt}$  and the heat absorbed by the PCM is also reduced, and the contribution efficiency of PCM will be gradually substituted by the  $R_{wt}$ . The same conclusion can be drawn from the decreasing difference between Model-1 (Model-3) and Model-2 due to the change in  $R_{wt}$ . Moreover, as shown in Fig. 4-6(b), the  $\varphi$  can be added by 3.71h-4.86h by applying PCM compared with model-0, while the change in  $\varphi$  is less as the  $R_{wt}$  is increased. This result is consistent with the literature [14]. Similarly, it can be also observed from Model-2 that the  $\varphi$  increases only by 0.43h when the  $R_{wt}$  is increased from  $2.0(\text{m}^2 \text{ K})/\text{W}$  to  $5.0(\text{m}^2 \text{ K})/\text{W}$ . This means that the effect of PCM application on  $\varphi$  is nearly independent of the  $R_{wt}$  under the same PCM location.

From Fig. 4-6 (c) and (d) can be concluded that the  $q_{peak}$  and  $q_{ave}$  can be significantly reduced when the LBW is integrated with PCM, with percentages as high as 53.02%-63.47% and 22.50%-26.01%. However, the  $q_{peak}$  is reduced from  $6.85\text{W}/\text{m}^2$ - $8.2\text{W}/\text{m}^2$  to  $2.76\text{W}/\text{m}^2$ - $3.59\text{W}/\text{m}^2$  as the  $R_{wt}$  is improved from  $2.0(\text{m}^2 \text{ K})/\text{W}$  to  $5.0(\text{m}^2 \text{ K})/\text{W}$ , the contribution efficiency of PCM is lowered by 40.29%-43.78%. The result suggests that the PCM contribution efficiency is higher for LBW of lower  $R_{wt}$  and it is resulted from that the lower  $R_{wt}$  allows the PCM layer received the thermal disturbance with the high-temperature amplitude, so it can be absorbed/released more thermal quantity. Meanwhile, the  $q_{peak}$  differences between Model-2 and Model-1 (Model-3) only decrease from  $1.35(1.39)\text{W}/\text{m}^2$  to  $0.83(0.79)\text{W}/\text{m}^2$  when the  $R_{wt}$  is enhanced from  $2.0(\text{m}^2 \text{ K})/\text{W}$  to  $5.0(\text{m}^2 \text{ K})/\text{W}$ , which can be considered that the  $R_{wt}$  has basically no effect on the selection of the suitable PCM location under the suitable phase-transition temperature. In addition, it can be easily observed that the  $q_{ave}$  is reduced by  $1.48\text{W}/\text{m}^2$ ,  $1.09\text{W}/\text{m}^2$ ,  $0.91\text{W}/\text{m}^2$  and  $0.74\text{W}/\text{m}^2$  for Model-2(optimal location) compared to Model-0 (no PCM) as the  $R_{wt}$  is improved from  $2.0(\text{m}^2 \text{ K})/\text{W}$  to  $5.0(\text{m}^2 \text{ K})/\text{W}$ , which is a small difference. It can summarize a conclusion that the contribution efficiency of PCM to  $q_{ave}$  is less influenced by the  $R_{wt}$ , This further illustrates that the core contribution from the PCM layer is not thermal insulation improvement but thermal adjustment enhancement.

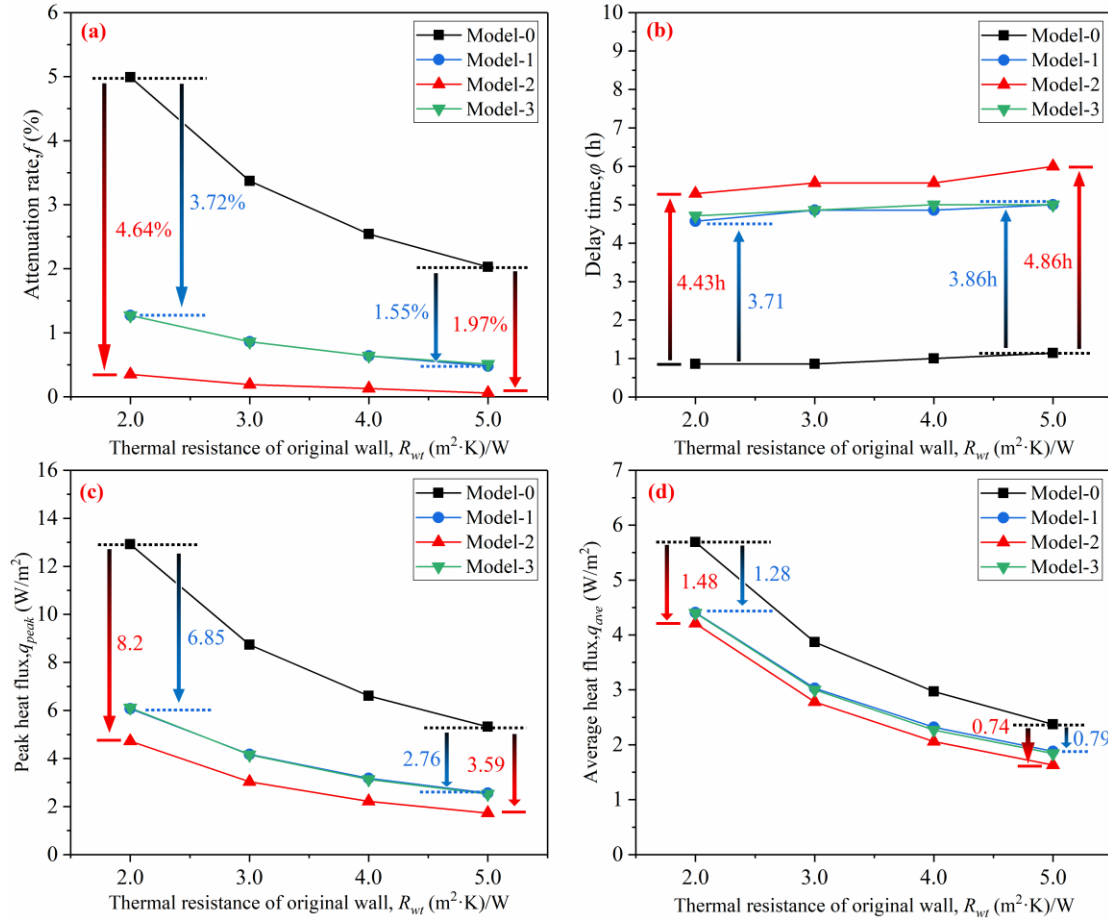


**Fig. 4-6. The (a) attenuation rate, (b) delay time, (c) peak heat flux and (d) average heat flux under the different PCM locations and  $R_{wt}$ .**

#### 4.4.2 Effect of the PCM thickness under different $R_{wt}$

The total thermal storage and release capacity of the wall is directly determined by the amount of PCM when other parameters are fixed. Based on the above analysis, PCM installed in the middle (Model-2) is studied on subsequent related issues in this paper. The phase-transition temperature is chosen to be 22-32 °C, and other parameters are set according to the basic value in table 1. As a result in Fig. 4-7(a) can be derived that even if the PCM is thinner (only 5mm) can still reduce the  $f$  by 79.56% for a small  $R_{wt}$  [ $2.0(m^2 \cdot K)/W$ ], however, the  $f$  is reduced by 0.67%, 0.1% and 0.09% respectively for every 5mm added. The above data can be easily determined that the contribution efficiency of PCM is not proportional to its thickness, the  $f$  gradually tends to a relatively stable state when the thickness exceeds 10mm. Furthermore, when the  $R_{wt}$  is increased from  $2.0(m^2 \cdot K)/W$  to  $5.0(m^2 \cdot K)/W$  based on 10mm PCM, the difference in  $f$  is reduced from 4.64% to 1.97%, which is equivalent to the PCM contribution efficiency is reduced by 57.54%. Meanwhile, the contribution efficiency between different PCM thicknesses also tends to be the same with the  $R_{wt}$  is enhanced. This phenomenon is

sufficient to explain that the optimal thickness exists in PCM applications, and its value shows a certain correlation with the  $R_{wt}$ . The optimal thickness of PCM is 10mm when the  $R_{wt}$  is determined to be  $2.0(\text{m}^2 \text{ K})/\text{W}$ , while it is recommended that the PCM thickness should not exceed 5mm when the  $R_{wt}$  is enhanced to  $5.0(\text{m}^2 \text{ K})/\text{W}$  or higher. Nevertheless, the above findings differ significantly from the literature [26-28], which may be caused by different PCM application environments (wall structural forms and outdoor climatic conditions). In addition, it is drawn from the  $\phi$  shown in Fig. 4-7(b) that the thicknesses of PCM have an obvious effect on it, the  $\phi$  can be added by 3.57-4h compared to 0mm when the PCM thickness is taken as 5mm. While the  $\phi$  can be increased by 6.57h-6.86h (increased by 71.5%-84.03%) when the thickness is added to 20mm compared to 5mm. Meanwhile, the  $\phi$  shows some increase (0.43h) with enhancing the  $R_{wt}$  when the thickness of PCM is less than 10mm, but beyond 10mm, the  $R_{wt}$  has little effect on the  $\phi$  (only 0.29h) under the same thickness.

Furthermore, it is observed in Fig. 4-7(c) that the conclusion is similar to Fig. 4-7(a), that is, the  $q_{peak}$  under the different PCM thicknesses gradually tends to be stable (same contribution efficiency) with the increase of  $R_{wt}$ . Meanwhile, the contribution efficiency of the PCM to inhibit the  $q_{peak}$  is declined by 57.07% when the  $R_{wt}$  is increased from  $2.0(\text{m}^2 \text{ K})/\text{W}$  to  $5.0(\text{m}^2 \text{ K})/\text{W}$  with the thickness is taken as 10mm. The above shows that it is meaningless to blindly increase PCM thickness. Meanwhile, the  $q_{ave}$  are presented in Fig. 4-7(d) shows that the increase in PCM thicknesses (more than 5mm) has little effect on it (even if the  $R_{wt}$  is small). The  $q_{ave}$  is only reduced by  $0.52\text{W}/\text{m}^2$  [ $R_{wt}$ ,  $2.0(\text{m}^2 \text{ K})/\text{W}$ ] and  $0.22\text{W}/\text{m}^2$  [ $R_{wt}$ ,  $5.0(\text{m}^2 \text{ K})/\text{W}$ ] as PCM thickness is increased from 5mm to 20mm. This phenomenon is because thicker PCM provides a higher heat storage capacity per unit surface, which leads to a higher thermal regulation mechanism. However, the additional PCM added only plays a certain role of thermal resistance for the relatively stable heat from the outside, and the total heat storage and release capacity are not fully utilized. This further illustrates that the main function of PCM is thermal regulation rather than thermal insulation. In summary, considering the cost of materials and thermal performance improvement effect, the PCM thickness should not exceed 10mm for different  $R_{wt}$ , and the PCM contribution efficiency to the performance improvement of low  $R_{wt}$  is much higher than the high  $R_{wt}$  for the same thickness. The main reason is that it not only suppresses the influence of outdoor temperature on the indoor but also reduces the heat storage and release of the PCM when the  $R_{wt}$  is large.

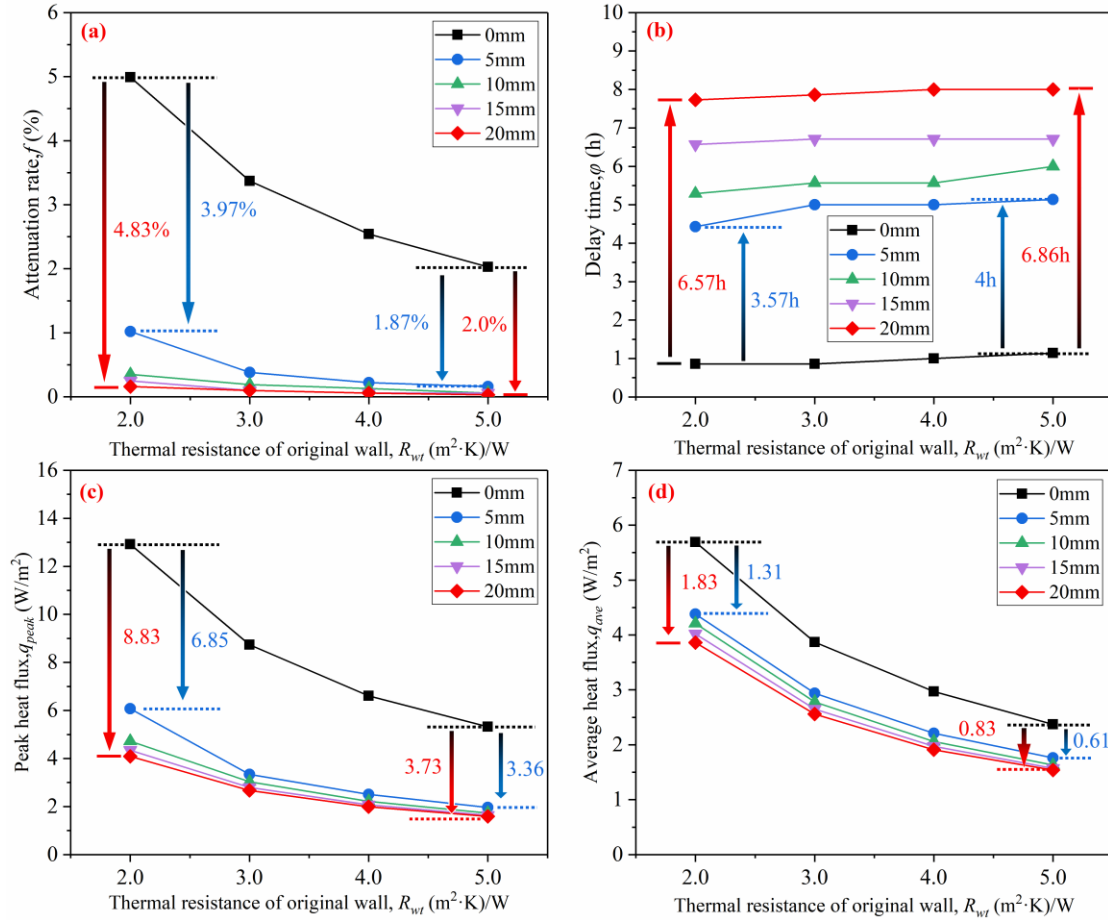


Fig. 4-7. The (a) attenuation rate, (b) delay time, (c) peak heat flux and (d) average heat flux under the different PCM thicknesses and  $R_{wt}$ .

#### 4.4.3 Effect of the PCM latent heat under different $R_{wt}$

The thermal storage and release capacity of PCM is mainly measured by PCM latent heat under the appropriate phase-transition temperature. The thermal inertia of LBW can be enhanced by integrating PCM, but the magnitude is closely related to the latent heat of PCM. For this reason, five groups of data are selected as the research indicators from 25 kJ/kg to 225 kJ/kg with an interval of 50 kJ/kg based on the above-optimized parameters to analyze the effects of different latent heats on the thermal performance of walls with different  $R_{wt}$ . As shown in Fig. 4-8(a) and (b), the greater the latent heat, the lower the  $f$  and the greater the  $\phi$  at the same  $R_{wt}$ . With the latent heat increasing from 25kJ/kg to 225kJ/kg, the  $f$  can be reduced by 86.67%-84.72% and the  $\phi$  is improved by 1.57h-2h. The  $f$  is reduced by 92.99%-97.04% and the  $\phi$  can be increased by 2.43h-5h compared to the reference wall (no PCM). Furthermore, the effect of increasing latent heat on the  $f$  and  $\phi$  is more noticeable when the  $R_{wt}$  is small. As the  $R_{wt}$  increased from 2.0( $m^2 \cdot K$ )/W to 5.0( $m^2 \cdot K$ )/W, the contribution efficiency of the latent heat increment (from 25 kJ/kg to 225 kJ/kg) on the  $f$  decreased by 79.9%, and the  $\phi$  decreased from

2h to 1.57h. Meanwhile, it is easy to find that the  $f$  and  $\varphi$  also have a substantial improvement even if the latent heat is chosen to be small 25kJ/kg, the contribution can be 54.11%-77.83% and 282.56%-300.88% compared to the reference wall. It means that the heat storage and release capacity of the wall have a remarkable effect on thermal performance. In addition, it is easy to see that the PCM contribution efficiency is significantly reduced as the latent heat continues to increase beyond 125 kJ/kg. From 25 kJ/kg to 125 kJ/kg at low  $R_{wt}$  [2.0(m<sup>2</sup> K)/W], the  $f$  decreases by 1.59%, yet is reduced by only 0.35% from 125 kJ/kg to 225 kJ/kg. Similar conclusions are also drawn in Fig. 4-8(b). This phenomenon has a similar conclusion to the increased PCM thickness, that is, its heat storage capacity is improved with the increase in latent heat, but beyond a certain value, its effect gets stable because of the limited outdoor heat.

Besides, it is also evident from Fig. 4-8(c) that the smaller the  $R_{wt}$  [2.0(m<sup>2</sup> K)/W], the higher the contribution on the reduction of  $q_{peak}$  (40.66%) when the latent heat is raised from 25 kJ/kg to 225 kJ/kg, while its contribution drops to 31.76% when the  $R_{wt}$  is set to 5.0(m<sup>2</sup> K)/W. Meanwhile, when the latent heat is determined (such as 125 kJ/kg), the  $q_{peak}$  decreases by 7.51W/m<sup>2</sup>, 5.41W/m<sup>2</sup>, 4.17W/m<sup>2</sup>, and 3.42W/m<sup>2</sup>, respectively for each 1.0(m<sup>2</sup> K)/W increase in  $R_{wt}$  from 2.0(m<sup>2</sup> K)/W to 5.0(m<sup>2</sup> K)/W. This phenomenon is mainly due to the increase in  $R_{wt}$  inhibiting the heat absorption and release of the PCM, resulting in a lower contribution efficiency of the PCM in reducing the  $q_{peak}$ . The results show that the latent heat is not proportional to the improvement of thermal performance, the differences of latent heat basically converge with the  $R_{wt}$  is boosted. So it can be presumed that the optimal value of latent heat under higher  $R_{wt}$  is less than that of a low  $R_{wt}$ . However, these results are quite different from the previous findings, where the effect tends to be relatively stable after latent heat exceeds 178 kJ/kg [29], 175 kJ/kg [11], 125 kJ/kg [8], 90 kJ/kg [7] and 50 kJ/kg [15]. It indicates that different structures (or  $R_{wt}$ ) are a very important factor affecting the optimal latent heat selection of PCM. Furthermore, Fig. 4-8(d) reveals that the  $q_{ave}$  reduction rate is less affected by the latent heat is heightened for the same  $R_{wt}$ , although these difference starts to increase under different latent heats as the  $R_{wt}$  is enlarged, the result is negligible which is only increased from 0.05 W/m<sup>2</sup> to 0.18 W/m<sup>2</sup>. This further illustrates that the PCM only adjusts the temperature fluctuation through its inherent thermal mass but does not weaken the heat transfer effect to a certain extent.

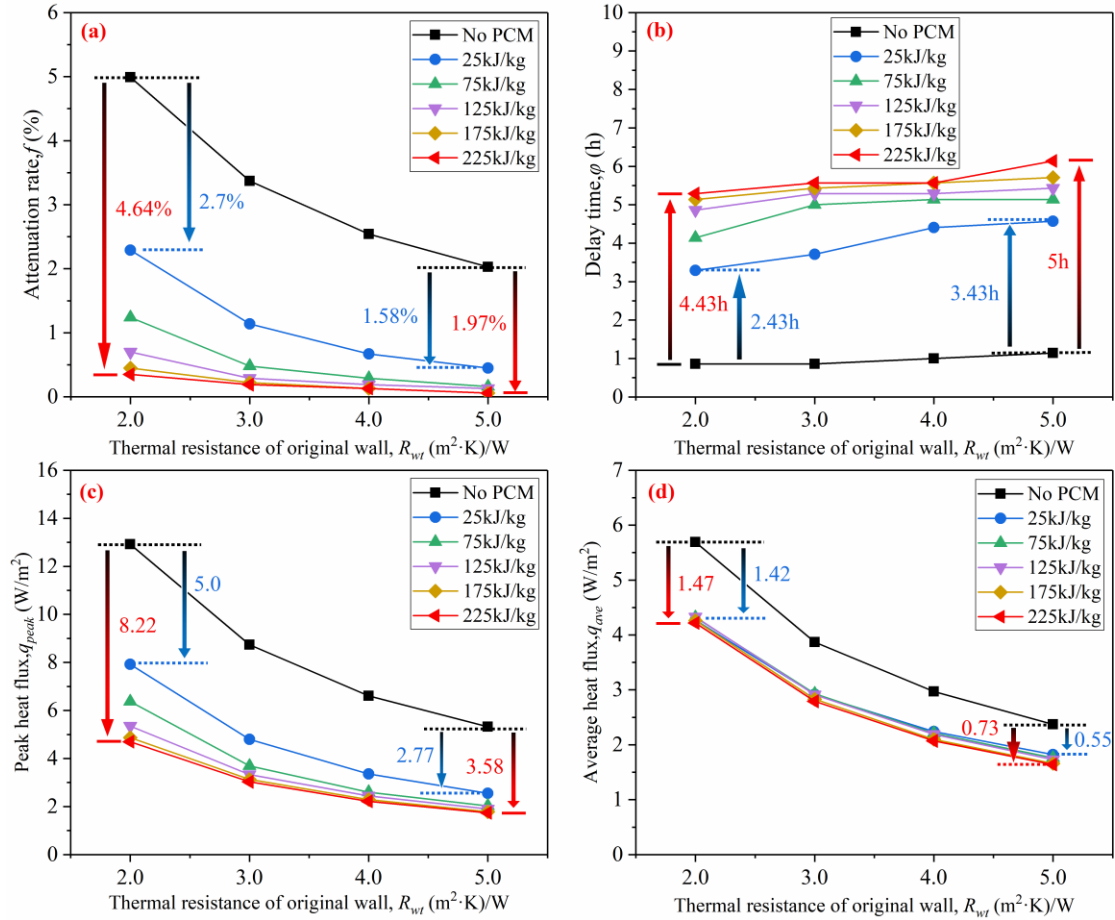


**Fig. 4-8. The (a) attenuation rate, (b) delay time, (c) peak heat flux and (d) average heat flux under the different PCM latent heat and  $R_{wt}$ .**

#### 4.4.4 Effect of the thermal conductivity coefficient of PCM under different $R_{wt}$

The thermal conductivity coefficient affects the thermal insulation performance of the material, indoor comfort and energy consumption of the building. Thus, four groups of different thermal conductivity coefficient values [solid (liquid),  $W/(m \cdot K)$ ] of PCM from minor to large are selected for analysis, and other parameters are set according to the basic value in table 1 except for the above optimization PCM parameters (includes: middle location, 22-22°C, 10mm thickness, 125 kJ/kg latent heat). As shown in Fig. 4-9(a) indicates the  $f$  change is small when the thermal conductivity is changed from 0.75 (0.375) to 0.05 (0.025), and the difference is smaller (only 0.07%) as the  $R_{wt}$  is heightened [5.0( $m^2 \cdot K$ )/W]. It is mainly due to the thinness of the PCM (only 10mm), whose variation in thermal conductivity has a small effect on the total thermal resistance of the wall, which is consistent with the results of the literature [8,17]. However, Fig. 4-9(b) shows that the smaller the thermal conductivity, the longer  $\phi$ . While the high  $\phi$  cannot be noticed for indoor thermal comfort under the small  $f$  (only 0.06%-0.73%, which leads to internal surface temperature fluctuations of less than 0.5 °C [8]). Meanwhile, it

can be clearly seen that the  $\varphi$  variation range is 0.28h-0.85h for different  $R_{wt}$  when the thermal conductivity is reduced from 0.75(0.375) to 0.25(0.125), while the  $\varphi$  variation range is increased to 1.57h-2.86h when the thermal conductivity is reduced from 0.25(0.125) to 0.05(0.025). The results are caused by a high total thermal resistance (due to low thermal conductivity coefficient) of the wall prevents the impact of outdoor temperature peak period on indoor temperature, and the thermal storage effect of PCM is also delayed. In the meantime, the reference wall is compared to suggest that the  $\varphi$  enhances 5.85h-7.86h and the  $f$  reduces 90.98%-97.04% respectively when the thermal conductivity is determined to be 0.05(0.025). It can be clearly shown that the phenomena are mainly caused by the PCM latent heat.

Similar conclusions are also drawn in Fig. 4-9(c) and (d), that is, the influence degree on the  $q$  is more evident after reducing from 0.25(0.125) to 0.05(0.025). It shows that the contribution efficiency of PCM thermal conductivity less than 0.25 (0.125) is higher when the PCM is integrated into the LBW, however, this contribution gradually tends to be the same as the  $R_{wt}$  is increased. In addition, taking the optimal value of 0.05 (0.025) as an example, compared to the reference wall when the  $R_{wt}$  is increased from 2.0(m<sup>2</sup> K)/W to 5.0(m<sup>2</sup> K)/W, the reduction of  $q_{peak}$  is reduced from 8.54W/m<sup>2</sup> to 3.56W/m<sup>2</sup> and the  $q_{ave}$  is reduced from 1.91W/m<sup>2</sup> to 0.73W/m<sup>2</sup>. It is clear that even if the thermal conductivity is low, its contribution efficiency will be decreased as the  $R_{wt}$  increases. However, it can still reduce 66.10%-66.92% of the  $q_{peak}$  and 30.8%-33.57% of the  $q_{ave}$  compared to the reference wall (no PCM). As a result, a suitable PCM integrated into LBW can not only suppress temperature fluctuations but also help to improve the building energy-saving.

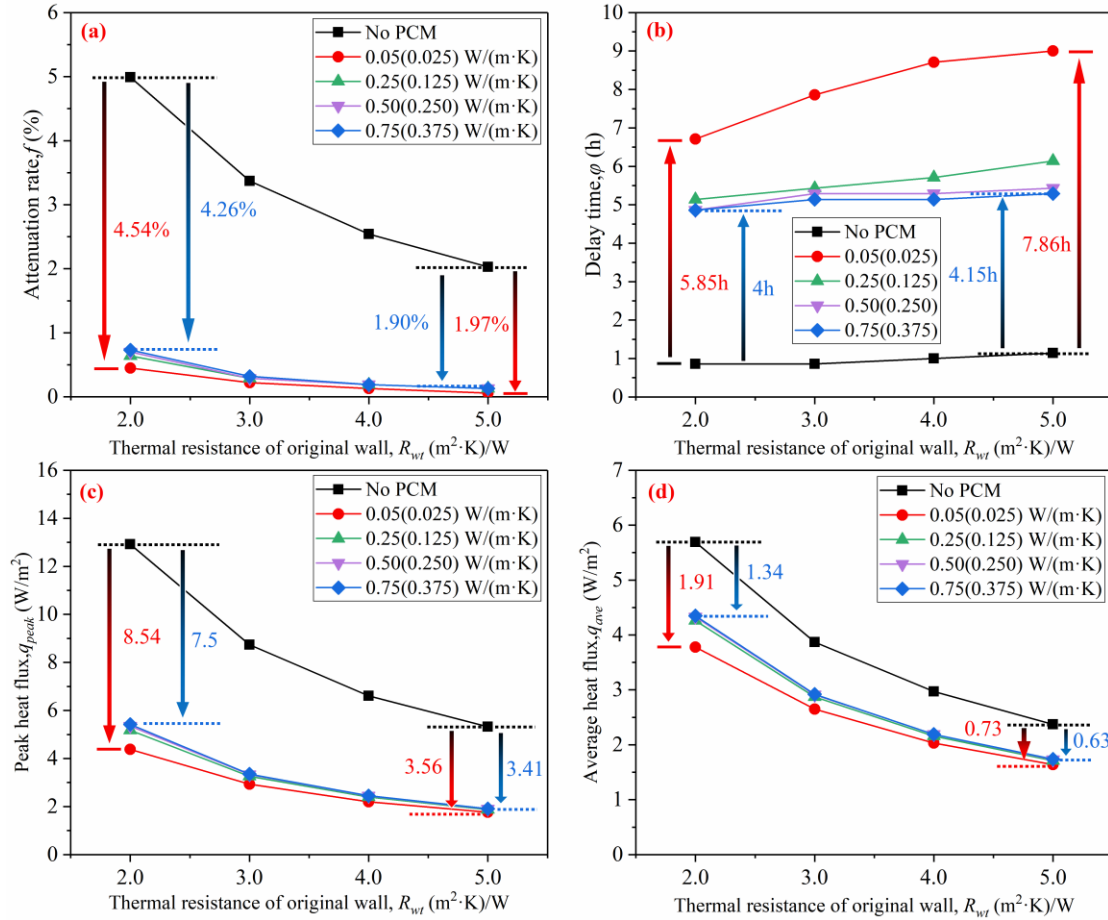


**Fig. 4-9. The (a) attenuation rate, (b) delay time, (c) peak heat flux and (d) average heat flux under the different thermal conductivity coefficients of PCM and  $R_{wt}$ .**

#### 4.5 Summary

The effect of PCM on the thermal performance of lightweight building walls (LBW) depends mainly on the heat absorption and release of PCM. However, the absorption and release efficiency of the PCM is influenced by the thermal resistance of the original walls ( $R_{wt}$ ), which then affects its contribution efficiency to improve the thermal performance of LBW. Therefore, typical two-dimensional heat-transfer models of LBW with different  $R_{wt}$  were built in this paper to analyze the influence laws and contribution of PCM parameters on the thermal performance of LBW with different  $R_{wt}$ . The main conclusions are gained as follows:

- LBW with integrating PCM can significantly improve their thermal performance. The suitable phase-transition temperature of PCM is more correlated with PCM location and less correlated with  $R_{wt}$ , but the greater the  $R_{wt}$  the lower the degree of phase-change of the PCM.
- Under a suitable phase-transition temperature, the difference between PCM installation on

the inside and outside is small and the suitable PCM location is almost independent of  $R_{wt}$ , the middle of the wall is the best choice for PCM installation.

- Based on suitable phase-transition temperature (22-32°C) and location (middle), PCM thickness is not proportional to its contribution efficiency, and its influence is more noticeable as the  $R_{wt}$  decreased. Also, the contribution efficiency between different PCM thicknesses tends to be the same with the  $R_{wt}$  is enhanced. In addition, the optimal thickness exists in PCM applications, and its value shows a certain correlation with the  $R_{wt}$ . The optimum thickness is 10mm when the  $R_{wt}$  is 2.0(m<sup>2</sup> K)/W, while no more than 5mm is recommended when the  $R_{wt}$  is enhanced to 5.0(m<sup>2</sup> K)/W or higher.
- The smaller the  $R_{wt}$ , the more obvious the effect of PCM latent heat. The optimal latent heat corresponding to low  $R_{wt}$  is 125 kJ/kg, beyond which the contribution efficiency of latent heat increment can be neglected. Meanwhile, the optimal value and its contribution efficiency are diminished and gradually converge with the  $R_{wt}$  is boosted.
- The influence and contribution efficiency with thermal conductivity less than 0.25(0.125)W/(m K) are more prominent, while its advantages gradually disappear with the increase of  $R_{wt}$ .
- Under suitable PCM parameters compared to the reference wall (no PCM), when the  $R_{wt}$  increased from 2.0(m<sup>2</sup> K)/W to 5.0(m<sup>2</sup> K)/W, the attenuation rate ( $f$ ) can be reduced by 90.98%(4.99%)-97.04%(2.03%), the delay time ( $\varphi$ ) increases 5.85h(0.86h)-7.86h(1.14h), the peak heat flux ( $q_{peak}$ ) and average heat flux ( $q_{ave}$ ) can be reduced by 66.10%(12.92W/m<sup>2</sup>)-66.92%(5.32W/m<sup>2</sup>) and 33.57%(5.69W/m<sup>2</sup>)-30.8%(2.37W/m<sup>2</sup>), respectively.

This paper delves into the appropriate parameters and applications of PCM under different  $R_{wt}$  of LBW, and the research conclusions are more informative for improving the indoor thermal environment and energy saving of different types of lightweight buildings. However, the study in this paper is analyzed in the same thermal environment, but the application effect of PCM is not only related to PCM parameters and  $R_{wt}$  but also different climates have different effects on the application of PCM. Meanwhile, the outdoor thermal environment of the wall in different directions is also quite different due to the shading effect of the actual building, especially the solar radiation intensity. This difference directly determines the thermal boundary conditions of the walls in different directions. Therefore, the application of PCM in different climates (or walls with different directions) will be the focus of future research.

## References

- [1] B. N émeth, A. Ujhidy, J. T óth, J. Gyenis, T. Feczko, Testing of microencapsulated phase-change heat storage in experimental model houses under winter weather conditions, *Building and Environment* 49 (2021) 108119.
- [2] A. D. Gracia, L. Navarro, J. Coma, S. Serrano, J. Roman í G. Pérez, L. F. Cabeza, Experimental set-up for testing active and passive systems for energy savings in buildings—lessons learnt, *Renewable and Sustainable Energy Reviews* 82 (2018) 1014-1026.
- [3] R. Cai, Z. Sun, H. Yu, E. Meng, J. Wang, M. Dai, Review on optimization of phase change parameters in phase change material building envelopes, *Journal of Building Engineering* 35 (2020) 101979.
- [4] N. Soares, A. R. Gaspar, P. Santos, J. J. Costa, Multi-dimensional optimization of the incorporation of PCM-drywalls in lightweight steel-framed residential buildings in different climates, *Energy and buildings* 70 (2014) 411-421.
- [5] J. Lei, J. Yang, E. H. Yang, Energy performance of building envelopes integrated with phase change materials for cooling load reduction in tropical Singapore, *Applied Energy* 162 (2016) 207-217.
- [6] X. Long, W. Zhang, Y. Li, L. Zheng, Thermal performance improvement of lightweight buildings integrated with phase change material: An experimental and simulation study, *Advances in Mechanical Engineering* 9(6) (2017) 1-8.
- [7] G. Zhou, Y. Yang, X. Wang, J. Cheng, Thermal characteristics of shape-stabilized phase change material wallboard with periodical outside temperature waves, *Applied Energy* 87(8) (2010) 2666-2672.
- [8] Y. Gao, F. He, X. Meng, Z. Wang, W. Gao, Thermal behavior analysis of hollow bricks filled with phase-change material (PCM), *Journal of Building Engineering* 31 (2020) 101447.
- [9] C. Jia, X. Geng, F. Liu, Y. Gao, Thermal behavior improvement of hollow sintered bricks integrated with both thermal insulation material (TIM) and Phase-Change Material (PCM), *Case Studies in Thermal Engineering* 25 (2021) 100938.
- [10] Y. Li, E. Long, L. Zhang, X. Dong, S. Wang, Energy-saving potential of intermittent heating system: Influence of composite phase change wall and optimization strategy, *Energy Exploration & Exploitation* 39(1) (2021) 426-443.
- [11] Z. Liu, J. Hou, X. Meng, B. J. Dewancker, A numerical study on the effect of phase-change material (PCM) parameters on the thermal performance of lightweight building walls, *Case Studies in Construction Materials* 15 (2021) e00758.
- [12] H. Ling, C. Chen, H. Qin, S. Wei, J. Lin, N. Li, M. Zhang, N. Yu, Y. Li, Indicators

- evaluating thermal inertia performance of envelopes with phase change material, *Energy and Buildings* 122 (2016) 175-184.
- [13] X. Sun, J. Jovanovic, Y. Zhang, S. Fan, Y. Chu, Y. Mo, S. Liao, Use of encapsulated phase change materials in lightweight building walls for annual thermal regulation, *Energy* 180 (2019) 858-872.
- [14] Q. Wu, J. Wang, X. Meng, Influence of wall thermal performance on the contribution efficiency of the Phase-Change Material (PCM) layer, *Case Studies in Thermal Engineering* 28 (2021) 101398.
- [15] R.A. Kishore, M. Bianchi, C. Booten, J. Vidal, R. Jackson, Optimizing PCM-integrated walls for potential energy savings in US. Buildings, *Energy and Buildings* 226 (2020) 110355.
- [16] J. H. Park, J. Lee, S. Wi, J. Jeon, S. J. Chang, J. D. Chang, S. Kim, Optimization of phase change materials to improve energy performance within thermal comfort range in the South Korean climate, *Energy and Buildings* 185 (2019) 12-25.
- [17] R. A. Kishore, M. V. A. Bianchi, C. Booten, J. Vidal, R. Jackson, Parametric and sensitivity analysis of a PCM-integrated wall for optimal thermal load modulation in lightweight buildings, *Applied Thermal Engineering* 187 (2021) 116568.
- [18] U. Berardi, S. Soudian, Experimental investigation of latent heat thermal energy storage using PCMs with different melting temperatures for building retrofit, *Energy and buildings* 185 (2019) 180–195.
- [19] M. Bimaganbetova, S. A. Memon, A. Sheriyev, Performance evaluation of phase change materials suitable for cities representing the whole tropical savanna climate region, *Renewable Energy* 148 (2020) 402-416.
- [20] D. A. Neeper, Thermal dynamics of wallboard with latent heat storage, *Solar energy* 68(5) (2000) 393-403.
- [21] I. Adilkhanova, S. A. Memon, J. Kim, A. Sheriyev, A novel approach to investigate the thermal comfort of the lightweight relocatable building integrated with PCM in different climates of Kazakhstan during summertime, *Energy* 217 (2021) 119390.
- [22] Z. Wang, Y. Qiao, Y. Liu, J. Bao, Q. Gao, J. Chen, H. Yao, L. Yang, Thermal storage performance of building envelopes for nearly-zero energy buildings during cooling season in Western China: An experimental study, *Building and Environment* 194 (2021) 107709.
- [23] A. H. N. Al-mudhafar, M. T. Hamzah, A. L. Tarish, Potential of integrating PCMs in residential building envelope to reduce cooling energy consumption, *Case Studies in Thermal Engineering* 27 (2021) 101360.
- [24] E. Tunçbilek, M. Arıcı, M. Krajčík, S. Nižetić, H. Karabay, Thermal performance based

- optimization of an office wall containing PCM under intermittent cooling operation, *Applied Thermal Engineering* 179 (2020) 115750.
- [25] D. K. Bhamare, M. K. Rathod, J. Banerjee, Proposal of a unique index for selection of optimum phase change material for effective thermal performance of a building envelope, *Solar Energy* 218 (2021) 129-141.
- [26] E. Meng, H. Yu, G. Zhan, Y. He, Experimental and numerical study of the thermal performance of a new type of phase change material room, *Energy conversion and management* 74 (2013) 386-394.
- [27] W. Xiao, X. Wang, Y. P. Zhang, Thermal analysis of lightweight wall with shapestabilized PCM panel for summer insulation, *J. Eng. Thermophys* 30 (2009) 1561-1563.
- [28] J. Bohórquez-Órdenes, A. Tapia-Calderón, D. A. Vasco, O. Esuardo-Flores, A. N. Haddad, Methodology to reduce cooling energy consumption by incorporating PCM envelopes: A case study of a dwelling in Chile, *Building and Environment* 206 (2021) 108373.
- [29] F. Kuznik, J. P. A. Lopez, D. Baillis, K. Johannes, Phase change material wall optimization for heating using metamodeling, *Energy and Buildings* 106 (2015) 216-224.
- [30] B. Li, S. Nie, Y. Hao, T. Liu, J. Zhu, S. Yan, Stearic-acid/carbon-nanotube composites with tailored shape-stabilized phase transitions and light-heat conversion for thermal energy storage, *Energy Conversion and Management* 98 (2015) 314-321.
- [31] A. Sari, Thermal energy storage characteristics of bentonite-based composite PCMs with enhanced thermal conductivity as novel thermal storage building materials, *Energy Conversion and Management* 117 (2016) 132-141.
- [32] Y. Zhang, K. Lin, Q. Zhang, H. Di. Ideal thermophysical properties for free-cooling (or heating) buildings with constant thermal physical property material, *Energy and Buildings* 38(10) (2006) 1164-1170.
- [33] X. Xie, B. Xu, X. Chen, G. Pei, Turning points emerging in the effect of thermal conductivity of phase change materials on utilization rate of latent heat in buildings, *Renewable Energy* 179 (2021) 1522-1536.
- [34] W. Xu, Research and comparison on international building energy codes & standards, China Architecture & Building Press, Beijing, 2012, pp. 235-280.
- [35] L. Zhang, Z. Liu, C. Hou, J. Hou, D. Wei, Y. Hou, Optimization analysis of thermal insulation layer attributes of building envelope exterior wall based on DeST and life cycle economic evaluation, *Case Studies in Thermal Engineering* 14 (2019) 100410.
- [36] C. Wang, S. Deng, J. Niu, E. Long. A numerical study on optimizing the designs of applying PCMs to a disaster-relief prefabricated temporary-house (PTH) to improve its summer daytime indoor thermal environment, *Energy* 181 (2019) 239-249.

- [37] China Academy of Building Research, Code for Thermal Design of Civil Building (GB 50176-2016), China Architecture & Building Press, Beijing, 2016.
- [38] B. S. Hua, S. Tian, W. Jing, Accuracy of TMY2 and stochastic climatic model, *Hv & Ac.* 34 (1) (2004) 5-7.
- [39] National Renewable Energy Laboratory. <https://nsrdb.nrel.gov>, 2021. (Accessed 6 March 2021).
- [40] J.P. Liu, Building Physics Fourth Edition, China Architecture & Building Press, Beijing, 2009.

### Nomenclature

$R_{wt}$	Thermal resistance of the original walls, [(m <sup>2</sup> K)/W]
$t_m$	Phase-transition temperature, (°C)
$L_p$	Phase change latent heat, (kJ/kg)
$d$	Material thickness, (m)
$\lambda$	Thermal conductivity, [W/(m K)],Solid (Liquid)
$k$	Heat transfer coefficient, [W/(m <sup>2</sup> K)]
$c_p$	Specific heat, [J/(kg K)]
$\rho$	Density, (kg/m <sup>3</sup> )
$T_i$	Material temperature, (°C)
$T_p$	PCM temperature, (°C)
$h_{in}$	Convective heat transfer coefficient of inner surface, [W/(m <sup>2</sup> ·K)]
$h_{out}$	Convective heat transfer coefficient of outer surface, [W/(m <sup>2</sup> ·K)]
$q_{peak}$	Inner surface peak heat flux, (W/m <sup>2</sup> )
$q_{ave}$	Inner surface average heat flux, (W/m <sup>2</sup> )
$H_p$	Enthalpy of PCM, (kJ/kg)
$M_t$	Measured temperatures at each hour, (°C)
$S_t$	Simulated temperatures at each hour, (°C)
$\overline{M}_t$	Average of the measured data values, (°C)
$T$	Temperature, (°C)
$t$	Time, (s)
$\alpha$	Solar radiation absorptivity of outer surface, -
$q$	Inner surface heat flux, (W/m <sup>2</sup> )
$\mu$	Solar radiation intensity, (W/m <sup>2</sup> )
$\delta$	Wall thickness, (m)
$h$	Wall height, (m)
$\beta$	Liquid fraction, -
$\varphi$	Delay time, (h)
$f$	Attenuation rate, (%)
$m$	Internal iteration number, -
$n$	Total number of hours, $t$

### Subscripts

$x$	Wall thickness direction
$y$	Wall height direction
$i$	Representatives OSB, glass wool or gypsum board

*p* Phase-change materials

*s* Solid states

*l* Liquid states

***Abbreviations***

LBW Lightweight Building Walls

PCM Phase-Change Materials

OSB Oriented Strand Board

TMY2 Typical Meteorological Year 2

## ***Chapter 5. Thermal performance analysis of lightweight wall in different directions integrated with PCM***

<i>5.1 Introduction.....</i>	<i>5-1</i>
<i>5.2 Physical model and thermal boundaries.....</i>	<i>5-3</i>
<i>5.2.1 Physical model description.....</i>	<i>5-3</i>
<i>5.2.2 Experimental system and indoor and outdoor thermal boundaries.....</i>	<i>5-4</i>
<i>5.2.3 Model validation.....</i>	<i>5-6</i>
<i>5.3 Selection of phase-transition temperature of PCM for walls in different directions .....</i>	<i>5-7</i>
<i>5.4 Effect of the other PCM parameters on the walls of different directions.....</i>	<i>5-10</i>
<i>5.4.1 Effect of the PCM location on the walls of different directions.....</i>	<i>5-10</i>
<i>5.4.2 Effect of the PCM thickness on the walls of different directions.....</i>	<i>5-12</i>
<i>5.4.3 Effect of the PCM latent heat on the walls of different directions.....</i>	<i>5-14</i>
<i>5.4.4 Effect of the thermal conductivity coefficient of PCM on the walls of different directions.....</i>	<i>5-16</i>
<i>5.5 Summary .....</i>	<i>5-18</i>
<i>References.....</i>	<i>5-20</i>
<i>Nomenclature.....</i>	<i>5-24</i>



## 5.1 Introduction

Buildings have attracted worldwide attention due to their high energy consumption in today's relatively energy-poor situation [1]. Energy consumption for air-conditioning is rapidly increasing to create a comfortable indoor thermal environment, which has a detrimental impact on sustainable development. However, the energy consumption of air-conditioning and heating caused by the heat transfer of building envelope accounts for more than 70% of the whole life cycle energy consumption [2]. Improving the thermal performance of the building envelope is a common way to obtain a stable indoor thermal environment and reduce energy consumption [3]. Heavy structures (such as concrete and clay brick) are used as traditional techniques to enhance the thermal stability of buildings [4,5]. With the widespread development of lightweight buildings in recent years, traditional methods of heat storage no longer meet the requirements. Nevertheless, lightweight buildings usually have sizeable indoor temperature fluctuations due to lower thermal mass. Specifically, the delay and attenuation of solar radiation heat irradiated on the exterior wall in summer are not obvious, resulting in high indoor temperature. Wang et al. [6] found that the indoor temperature of light buildings in summer was up to 10 °C higher than outdoor by measurements. High indoor temperature fluctuations not only diminish indoor thermal comfort but also increase the energy consumption of air-conditioning. However, phase change materials (PCM) have been concerned as innovative materials for architecture by absorbing large amounts of heat at higher temperatures with small volumes and releasing it at lower temperatures to reach the purpose that suppressing indoor temperature fluctuations [7,8].

Kuznik and Virgone [9] and Xu et al. [10] installed shape-stabilized PCM in lightweight building walls (LBW) and found that PCM could effectively control the fluctuation and rise of indoor air temperature in summer, with the maximum indoor temperature could be reduced by 8.5 °C. Liu et al. [11] installed shape-stabilized PCM in passive heating buildings observed that it could reduce the non-uniformity of radiant temperature by 20%. In addition, to evaluate the thermal inertia of PCM integrated LBW, Ling et al. [12] proposed a simplified method for calculating the heat storage coefficient of PCM by dimensional analysis and numerical simulation. Based on this method, Sun et al. [13] concluded that the thermal inertia index of LBW could be improved by 60.3% when a suitable PCM was employed. Moreover, Adilkhanova et al. [14-17] assessed the effect of PCM applied to lightweight buildings based on different climatic conditions by using EnergyPlus. According to the studies, PCM can effectively minimize indoor discomfort, but the energy-saving rate depends on climatic conditions and the thermal insulation features of the envelope.

It can be determined from numerous studies that the PCM applied to LBW can enhance their thermal performance and keep indoor temperature fluctuations within a specific comfort level [18,19]. However, its thermal performance improvement effect mainly depends on the heat storage and release capacity of PCM, while the latent heat storage and release capacity of PCM are highly dependent on the exchange between the wall surface and the ambient thermal environment for PCM integrated LBW. [13]. As a result, many scholars have evaluated the effects of PCM on LBW under different outdoor thermal environments. Among them, Sarri et al. [20] pointed out that PCM combined with shading equipment under natural conditions was more conducive to improving indoor thermal comfort hours in most climate zones of Algerian, and its energy-saving potential can reach 44.13-59.11%. Sun et al. [21] studied the influence of PCM integrated LBW on energy consumption in humid environments. It was presented that the energy-saving rate dropped from 1.64% to 1.32% when the humidity increased from 40% to 90%, but the effect was not significant in winter. Fateh et al. [22] investigated the effects of solar radiation (solar radiation was regarded as the time-varying heat source at the boundary) and concluded that the appropriate PCM could save 75% of the heating load. Zwanzig et al. [23] discovered the high dependence of PCM performance on weather conditions through energy-saving potential analysis and emphasized the necessity of selecting different PCM in different climatic regions. For PCM itself, several parameters obtained by Kishore et al. [24] will greatly affect the performance of PCM, mainly including PCM location, phase-transition temperature, thickness, and latent heat. Zhou et al. [25] studied the effect of different PCM parameters on the delay time and attenuation coefficient of shape-stabilized phase change material wallboard based on the enthalpy method model and revealed that the phase-transition temperature was an important factor affecting the evaluation index, and there were relatively optimal values of PCM latent heat and thickness under a certain external heat disturbance. Wang et al. [26] used EnergyPlus single-zone model to study the thermal performance of PCM wall panels in lightweight buildings in Shanghai from the points of phase-transition temperature, location, and thickness. It was found that the appropriate phase-transition temperature varied for different room locations and it had seasonal differences due to different solar radiation intensities.

From previous studies, we can easily find that the integration of PCM in LBW has been widely studied and optimized, which proves its effectiveness in reducing energy consumption and improving indoor thermal comfort, but its application effect is affected by PCM parameters and outdoor thermal environment [14-17, 24, 26]. Most of the research was mainly focused on the influence of PCM on the thermal performance of LBW and the indoor thermal environment in different climatic zones or uniform climatic environments. However, the outdoor thermal

environment of the wall in different directions is quite different, especially the solar radiation intensity, due to the shading effect of the building (or itself). This difference directly determines the thermal boundary conditions of the walls in different directions, while the latent heat storage and release of PCM are highly dependent on the heat exchange between the wall surfaces and the ambient environment [13]. Hence, a small-scale lightweight building was manufactured in Qingdao and the outdoor thermal environment of the wall in different directions was tested. Based on this, a typical two-dimensional numerical model of LBW integrated PCM was built in this study and validated by experiment to evaluate the influence rules and difference of PCM on the thermal performance of the walls in different directions. At the same time, the suitable PCM parameters and the important ordering of PCM applications for the walls in different directions were proposed. The research results can provide theoretical reference and data support for the use of PCMs in lightweight buildings to maximize economic benefits.

## 5.2 Physical model and thermal boundaries

### 5.2.1 Physical model description

The main purpose of this chapter is to evaluate the appropriate PCM parameters and configurations for the walls of lightweight buildings with different orientations (different thermal boundaries). Therefore, the establishment of physical models is still based on the two-dimensional physical model in Chapter 3. However, in order to visualize more in this chapter the physical model corresponding to the study, the heat transfer model of the typical lightweight wall with different PCM locations is described again, as shown in Fig. 5-1. Among them, Model-0 is still a reference wall without PCM, then, Model-1, Model-2 and Model-3 are used as comparison models to explore the suitable PCM location in different directions for walls. The relevant thermo-physical parameters of materials are listed in Table 1.

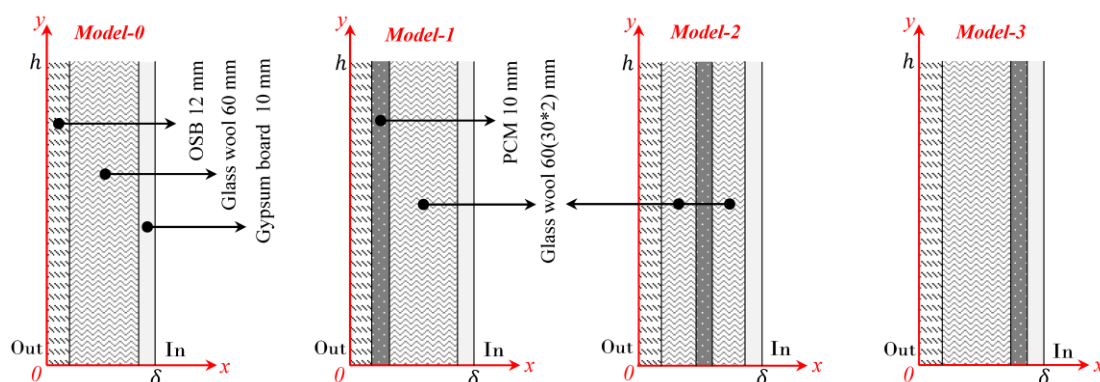


**Fig. 5-1. Schematic diagram of the two-dimensional geometric model of the LBW and the location of the PCM.**

**Table 5-1 Thermo-physical parameters of wall materials [10,27].**

Material	$t_m(^{\circ}\text{C})$	$L_p(\text{kJ/kg})$	$\lambda[\text{W}/(\text{m K})]$ , Solid (Liquid)	$c_p[\text{J}/(\text{kg K})]$	$\rho(\text{kg}/\text{m}^3)$
PCM	18-26	216	0.5(0.25)	1785	1300
OSB	-	-	0.105	1400	593
Glass wool	-	-	0.035	1220	40
Gypsum board	-	-	0.33	1050	1050
Plywood	-	-	0.17	2510	600
EPS	-	-	0.039	1380	20

### 5.2.2 Experimental system and indoor and outdoor thermal boundaries

To obtain the outdoor thermal environment variation over time for different orientations of LBW, a small-scale lightweight building was manufactured and tested in Qingdao (China), which is presented in Fig. 5-2. The test parameters mainly include solar radiation intensity of walls in different directions, indoor and outdoor air temperature, inner and outer surface temperature, inner surface heat flux intensity, and outdoor wind speed. The lightweight building (experimental system) is composed of a 1.2m×1.0m×1.0m lightweight timber structure with walls are 12mm Plywood, 20mm EPS, 20mm PCM, and 5mm Plywood in order from the outside to the inside and the relevant material parameters are shown in Table 1. For testing, four JTR05 dual-channel thermal environment testers were placed in different directions of their walls (East, West, South, North) to test the solar radiation intensity and air temperature in different directions. The inner and outer surface temperature and inner surface heat flux of the walls were recorded by the JTNT-A multi-channel temperature and heat flux tester. The JTR13 Multi-parameter outdoor weather station measured the outdoor wind speeds. Table 2 gives the accuracy and measurement range of the test instruments. The above data was recorded at 15min intervals and the test site was unobstructed during the test period, which lasted 168h from 18-24 July 2021(the hottest month of the summer).

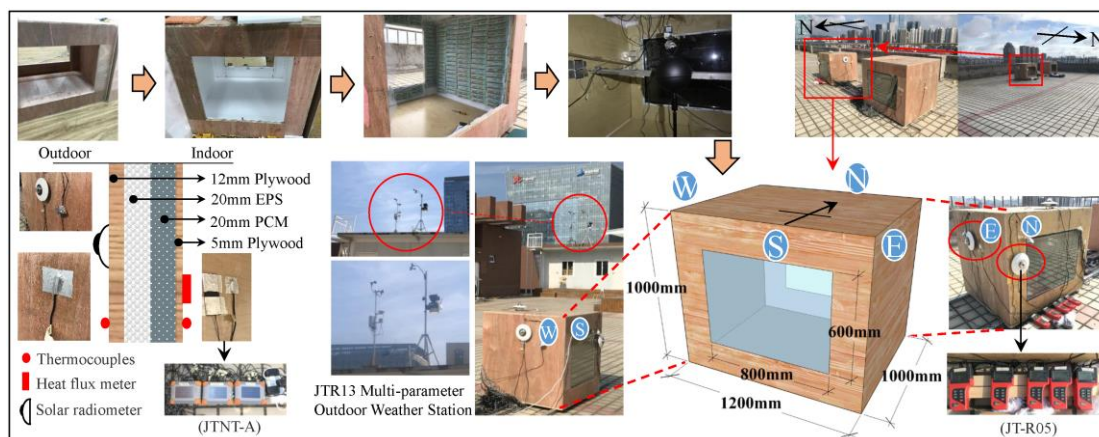


**Fig. 5-2. Experimental system and measurement point arrangement.**

**Table 5-2 Related parameters of experimental instruments.**

Test parameters	Picture	Brand and Model	Range	Accuracy	Resolution
Surface temperature		Jantytch, JTNT-A	-50°C-120°C	±0.5°C	0.1°C
Surface heat flux			0-2000W/m <sup>2</sup>	±4%	0.1W/m <sup>2</sup>
Solar radiation intensity		Jantytch, JTR05	0-2000W/m <sup>2</sup>	±2%	1W/m <sup>2</sup>
Air temperature			-50°C-50°C	±0.5°C	0.1°C
Wind speed			0-30m/s	±1m/s	0.1m/s
Wind direction		Jantytch, JTR13	16 directions (360 °)	±5%	1 °

Considering the stability of the experimental equipment and the typicality of the weather data, the data of July 22-24 (consecutive 72h) are selected for analysis in this study, as shown in Fig. 5-3. It can be obtained that the outdoor thermal environment of the wall differs considerably in different directions where the maximum difference in temperature can be 5-6 °C and the difference in solar radiation intensity is up to 68-72%. The results show that different thermal boundaries exist for the walls in different directions, which means that their thermal performance will also be quite different under different thermal boundaries. For this reason, this paper provides an in-depth analysis of the effect of different directions of LBW integrated PCM on the thermal performance of the wall based on the meteorological parameters of the measured data in different directions (see Fig. 5-3) as the outdoor thermal boundary. The indoor air temperature maintains 26 °C. Adiabatic boundaries were applied to the top and bottom surfaces of the numerical model. The indoor convective heat transfer coefficient ( $h_{in}$ ) is taken as 8.7W/(m<sup>2</sup>·K) [28,29]. However, for the outdoor convective heat transfer coefficient ( $h_{out}$ ), it is necessary to point out that the outdoor wind speed ( $v$ ) fluctuates considerably (the daily wind speed measured between 1.6m/s and 13.8m/s, with an average of 5m/s) due to the climatic characteristics of Qingdao (oceanic temperate monsoon climate). To facilitate the analysis of the numerical results, the average wind speed of 5m/s is used as the calculation boundary of the  $h_{out}$ , and it is obtained by equation (1) [28]:

$$h_{out}=5+3.6v \quad (5-1)$$

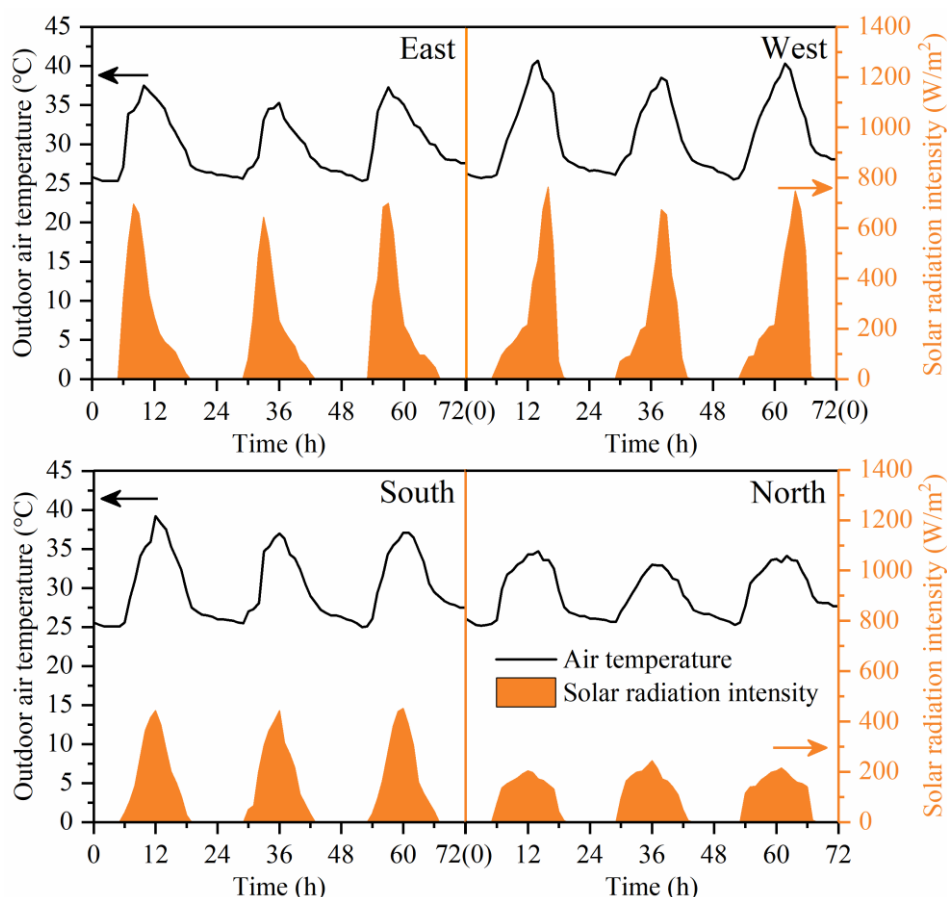


**Fig. 5-3. Variation of outdoor air temperature and solar radiation intensity over time in different directions of building.**

### 5.2.3 Model validation

To ensure the accuracy and reliability of the numerical model, the inner and outer surface temperatures of walls in different directions in the experimental system were used to validate. Fig. 5-4 gives the measured and numerical results of the walls integrated with PCM in different directions, and it can be easily found that the numerical results have the same variation trend with experiments. However, to ensure the validation accuracy, two metrics: root mean square error (RMSE) and coefficient of variation ( $CV_{(RMSE)}$ ) were employed in this study to evaluate [30,31]. Of those, the RMSE measures the average spread of errors which provided a measure for the model's dispersion [30,32],  $CV_{(RMSE)}$  is the coefficient of variation in RMSE, it is described by Equations (2-54) and (2-55), respectively.

Table 3 gives the RMSE and  $CV_{(RMSE)}$  of numerical results for the outer and inner surfaces in different directions, and it can be obtained that the maximum RMSE/ $CV_{(RMSE)}$  are 2.62°C/8.22% for the outer surface and 1.07°C/3.14% for the inner surface. The main reasons for the errors are that: (1) On the convective heat transfer boundary, the stable convective heat

transfer coefficients used in the simulation, while its convective heat transfer conditions are unstable in the experimental test due to the more complex environment, which will also make the results produce certain errors [25]; (2) The experimentally tested PCM has some supercooling effect but the supercooling was ignored in this study; (3) Considering the ideality of numerical simulation, the sensitivity and accuracy of the experimental instruments will also have some influence on the experimental results. Nevertheless, the above errors (see Table 3) are still small compared to the ASHRAE criterion of  $CV_{(RMSE)}$  less than 30% [33], indicating that the numerical models in this study can be used to solve the heat transfer problem of LBW integrated with PCM.

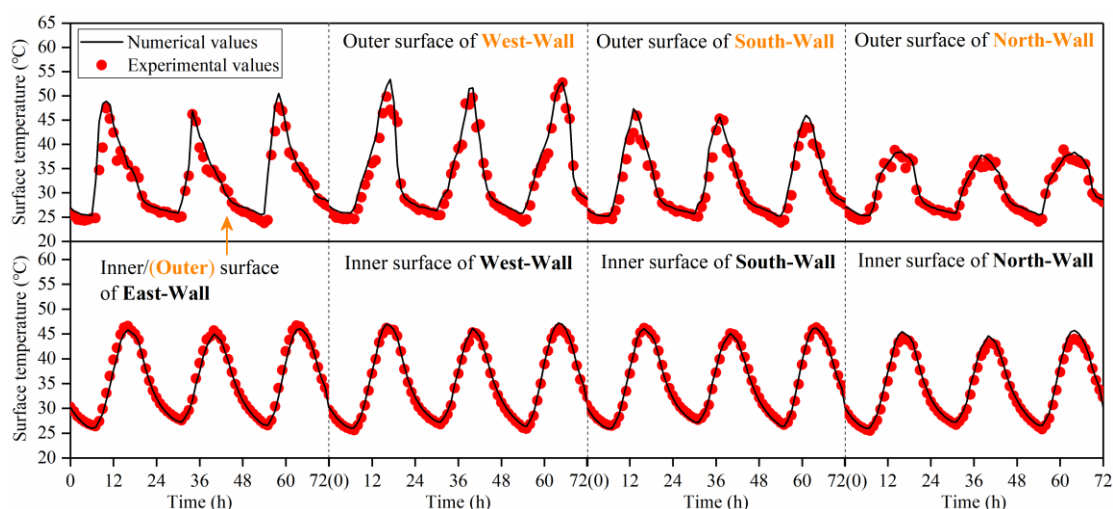


**Fig. 5-4. Comparison of numerical and experimental results of the inner and outer surface temperatures of walls in different directions.**

**Table 5-3 RMSE and CV of results for the outer/inner surface in different directions.**

Directions (outer surface/ inner surface)	East	West	South	North
RMSE (°C)	2.62/0.88	2.35/0.64	2.05/0.79	0.99/1.07
$CV_{(RMSE)}$ (%)	8.22/2.46	7.03/1.84	6.49/2.24	3.22/3.14

### 5.3 Selection of phase-transition temperature of PCM for walls in different directions

The phase-transition temperature of PCM determines the degree of phase change. The phase change will not occur or quickly complete (only acts as thermal resistance) when the phase-transition temperature is lower or higher than the actual temperature range, but both whether and how much the phase change of PCM happens depends on the overlap ratio between its temperature fluctuation and its phase-transition temperature [34]. However, when PCM is integrated into building walls, the degree of phase change is mainly decided by the heat

transferred through the wall under the interaction of indoor and outdoor thermal environments and it has a significant impact on the thermal performance of the wall. As a result, gaining a suitable phase-transition temperature is the primary task in this study.

Fig. 5-5 depicts the variation of the inner surface temperature of LBW in different directions under different phase-transition temperatures and PCM locations. It can be noted that the amplitude of internal surface temperature varies greatly under different phase-transition temperatures. Taking Model-1 as an example, the effect of inhibiting the fluctuation of internal surface temperature is weak when the phase-transition temperature is chosen to be low. This is mainly due to the PCM undergoing a rapid phase transition due to the strong thermal interaction with the outdoor temperature when the phase-transition temperature is low so that the thermal regulation ability of PCM is substantially weakened, which is proved in our previous studies [35]. However, the temperature fluctuation of the inner surface is remarkably reduced as the phase-transition temperature is raised. It indicates that an appropriate phase-transition temperature can improve the thermal storage and release capacity of PCM to suppress the effect of outdoor temperature fluctuations on the indoors. In addition, one obvious characteristic that can be seen is that many overlapping curves appear when the inner surface temperature fluctuations are minimal no matter where the PCM is installed (different locations or directions). From Model-1 can be drawn that the phase-transition temperatures corresponding to the inner surface temperature overlap curves (relative optimal) within the east and south-facing walls are 26-36 °C, and 28-38 °C respectively, while the west-facing wall has no overlap, with an optimum value of 28-38 °C. The north-facing wall has the most overlapping curves, which are 24-34 °C, 26-36 °C, and 28-38 °C severally. The main reason is that the actual temperature change of PCM is in the range of phase-transition temperature under the interaction of the outdoor and indoor temperature [35]. Meanwhile, it can also be obtained that the same phase-transition temperature exhibits different thermal performance on walls in different directions due to differences in the outdoor environment. For example, the north-facing walls at 24-34°C have reached the optimum for suppressing inner surface temperature fluctuations, while the walls in other directions need higher phase-transition temperatures. The above phenomenon indicates a significant difference in the choice of suitable phase-transition temperatures for the walls in different directions even at the same PCM location.

Furthermore, different PCM installation locations in the same wall direction also exhibit different phase-transition temperature overlapping curves. Taking the east-facing wall as an example, the phase-transition temperature of the overlapping curve decreases gradually from the outside to the inside of the PCM installation location. It shows that the heat transferred from the outdoor to the PCM gradually decreases when the PCM is located away from the outside

due to the thermal resistance of the original walls. The influence of indoor temperature on PCM is stronger than that of outdoor at this time, which is also why the phase-transition temperature is taken to be lower (or close to indoor temperature) when the PCM is installed on the inside. Based on the above results, it can be considered that the suitable phase-transition temperature of PCM should be selected according to different wall directions and PCM locations to maximize the characteristics of PCM. However, it needs to be pointed out that although the effects of suppressing the fluctuation of the inner surface temperature are similar (or same) at the above suitable phase-transition temperatures (phase-transition temperatures under the overlapping curve) mentioned, the liquid fraction of PCM is gradually decreased as the phase-transition temperature is enlarged at the lowest suitable temperature, i.e., the PCM utilization starts to be reduced, which have been found in our previous study [35]. As a result, selecting the PCM with low phase-transition temperatures among suitable phase-transition temperatures will also play a greater role in the transition season. Since the outdoor temperature selected in this study is the highest of the year, it is determined that the suitable phase-transition temperatures for Model-1 in different directions are 26-36 °C (East and South), 28-38 °C (West), and 24-34 °C (North) respectively. Model-2 are 20-30 °C (East, South, and North) and 22-32 °C (West). Model-3 is 18-28 °C in all directions.

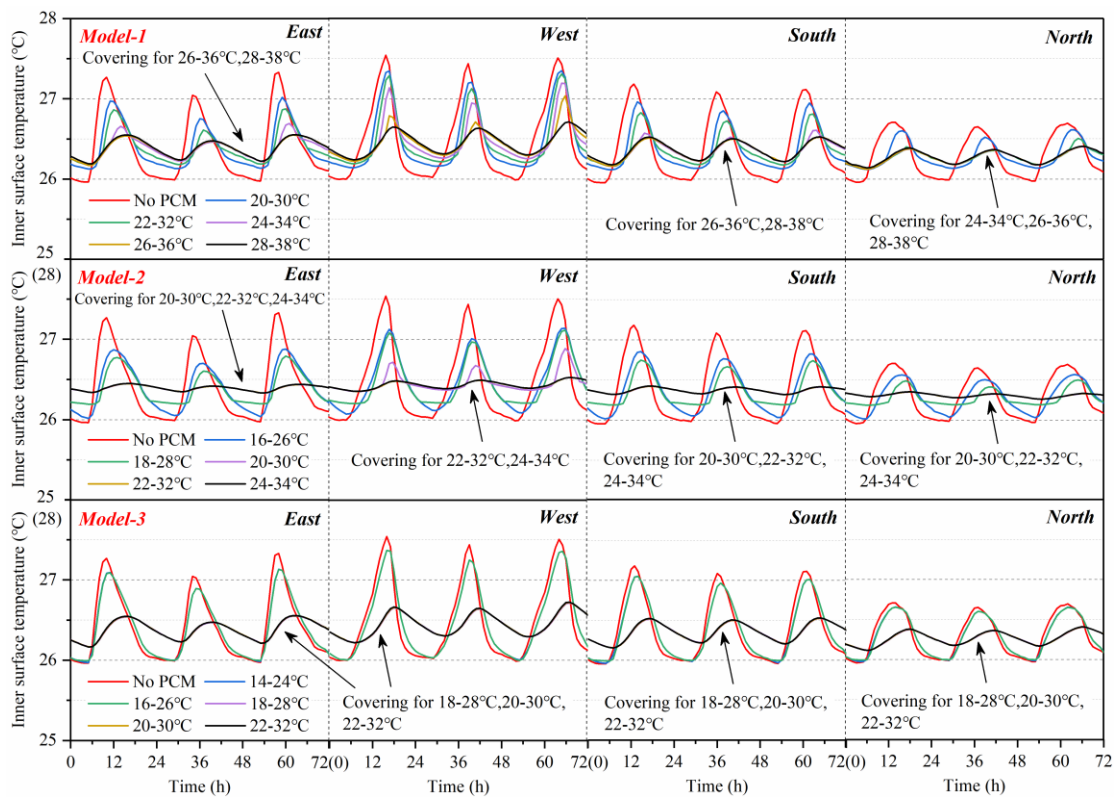


**Fig. 5-5. Variation of inner surface temperature of the wall in different directions with time under different phase-transition temperatures and locations of PCM.**

## 5.4 Effect of the other PCM parameters on the walls of different directions

### 5.4.1 Effect of the PCM location on the walls of different directions

The different locations of PCM in the wall determine the degree of interaction with the indoor and outdoor environment [24]. Meanwhile, for the thermal performance analysis of the wall, the attenuation rate ( $f$ ) and delay time ( $\varphi$ ) of the inner surface temperature are two important factors affecting the indoor comfort, and the peak heat flux ( $q_{peak}$ ) and average heat flux ( $q_{ave}$ ) of the inner surface are essential elements affecting the energy-saving [34]. Thus, based on the above suitable phase-transition temperatures, it can be noted from Fig. 5-6(a) that the selection of suitable PCM for different PCM locations can markedly reduce the  $f$  (72.7-93.4%) and improve the  $\varphi$  (2.34h-6h). Nevertheless, the  $f$  and  $\varphi$  still appear to vary considerably even if the PCM is given the suitable phase-transition temperature at different locations. Model-1 and Model-3 have basically the same effect on the thermal performance of the walls in different directions, while Model-2 performs more prominently. From the east-facing wall can be drawn that Model-1 and Model-3 can reduce the  $f$  by 75.7%-76.6% and improve the  $\varphi$  by 376% compared to the reference wall, whereas the Model-2 is noticeably better than Model-1 and Model-3, with the  $f$  can continue to be reduced based on Model-1(3) by 16%(17%) and a 1h (1h) increase in  $\varphi$ . The results show that a reasonable choice of PCM location at a suitable phase-transition temperature is also an effective way to improve the thermal performance of LBW. In addition, PCM location have nearly the same effect on the  $f$  in different directions under the appropriate phase change temperature, but the differences in  $\varphi$  are distinct. The  $\varphi$  of the west-facing wall is the shortest compared to the reference wall, basically 2.34h-2.67h, while the other directions are basically between 4.33h-6h. The above result illustrates the difference in thermal performance of the walls in different directions even though the PCM parameters are the same.

Based on the above findings, the  $q_{peak}$  and  $q_{ave}$  of the wall in different directions are presented in Fig. 5-6(b), and it is derived that the  $q_{peak}$  can be lowered obviously after adding suitable PCM to the wall in different directions, but still the best performance is Model-2. Also, taking Model-2 as an example, it can be obtained that the  $q_{peak}$  reduction rate of the walls in different directions is 64.8%, 64.4%, 62.9%, and 52.9% for the east, west, south, and north, respectively compared to the reference wall (no PCM). The result indicates that the application effects of PCM are more pronounced on the east and west-facing walls. In addition, it can be seen that the variation of PCM location has less effect on  $q_{ave}$  for the wall in different directions, but there is still some divergence on its optimal PCM location. Among them, Model-1 is more suited to north-facing walls, while Model-2 performs optimally in east-facing walls for all

evaluation indicators. Moreover, it can be seen for west-facing walls that although Model-2 is more beneficial in the  $f$  and  $q_{peak}$ , Model-3 outperforms Model-2 and Model-1 in terms of the  $\phi$  and the  $q_{ave}$ . Nevertheless, it is necessary to point out that the fluctuations of the inner surface temperature are only less than 0.5 °C under the  $f$  differs by 0.97% compared to Model-2, which can be ignored for indoor thermal comfort, and the  $q_{peak}$  is also only 1.15W/m<sup>2</sup> in difference. As a result, combining indoor thermal comfort and energy savings over the whole cycle, Model-3 is preferable for west-facing walls, where it reduces the  $q_{peak}$  by 55.7% and the  $q_{ave}$  by 14.4% compared to the reference wall. The above analysis concludes that there is an optimal PCM location for the LBW, but the optimal location is affected by the walls in different directions. East and south-facing walls are better suited to the middle of the LBW, while the inside and outside for west and north-facing walls.

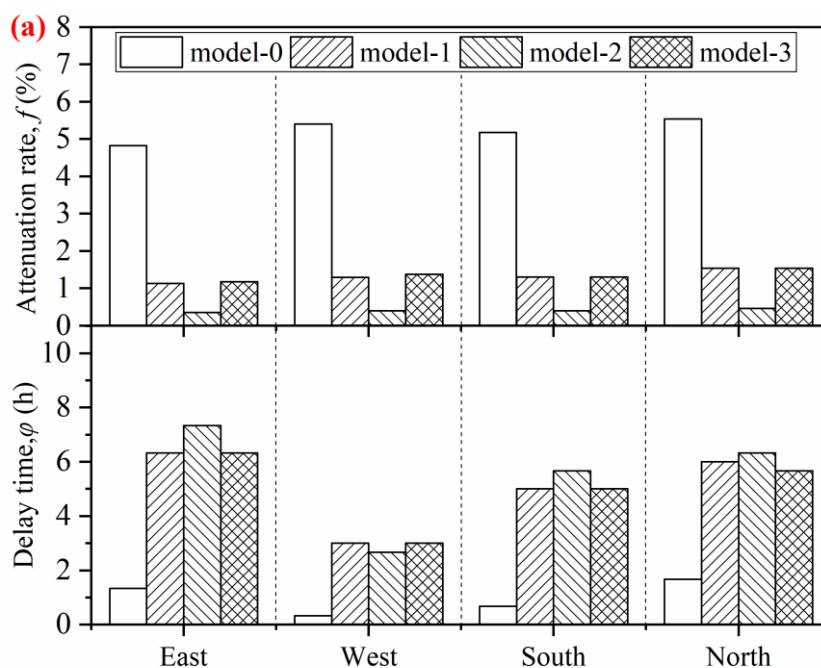


**Fig. 5-6. The (a) attenuation rate, delay time and (b) inner surface heat flux for different wall directions and PCM locations.**

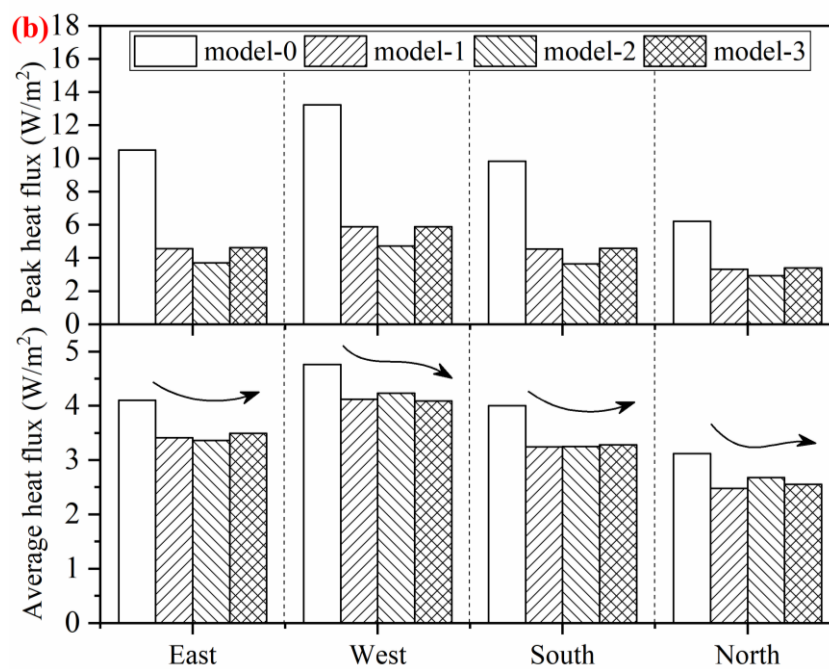


Fig. 5-6. (Continued).

#### 5.4.2 Effect of the PCM thickness on the walls of different directions

The amount of PCM is another major factor affecting the thermal performance of the LBW when other parameters are fixed. For this reason, the effect of increasing different PCM thicknesses on the thermal performance of the walls in different directions is analyzed in this paper based on the above suitable phase-transition temperature and the optimum location. The rest of the unstudied parameters are set according to the actual values. Fig. 5-7(a) demonstrates that the  $f$  can be reduced by 45.9-97.5% and the  $\phi$  can be added by 2h-8h for the wall in all directions are endowed with PCM from 5mm to 20mm based on the reference wall, suggesting that the thicker the PCM is, the better its effect on suppressing temperature fluctuations, but it is clear that its influence begins to diminish beyond a certain thickness. Taking the east-facing wall as an example, it can be found each increase of 5mm on the basis of 5mm that the  $f$  only decreases by 0.74%, 0.16%, and 0.04%, and the  $\phi$  increases by 2h, 0.66h, and 1h. From the above data, it is smaller changes in the evaluation index ( $f$  and  $\phi$ ) and cannot be noticed for improving indoor thermal comfort when the thickness exceeds 10mm ( $f$  changes only 0.04%-0.16%, which leads to internal surface temperature fluctuations of less than 0.5°C), which was also mentioned in the literature [34,36]. Furthermore, it is different regarding the  $f$  and  $\phi$  of walls in different directions when the same thickness is increased. Among them, the influence on east and south-facing walls is the most prominent, followed by the north and west-facing walls. Taking 5mm as an example, the  $f$  can be cut by 76.6% and 79.1% and the  $\phi$  added by 4.34h and 4h for east and south-facing walls respectively, while for the west and north-facing

walls, the  $f$  is only cut by 52.8% and 45.8% and the  $\varphi$  is only added by 2h and 3.33h. By contrast, in the west and north-facing walls reach the same results as the east and south-facing walls, its PCM thickness needs to be enlarged to 10mm or more. Therefore, it can be summarized that there are some differences in the amount of PCM in different directions.

However, the energy-saving effect under different thicknesses can more accurately reflect the optimal amount of PCM when the cost of PCM (increase linearly [37]) is considered. For this reason, Fig. 5-7(b) displays the heat flux of different directional walls at different thicknesses. It can be observed that the reduction effect of the  $q_{peak}$  is weakened at thicknesses above 10mm, but it is discrepant for walls in different directions. The PCM thickness is increased from 10 mm to 20 mm with  $q_{peak}$  reduction rates of 7.6%, 17.7%, 7.4%, and 9.4% for east, west, north, and south-facing walls, respectively. This phenomenon is mainly related to the different heat gain of PCM due to the different ambient environments in different wall directions, which further shows that the PCM parameters should be determined according to different directions to better perform the function of PCM. Furthermore, based on the changes in the  $q_{ave}$  it can be concluded that the increase in thickness has less effect on the  $q_{ave}$  while some differences still appear for different wall orientations. For example, for each 5mm growth based on 5mm, the  $q_{ave}$  can be reduced by 0.6%, 1.2%, and 1.5% for east-facing walls, while the west-facing walls by 0.5%, -0.5%, and -0.7% respectively. From the above data, the energy-saving effect varies for the same thickness of PCM in different directions. The  $q_{ave}$  of the west-facing wall has a negative change with increasing PCM thickness, and this feature is more noticeable in the north-facing wall. The main reason is that although the PCM can lower the peak temperature at different outdoor thermal boundaries (different directions), the additional increase in PCM is not utilized only acts as a thermal resistance due to the limited outdoor heat, and its thermal regulation capacity is gradually replaced by the increase in thermal resistance due to the thickness is added [36], which can also explain why the reduction in  $q_{peak}$  is gradually weakened with the increase in PCM thickness. At the same time, the minimum temperature is raised due to the PCM heat release, and the higher thermal resistance will lead to the indoor temperature being difficult to be transferred to the outdoors so that the  $q_{ave}$  grows rather than falls, which is similar to the conclusion of insulation materials [38]. The above results are sufficient to explain that PCM thickness is not thicker the better when integrating PCM in LBW. Considering the cost [37] and energy-saving of PCM, blindly increasing the thickness of PCM cannot yield higher benefits, and relatively optimal thickness exists for walls in different directions. Finally, founded on the above analysis, the appropriate PCM thickness for the east and west-facing walls is determined to be 10mm, and for the south and north-facing walls is 5mm when PCM application effectiveness and cost are considered simultaneously.

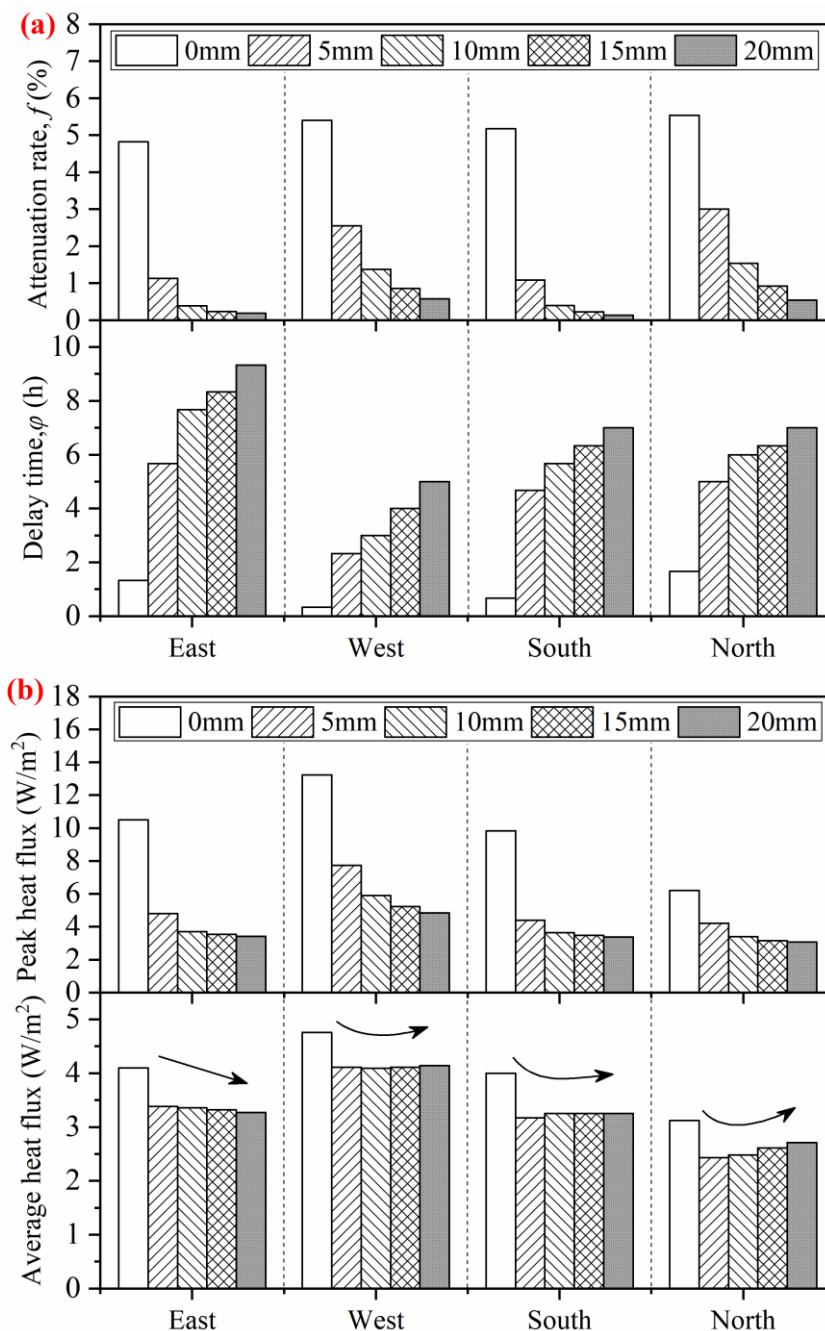


**Fig. 5-7. The (a) attenuation rate, delay time and (b) inner surface heat flux for different wall directions and PCM thicknesses.**

### 5.4.3 Effect of the PCM latent heat on the walls of different directions

The thermal inertia of LBW can be enhanced by integrating PCM, but the magnitude is closely related to the latent heat of PCM. For this purpose, five groups of data are selected from 25kJ/kg to 225kJ/kg in 50kJ/kg intervals to analyze the thermal performance of the wall in different directions. As shown in Fig. 5-8(a), the  $f$  and  $\phi$  change linearly as the latent heat of PCM is increased, with the higher the latent heat, the lower the  $f$  and the greater the  $\phi$ . Yet, the

change of the  $f$  and  $\phi$  of walls in different directions are different for the same latent heat being raised. The east-facing wall is most prominent, while the  $\phi$  for the west-facing wall and the  $f$  for the north-facing wall are less affected. For each 50kJ/kg increase based on 25kJ/kg, the decline in  $f$  are 45.1%, 37.1%, 34.6% and 31.4% for the east-facing wall and 15.1%, 13.3%, 22.5% and 17.9% for the west-facing wall respectively. In terms of the  $\phi$ , the east-facing wall can be upped to a maximum of 6h and the west-facing wall is only 2.67h. Meanwhile, it can be found that the  $\phi$  of the west-facing wall is basically unchanged when the latent heat is increased exceeds 175kJ/kg, and the  $f$  is only reduced by 0.29%, whereas the other directions of the wall also show different degrees of attenuation for improving the  $f$  and  $\phi$ . The above data indicates the effect of increasing the latent heat in different directions can be considered not very meaningful when beyond a specific value under the relatively stable outdoor heat, the relative optimum value exists in different directions, which is similar conclusions with PCM thickness.

In addition, from Fig. 5-8(b) can be discovered that the  $q_{peak}$  is greatly diminished and the  $q_{ave}$  is less variable as the latent heat is heightened. It is further explained that the main function of PCM is to regulate indoor temperature fluctuations by their superior heat storage and release capacity rather than to reduce energy consumption through insulation. At the same time, using 125kJ/kg as an example, the  $q_{peak}$  energy-saving rates for all walls compare to the reference wall can be drawn as 59.1% (East), 52.7% (West), 42.8% (South), and 20.3% (North) respectively. It shows that there is still a large distinction in the energy savings in different directions with the same latent heat, and the change in latent heat has the least effect on the north-facing walls. In another way, considering the energy savings over the whole cooling cycle, it can be concluded from the  $q_{ave}$  that for east and north-facing walls the lower the latent heat, the more energy-saving it is, nevertheless, it is still recommended 125 kJ/kg for the latent heat when the indoor thermal comfort ( $f$  and  $\phi$ ) are considered. By contrast, the west and south-facing walls show a decrease and then increase with the enhancement of latent heat, and the highest energy savings are observed at 175kJ/kg and 75kJ/kg with 13.9% and 22.3% respectively. It is mainly because the higher PCM latent heat reduces the peak temperature while also increasing the minimum temperature value by releasing latent heat that reduces the energy-saving effect in the whole cooling period. Moreover, a clear feature is displayed that even if the latent heat is chosen to be smaller at 25kJ/kg, the thermal performance of the wall is remarkably improved compared with the reference wall, the  $q_{peak}$  and the  $q_{ave}$  energy-saving rate can also reach 7.7-43.0% and 11.8-21.0% in different directions. As a result, it shows that improving the thermal storage capacity of the wall not only improves the indoor thermal environment but also helps to enhance building energy-saving.

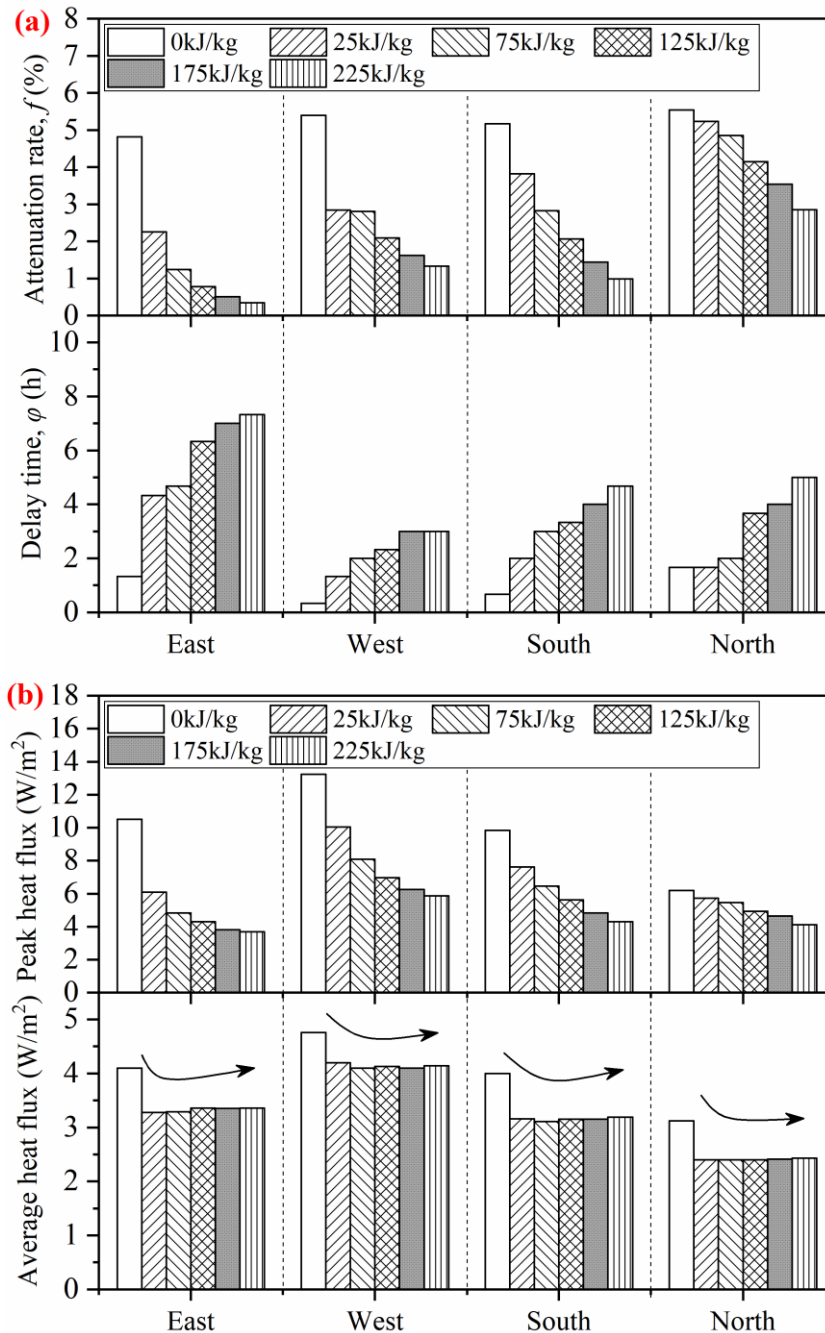


**Fig. 5-8. The (a) attenuation rate, delay time and (b) inner surface heat flux for different wall directions and latent heats of PCM.**

#### 5.4.4 Effect of the thermal conductivity coefficient of PCM on the walls of different directions

The thermal conductivity coefficient affects the thermal insulation performance of the material, indoor comfort and energy consumption of the building. Thus, Fig. 5-9 depicts the variation of wall thermal performance on different PCM thermal conductivity [solid (liquid)] based on the above all optimized parameters. From Fig. 5-9(a), a lower thermal conductivity

can dramatically reduce the  $f$  and extend the  $\varphi$ . However, the  $f$  and  $\varphi$  of the walls in different directions differ for the same thermal conductivity. For example, with a value of 0.05 (0.025) W/(m K), the  $f$  of the east and west-facing walls can be reduced by 81.5% and 85.4%, and the  $\varphi$  increased by 5.34h and 5h respectively, while the south and north-facing walls can only reduce the  $f$  by a maximum of 44.4% and 53.0%, and the  $\varphi$  is increased only 2.33 h and 3.33h. Additionally, although there are different thermal performances in different directions with the change of thermal conductivity, all show a common characteristic that its impact on the  $f$  and  $\varphi$  is more significant when the thermal conductivity is less than 0.25 (0.125) W/(m K), above this value, its impact is very small. The main reason is that the lower thermal conductivity improves the total thermal resistance of the wall, thus blocking the disturbance from outside to inside. Moreover, the change of thermal conductivity has the most significant influence on the east-facing walls in terms of the  $\varphi$ , followed by the west and north-facing walls, with a lesser effect on the south-facing walls.

In addition, as can be seen from the variation of  $q$  given in Fig. 5-9(b), the  $q_{peak}$  and the  $q_{ave}$  of the wall in different directions can be reduced by 10.1-25.3% and 5.5-14.7% when the thermal conductivity of PCM is reduced from 0.25 (0.125) W/(m K) to 0.05 (0.025) W/(m K), whereas, the reduction of the  $q_{peak}$  and  $q_{ave}$  is only 1.7-6.6% and 0.9-2.9% when it is decreased from 0.75 (0.375) W/(m K) to 0.25 (0.125) W/(m K). The results show that reducing the thermal conductivity of PCM can effectively improve the energy-saving of LBW in both  $q_{peak}$  and  $q_{ave}$ , while the effects are more noticeable after decreasing to 0.25 (0.125) W/(m K), which is consistent with previous studies [35]. Nonetheless, the energy-saving of the same thermal conductivity still shows some diversity for walls in different directions. Taking the optimal value of 0.05 (0.025) W/(m K) for example, compared with the reference wall, the reduction of the  $q_{peak}$  is 62.8% (East), 66.4% (West), 41.9% (South), and 34.8% (North), and the  $q_{ave}$  being reduced by 29.5% (East), 28.2% (West), 27.5% (South) and 27.9% (North), respectively. The above data point out that the  $q_{peak}$  energy-saving is highest for west-facing walls at the optimum PCM parameters, followed by east, south, and north-facing walls. However, unlike the  $q_{peak}$  (West > East > South > North), the reduction of  $q_{ave}$  is ordered as East > West > North > South. The difference in this order is mainly caused by the solar radiation intensity received by the walls in different directions. The stronger the solar radiation, the higher the heat gained by the PCM and the higher the heat released at the same time, which can also be explained by the west-facing wall. That is, while the  $q_{peak}$  of the west-facing wall exhibits the highest energy saving, its  $q_{ave}$  still exhibits a higher level. This result is also sufficient to indicate that the application potential of PCM will be different due to the difference in the building environment caused by different directions. Based on the above results, the east and west-facing walls are

preferred when PCM is installed on LBW under the application potential and cost of PCM are considered simultaneously, followed by the south and north-facing walls.

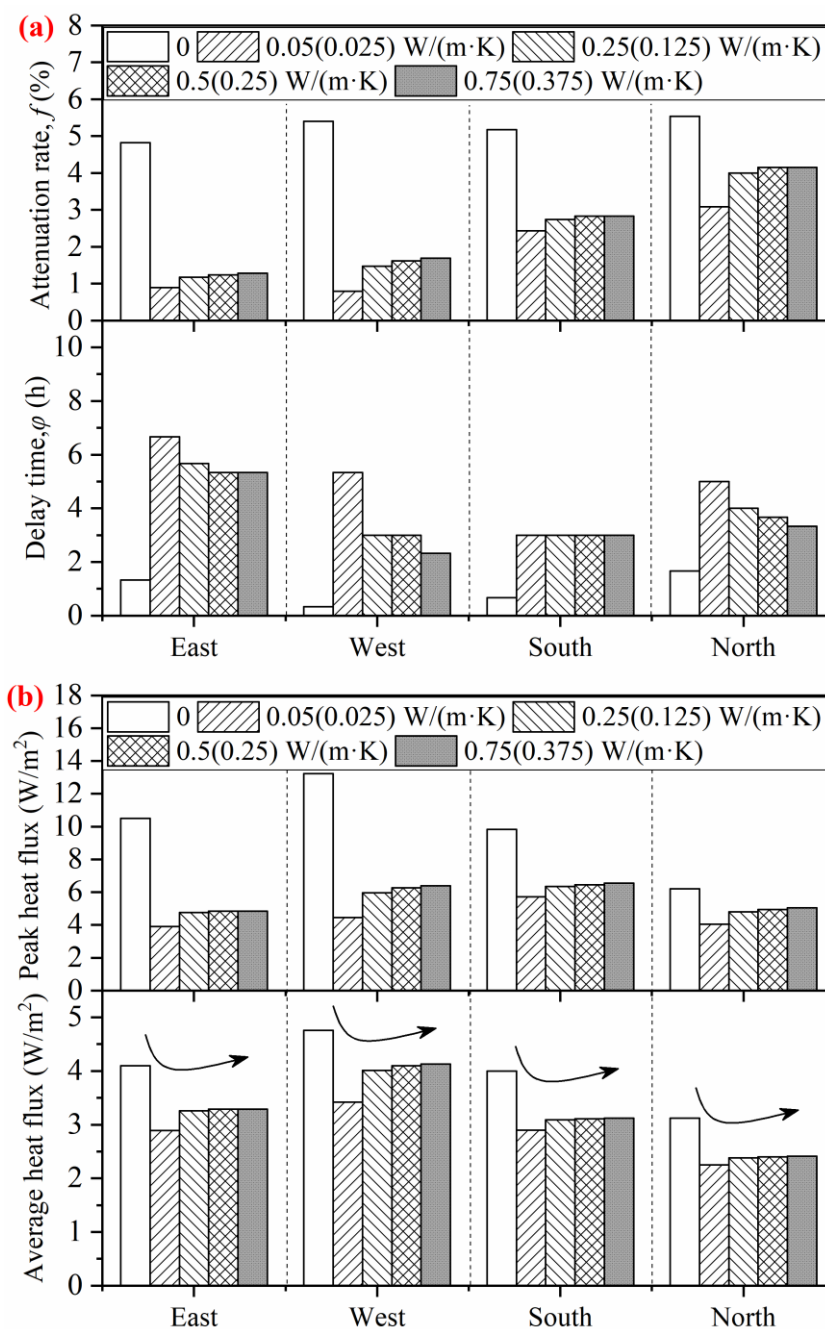


**Fig. 5-9. The (a) attenuation rate, delay time and (b) inner surface heat flux for different wall directions and thermal conductivity coefficients of PCM.**

### 5.5 Summary

The effect of PCM on the thermal performance of lightweight wall is highly dependent on the exchange between the wall surface and the ambient environment. However, the outdoor thermal environment of the wall in different directions is quite different due to the shading

effect of the building (or itself). Therefore, the effect rules and suitable parameters of PCM on the thermal performance of LBW in different directions are discussed in-depth and obtained based on measured outdoor thermal boundaries in this paper. The main conclusions are gained as follows:

- (1) PCM can effectively improve the thermal performance of LBW, but the suitable phase-transition temperature is different for different PCM installation locations (inside, middle, and outside). The suitable phase-transition temperature for Model-1 is 26-36 °C (East and South), 28-38 °C (West), and 24-34 °C (North) respectively. Model-2 are 20-30 °C (East, South, and North) and 22-32 °C (West). Model-3 is 18-28 °C in all directions.
- (2) There are different optimal locations of PCM in different directions of the wall at an appropriate phase-transition temperature. Among them, PCM installed in the east and south-facing wall is more adapted to the middle location, while the inside and outside is optimal for the west and north-facing walls, respectively.
- (3) PCM is not the thicker the better when PCM application effectiveness and cost are considered simultaneously. Optimum thicknesses exist for walls in different directions, the east and west-facing walls are 10mm and 5mm for the south and north-facing walls.
- (4) Walls with different directions exhibit different thermal performance for the same PCM latent heat. For east and north-facing walls the lower the latent heat the more energy-saving (it is recommended 125 kJ/kg when considering indoor comfort), while the west and south-facing walls show a decrease and then increase as the latent heat is increased, with the highest energy savings at 175kJ/kg and 75kJ/kg.
- (5) The thermal performance of the wall can be improved when the thermal conductivity of PCM is dropped, its improvement can be more evident for the value less than 0.25(0.125) W/(m K) based on other suitable parameters.
- (6) Under suitable PCM parameters compared to the reference wall (no PCM), the greatest improvement in thermal performance are observed in the east and west-facing walls, which reduced the  $q_{peak}$  by 62.8% and 66.4% and the  $q_{ave}$  by 29.5% and 28.2%, as well as the  $f$  is reduced by 81.5% and 85.4%, and the  $\phi$  is added by 5.34h and 5h respectively. By contrast, the thermal performance improvement in the south and north-facing walls are relatively minor but still reduces the  $q_{peak}$  and  $q_{ave}$  by 34.8-41.9% and 27.5-27.9%. Meanwhile, the  $f$  is declined by 44.4-53.0%, and the  $\phi$  added 2.33h-3.33h, severally. As a result, the east and west-facing walls are given priority in PCM installation.

## References

- [1] R. Ruparathna, K. Hewage, R. Sadiq, Improving the energy efficiency of the existing building stock: A critical review of commercial and institutional buildings, *Renewable and sustainable energy reviews* 53 (2016) 1032-1045.
- [2] E. Long, Z. Zang, X. Ma, Are the energy conservation rates (RVRs) approximate in different cities for the same building with the same outer-wall thermal insulation measures?, *Building & Environment* 40(4) (2005) 537-544.
- [3] L. Yang, J. C. Lam, C. L. Tsang, Energy performance of building envelopes in different climate zones in China, *Applied Energy* 85(9) (2008) 800-817.
- [4] D. H. W. Li, L. Yang, J. C. Lam, Zero energy buildings and sustainable development implications—A review, *Energy* 54 (2013) 1-10.
- [5] L. Yang, Y. Qiao, Y. Liu, X. Zhang, C. Zhang, J. Liu, A kind of PCMs-based lightweight wallboards: Artificial controlled condition experiments and thermal design method investigation, *Building and Environment* 144 (2018) 194-207.
- [6] C. Wang, X. Huang, S. Deng S, E. Long, J. Niu, An experimental study on applying PCMs to disaster-relief prefabricated temporary houses for improving internal thermal environment in summer, *Energy and Buildings* 179 (2018) 301-310.
- [7] A. D. Gracia, L. Navarro, J. Coma, S. Serrano, J. Roman í G. Pérez, L. F. Cabeza, Experimental set-up for testing active and passive systems for energy savings in buildings—lessons learnt, *Renewable and Sustainable Energy Reviews* 82 (2018) 1014-1026.
- [8] X. Chen, J. Ren, Z. Xie, K. Dong, Temperature and Energy Consumption Simulation of Phase Change Materials Applied to Building Exterior Wall, *Building Energy Efficiency* 45(4) (2017) 56-62.
- [9] F. Kuznik, J. Virgone, Experimental assessment of a phase change material for wall building use, *Applied Energy* 86(10) (2009) 2038-2046.
- [10] L. Xu, H. Wang, Y. Gao, J. Wang, E. Long, R. Zhao, Study on Performance of Composite PCM (Phase-change Material)'s Adjusting Indoor Thermal Environment of Light Weight Enclosure Buildings, *Building Science* 029(012) (2013) 45-49,107.
- [11] S. Liu, B. Chen, R. Zhao, J. Sun, Experiment study on effect of TCM on thermal environment of passive solar houses, *Renewable Energy Resources* 33(10) (2015) 1459-1464.
- [12] H. Ling, C. Chen, H. Qin, S. Wei, J. Lin, N. Li, M. Zhang, N. Yu, Y. Li, Indicators evaluating thermal inertia performance of envelopes with phase change material, *Energy and Buildings* 122 (2016) 175-184.
- [13] X. Sun, J. Jovanovic, Y. Zhang, S. Fan, Y. Chu, Y. Mo, S. Liao, Use of encapsulated phase

- change materials in lightweight building walls for annual thermal regulation, *Energy* 180 (2019) 858-872.
- [14] I. Adilkhanova, S. A. Memon, J. Kim, A. Sheriyev, A novel approach to investigate the thermal comfort of the lightweight relocatable building integrated with PCM in different climates of Kazakhstan during summertime, *Energy* 217 (2021) 119390.
- [15] P. Marin, M. Saffari, A. De Gracia, X. Zhu, M. M. Farid, L. F. Cabeza, S. Ushak, Energy savings due to the use of PCM for relocatable lightweight buildings passive heating and cooling in different weather conditions, *Energy and Buildings* 129 (2016) 274-283.
- [16] Y. Hong, L. Long, H. Zhang, R. Zou, The performance evaluation of shape-stabilized phase change materials in building applications using energy saving index, *Applied energy* 113 (2014) 1118-1126.
- [17] N. Soares, A. R. Gaspar, P. Santos, J. J. Costa, Multi-dimensional optimization of the incorporation of PCM-drywalls in lightweight steel-framed residential buildings in different climates, *Energy and buildings* 70 (2014) 411-421.
- [18] H. Akeiber, P. Nejat, M. Z. A. Majid, M. A. Wahid, F. Jomehzadeh, I. Z. Famileh, J. K. Calautit, B. R. Hughes, S. A. Zaki, A review on phase change material (PCM) for sustainable passive cooling in building envelopes, *Renewable and Sustainable Energy Reviews* 60 (2016) 1470-1497.
- [19] A. Sari, Thermal energy storage characteristics of bentonite-based composite PCMs with enhanced thermal conductivity as novel thermal storage building materials, *Energy Conversion and Management* 117 (2016) 132-141.
- [20] A. Sarri, D. Bechki, H. Bouguettaia, S. Al-Saadi, M. M. Farid, Effect of using PCMs and shading devices on the thermal performance of buildings in different Algerian climates. A simulation-based optimization, *Solar Energy* 217 (2021) 375-389.
- [21] X. Sun, Z. Zhu, S. Fan, J. Li, Thermal performance of a lightweight building with phase change material under a humid subtropical climate, *Energy and Built Environment* 11 (2020) 01-13.
- [22] A. Fateh, D. Borelli, F. Devia, H. Weinlader. Summer thermal performances of PCM-integrated insulation layers for light-weight building walls: effect of orientation and melting point temperature, *Thermal Science and Engineering Progress* 6 (2018) 361-369.
- [23] S. D. Zwanzig, Y. Lian, E. G. Brehob, Numerical simulation of phase change material composite wallboard in a multi-layered building envelope, *Energy Conversion and Management* 69 (2013) 27-40..
- [24] R. A. Kishore, M. V. Bianchi, C. Booten, J. Vidal, Parametric and sensitivity analysis of a PCM-integrated wall for optimal thermal load modulation in lightweight buildings,

- Applied Thermal Engineering 187 (2021) 116568.
- [25] G. Zhou, Y. Yang, X. Wang, J. Cheng, Thermal characteristics of shape-stabilized phase change material wallboard with periodical outside temperature waves, *Applied Energy* 87(8) (2010) 2666-2672.
- [26] H. Wang, W. Lu, Z. Wu, G. Zhang, Parametric analysis of applying PCM wallboards for energy saving in high-rise lightweight buildings in Shanghai, *Renewable Energy* 145 (2020) 52-64.
- [27] Ministry of housing and urban-rural development, Code for Thermal Design of Civil Building (GB 50176-2016), China Architecture & Building Press, Beijing, China, 2016, pp. 77-84.
- [28] J.P. Liu, *Building Physics Fourth Edition*, China Architecture & Building Press, Beijing, China, 2009, pp. 15-23.
- [29] X. Meng, T. Luo, Y. Gao, L. Zhang, X. Huang, C. Hou, Q. Shen, E. Long, Comparative analysis on thermal performance of different wall insulation forms under the air-conditioning intermittent operation in summer, *Applied thermal engineering* 130 (2018) 429-438.
- [30] C. Wang, S. Deng, J. Niu, E. Long. A numerical study on optimizing the designs of applying PCMs to a disaster-relief prefabricated temporary-house (PTH) to improve its summer daytime indoor thermal environment, *Energy* 181 (2019) 239-249.
- [31] C. Amaral, T. Silva, F. Mohseni, J. S. Amaral, V. S. Amaral, Experimental and numerical analysis of the thermal performance of polyurethane foams panels incorporating phase change material, *Energy* 216 (2021) 119213.
- [32] R. H. Inman, H. T. C. Pedro, C. F. M. Coimbra, Solar forecasting methods for renewable energy integration, *Progress in energy and combustion science* 39(6) (2013) 535-576.
- [33] ASHRAE, *Guideline 14-2014: Measurement of Energy and Demand Savings*, Atlanta, 2014, pp. 17-20.
- [34] Y. Gao, F. He, X. Meng, Z. Wang, M. Zhang, H. Yu, W. Gao, Thermal behavior analysis of hollow bricks filled with phase-change material (PCM), *Journal of Building Engineering* 31 (2020) 101447.
- [35] Z. Liu, J. Hou, X. Meng, B. J. Dewancker, A numerical study on the effect of phase-change material (PCM) parameters on the thermal performance of lightweight building walls, *Case Studies in Construction Materials* 15 (2021) e00758.
- [36] Z. Liu, J. Hou, Y. Huang, J. Zhang, X. Meng, B. J. Dewancker, Influence of phase change material (PCM) parameters on the thermal performance of lightweight building walls with different thermal resistances, *Case Studies in Thermal Engineering* 31 (2022) 101844.

- [37] F. Souayfane, P. H. Biwolé, F. Fardoun, P. Achard, Energy performance and economic analysis of a TIM-PCM wall under different climates, *Energy* 169 (2019) 1274-1291.
- [38] L. Zhang, Z. Liu, C. Hou, J. Hou, D. Wei, Y. Hou, Optimization analysis of thermal insulation layer attributes of building envelope exterior wall based on DeST and life cycle economic evaluation, *Case Studies in Thermal Engineering* 14 (2019) 100410.

### Nomenclature

$t_m$	Phase-transition temperature, (°C)
$L_p$	Phase change latent heat, (kJ/kg)
$\lambda$	Thermal conductivity, [W/(m K)],Solid (Liquid)
$c_p$	Specific heat, [J/(kg K)]
$\rho$	Density, (kg/m <sup>3</sup> )
$T_i$	Material temperature, (°C)
$T_p$	PCM temperature, (°C)
$h_{in}$	Convective heat transfer coefficient of inner surface, [W/(m <sup>2</sup> ·K)]
$h_{out}$	Convective heat transfer coefficient of outer surface, [W/(m <sup>2</sup> ·K)]
$v$	Outdoor wind speed, (m/s)
$q_{peak}$	Inner surface peak heat flux, (W/m <sup>2</sup> )
$q_{ave}$	Inner surface average heat flux, (W/m <sup>2</sup> )
$H_p$	Enthalpy of PCM, (kJ/kg)
$M_t$	Measured temperatures at each hour, (°C)
$S_t$	Simulated temperatures at each hour, (°C)
$\overline{M}_t$	Average of the measured data values, (°C)
$T$	Temperature, (°C)
$t$	Time, (s)
$\alpha$	Solar radiation absorptivity of outer surface, -
$q$	Inner surface heat flux, (W/m <sup>2</sup> )
$\mu$	Solar radiation intensity, (W/m <sup>2</sup> )
$\delta$	Wall thickness, (m)
$h$	Wall height, (m)
$\beta$	Liquid fraction, -
$\varphi$	Delay time, (h)
$f$	Attenuation rate, (%)
$m$	Internal iteration number, -
$n$	Total number of hours, $t$

### Abbreviations

LBW	Lightweight Building Walls
PCM	Phase-Change Materials
OSB	Oriented Strand Board
EPS	Expanded Polystyrene
TMY2	Typical Meteorological Year 2

**Chapter 6. Effectiveness of different kinds/configurations of PCM  
for improving the thermal performance of lightweight wall in  
summer and winter**

6.1	Introduction.....	6-1
6.2	Physical model and boundary conditions .....	6-4
6.2.1	Physical model.....	6-4
6.2.2	Boundary conditions .....	6-5
6.3	Utilization versus effectiveness of the PCM under different models.....	6-6
6.3.1	The variation of temperature and liquid fraction of PCM with different models .....	6-6
6.3.2	Effectiveness of different models .....	6-9
6.4	Utilization versus effectiveness of the PCM under different transition ranges.....	6-11
6.4.1	The variation of liquid fraction of PCM and inner surface temperature with different transition ranges.....	6-11
6.4.2	Effectiveness of different transition ranges of PCM .....	6-13
6.5	Effectiveness of the PCM under different thicknesses.....	6-14
6.6	Effectiveness of the PCM under different latent heats .....	6-17
6.7	Summary .....	6-19
	References.....	6-21
	Nomenclature.....	6-27



## 6.1 Introduction

Nowadays, most people spend 90% of their daily lives indoors and rely on mechanical heating and air conditioning, making the building industry considered the single largest contributor to the world's energy consumption and greenhouse gas emissions [1,2]. Of these, more than 70% of total energy consumption is caused by the heat transfer loss in building envelopes [3], so it is vital to improve the thermal performance of the building envelopes. At present, improving the thermal performance of walls can be done by enhancing their heat storage and release capacity, including both sensible and latent heat storage. However, sensible heat storage has been used by architects to passively store/release thermal energy for centuries, but to store the same amount of energy requires a much larger volume of material compared to latent heat storage, especially in lightweight buildings (lower thermal mass), which will lead to a significant increase in building costs. So a new material is urgently needed for traditional insulation forms [4-6] to change the current composition of heat storage materials for envelopes.

Phase change materials (PCM) are used in different heat-related applications to overcome the mismatch between heat supply and demand as an advanced energy storage material that can store and release large amounts of heat in a small volume during phase change [7-12]. Simultaneously, in high-energy consumption buildings, integrating PCM into the envelopes to regulate the indoor thermal environment and reduce energy consumption has also proven to have a high potential [13-16]. For example, Lei et al. [17] found that it could reduce envelope heat gain by 21-32% in summer for Singapore in a tropical climate, and Soares et al. [18] concluded it could reduce energy demand by 10-60% in different climates of Europe for applying PCM to lightweight building walls (LBW). Meanwhile, Marin et al. [19] studied the impact of PCM applied to lightweight buildings on energy consumption under different climatic conditions, and it observed that the potential for PCM to reduce heating and cooling energy consumption was more remarkable in arid and warm temperate climates areas, while it was limited in tropical and snowfall-dominated areas. In addition, Li et al. [20] derived based on simulation analysis (EnergyPlus) that integrating PCM in a normal foamed concrete wall could reduce the yearly heating energy consumption by 4.74% in hot summer and cold winter zone (China). In the meantime, PCM applications in microclimatic environments have been studied by many scholars. Sun et al. [21] studied the energy-saving potential of PCM-integrated lightweight buildings in humid environments, and it was presented that the energy-saving rate decreased from 1.64% to 1.32% when the humidity increased from 40% to 90% in summer, while the effect was not significant in winter. Sarri et al. [22] found that PCM combined with shading equipment under natural conditions was more conducive to improving indoor thermal comfort hours in most climate zones of Algerian, and its potential could reach 44.13%~59.11%.

Fateh et al. [23] explored the effects of solar radiation (solar radiation was regarded as the time-varying heat source at the boundary) and concluded that the appropriate PCM could reduce heat gain by 75% in summer. Moreover, the related reviews [24-28] also summarized the high application potential of PCM in other building envelopes, including different types of walls, roofs, ceilings, floors, and windows.

However, PCM operates effectively in the envelope and is mainly accomplished by absorbing (heat storage) the heat transferred through the walls under the interaction between the indoor and outdoor thermal environment during the high-temperature hours (day-time) and releasing it during the low-temperature hours (night-time) [29]. In this case, energy wastage and demand are further mitigated and reduced [30]. Nevertheless, whether PCM can effectively operate in building envelopes are dependent on many factors, including the indoor and outdoor thermal environment [18,19,31], the thermal properties of original walls [32,33], and the PCM parameters [34,35] (phase-transition temperature, location, thickness, latent heat, thermal conductivity). It is also the reason for the large differences in the application potential of PCM in the different findings mentioned above [17-28]. Therefore, many studies have also been done to optimize the application of PCM, and results were obtained by experiments or numerical simulations. Jangeldinov et al. [36] used EnergyPlus to evaluate the effectiveness of eleven melting temperature ranges of PCM in eight cities with warm summer humid continental climates. The results demonstrated that the optimum PCM was PCM24-26 °C in cities where cooling energy savings were the highest, while it was found to be PCM 21 °C in cities where heating energy savings were the highest. Kabdrakhmanova et al. [37] used DesignBuilder to simulate eight cities in subtropical climate regions, and the findings were that PCM 24 °C showed high energy efficiency for most cities, while for Nanning and Asuncion PCM 27 °C was the most efficient. Meanwhile, Nurlybekova et al. [38] concluded that PCM18 °C had the best effect on reducing peak temperatures and temperature fluctuations in winter, while the higher temperature of PCM was required in summer and transition seasons, and found that the performance of PCM was related to local climatic conditions. However, Mohseni et al. [39] considered the optimum phase-transition temperature to be seasonal and arrived at a suitable phase-transition temperature of 25 °C in summer and 21 °C in winter. Furthermore, Kishore et al. [40] suggested that the phase-transition temperature range ( $\Delta T$ ) was also a critical factor in PCM utilization, with increasing the  $\Delta T$  would result in lower daily utilization but higher annual utilization of PCM for which the optimum value existed ( $\Delta T=4^{\circ}\text{C}$ ). Staszczuk et al. [41] believed that the effective use of PCM was required to precisely adjust the  $\Delta T$  to suit the actual building conditions. In addition, Meng et al. [42] evaluated the thermal behavior of double-layer PCM (with different phase-transition temperatures) in lightweight buildings. It was found

that indoor temperatures could be reduced by 4.28-7.7 °C and temperature fluctuations by 28.8-67.8% in summer and that temperature increases were 6.93-9.48 °C, and temperature fluctuations were reduced by 17.7-25.4% in winter. Bhamare et al. [43] established a mathematical model using MATLAB to assess the effectiveness of different phase-transition temperatures in different climatic zones of India, and found that the effectiveness of PCM was strongly dependent on climatic conditions.

Additionally, Kishore et al. [40] found that the utilization and effectiveness of PCM would also be affected by the latent heat and the thickness of PCM, and its effectiveness and load transfer capacity were improved with increasing latent heat and thickness. Elawady et al. [14] also concluded that the thicker the PCM, the better the performance. While Wijesuriya et al. [44] observed by EnergyPlus that PCM was integrated into the building envelopes, the flexibility of its impact on load was saturated when the thickness and latent heats were more than 1.91cm and 200kJ/kg, respectively. Nonetheless, different scholars still have different views on the above conclusions. Kuznik [45], Xiao [46], Cheng [47], and Meng et al. [48] believed that the PCM thicknesses of 10mm, 20mm, and 30-40mm, respectively, were the most effective for their applications by studying different types of walls. By contrast, Bohárquez-Órdenes et al. [49] based on simulations (DesignBuilder) found that different optimum thicknesses existed for different locations, with ideal PCM layer thicknesses of 4mm and 8mm for ceilings and walls separately. Moreover, concerning latent heat, different scholars deemed its optimum values to be 178 kJ/kg [50], 120 kJ/kg [51], and 90 kJ/kg [52] when PCM was integrated into different walls. As a consequence, in our previous study [33], we evaluated the influence rules and contribution efficiency of PCM parameters on the thermal performance of LBW with a different thermal resistance of the original walls ( $R_{wt}$ ). The results showed that the effectiveness (contribution efficiency) of PCM was gradually replaced with  $R_{wt}$  was boosted. It is clear from the above findings that there are many obstacles to applying PCM in buildings, a fundamental one being that different structures have different requirements for the thermal properties of PCM. It is imperative to assess the effectiveness of PCM-related parameters in buildings.

With the above review, it is not difficult to discover that PCM can effectively improve the thermal performance of the walls, but its application effect varies greatly in different regions. Among these, the ambient temperature is a determining factor in the thermal performance of PCM-integrated building components [19,21-23,36-43,53-56]. However, most studies on PCM applications have focused on a specific season, and the study that both consider the effectiveness of PCM in different seasons, especially in summer and winter (vary considerably) is insufficient. For PCM, the inherent phase-transition temperature may have satisfactory

results in summer (winter) but may have unsatisfactory or negative consequences in winter (summer). Finding the optimum PCM kinds and configurations to improve the thermal performance of buildings in different climates/seasons has not been well solved. Furthermore, compared to traditional buildings, lightweight buildings have been widely developed owing to their sustainability advantages [33], but their lower thermal mass (i.e., thermal storage capacity) results in a poorer ability to suppress temperature fluctuations [57]. Hence, based on the previous research [34], the typical summer and winter climate (TMY2) [58,59] in Fukuoka (Japan) was adopted as the thermal boundary, and a typical two-dimensional LBW numerical model was built in this study with the heat transfer process of melting-solidifying and validated. Based on this, the influence laws and effectiveness of different PCM kinds/configurations on the thermal performance of LBW in summer and winter are evaluated in-depth and suitable PCM for both summer and winter is proposed. The research results are helpful in achieving long-term thermal comfort and low-energy operation of lightweight buildings, and it can also provide data support and theoretical references for the efficient application and maximize economic benefits of PCM in lightweight buildings for local or other regions.

## **6.2 Physical model and boundary conditions**

### **6.2.1 Physical model**

In our previous study [34], it was found that suitable phase-transition temperatures for different PCM locations in the LBW (outside, middle, and inside) were significantly different. However, the influence of PCM locations on the thermal performance of LBW (including the LBW with the different  $R_{wt}$  [33]) is small under the suitable phase-transition temperatures, the middle (22-32 °C) was the best choice by comparing all evaluation indexes. Therefore, based on the previous research results [34], a reference model (Model-0, without PCM) and four comparison models (Model-1 to Model-4) are built in this study, as shown in Fig. 6-1. Among them, on the basis of Model-0, two models (Model-1 and Model-2) of different phase-transition temperatures (14-24 °C and 22-32 °C) are proposed to explore the thermal behavior of LBW integrated with different PCM types under winter and summer. Then, to find a PCM configuration that applies to both summer and winter, the Model-3 (double-layer PCM) with different phase-transition temperatures is established at the same thickness based on Model-1 and Model-2. A special note here is that the order of the PCM is ignored in this Model-3. Due to this fact, the order of the two PCM is not important when the PCM thickness is small (<0.5 in. or 1.27cm), which was found through a relevant study [40]. Simultaneously, Model-4 is also presented as a comparison to analyze the effectiveness of the double-layer PCM in different configurations (location and phase-transition temperatures) in winter and summer. Table 1

shows the relevant thermophysical parameters of wall materials [60-63].

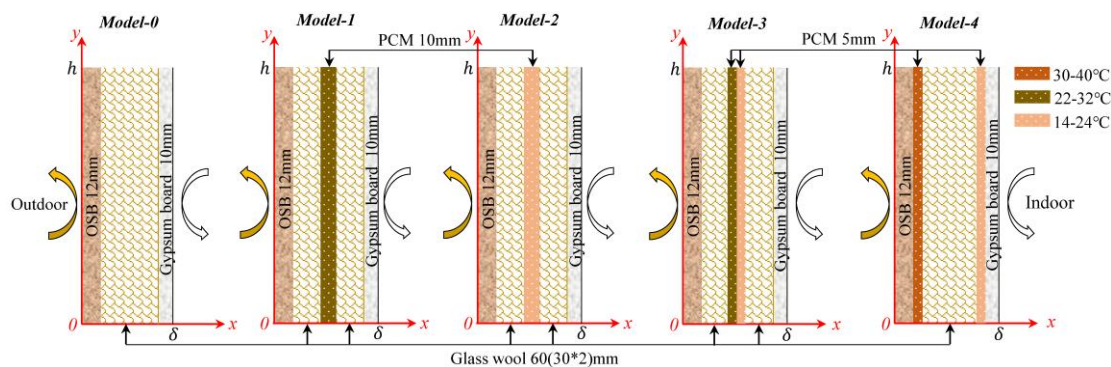


**Fig. 6-1. Schematic diagram of the two-dimensional geometric model of the LBW with different PCM kinds/configurations.**

**Table 6-1 Thermo-physical parameters of wall materials [60-63].**

Material	$t_m$ (°C)	$L_p$ (kJ/kg)	$d_p$ (mm)	$\lambda$ [W/(m K)], Solid (Liquid)	$c_p$ [J/(kg K)]	$\rho$ (kg/m <sup>3</sup> )
PCM	30-40/22-32/14-24	216	5/10	0.5(0.25)	1785	1300
OSB	-	-	12	0.105	1400	593
Glass wool	-	-	30/60	0.035	1220	40
Gypsum board	-	-	10	0.33	1050	1050

## 6.2.2 Boundary conditions

In this study, to analyze the thermal behavior of LBW integrated with PCM under summer and winter conditions, the numerical simulations were carried out using weather conditions from Jul. 1 to Aug. 5 in the summer climate (Typical Meteorological Year 2, TMY2) [58] and from Jan. 1 to Jan. 29 in winter in Fukuoka (Japan). The TMY2 is a dataset of hourly values of solar radiation and meteorological elements for a one-year period, and it was downloaded from the National Renewable Energy Laboratory [59]. The first simulation period (Jul. 1 to Jul. 29 and Jan. 1 to Jan. 22) was done to eliminate the influence of the initial temperature distribution, and the second simulation period (Jul. 30 to Aug.5 and Jan. 23 to Jan. 29) (7 consecutive days) was carried to analyze the wall thermal behavior. Fig. 6-2 shows the variation of outdoor air temperature and solar radiation intensity from Jul. 30 to Aug.5 (summer) and Jan. 23 to Jan. 29 (winter). The indoor air temperature maintains 26 °C in summer and 20 °C in winter.

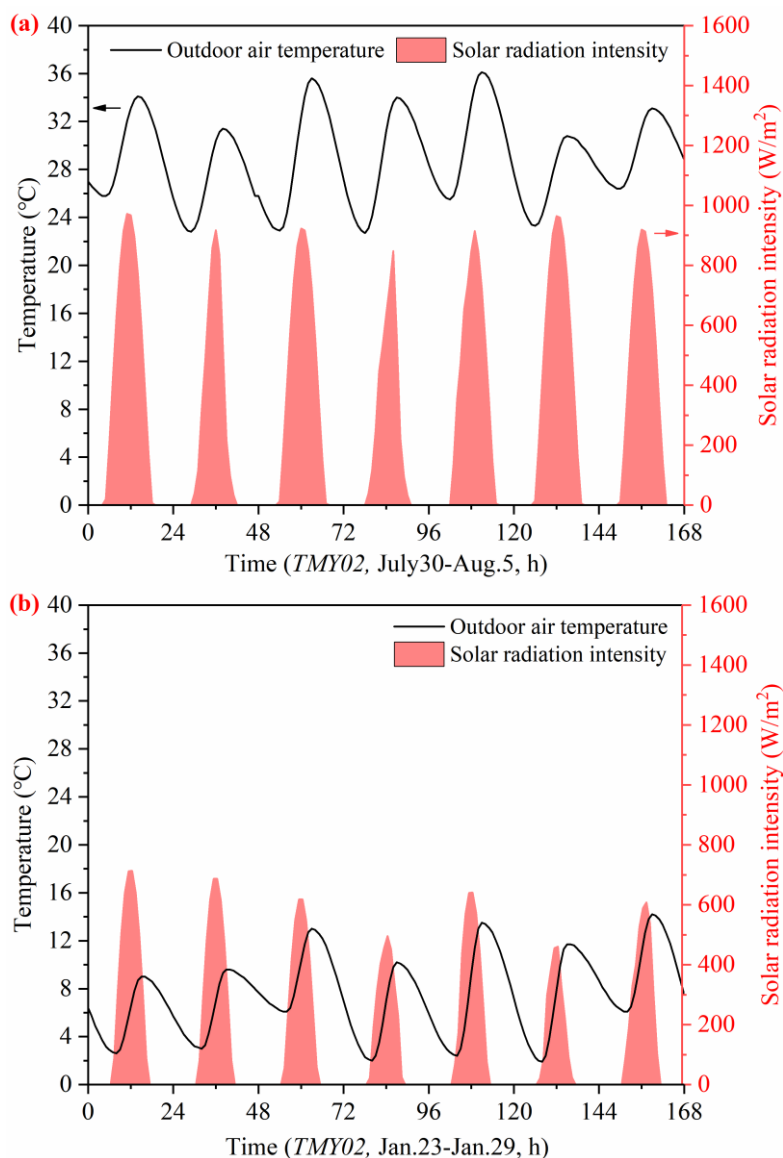


**Fig. 6-2. Variation of outdoor air temperature and solar radiation intensity with time in (a) summer and (b) winter.**

### 6.3 Utilization versus effectiveness of the PCM under different models

#### 6.3.1 The variation of temperature and liquid fraction of PCM with different models

Considering that the actual temperature of the PCM determines the degree of phase change [34,64], Fig. 6-3 gives the variation of temperature and a liquid fraction (%) of PCM with time for different models to analyze the thermal behavior of different kinds/configurations (different models) of PCM in winter and summer. As can be seen in Fig. 6-3(a), the magnitude of the actual temperature fluctuations of PCM at different Models varies considerably under summer conditions due to the interaction of indoor and outdoor temperatures when PCM is integrated into LBW. Taking Model-1 and Model-2 as an example, when the phase-transition temperature is taken as the appropriate temperature of 22-32 °C (Model-1) [34], the PCM temperature is

29.45-31.66 °C. Whereas the PCM temperature is 25.58-37.60 °C when it is chosen as 14-24 °C (Model-2), and its temperature fluctuation increased by 444.9% compared to Model-1. The main reason is that the PCM is basically in the solid or liquid state when the phase-transition temperature of the PCM selected is lower or higher than the actual temperature change of PCM, and its temperature change is mainly dominated by sensible heat, and its latent heat utilization rate is close to zero. The above phenomenon can be more intuitively derived in Fig. 6-3(b). The PCM liquefies rapidly and its liquefaction rate is maintained at 100% (liquid fraction) when the selected phase-transition temperature is low (14-24 °C) in summer. It is mainly caused by the fact that the temperature transferred to the PCM through the wall is above 24 °C under the interaction of the indoor and outdoor thermal environment in summer. In comparison, the above phenomenon for winter is often the opposite. From Fig. 6-3(c), it can be concluded that although the PCM (22-32 °C) is suitable in summer (Model-1), its actual temperature variation in winter is 12.26-20.21 °C, which is much lower than the minimum value (22 °C) of the phase-transition temperature, and its temperature fluctuation also appears to be higher compared to summer (2.21 °C), reaching 7.95 °C. By contrast, for PCM (14-24 °C) with poor performance in summer (Model-2), the actual temperature in winter is 14.19-16.03 °C, and its changes are all in the phase-transition temperature range (14-24 °C). Concurrently, in Fig. 6-3(d) the liquid fraction is found to be 0% for PCM (Model-1 and Model-3) at 22-32 °C and 1.9-20.3% for PCM (Model-2) at 14-24 °C. The above data are sufficient to explain that the appropriate phase-transition temperature is not only related to the PCM location but is also influenced by the difference between the indoor and outdoor temperatures, which is consistent with the findings of the literature [18,19,31,65,66]. As a result, it can be drawn that it is very essential to choose the correct PCM for the different thermal environments. Otherwise, the heat absorption and release capacity of the PCM will not be utilized and will only work as thermal resistance, which reduces the economic value of the PCM.

Based on the above characteristics, it can be noted from Model-3 that the application of double-layer PCM results in a significant reduction in PCM temperature fluctuations (see Fig. 6-3 (a) and (c)) compared to Model-2 for summer (25.57-37.60 °C) and Model-1 for winter (14.26-20.21 °C), with a reduction of 51.9% and 67.7%, respectively. Nonetheless, there is a slight increase in PCM temperature fluctuations compared to the optimal Model-1 for summer and Model-2 for winter, which is mainly related to the PCM thickness [35]. At the same time, it is also found that occasionally extreme high temperatures in summer (>32 °C) also cause a rapid rise in the PCM temperature even if suitable phase-transition temperatures are adopted. Under this condition, the liquid fraction remained at 100%. This result also further demonstrates that the phase-transition temperature range ( $\Delta T$ ) of the PCM has a significant effect on its

effectiveness of PCM. In addition, it can be observed from Fig. 6-3 (b) and (d) that the liquid fraction of PCM is 67.8-100% for 22-32 °C in summer and 0.3-26.0% for 14-24 °C in winter when the double-layer PCM (Model-3) is selected. The above data indicates that a layer of PCM is in operation in winter and summer, allowing the room to remain comfortable for extended periods.

Simultaneously, Model-4 as a comparison (double-layer PCM), reveals that the temperature fluctuation and utilization of PCM close to the outside (30-40 °C) is high (liquid fraction is 0-100%), but at this time, the liquid fraction of the inner PCM (14-24 °C) remains at 100%. In contrast, the temperature of outside PCM (30-40 °C) is 3.9-25.5 °C in winter with a liquid fraction of 0, and for the inner PCM (14-24 °C), which ranged from 18.9-19.8 °C with a liquid fraction of 49.3-58.1%. This is the same conclusion as Model-3 in that the use of a double-layer PCM always has a layer of PCM playing a latent heat role in both summer and winter. A clear difference is that the utilization of PCM in Model-4 is higher than in Model-3 in both summer and winter, but whether this is proportional to its effectiveness in improving the thermal performance of the walls needs to be further explored.

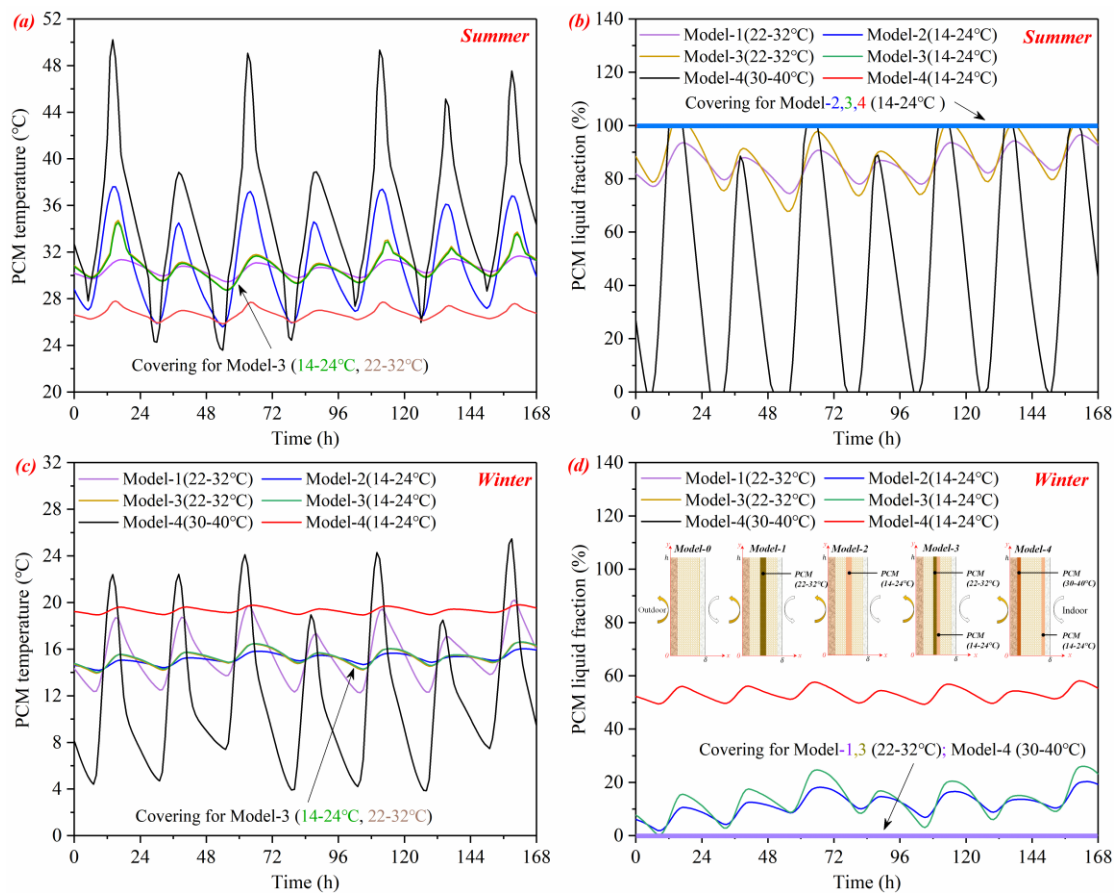


**Fig. 6-3. Variation of PCM temperatures and liquid fractions with time under different phase-transition temperatures for summer and winter.**

### 6.3.2 Effectiveness of different models

From the above study, it is drawn that the PCM of different Models exhibits different temperature variations and utilization rates in summer and winter. However, whether there is a positive relationship between PCM utilization and application effectiveness of the integrated walls considering the thermal resistance of the wall [33] needs further discussion. For this reason, Fig. 6-4 gives the effects of different Models on the thermal performance of the LBW, it can be found that different models have remarkable differences in winter and summer, but a common conclusion can still be drawn that the application of PCM can effectively improve the thermal performance of LBW. As shown in Fig. 6-4(a), Model-1 performs the best in summer, with a 91.6% reduction in the  $f$  compared to Model-0 (reference wall), followed by Model-3, Model-4, and Model-2 with 81.0%, 40.4%, and 32.8% reductions respectively. Whereas, Model-1 shows the smallest reduction in  $f$  for winter, which is the opposite in Model-2. It further illustrates the importance of choosing the proper temperature for the different seasons. Nevertheless, it can be clearly observed that the  $f$  can still be reduced by 32.8% (Model-1 for winter) and 35.5% (Model-2 for summer), even though the thermal performance is poorer in the opposite season. This phenomenon shows that the PCM can still play heat-insulated (summer) and heat preservation (winter) due to its low thermal conductivity when it only has a sensible heat effect (solid or liquid), which also provides direction for double-layer PCM to use. As a result, the application of double-layer PCM (Model-3) can reduce the  $f$  by 81.0% and 85.1% in summer and winter. Compared with the optimal Model-1 in summer and Model-2 in winter, the difference is only 0.53% and 0.32% although the  $f$  is raised, which brings the internal surface temperature fluctuations is less than 0.5 °C and it is not worthy of concern for indoor thermal comfort [64]. Furthermore, Model-4 does not display an absolute advantage compared to the other three Models for summer or winter. It shows that the application effect of PCM is not consistent with the utilization rate of PCM. Also, it is important to point out from Fig. 6-4(b) that the  $\varphi$  can be improved from 0.86h to 2.71-5.29h (summer) and 2.86-6h (winter) for different Models compared to Model-0. Among them, the  $\varphi$  for Model-3 is decreased from 5.29h to 4.43h in summer compared to Model-1 but can be added from 2.86h to 5.43h in winter, which is a more noticeable improvement in winter compared to the reduction rate in summer. A similar but opposite conclusion can be drawn for Model-3 compared to Model-2. Therefore, Model-3 is more favorable for improving indoor thermal comfort when considered from a year-round perspective.

Moreover, Fig. 6-4 (c) and (d) demonstrate the variation of heat flux on the inner surface under different models, where the energy-saving objective is to reduce heat gain in summer and heat loss in winter. As observed in Fig. 6-4(c), the  $q_{peak}$  can be reduced by up to 63.5% (Model-

1) in summer and 36.5% (Model-2) in winter, but this is not optimal when both summer and winter are concerned. The best Model-1 in summer only reduces the  $q_{peak}$  by 10.8% in winter, and the best Model-2 in winter only reduces by 26.9% in summer, but the results still show certain energy savings. The foremost reason is that the PCM provides thermal insulation due to its lower thermal conductivity, even though it cannot regulate heat when PCM is in a liquefied or solidified state. The above results also reveal that the efficient application of PCM is highly dependent on outdoor climatic conditions. In addition, it can be noticed that the application of double-layer PCM (Model-3) shows superior thermal regulation in both summer and winter. The peak heat gain in summer and heat loss in winter can be reduced by 54.8% and 33.6%, separately. What's more, it can still reduce 33.4% summer heat gain and 17.4% winter heat loss when it is compared with Model-4. Further, it can be seen in Fig. 6-4(d) that the PCM integrated into LBW can reduce the  $q_{ave}$  by 21.9-25.6% in summer and 11.8-14.8% in winter compared to Model-0 (no PCM), while the difference between the different Models are minor and can be ignored, with a maximum difference of 0.22 W/m<sup>2</sup> in summer and 0.11 W/m<sup>2</sup> in winter. Based on the above results, it can be easily concluded that Model-3 is a good choice for year-round operation. Meanwhile, it is worth pointing out that energy saving ( $q_{peak}$  or  $q_{ave}$ ) is better in summer than in winter, contrary to the findings in the literature [39]. It can be attributed to the fact that the temperature difference between indoors and outdoors in this study is greater in summer than in winter, considering the role of solar radiation so that the cooling load demand is higher than the heating load.

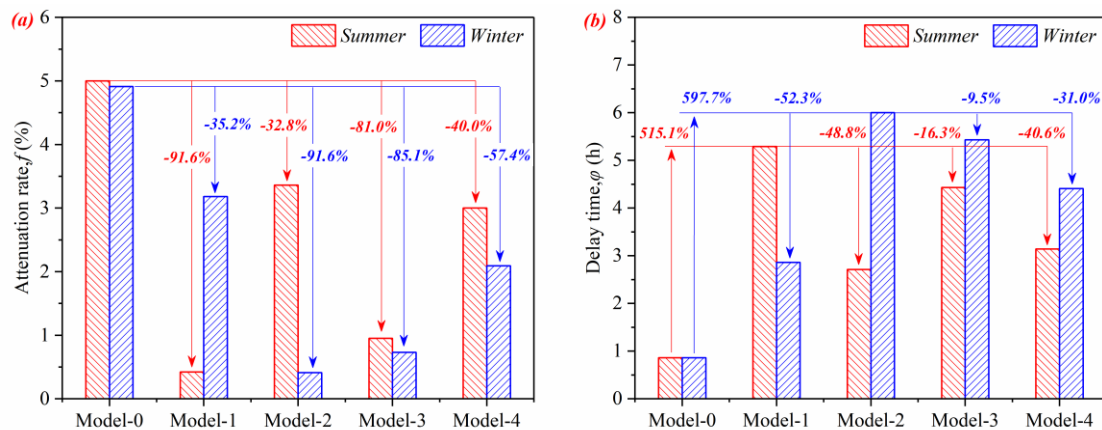


**Fig. 6-4. The (a) attenuation rate, (b) delay time, (c) peak heat flux and (d) average heat flux under the different Models for summer and winter.**

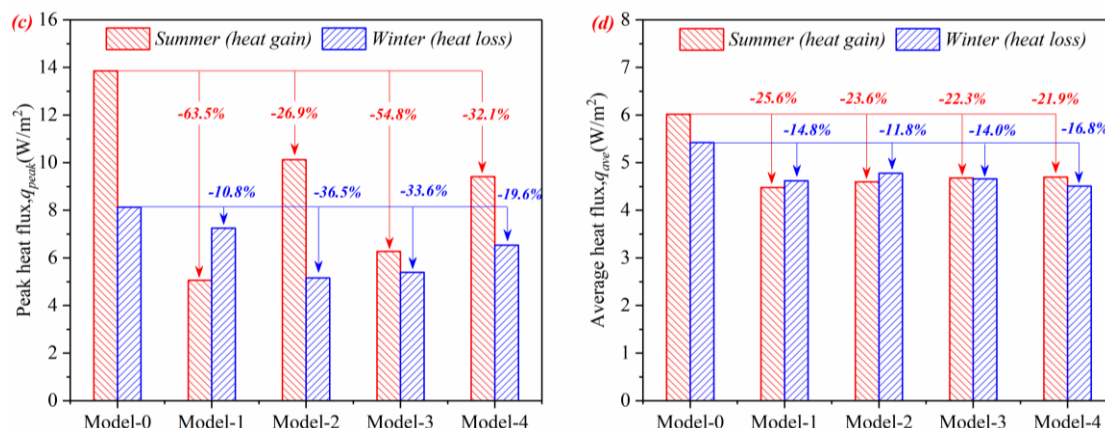


Fig. 6-4. (Continued).

## 6.4 Utilization versus effectiveness of the PCM under different transition ranges

### 6.4.1 The variation of liquid fraction of PCM and inner surface temperature with different transition ranges

Based on the above results, the phase-transition temperature range ( $\Delta T$ ) is the crucial factor affecting the utilization of the PCM when the PCM location is determined. A narrower  $\Delta T$  provides higher energy density, but it limits PCM utilization. In contrast, a more extensive  $\Delta T$  can provide a higher utilization rate (longer applicable cycles), while the energy storage capacity of the temperature change will be diminished [40]. Thus, to analyze the thermal performance of PCM at different  $\Delta T$ , this paper discusses the relevant issues based on Model-3 (optimal) derived from the above study. Nonetheless, there is worth explaining that the thermal performance of PCM is the best when the actual PCM temperature of PCM is within  $\Delta T$ , in contrast when the average value of PCM temperature (actual temperature of the PCM) is close to the maximum or minimum value of the  $\Delta T$ , the change of the  $\Delta T$  (especially narrowing the  $\Delta T$ ) often leads to the situation that PCM cannot be effectively used, which is also reflected in Fig. 6-3. Hence, to avoid the above situation and to more accurately reflect the effects of the  $\Delta T$ , the  $\Delta T$  of 2 °C, 6 °C, 10 °C, and 14 °C are selected for discussion in this study, based on the average PCM temperature (30 °C in summer and 15 °C in winter) of the double-layer PCM in Model-3 obtained in the above result.

Fig. 6-5 demonstrates the variation of the PCM liquid fraction and the inner surface temperature over time for different  $\Delta T$ . It can still be determined that when the phase-transition temperature is low in summer and high in winter, it remains in a liquefied (100% liquid fraction) and solidified (0% liquid fraction) state due to the difference between summer and winter climatic conditions, which only serve to enhance the thermal resistance of the wall. Accordingly, in this study, only the parts in the double-layer PCM that are suitable for summer

and winter are analyzed, it is denoted as PCM-a and PCM-b, respectively. It is evident from Fig. 6-5(a) and (b) that the PCM liquid fraction (utilization rate) is enlarged with the  $\Delta T$  is narrowed, the mean values of 56.1%/54.4% ( $\Delta T=14^{\circ}\text{C}$ ), 58.4%/56.1% ( $\Delta T=10^{\circ}\text{C}$ ), 63.9%/59.8% ( $\Delta T=6^{\circ}\text{C}$ ) and 83.5%/74.9% ( $\Delta T=2^{\circ}\text{C}$ ) for summer/winter. However, it is noticed that the PCM liquid fraction will reach 100% for a certain time in summer when the  $\Delta T$  is narrow ( $\Delta T=2^{\circ}\text{C}$ ). The main reason for this is that the temperature transferred to the PCM through the wall is partially above the phase-transition temperature range due to the interaction between indoor and outdoor temperatures, causing the PCM to melt rapidly and lose its latent heat storage capacity. It shows that although the narrow  $\Delta T$  improves the daily utilization rate of PCM, the total utilization rate of latent heat is reduced over longer temperature cycles. Moreover, it can be derived from the inner surface temperature variation (in summer) given in Fig. 6-5(c), where the narrower the phase-transition temperature range ( $\Delta T=2^{\circ}\text{C}$ ), the worse the ability to adapt to the environment and the inner surface temperature undergoes a rapid response with large fluctuations due to the melting of the PCM (latent heat is displaced by sensible heat) under higher outdoor temperature fluctuations. As a result, suitable  $\Delta T$  is required to utilize PCM heat storage and release capacity better. Meanwhile, from the above data, it can be observed that the liquid fraction of PCM is lowered with the expansion of the  $\Delta T$ , but the difference is gradually minimized. It can be drawn that the utilization rate of PCM is not proportional to the  $\Delta T$ . Furthermore, as shown in Fig. 6-5(c) and (d), the amplitude of the inner surface temperature is curbed as the  $\Delta T$  is reduced, with the best performance being  $\Delta T=6^{\circ}\text{C}$  in summer and  $\Delta T=2^{\circ}\text{C}$  in winter. Whereas the fluctuations in internal surface temperature only differ by  $0.07^{\circ}\text{C}$  in winter  $\Delta T=2^{\circ}\text{C}$  compared to  $\Delta T=6^{\circ}\text{C}$ . To extend the period of PCM use,  $\Delta T=6^{\circ}\text{C}$  is still the preferred choice.

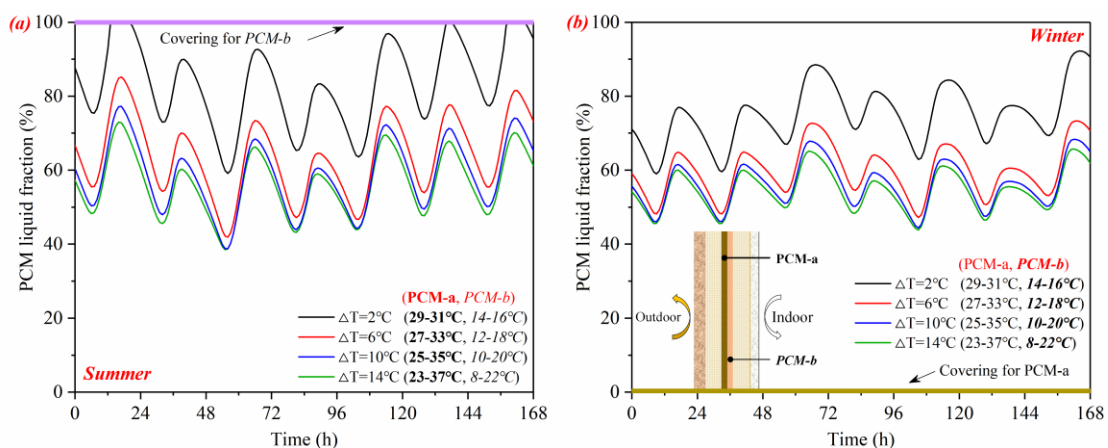


**Fig. 6-5. Variation of PCM liquid fractions and inner surface temperatures with time under different PCM transition temperature ranges for summer and winter.**

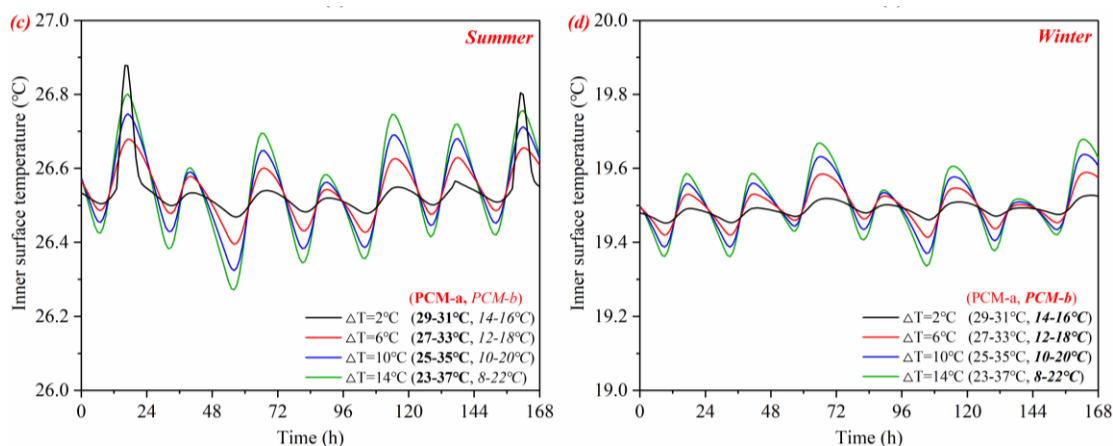


Fig. 6-5. (Continued).

#### 6.4.2 Effectiveness of different transition ranges of PCM

Fig. 6-6 gives the thermal performance indexes of walls under different  $\Delta T$  to more intuitively analyze the effectiveness of PCM in improving the thermal performance of the wall under different phase-transition temperature ranges ( $\Delta T$ ). As shown in Fig. 6-6(a), the narrower the  $\Delta T$ , the greater the reduction in the  $f$ . The  $\Delta T$  narrows from  $14^\circ\text{C}$  to  $2^\circ\text{C}$ , and the  $f$  can be reduced from 0.98%/0.96% (summer/winter) to 0.45%/0.18%, a reduction of up to 54.1%/81.3%, indicating that the level of indoor comfort is improved by the narrower the  $\Delta T$ . Nevertheless, it is more noticeable that the  $f$  in summer is only decreased from 0.48% to 0.42% when  $\Delta T=6^\circ\text{C}$  continues to narrow to  $\Delta T=2^\circ\text{C}$ , which means that the application effect of PCM is weakened. In addition, it can be seen from the  $\varphi$  in Fig. 6-6(b) that the change in the  $\Delta T$  has a smaller effect in summer, with the  $\varphi$  added only by 0.43h from  $14^\circ\text{C}$  to  $2^\circ\text{C}$  ( $\Delta T$ ), while the effect is pronounced in winter, the  $\varphi$  can increase 2h. By contrast, the same conclusion can still be obtained that the  $\Delta T=6^\circ\text{C}$  is relatively optimal because the increment of the  $\varphi$  in winter shows a certain attenuation as the  $\Delta T$  becomes narrower, increasing by 0.58h, 0.71h, and 0.72h for every  $4^\circ\text{C}$  decreases compared to  $\Delta T=14^\circ\text{C}$ , relatively highest increments of  $\Delta T = 6^\circ\text{C}$ , after which it can be neglected.

Meanwhile, with the changes of  $q_{peak}$  in Fig. 6-6(c), it can be found that the  $q_{peak}$  is reduced by 56.0%, 58.4%, 61.3%, and 60.5% in summer, respectively, as the  $\Delta T$  is reduced (from  $14^\circ\text{C}$  to  $2^\circ\text{C}$ ) compared to the reference wall (no PCM), with the optimum at  $\Delta T=6^\circ\text{C}$  (61.3%). Nevertheless, no obvious inflection point is found in reducing heat loss in winter. The increment of energy-saving rate is 2.6%, 3.2%, and 2.9% for every  $4^\circ\text{C}$  decreases compared with  $\Delta T=14^\circ\text{C}$ , while it still can be observed to be progressively weaker after  $\Delta T=6^\circ\text{C}$ . This further suggests that there is a relatively optimal value (non-proportional) for  $\Delta T$  in the energy savings of the walls. Besides, from the results in Fig. 6-6(d), it is revealed that the effect of  $\Delta T$  on the

$q_{ave}$  is smaller yet still exists differently. The narrower the  $\Delta T$  more energy savings ( $q_{ave}$ ) it is in summer, while the opposite conclusion is obtained in winter. This is mainly related to the difference in load demand between winter and summer. The inner surface temperature needs to be lowered in summer and raised in winter. A narrow  $\Delta T$  of PCM under the action of latent heat will lead to an increased demand for heat storage in winter owing to the limited heat from outdoors. When the appropriate  $\Delta T$  is determined to be  $6^{\circ}\text{C}$ , the  $q_{peak}$  can be saved by 61.3% (summer) and 39.9% (winter), and the  $q_{ave}$  can be reduced by 22.4% (summer) and 19.2% (winter) compared to the reference wall (no PCM). As a consequence, the above data confirm the fact that the double-layer PCM proposed in this study not only regulates the indoor thermal environment in summer and winter but also has a more noteworthy effect on energy savings.

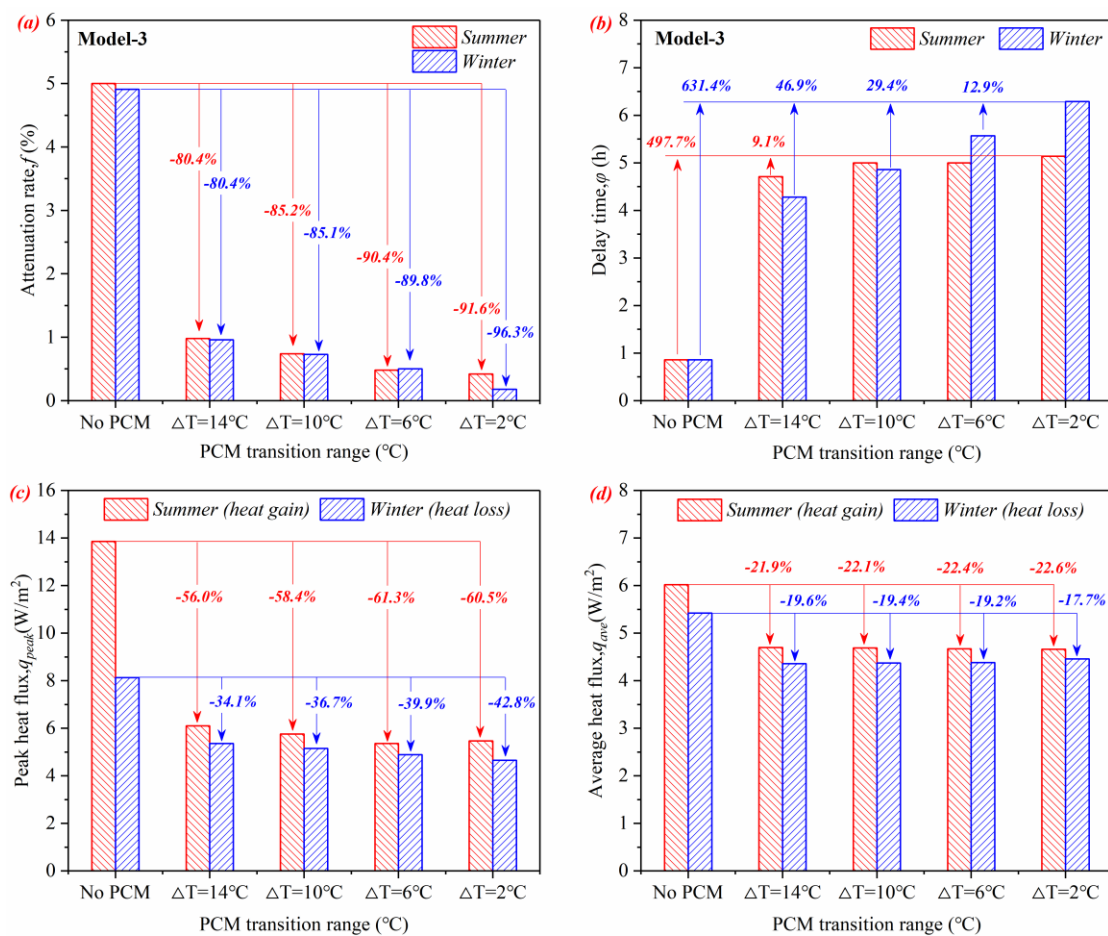


**Fig. 6-6.** The (a) attenuation rate, (b) delay time, (c) peak heat flux and (d) average heat flux under different PCM transition temperature ranges for summer and winter.

### 6.5 Effectiveness of the PCM under different thicknesses

The amount of PCM is another important factor influencing the total thermal storage and release capacity of the wall at a fixed phase change material parameter. Therefore, the effect of different thicknesses of PCM on the thermal performance of walls in summer and winter is

given in Fig. 6-7 based on the optimal configurations derived from the above conclusions (Model-3,  $\Delta T=6^{\circ}\text{C}$ ). It is clear that the double-layer of PCM integrated with the LBW exhibits a noticeable improvement in both summer and winter at suitable phase-transition temperatures even though the PCM thin is only 5mm (2.5mm+2.5mm). As a presentation in Fig. 6-7(a), 5mm (2.5mm+2.5mm) double-layer PCM reduces the  $f$  by 80.4% in summer and 67.6% in winter compared to the reference wall (no PCM). The  $f$  is reduced by 90.4% and 89.9% in summer and winter, respectively when the thickness is increased to 10mm (5mm+5mm), and the  $f$  gradually decreases and stabilizes as the thickness continues to increase on this basis. This means that in a relatively stable indoor and outdoor thermal environment (under comprehensive outdoor temperature,  $T_{sa}=T_a + GI/h_{out}$  [33]), heat transferred to the PCM through the wall does not completely melt the thicker PCM. The additional PCM only plays a certain role in thermal resistance where the heat storage and release capacity has not been exerted. At the same time, a significant difference can be found that the difference in  $f$  between summer and winter is greater when the PCM thickness is 5mm. This phenomenon is mainly caused by the different thermal conductivity [W/(m K)] in different states (solid and liquid) of the double-layer PCM. The 2.5mm PCM-b (12-18 °C) of the double-layer is completely liquefied in summer, and its thermal conductivity (0.25) is lower than that of the 2.5mm PCM-a (27-33 °C) in the solid-state in winter (0.5). The equivalent thickness exhibits different thermal properties in the total thermal resistance of the wall, which further suggests that the lower the thermal conductivity of the PCM, the better for the wall, a conclusion that has also been demonstrated in previous studies [34].

Nonetheless, the above differences are largely eliminated with increasing PCM thickness, suggesting that the difference in total thermal resistance due to another layer of PCM in a different season (or different phase state) can be balanced out by the superior thermal regulation capacity of thicker PCM. As a result, the advantages of the double-layer PCM proposed in this study in terms of year-round thermal comfort are also further highlighted (the PCM-unutilized can act as insulation in summer or winter). Moreover, it can be noticed in Fig. 6-7(b) that even though only a thin layer of PCM (2.5mm) contributes to the thermal regulation, the  $\varphi$  can still be extended to 4.57h (summer) and 4h (winter) with the combined effect of another layer of PCM (liquid or solid) for thermal insulation. As the PCM thickness increases to 20mm (10mm+10mm), the  $\varphi$  increases to 6.14h (summer) and 6.29 (winter), during which the  $\varphi$  increases somewhat linearly in the summer but the advantage of the increase in  $\varphi$  can be ignored in winter after the thickness exceeds 10mm. It is also found that the difference in  $\varphi$  between winter and summer decreases to 0.15h (20mm) from 0.57h (10mm) with increasing PCM thickness. The above data show that the advantage of PCM in transferring peak temperature

(the  $\varphi$ ) in summer over that in winter will gradually become the same with the increase in thickness.

In addition, Fig. 6-7(c) presents the variation of the  $q_{peak}$  with thickness, and it can be derived that the  $q_{peak}$  gradually is decreased as the thickness of PCM is increased, but the reduction does not seem to show a certain significance. Take summer as an example, the  $q_{peak}$  reduction rate is 5.8%, 2.1%, and 1.4% for each additional 5mm (2.5mm+2.5mm) on the basis of 5mm (2.5mm+2.5mm). Thus, it can be obtained that the reduction rate of  $q_{peak}$  does not need to be noticed when the PCM thickness exceeds 10mm (5mm+5mm) in consideration of cost. Further, it can be viewed that the change of  $q_{ave}$  given in Fig. 6-7 (d) yields a poor correlation with the increase in PCM thickness. The  $q_{ave}$  reduction rate increases by only 1.9% [20mm (10mm+10mm)] in summer after 10mm (5mm+5mm) although the increase of PCM thickness can reduce the  $q_{ave}$  to some extent. By contrast, the  $q_{ave}$  increases slightly in winter as continued increases in thickness. This phenomenon can be explained by the fact that the increased PCM thickness improves the heat storage capacity of the wall in summer to suppress the effect of outdoor temperatures, while it also increases the heat loss caused by heat absorption from stable indoors due to the limited outdoor heat in winter. Furthermore, a remarkable feature is that the difference in  $q_{peak}$  (or  $q_{ave}$ ) is gradually minimized with the PCM thickness added in summer and winter. The difference in  $q_{peak}$  and  $q_{ave}$  decreases respectively to 0.25W/m<sup>2</sup> and 0.18W/m<sup>2</sup> when the PCM thickness is increased to 20mm (10mm+10mm) compared to the 5.56W/m<sup>2</sup> ( $q_{peak}$ ) and 0.6W/m<sup>2</sup> ( $q_{ave}$ ) of the reference wall (no PCM), a reduction of 95.5% and 70%. It can be concluded that the influence of the outdoor environment on the indoors is significantly mitigated by the superior thermal regulation and insulation capacity of the wall (due to the increased PCM thickness). In summary, the thickness of the double-layer PCM is recommended to be 10mm (5mm+5mm) considering the economics of PCM.

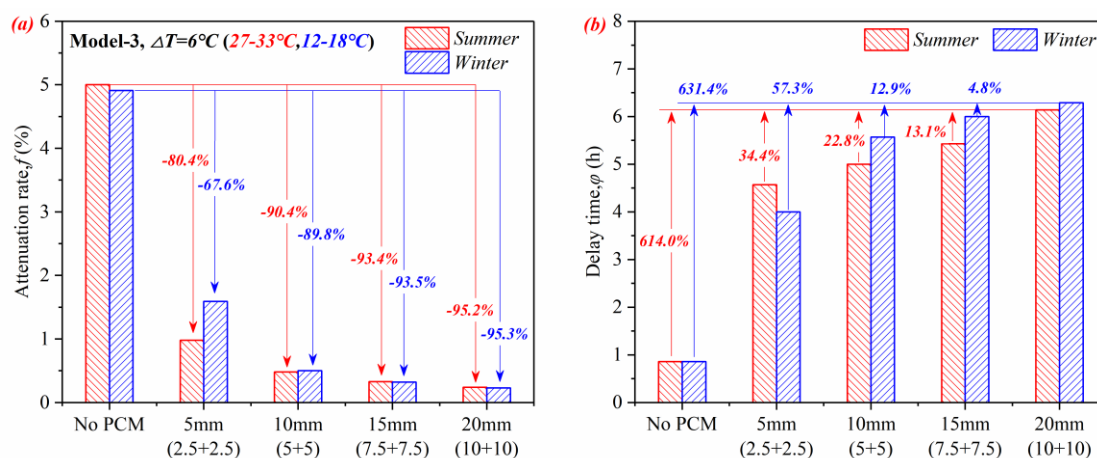


**Fig. 6-7. The (a) attenuation rate, (b) delay time, (c) peak heat flux and (d) average heat flux under different PCM thicknesses for summer and winter.**

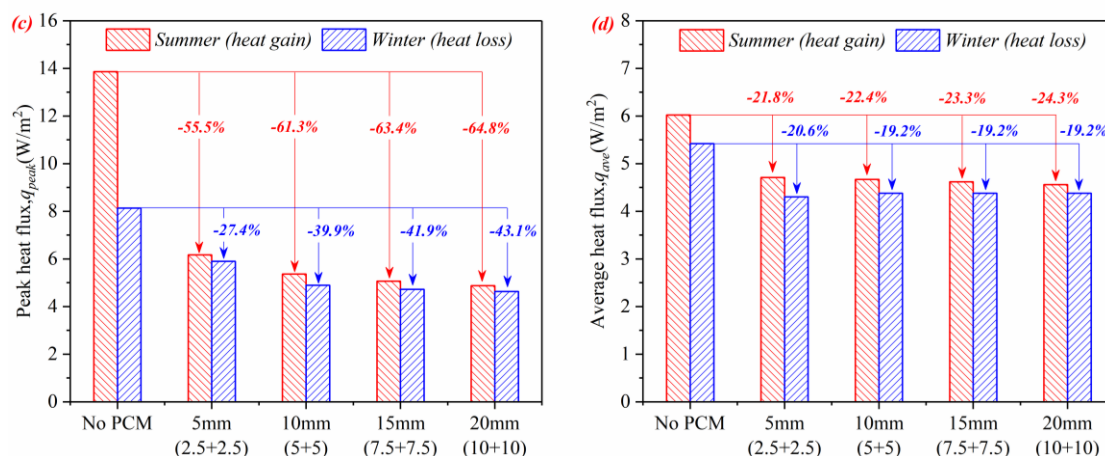


Fig. 6-7. (Continued).

## 6.6 Effectiveness of the PCM under different latent heats

The change of latent heat of PCM is expected to substantially impact the heat storage capacity of PCM and the application effectiveness of integration in LBW. The literature [40] found that an increase in latent heat reduces the daily fluctuation range of the PCM liquid fraction, which implies a reduction in the daily utilization rate of PCM, but whether the thermal performance of the wall also is affected due to it needs further investigation. Therefore, five data groups are selected for analysis based on the appropriate PCM parameters/configurations described above [Model-3,  $\Delta T=6^\circ C$  (27-33 $^\circ C$ , 12-18 $^\circ C$ ), 5mm+5mm] with an interval of 50kJ/kg and an initial value of 25kJ/kg. Fig. 6-8 shows the variation laws of wall thermal performance indexes with latent heat in summer and winter. It can be found that there is a measurable improvement with the increase in latent heat in the thermal performance of the wall in both summer and winter, but the application effect is still not directly proportional to the increase in latent heat. Fig. 6-8(a) indicates the  $f$  can be cut from 2.35% (summer) and 2.14% (winter) to 0.77% and 0.77%, respectively when the latent heat is improved from 25kJ/kg to 125kJ/kg. However, increasing latent heat from 125kJ/kg to 225kJ/kg only reduces the  $f$  from 0.77% to 0.48% (summer) and 0.45% (winter), and its contribution efficiency is reduced by 81.6% and 76.6%, respectively. The results demonstrate that double-layer PCM applications still show high benefits when the latent heat is 125kJ/kg in both summer and winter. Concurrently, the increase in latent heat of the double-layer PCM still eliminates the difference in  $f$  due to seasonal differences, a result similar to that concluded for the increase in PCM thickness. Moreover, Fig. 6-8(b) illustrates that the  $\varphi$  does not change for summer when the latent heat value exceeds 125kJ/kg, whereas it shows some tendency to increase in winter, but it is only a 0.71h increase from 4.86h (125kJ/kg) to 5.57h (225kJ/kg), which it is not noticeable for the lower  $f$ . Additionally, the above results are compared to previous studies [34] where the

optimal latent heat is taken to be essentially the same, but where previous studies found that a 10mm single layer PCM could achieve effect in summer, the 5mm PCM in the double-layer PCM proposed in this study (because the heat storage and release capacity of only one layer of PCM is effectively utilized in summer) can still achieve similar application potential under the same original wall and ensure the application effectiveness in winter. It shows that the double-layer PCM proposed in this study has higher economic efficiency for the same PCM thickness (10mm).

Furthermore, it can be seen from the variation in the  $q_{peak}$  given in Fig. 6-8(c) that the  $q_{peak}$  reduction rate appears relatively stable after exceeding 125kJ/kg in both summer and winter, which means that PCM with high latent heat will not bring higher economic benefits (the effectiveness of PCM is reduced). Simultaneously, it is important to mention that although the findings are similar to the PCM thickness, the increase in thickness results in a higher peak energy saving than the increase in latent heat for double-layer PCM, as can be easily seen in Fig. 6-7 and 8. This result is mainly since the increase in thickness of the double-layer PCM increases the thermal storage capacity and the total thermal resistance of the wall to a certain extent (one layer of PCM is the liquid or solid state in summer or winter), whereas the latent heat can only enhance the thermal storage capacity of the wall and its high latent heat will not be fully utilized and becomes meaningless due to the relatively stable indoor and outdoor thermal environment. Another distinguishing feature is that the double-layer PCM shows a superior result for the energy saving of  $q_{peak}$  (heat gain in summer and heat loss in winter) in summer than in winter, which means the demand for latent heat is higher in summer than in winter. Primarily because of the higher outdoor temperature fluctuations in summer in this study, which results in higher utilization of the PCM (latent heat is fully utilized) and a higher attenuation effect on its peak temperature, whereas the magnitude of heat absorbed (or released) by the PCM in winter is lower than in summer due to the lower outdoor temperature under the same latent heat of PCM. The above is also why the conclusion is contrary to the literature [40]. In addition, it can be observed from Fig. 6-8(d) that the increase in latent heat has little effect on the  $q_{ave}$ , with an energy-saving changes rate of only 0.4% (summer) and 1.7% (winter). It suggests that the PCM only adjusts the temperature fluctuation (peak-cutting and valley-filling) through its inherent thermal mass but does not weaken the heat transfer effect to a certain extent, which is in agreement with the findings of [34,64]. Meanwhile, it is clearly exhibited that the  $q_{ave}$  can still be reduced by 19.0%-22.3% with a small latent heat (25kJ/kg) compared to a reference wall (no PCM). As a result, it can be verified that the increased thermal storage capacity of the wall not only improves indoor comfort but also has a positive impact on energy saving for summer and winter. Based on the above suitable PCM kind/configurations [Model-

3,  $\Delta T=6^{\circ}\text{C}$ , 5mm+5mm, 125kJ/kg], the  $f$  can be reduced by 84.6%/84.3%, and the  $\phi$  is added to 5h/4.86h, the  $q_{peak}$  and  $q_{ave}$  are reduced by 58.2%/36.4% and 22.1%/19.4% respectively in summer/winter compared to the reference wall (no PCM). It further demonstrates that the application of double-layer PCM proposed in this study is helpful for long-term thermal comfort and low-energy operation of buildings.

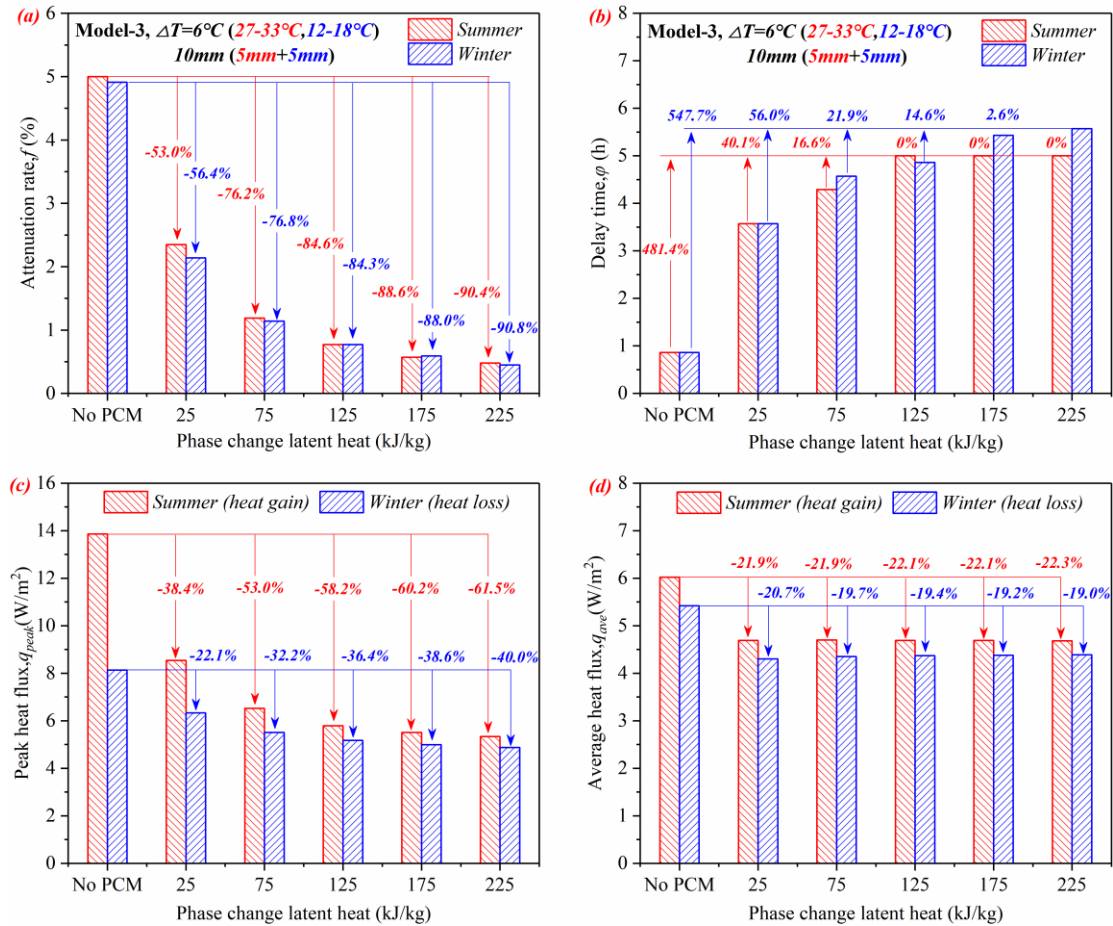


**Fig. 6-8. The (a) attenuation rate, (b) delay time, (c) peak heat flux and (d) average heat flux under different PCM latent heats for summer and winter.**

### 6.7 Summary

The effect of phase-change materials (PCM) on the thermal performance of walls has been extensively studied. However, the phase-transition temperature of PCM is usually fixed and its advantages (heat storage and release capacity) are limited to a certain season. Therefore, based on previous studies, the effectiveness of different kinds/configurations of PCM in lightweight building walls (LBW) for summer and winter were evaluated in this study, and the influence rules and energy-saving potential of PCM parameters (phase-transition temperature range, thickness, and latent heat) on the thermal performance of LBW in summer and winter were further explored. The main findings are as follows:

- Conventional single-layer PCM integrated into the LBW performs excellent heat storage and release capacity only part of the time within the phase-transition temperature range. In contrast, double-layer PCM applications exhibit superior thermal regulation ability in both summer and winter under the same PCM thickness.
- Double-layer PCM is located together in the middle of the wall is preferable to it being positioned separately on the outside and inside of the wall (single layer) under suitable phase-transition temperature.
- The effectiveness of wall thermal performance improved by the double-layer PCM is poorly correlated with the utilization rate ( $0 < \text{liquefaction rate} < 100\%$ ) of PCM under appropriate phase-transition temperatures, while it is strongly correlated with the indoor-outdoor temperature difference at comprehensive outdoor temperature (the common effect of solar radiation intensity and temperature). In this study, the application effectiveness of PCM in summer is better than in winter.
- PCM utilization is not proportional to phase-transition temperature ranges ( $\Delta T$ ), it tends to be the same as the  $\Delta T$  is expanded. The narrower  $\Delta T$  results in a higher average utilization rate (liquid fraction) at a suitable phase-transition temperature. However, the narrower the  $\Delta T$ , the worse the ability to adapt to the environment, which means a lower application effect. The  $\Delta T$  performs best in this study at  $6^\circ\text{C}$  ( $27\text{-}33^\circ\text{C}$ ,  $12\text{-}18^\circ\text{C}$ ).
- The effectiveness of double-layer PCM reaches saturation when thickness and latent heat exceed  $10\text{mm}$  ( $5\text{mm}+5\text{mm}$ ) and  $125\text{kJ/kg}$ , respectively. Nevertheless, the difference in application effect due to different total thermal resistance of the wall caused by another layer of PCM in different seasons (or different phase states) is diminished by enhancing the thermal storage capacity of the PCM.
- Compared with the reference wall (no PCM) in summer/winter, the PCM kinds/configurations [Model-3,  $\Delta T=6^\circ\text{C}$  ( $27\text{-}33^\circ\text{C}$ ,  $12\text{-}18^\circ\text{C}$ ),  $5\text{mm}+5\text{mm}$ ,  $125\text{kJ/kg}$ ] proposed in this study can reduce the attenuation rate ( $f$ ) by  $84.6\%/84.3\%$ , the delay time ( $\varphi$ ) is added to  $5\text{h}/4.86\text{h}$ , the peak ( $q_{peak}$ ) and average heat flux ( $q_{ave}$ ) are decreased by  $58.2\%/36.4\%$  and  $22.1\%/19.4\%$ , respectively.

## References

- [1] A. Allouhi, Y. E. Fouih, T. Kousksou, A. Jamil, Y. Zeraoui, Y. Mourad, Energy consumption and efficiency in buildings: current status and future trends, *Journal of Cleaner Production* 109 (2015) 118-130.
- [2] X. Cao, X. Dai, J. Liu, Building energy-consumption status worldwide and the state-of-the-art technologies for zero-energy buildings during the past decade, *Energy and buildings* 128 (2016) 198-213.
- [3] X. Meng, T. Luo, Y. Gao, L. Zhang, X. Huang, C. Hou, Q. Shen, E. Long, Comparative analysis on thermal performance of different wall insulation forms under the air-conditioning intermittent operation in summer, *Applied Thermal Engineering* 130 (2018) 429-438.
- [4] L. Zhang, Z. Liu, C. Hou, J. Hou, D. Wei, Y. Hou, Optimization analysis of thermal insulation layer attributes of building envelope exterior wall based on DeST and life cycle economic evaluation, *Case Studies in Thermal Engineering* 14 (2019) 100410.
- [5] J. Hou, T. Zhang, Z. Liu, C. Hou, H. Fukuda, A study on influencing factors of optimum insulation thickness of exterior walls for rural traditional dwellings in northeast of Sichuan hills, China, *Case Studies in Construction Materials* 16 (2022) e01033.
- [6] X. Meng, Y. Huang, Y. Cao, Y. Gao, C. Hou, L. Zhang, Q. Shen, Optimization of the wall thermal insulation characteristics based on the intermittent heating operation, *Case Studies in Construction Materials* 9 (2018) e00188.
- [7] Y. Lin, Y. Jia, G. Alva, G. Fang, Review on thermal conductivity enhancement, thermal properties and applications of phase change materials in thermal energy storage. *Renew Sustain Energy Rev* 82 (2018) 2730–2742.
- [8] A. D. Gracia, L. Navarro, J. Coma, S. Serrano, J. Roman í G. Pérez, L.F. Cabeza, Experimental set-up for testing active and passive systems for energy savings in buildings—lessons learnt, *Renew. Sustain. Energy Rev.* 82 (2018) 1014–1026.
- [9] L. Yang, X. Jin, Y. Zhang, K. Du, Recent development on heat transfer and various applications of phase-change materials, *Journal of Cleaner Production* 287 (2021) 124432.
- [10] J. Huang, Y. Luo, M. Weng, J. Yu, L. Sun, H. Zeng, Y. Liu, W. Zeng, Y. Min, Z. Guo, Advances and Applications of Phase Change Materials (PCMs) and PCMs-based Technologies, *ES Mater Manuf* 13 (2021) 23-29.
- [11] B. Kalidasan, A. K. Pandey, S. Shahabuddin, M. Samykano, M. Thirugnanasambandam, R. Saidur, Phase change materials integrated solar thermal energy systems: Global trends and current practices in experimental approaches, *J Energy Storage* 27 (2020) 101118.
- [12] F. He, J. Zou, X. Meng, W. Gao, L. Ai, Effect of copper foam fin (CFF) shapes on thermal

- performance improvement of the latent heat storage units, *Journal of Energy Storage* 45 (2022) 103520.
- [13] Y. Gao, Q. Zheng, J. C. Jonsson, S. Lubner, C. Curcija, L. Fernandes, S. Kaur, C. Kohler, Parametric study of solid-solid translucent phase change materials in building windows, *Applied Energy* 301 (2021) 117467.
- [14] N. Elawady, M. Bekheit, A. A. Sultan, A. Radwan, Energy assessment of a roof-integrated phase change materials, long-term numerical analysis with experimental validation, *Applied Thermal Engineering* 202 (2022) 117773.
- [15] Z. Xiao, P. Mishra, A. M. Nejad, M. Tao, S. Granados-Focil, S. V. Dessel, Thermal optimization of a novel thermo-optically responsive SS-PCM coatings for building enclosures, *Energy and Buildings* 247 (2021) 111129.
- [16] Z. Liu, J. Hou, D. Wei, X. Meng, B. J. Dewancker, Thermal performance analysis of lightweight building walls in different directions integrated with phase change materials (PCM), *Case Studies in Thermal Engineering* 40 (2022) 102526.
- [17] J. Lei, J. Yang, E. H. Yang, Energy performance of building envelopes integrated with phase change materials for cooling load reduction in tropical Singapore, *Applied energy* 162 (2016) 207-217.
- [18] N. Soares, A. R. Gaspar, P. Santos, J. J. Costa, Multi-dimensional optimization of the incorporation of PCM-drywalls in lightweight steel-framed residential buildings in different climates, *Energy and buildings* 70 (2014) 411-421.
- [19] P. Marin, M. Saffari, A. D. Gracia, X. Zhu, M. M. Farid, L. F. Cabeza, S. Ushak, Energy savings due to the use of PCM for relocatable lightweight buildings passive heating and cooling in different weather conditions, *Energy and Buildings* 129 (2016) 274-283.
- [20] Y. Li, E. Long, L. Zhang, X. Dong, S. Wang, Energy-saving potential of intermittent heating system: influence of composite phase change wall and optimization strategy, *Energy Exploration & Exploitation* 39(1) (2021) 426-443.
- [21] X. Sun, Z. Zhu, S. Fan, J. Li, Thermal performance of a lightweight building with phase change material under a humid subtropical climate, *Energy and Built Environment* 3(1) (2022) 73-85.
- [22] A. Sarri, D. Bechki, H. Bouguettaia, S. N. Al-Saadi, S. Boughali, M. M. Farid, Effect of using PCMs and shading devices on the thermal performance of buildings in different Algerian climates. A simulation-based optimization, *Solar Energy* 217 (2021) 375-389.
- [23] A. Fateh, D. Borelli, F. Devia, H. Weinläder, Summer thermal performances of PCM-integrated insulation layers for light-weight building walls: effect of orientation and melting point temperature, *Thermal Science and Engineering Progress* 6 (2018) 361-369.

- [24] P. K. S. Rathore, N. K. Gupta, D. Yadav, S. K. Shukla, S. Kaul, Thermal performance of the building envelope integrated with phase change material for thermal energy storage: an updated review, *Sustainable Cities and Society* 79 (2022) 103690.
- [25] Q. Al-Yasiri, M. Szabó, Incorporation of phase change materials into building envelope for thermal comfort and energy saving: A comprehensive analysis, *Journal of Building engineering* 36 (2021) 102122.
- [26] M. Song, F. Niu, N. Mao, Y. Hu, S. Deng, Review on building energy performance improvement using phase change materials, *Energy and Buildings* 158 (2018) 776-793.
- [27] N. Zhu, S. Li, P. Hu, S. Wei, R. Deng, F. Lei, A review on applications of shape-stabilized phase change materials embedded in building enclosure in recent ten years, *Sustainable cities and society* 43 (2018) 251-264.
- [28] M. Saffari, A. de Gracia, S. Ushak, L. F. Cabeza, Passive cooling of buildings with phase change materials using whole-building energy simulation tools: A review, *Renewable and Sustainable Energy Reviews* 80 (2017) 1239-1255.
- [29] A. C. Rai, Energy performance of phase change materials integrated into brick masonry walls for cooling load management in residential buildings, *Building and Environment* 199 (2021) 107930.
- [30] P. K. S. Rathore, S. K. Shukla, An experimental evaluation of thermal behavior of the building envelope using macroencapsulated PCM for energy savings, *Renewable Energy* 149 (2020) 1300-1313.
- [31] I. Adilkhanova, S.A. Memon, J. Kim, A. Sheriyev, A novel approach to investigate the thermal comfort of the lightweight relocatable building integrated with PCM in different climates of Kazakhstan during summertime, *Energy* 217 (2021) 119390.
- [32] Q. Wu, J. Wang, X. Meng, Influence of wall thermal performance on the contribution efficiency of the Phase-Change Material (PCM) layer, *Case Studies in Thermal Engineering* 28 (2021) 101398.
- [33] Z. Liu, J. Hou, Y. Huang, J. Zhang, X. Meng, B. J. Dewancker, Influence of phase change material (PCM) parameters on the thermal performance of lightweight building walls with different thermal resistances, *Case Studies in Thermal Engineering* 31 (2022) 101844.
- [34] Z. Liu, J. Hou, X. Meng, B. J. Dewancker, A numerical study on the effect of phase-change material (PCM) parameters on the thermal performance of lightweight building walls, *Case Studies in Construction Materials* 15 (2021) e00758.
- [35] R. A. Kishore, M. V. A. Bianchi, C. Booten, J. Vidal, R. Jackson, Parametric and sensitivity analysis of a PCM-integrated wall for optimal thermal load modulation in lightweight buildings, *Applied Thermal Engineering* 187 (2021) 116568.

- [36] B. Jangeldinov, S. A. Memon, J. Kim, M. Kabdrakhmanova, Evaluating the Energy Efficiency of PCM-Integrated Lightweight Steel-Framed Building in Eight Different Cities of Warm Summer Humid Continental Climate, *Advances in Materials Science and Engineering* 2020 (2020) 4381495.
- [37] M. Kabdrakhmanova, S. A. Memon, A. Saurbayeva, Implementation of the panel data regression analysis in PCM integrated buildings located in a humid subtropical climate, *Energy* 237 (2021) 121651.
- [38] G. Nurlybekova, S. A. Memon, I. Adilkhanova, Quantitative evaluation of the thermal and energy performance of the PCM integrated building in the subtropical climate zone for current and future climate scenario, *Energy* 219 (2021) 119587.
- [39] E. Mohseni, W. Tang, Parametric analysis and optimisation of energy efficiency of a lightweight building integrated with different configurations and types of PCM, *Renewable Energy* 168 (2021) 865-877.
- [40] R. A. Kishore, C. Booten, M. V. A. Bianchi, J. Vidal, R. Jackson, Evaluating cascaded and tunable phase change materials for enhanced thermal energy storage utilization and effectiveness in building envelopes, *Energy and Buildings* 260 (2022) 111937.
- [41] A. Staszczuk, T. Kuczyński, The impact of wall and roof material on the summer thermal performance of building in a temperate climate, *Energy* 228 (2021) 120482.
- [42] E. Meng, H. Yu, B. Zhou, Study of the thermal behavior of the composite phase change material (PCM) room in summer and winter, *Applied Thermal Engineering* 126 (2017) 212-225.
- [43] D. K. Bhamare, M. K. Rathod, J. Banerjee, Proposal of a unique index for selection of optimum phase change material for effective thermal performance of a building envelope, *Solar Energy* 218 (2021) 129-141.
- [44] S. Wijesuriya, C. Booten, M. V. A. Bianchi, R. A. Kishore, Building energy efficiency and load flexibility optimization using phase change materials under futuristic grid scenario, *Journal of Cleaner Production* 339 (2022) 130561.
- [45] F. Kuznik, J. Virgone, J. Noel, Optimization of a phase change material wallboard for building use, *Applied Thermal Engineering* 28(11-12) (2008) 1291-1298.
- [46] W. Xiao, X. Wang, Y. P. Zhang, Thermal analysis of lightweight wall with shapestabilized PCM panel for summer insulation, *J. Eng. Thermophys* 30 (2009) 1561-1563.
- [47] C. Chen, H. Guo, Y. Liu, H. Yue, C. Wang, A new kind of phase change material (PCM) for energy-storing wallboard, *Energy and Buildings* 40(5) (2008) 882-890.
- [48] E. Meng, H. Yu, G. Zhan, Y. He, Experimental and numerical study of the thermal performance of a new type of phase change material room, *Energy conversion and*

- management 74 (2013) 386-394.
- [49] J. Bohárquez-Órdenes, A. Tapia-Calderón, D. A. Vasco, O. Estuardo-Flores, A. N. Haddad, Methodology to reduce cooling energy consumption by incorporating PCM envelopes: A case study of a dwelling in Chile, *Building and Environment* 206 (2021) 108373.
- [50] F. Kuznik, J. P. A. Lopez, D. Baillis, K. Johannes, Phase change material wall optimization for heating using metamodeling, *Energy and Buildings* 106 (2015) 216-224.
- [51] Y. P. Zhang, K. P. Lin, R. Yang, H. F. Di, Y. Jiang, Preparation, thermal performance and application of shape-stabilized PCM in energy efficient buildings, *Energy and buildings* 38(10) (2006) 1262-1269.
- [52] G. Zhou, Y. Zhang, K. Lin, W. Xiao, Thermal analysis of a direct-gain room with shape-stabilized PCM plates, *Renewable Energy* 33(6) (2008) 1228-1236.
- [53] S. Ramakrishnan, X. Wang, J. Sanjayan, J. Wilson, Thermal performance assessment of phase change material integrated cementitious composites in buildings: Experimental and numerical approach, *Applied energy* 207 (2017) 654-664.
- [54] H. Cui, S. A. Memon, R. Liu, Development, mechanical properties and numerical simulation of macro encapsulated thermal energy storage concrete, *Energy and buildings* 96 (2015) 162-174.
- [55] X. Shi, S. A. Memon, W. Tang, H. Cui, F. Xing, Experimental assessment of position of macro encapsulated phase change material in concrete walls on indoor temperatures and humidity levels, *Energy and buildings* 71 (2014) 80-87.
- [56] H. A. Hattan, M. Madhkhan, A. Marani, Thermal and mechanical properties of building external walls plastered with cement mortar incorporating shape-stabilized phase change materials (SSPCMs), *Construction and Building Materials* 270 (2021) 121385.
- [57] B. Németh, A. Ujhidy, J. Tóth, J. Gyenis, T. Feczák, Testing of microencapsulated phase-change heat storage in experimental model houses under winter weather conditions, *Building and Environment* 204 (2021) 108119.
- [58] B.S. Hua, S. Tian, W. Jing, Accuracy of TMY2 and stochastic climatic model, *Hv & Ac* 34 (1) (2004) 5-7.
- [59] National Renewable Energy Laboratory. <https://nslrdb.nrel.gov>, 2022. (Accessed 6 January 2022).
- [60] C. Wang, X. Huang, S. Deng, E. Long, J. Niu, An experimental study on applying PCMs to disaster-relief prefabricated temporary houses for improving internal thermal environment in summer, *Energy and Buildings* 179 (2018) 301-310.
- [61] Y. Li, J. Zhou, E. Long, X. Meng, Experimental study on thermal performance improvement of building envelopes by integrating with phase change material in an

- intermittently heated room, *Sustainable cities and society* 38 (2018) 607-615.
- [62] C. Wang, S. Deng, J. Niu, E. Long, A numerical study on optimizing the designs of applying PCMs to a disaster-relief prefabricated temporary-house (PTH) to improve its summer daytime indoor thermal environment, *Energy* 181 (2019) 239-249.
- [63] Ministry of housing and urban-rural development, Code for Thermal Design of Civil Building (GB 50176-2016), China Architecture & Building Press, Beijing, China, 2016, pp. 77-84.
- [64] Y. Gao, F. He, X. Meng, Z. Wang, M. Zhang, H. Yu, W. Gao, Thermal behavior analysis of hollow bricks filled with phase-change material (PCM), *Journal of Building Engineering* 31(2020) 101447.
- [65] Y. Hong, L. Long, H. Zhang, R. Zou, The performance evaluation of shape-stabilized phase change materials in building applications using energy saving index, *Applied energy* 113 (2014) 1118-1126.
- [66] H. Wang, W. Lu, Z. Wu, G. Zhang, Parametric analysis of applying PCM wallboards for energy saving in highrise lightweight buildings in Shanghai, *Renewable Energy* 145 (2020) 52-64.

## Nomenclature

$t_m$	Phase-transition temperature, (°C)
$L_p$	Phase change latent heat, (kJ/kg)
$d$	Material thickness, (m)
$\lambda$	Thermal conductivity, [W/(m K)],Solid (Liquid)
$c_p$	Specific heat, [J/(kg K)]
$\rho$	Density, (kg/m <sup>3</sup> )
$T_i$	Material temperature, (°C)
$T_p$	PCM temperature, (°C)
$\Delta T$	Phase-transition temperature ranges, (°C)
$h_{in}$	Convective heat transfer coefficient of inner surface, [W/(m <sup>2</sup> ·K)]
$h_{out}$	Convective heat transfer coefficient of outer surface, [W/(m <sup>2</sup> ·K)]
$q_{peak}$	Inner surface peak heat flux, (W/m <sup>2</sup> )
$q_{ave}$	Inner surface average heat flux, (W/m <sup>2</sup> )
$H_p$	Enthalpy of PCM, (kJ/kg)
$\delta$	Wall thickness, (m)
$h$	Wall height, (m)
$\beta$	Liquid fraction, -
$\varphi$	Delay time, (h)
$f$	Attenuation rate, (%)

## Subscripts

$x$	Wall thickness direction
$y$	Wall height direction
$i$	Representatives OSB, glass wool or gypsum board
$p$	Phase-change materials
$s$	Solid states
$l$	Liquid states

## Abbreviations

LBW	Lightweight Building Walls
PCM	Phase-Change Materials
OSB	Oriented Strand Board
TMY2	Typical Meteorological Year 2



**Chapter 7. Effect of PCM on the thermal performance of  
lightweight wall and indoor thermal environment under natural  
conditions**

7.1	Introduction.....	7-1
7.2	Material and methods .....	7-2
7.2.1	Experimental system description.....	7-2
7.2.2	Experimental equipment and test methods .....	7-4
7.2.3	Evaluation indicators.....	7-5
7.3	Experimental result and analysis .....	7-5
7.3.1	Summer condition.....	7-5
7.3.2	Transitional season conditions .....	7-7
7.3.3	Winter conditions.....	7-9
7.3.4	Indoor temperature analysis .....	7-10
7.3.5	Energy saving potential analysis.....	7-13
7.4	Summary .....	7-14
	References.....	7-16
	Nomenclature.....	7-18



## 7.1 Introduction

Recently, lightweight buildings have been widely developed but are less able to suppress temperature fluctuations compared to conventional buildings [1]. Specifically, the delay and attenuation of solar radiation heat irradiated on the exterior wall in summer are not obvious, resulting in high indoor temperature. Wang et al. [2] found that the indoor temperature of light buildings in summer was up to 10 °C higher than outdoor by measurements. High indoor temperature fluctuations not only diminish indoor thermal comfort but also increase the energy consumption of air-conditioning. However, phase change materials (PCM) have been concerned as innovative materials for architecture by absorbing large amounts of heat at higher temperatures with small volumes and releasing it at lower temperatures to reach the purpose that suppresses indoor temperature fluctuations [3,4].

Soares et al. [5] investigated the performance of adding PCM to lightweight steel buildings in Europe and found that PCM can reduce the energy demand by about 10-60% in various climate zones. Lei et al. [6] showed that PCM can reduce the heat gain of the building envelopes by 21%-32% per year in Singapore. Long et al. [7] concluded that in humid subtropical climates, the annual energy consumption of lightweight buildings with integrated PCM can be reduced by 23.85%. Gao et al. [8] filled PCM in hollow bricks and found that the results could reduce the attenuation rate from 13.07% to 0.92%-1.93% and increase the delay time from 3.83h to 8.83h-9.83h. While Jia et al. [9] revealed that Integrating both thermal insulation material and PCM could improve the thermal performance of hollow bricks comprehensively in the thermal resistance and thermal inertia. In addition, Li et al. [10] derived from EnergyPlus simulation-based analysis that integrating PCM in a normal foamed concrete wall could reduce the yearly heating energy consumption by 4.74%.

It can be determined from numerous studies that the PCM is applied to LBW can enhance their thermal performance and keep indoor temperature fluctuations within a specific comfort level [11]. But its thermal performance improvement effect mainly depends on the heat storage and release capacity of PCM, while the latent heat storage and release capacity of PCM are highly dependent on the exchange between the wall surface and the ambient thermal environment for PCM integrated LBW. [12]. Thus, many scholars have studied the effects of PCM on LBW under different outdoor thermal environments. Among them, Sarri et al. [13] found that PCM combined with shading equipment under natural conditions was more conducive to improving indoor thermal comfort hours in most climate zones of Algerian, and its energy-saving potential can reach 44.13%~59.11%. Sun et al. [14] studied the influence of PCM integrated LBW on energy consumption in humid environments, It was presented that the

energy-saving rate dropped from 1.64% to 1.32% when the humidity increased from 40% to 90%, but the effect was not significant in winter. Fateh et al. [15] studied the effects of solar radiation (solar radiation was regarded as the time-varying heat source at the boundary) and concluded that the appropriate PCM could save 75% of the heat load. Zwanzig et al. [16] obtained the high dependence of PCM performance on weather conditions through energy-saving potential analysis and emphasized the necessity of selecting different PCM in different climatic regions.

From the above studies, it is easy to find that the existing studies also mostly focus on the simulation analysis of lightweight buildings in a specific climate environment, while the research on the thermal performance of lightweight walls and the indoor thermal environment regulation by comparing and testing PCM under natural environment for a long time is insufficient. Meanwhile, numerical simulation is more ideal, and it is more important to analyze the application of PCM in the lightweight building by real measurement. Therefore, two experimental rooms (reference room and composite PCM room) of the same size were built in this paper to compare and analyze the performance of composite PCM in lightweight buildings by experiment, and to evaluate the energy-saving potential of lightweight buildings with composite PCM based on experimental data, thus providing important experimental support for the subsequent research.

## **7.2 Material and methods**

### **7.2.1 Experimental system description**

In this study, to monitor the thermal behavior of composite PCM lightweight buildings at different times of the year, two small-scale test rooms of the same size were constructed in Qingdao and exposed to different seasons (summer, transition season and winter) for a longer time, as shown in Fig. 7-1. In addition, the experimental tests relied on passive solar gain and ambient environment to activate the composite PCM system without machinery. The dimensions of the two box rooms are 1200mm (length) ×1000mm (width) ×1000mm (height), and the envelope is 12mm Plywood, 20mm PCM and 5mm Plywood from the outside to inside (see Fig. 7-2). The north and south directions of the room each have an 800mm (length) × 600mm (height) double hollow window (6mm+12A+6mm). Among them, Fig. 7-1(a) is the composite PCM box room, where the tubular PCM is arranged and fixed on the placement grid matching the size of each inner surface, and then installed on the inner surface around the box room using a steel frame as support. Considering the practical application, the PCM is located between EPS and inner Plywood to form a composite envelope structure. Fig. 7-1(b) is a reference box room without PCM. The experimental test site is located on the roof of a

university building in Qingdao with no shade around.

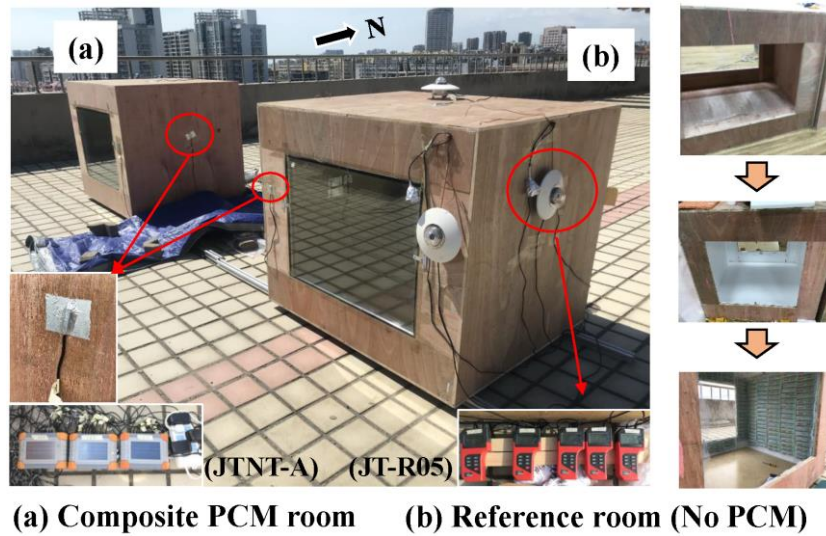


**Fig. 7-1. Experimental box room.**

The PCM used in the experiment is a new material that is easy to composite with the wall and was developed by the Chavez Institute of Environmental Studies in Canada and the University of British Columbia (UBC). The PCM is permanently encapsulated in an aluminum composite diaphragm to form a "TCM tube", also known as a natural temperature-controlled material. Normally a "TCM" tube weighs 100-120g, 175mm long, 45mm wide and 20-25mm thick, as shown in Fig. 7-2[17]. The thermal parameters of the relevant materials are given in Table 1.

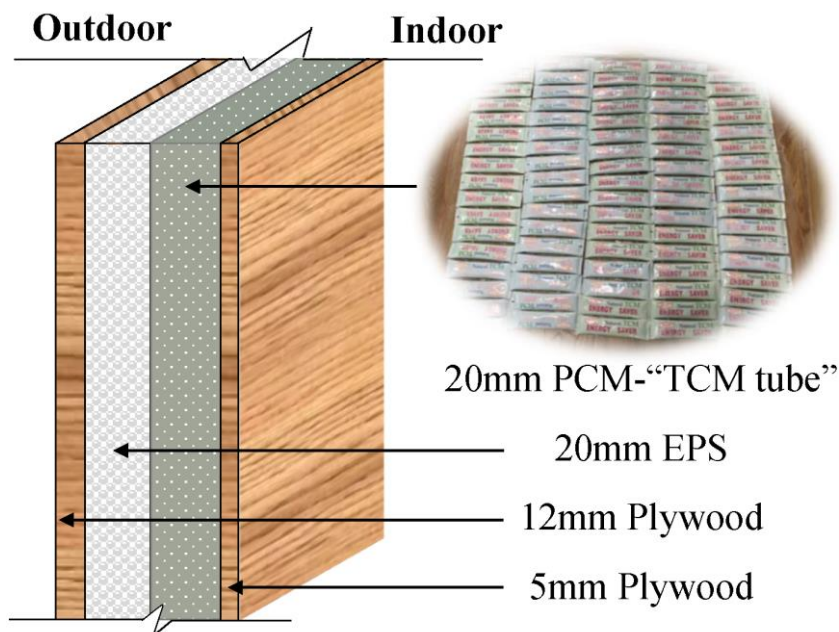


**Fig. 7-2. Diagram of envelope structure and PCM (TCM tube).**

**Table 7-1 Thermo-physical parameters of wall materials [17,18].**

Material	$t_m, (^{\circ}\text{C})$	$L_p, (\text{kJ/kg})$	$d, (\text{mm})$	$\lambda, [\text{W}/(\text{m K})]$	$c, [\text{J}/(\text{kg K})]$	$\rho (\text{kg}/\text{m}^3)$
PCM	18-26	216	20-25	0.5(0.25)	1785	1300
Plywood	-	-	5/12	0.17	2510	600
EPS	-	-	20	0.039	1380	20

### 7.2.2 Experimental equipment and test methods

The JTR05 dual-channel thermal environment tester produced by Beijing Jian Tong Technology Co., Ltd. was used for outdoor thermal environment testing, it can simultaneously test and record the total solar radiation and air temperature in the spectral range of 0.3~3.2 $\mu\text{m}$ . Its surface is coated with a high absorption rate black layer, the hot junction is on the induction surface, and the cold junction is in the body, the temperature difference potential generated between the hot and cold junction can reflect the total solar radiation. JTR05 storage interval 1-60min can continuously store 4000 groups of data, communication interface RS232. Moreover, the JTNT-A temperature and heat flux tester was used to record the inner and outer surface temperature of the wall, indoor air temperature and heat flux density. JTNT-A adopts a high-precision AD module, which can synchronously measure and record 12-way T-type thermocouple temperature and 6-way heat flux density, with storage interval 0.5s-60min, built-in high storage SD card and communication interface RS485. Table 2 gives the related parameters of the experimental equipment.

**Table 7-2 Related parameters of the experimental equipment.**

Equipment	Picture	Test parameters	Range	Accuracy	Resolution
JTR05		Solar radiation intensity	0~2000W/m <sup>2</sup>	Nonlinearity: $\pm 2\%$ ; Cosine response: $\leq \pm 7\%$	Sensitivity: 7~14mv/kw. m <sup>2</sup>
		Temperature	-50 $^{\circ}\text{C}$ ~50 $^{\circ}\text{C}$	$\pm 0.5^{\circ}\text{C}$ (normal < $\pm 0.2^{\circ}\text{C}$ )	0.1 $^{\circ}\text{C}$
JTNT-A		Heat flux	0~2000W/m <sup>2</sup>	$\pm 4\%$	0.1 W/m <sup>2</sup>
		Temperature	-50 $^{\circ}\text{C}$ ~120 $^{\circ}\text{C}$	$\pm 0.5^{\circ}\text{C}$	0.1 $^{\circ}\text{C}$

To obtain the solar radiation intensity and temperature variations in different directions of the room, five JTR05 units were placed in different directions (east, south, west, north and roof). Next, 22 thermocouples were arranged in the center of the inner and outer surfaces (top and five inner surfaces) and the center of the 2 test box rooms, and 10 heat flux meters were placed in the center of the inner surface in 5 directions. All data were collected by three JTNT-A units

and connected to the computer via RS232/RS485 for real-time data recording and output and the recording intervals were all set to 15 min. To ensure the accuracy of the test data, the experimental instruments were calibrated before the tests. Meanwhile, the tests were carried out from Jul. 15 to Jul. 25 (summer), Oct. 16 to Oct. 28 (transition season) and Dec. 22 to Dec. 31 (winter), 2021, respectively to reflect clearly the effect of PCM on the thermal performance of lightweight buildings in different seasons.

### 7.2.3 Evaluation indicators

Some evaluation indexes are proposed in this paper to evaluate more intuitively the influence of PCM on the thermal performance of lightweight building walls (LBW) and the improvement effect, including the delay time ( $\varphi$ ), attenuation rate ( $f$ ), peak heat flux ( $q_{peak}$ ) and load energy-saving rate ( $ESR$ ), which are described as equations (1)-(5) [19-20]:

$$\varphi = t_{T,w,in,max} - t_{T,out,max} \quad (7-1)$$

$$f = \frac{A_{w,in}}{A_{out}} \times 100\% \quad (7-2)$$

$$q_{peak} = q(t)_{max} \quad (7-3)$$

$$ESR = \frac{Q_1 - Q_2}{Q_1} \times 100\% \quad (7-4)$$

$$Q = KF\Delta T_{indoor} = \frac{F(T_{in} - T_{cool/heat})}{R_{wt}} \quad (7-5)$$

## 7.3 Experimental result and analysis

Due to the long test period and more experimental data, only three representative days in different seasons are selected for analysis in this paper, which is Jul. 22-Jul. 24, 2021 (summer), Oct. 20-Oct. 22, 2021 (transition season) and Dec. 28-Dec. 30, 2021 (winter), respectively. Meanwhile, the south-facing wall with typicality is discussed for wall thermal performance analysis, and the above evaluation indexes are calculated as 3-day average values. Considering the same thermal resistance ( $R_{wt}$ ), the equivalent heat flux is used in this paper to evaluate wall heat flux, i.e.  $q_{(T)} = \Delta T / R_{wt}$ .

### 7.3.1 Summer condition

Previous studies [19] found that LBW integrated PCM can effectively suppress inner surface temperature fluctuations to improve the energy-saving of cooling load during summer. However, the thermal performance of lightweight buildings and the application effect of PCM can be revealed more intuitively under non-mechanical operation. Therefore, Fig. 7-3 gives the variation of the inner surface temperature of the south wall in the natural state in summer. It is

obvious from Fig. 7-3(a) that the maximum inner surface temperature of the reference room (without PCM) can reach 49.2 °C when the outdoor temperature is high (39.2 °C). It shows that the indoor temperature in summer is far beyond the human thermal comfort range due to the lower thermal inertia of LBW, which is also an urgent problem to be solved in lightweight buildings. Meanwhile, from the perspective of comprehensive temperature ( $T_{sa}$ ) (considering the solar radiation effect), the inner surface temperature fluctuation of the reference room is basically the same as the  $T_{sa}$ , and the average temperature fluctuation is only reduced by 0.16%. The above phenomenon is mainly due to the low thermal inertia of LBW which does not play a significant role in delaying and attenuating the solar radiation heat irradiated on the external walls. However, compared to the reference wall when the LBW is integrated with PCM, the peak inner surface temperature can be reduced by 2.9 °C (average), and the attenuation rate ( $f$ ) is reduced by 18.08% from 99.84% to 81.79%, delay time ( $\varphi$ ) can be increased from 1.67h to 3.67h. But the difference in the average temperature of the inner surface between the reference wall (35.31 °C) and the composite PCM wall (34.02 °C) is only 0.99 °C. As a result, it indicates that the advantage of PCM is not in thermal insulation but in thermal regulation to suppresses temperature fluctuations and rises and shifts peak temperatures. Moreover, it can be seen from Fig. 7-3(b) that the peak heat flux ( $q_{peak}$ ) of the reference wall can be reduced by 8.73% and the delay time of  $q_{peak}$  can be increased by 6.5h. The above data can be intuitively concluded that PCM can effectively improve the energy-saving of buildings in high-temperature periods. At the same time, the heat flux of the composite PCM wall shows negative values (i.e.,  $T_{w,in} < T_{w,out}$ ) from 09:00 to 12:00, while the reference wall is continuously increasing at this time, a phenomenon sufficient to indicate the heat absorption of the PCM during high-temperature periods. The heat flux of the reference wall rise to the highest point at about 15:00 and then started to decrease, and tended to 0 after about 7h, while the composite PCM wall peaked at about 20:00 and decreased slowly, and no relatively stable trend is found. It means that the PCM is continuously exothermic and remains relatively stable until the exothermic completion, which is one of the reasons why PCM can maintain the indoor thermal stability of lightweight buildings.

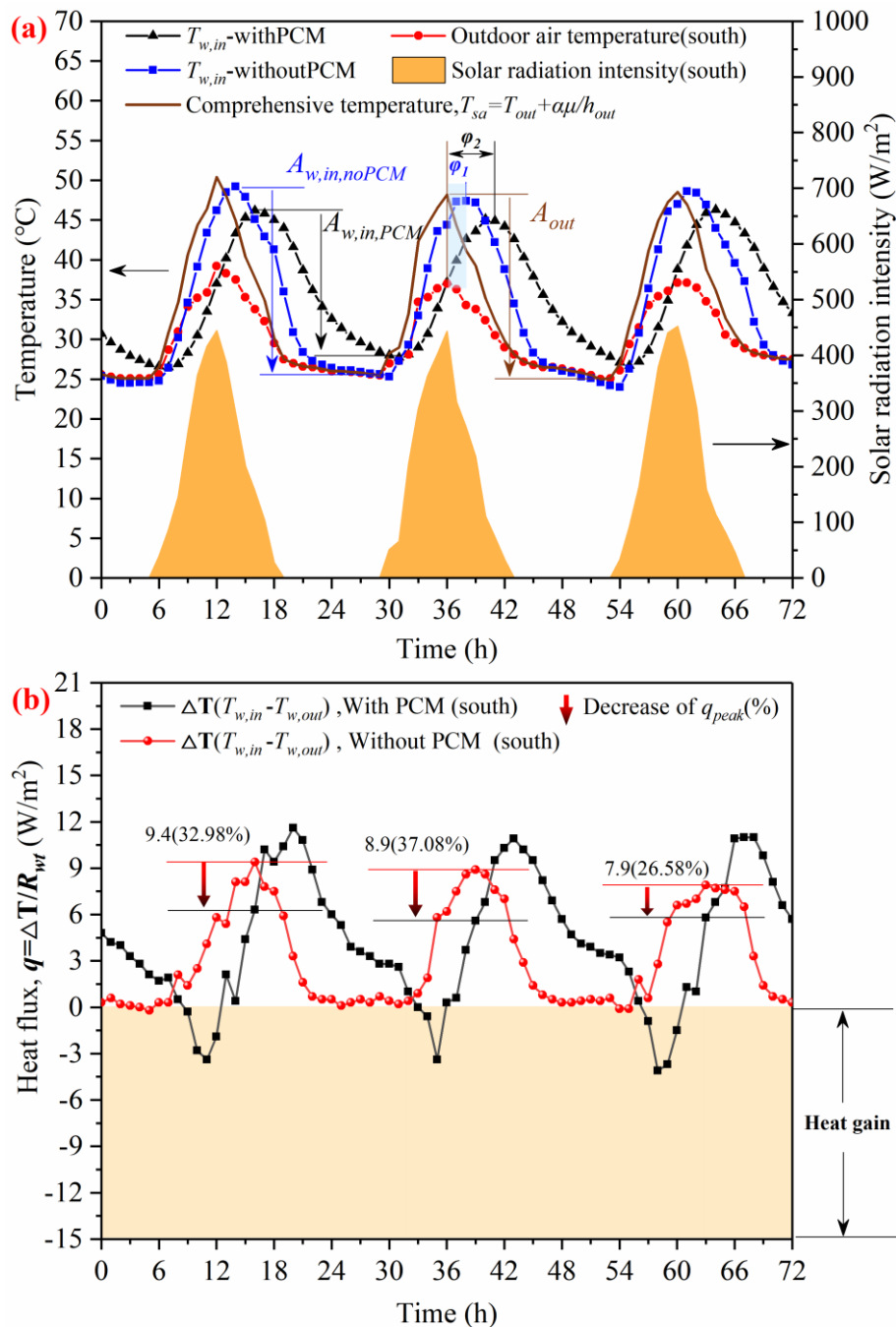
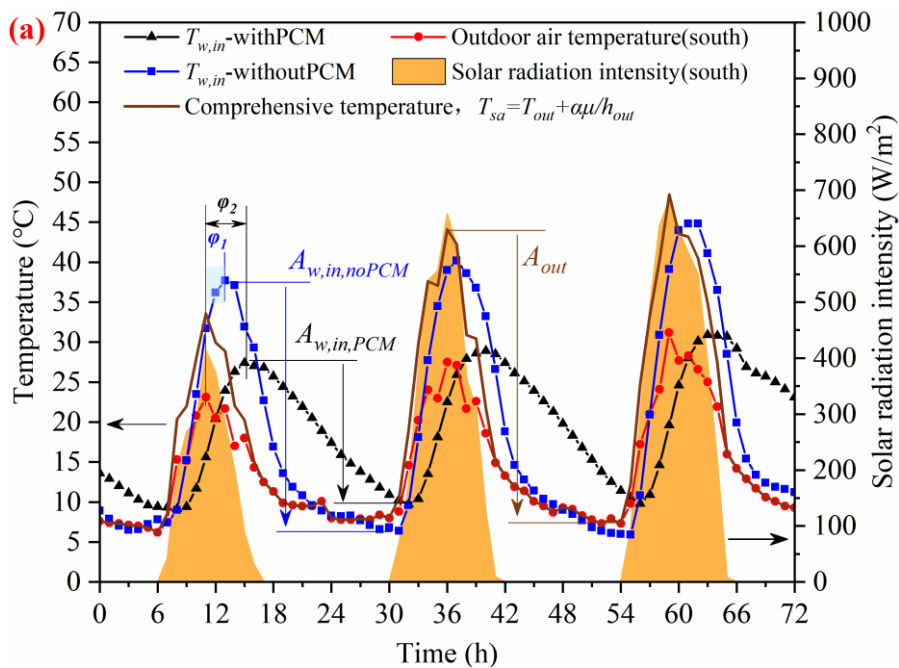


Fig. 7-3. Variation of (a) surface temperature and (b) heat flux with time in summer.

### 7.3.2 Transitional season conditions

From the above results, it can be drawn that PCM can suppress the summer peak temperature, but its latent heat application is limited due to the low phase-transition temperature (basically in the liquefied state) compared to the high temperature. Therefore, Fig.4 depicts the changes in the thermal performance of the wall during the transition season (Oct. 20-22). From Fig. 7-4(a), it can be found that the inner surface temperature of the reference wall is still high, which can reach up to 44.8 °C, and the average temperature is at 18.4 °C. The temperature

fluctuation ( $A_{w,in,ref}$ ) reaches 34.6 °C, and the  $f$  is 99.6%. While there is a significant reduction in the peak inner surface temperature of the composite PCM wall, with a maximum reduction of 13.9 °C and an average of 11.8 °C compared to the reference wall, reducing the  $f$  to 56.7% (reduction rate of 42.9%). It means that PCM is better in the transition season than summer for lightweight buildings, and its application basically maintains all day in a comfortable temperature range (preventing overcooling and overheating). The main reason is that the phase-transition temperature is 18-26°C, for summer, the temperature is higher ( $T > 26^\circ\text{C}$ ), and the lower phase-transition temperature makes PCM rapid phase change and basically keeps it in a liquid state only play the role of thermal resistance. And the PCM storage and release capacity can be effectively utilized in the transition season due to the large temperature difference throughout the day ( $T_{sa} = 6.2^\circ\text{C} - 44.12^\circ\text{C}$ ). This is also sufficient to explain that the application effect of PCM is highly related to the outdoor thermal environment, and the appropriate phase-transition temperature should be selected for different seasons. Furthermore, the  $\varphi$  of the reference wall is 1.67h, while the composite PCM wall is 4h, indicating that the application of PCM can effectively shift the time of peak temperature occurrence and improve indoor comfort while reducing energy use during peak time. It is also obvious from Fig. 7-4(b) that the peak energy-saving rate of composite PCM walls can reach 50.47% compared to the reference wall. In addition, it can be found that PCM energy saving contribution increases as the outdoor peak temperature rises. The phenomenon is mainly because the PCM absorbs heat more fully as the outdoor temperature fluctuation increases and has a higher latent heat utilization, which can also be concluded from the change in the negative value of heat flux ( $T_{w,in} < T_{w,out}$ ) as well.



**Fig. 7-4. Variation of (a) surface temperature and (b) heat flux with time in transition seasons.**

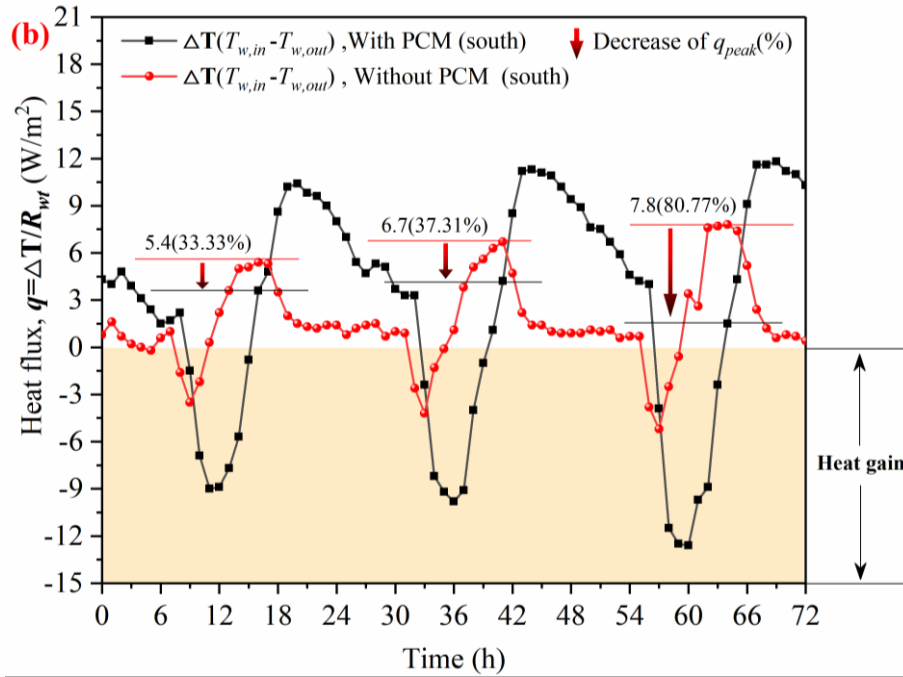


Fig. 7-4. (Continued).

### 7.3.3 Winter conditions

In winter, the phenomenon of indoor overcooling or overheating is more obvious under no mechanical equipment due to the low thermal inertia of LBW. As can be seen from Fig. 7-5(a) which gives the curve of the inner surface temperature with time in winter, the maximum inner surface temperature of the reference wall can reach 31.9 °C and the minimum temperature is -4.5 °C. The temperature fluctuations all day reached 36.4 °C, and the  $f$  is 91.69%. It illustrates that the outdoor environment has a greater impact on the indoor due to the low thermal mass of LBW. Although the indoor temperature can be increased in winter, taking into account the human thermal comfort needs, all day (24h) thermal comfort hours (16-25°C [21]) only accounted for 8% (reference building). Nevertheless, the  $f$  of composite PCM was 64.74%, which is 29.39% lower compared to the reference wall, and the  $\phi$  increased from 1h to 4h, and the thermal comfort hours increased to 27.8%. The peak temperature is decreased from 31.9 °C to 23.0 °C and the minimum temperature is improved by 1.9 °C. This is mainly because the solar radiation heat absorbed by the PCM during the day is released at night when the temperature drops. Moreover, Fig. 7-5(b) shows that the composite PCM can reduce the  $q_{peak}$  by 71.14% compared to the reference wall, meanwhile, the heat flux of the reference wall decreases from the peak to nearly 0 ( $T_{w,in}=T_{w,out}$ ) in only 3h, while the composite PCM starts to decrease slowly when the reference wall drops to the lowest and always remains positive ( $T_{w,in}>T_{w,out}$ ) until the heat gain of the second day after the heat release is completed ( $T_{w,in}<T_{w,out}$ ). This also further demonstrates that PCM can always ensure that the inner surface temperature is maintained at a

high level in its natural state due to latent heat, thereby improving indoor thermal comfort.

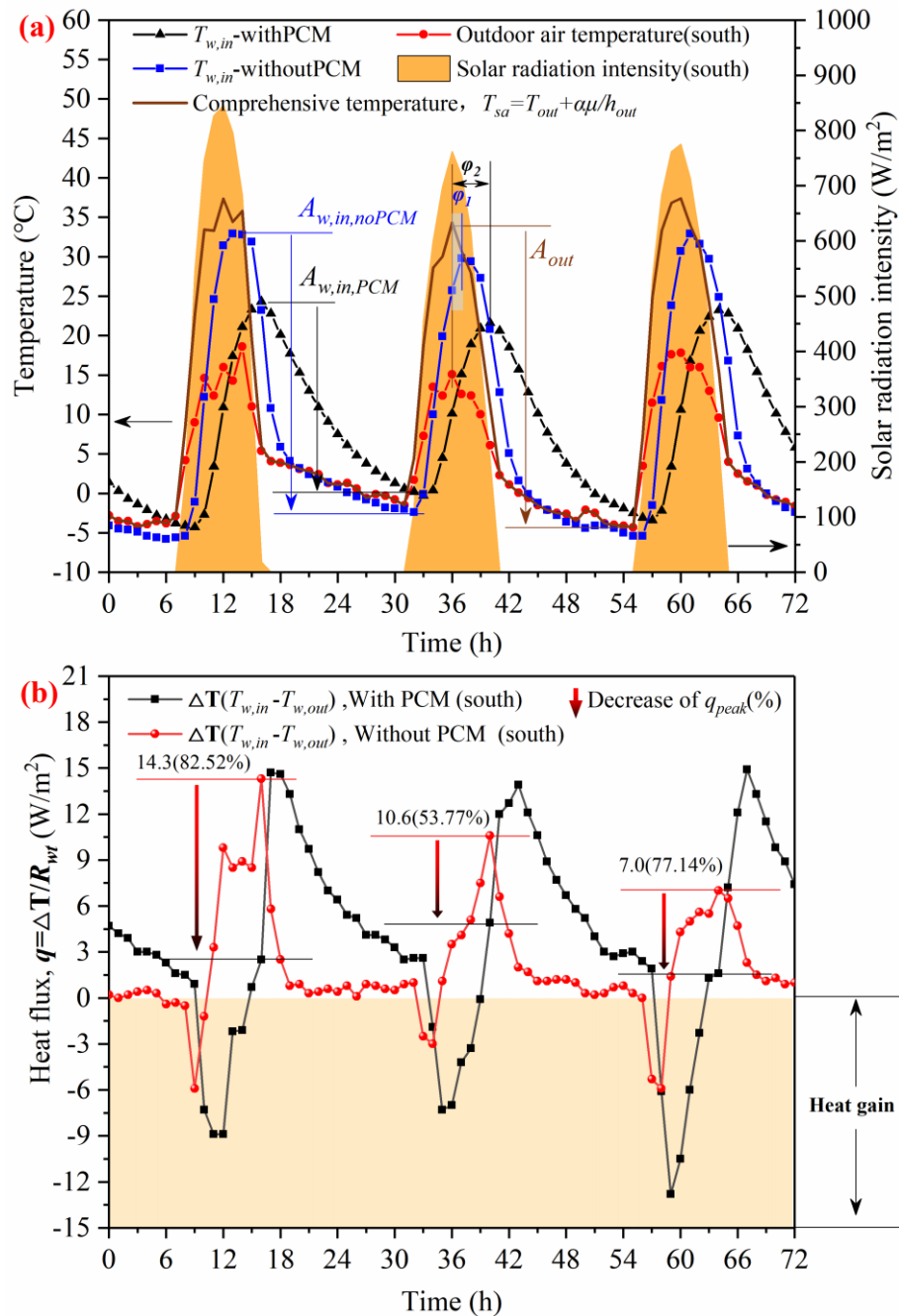


Fig. 7-5. Variation of (a) surface temperature and (b) heat flux with time in winter.

### 7.3.4 Indoor temperature analysis

The above results are sufficient to explain the ability of PCM to improve the thermal performance of LBW. However, considering the level of indoor thermal comfort, the variation of indoor and outdoor temperature in different seasons is presented in Fig. 7-6. As observed in Fig. 7-6(a), when the outdoor temperature is high (37.7°C) in summer, the indoor temperature

rises rapidly with the outdoor temperature due to the small heat storage and low thermal inertia of the reference building wall, and the maximum can reach 52.0°C under the higher solar radiation heat, which is 14.3°C higher than the outdoor temperature. While the composite PCM box room can better prevent the heat transfer to the room during the period of temperature rise due to the strong heat storage capacity of PCM, which has the effect of heat attenuation and temperature delay. The indoor temperature can be reduced by 3.3°C and improve the minimum by 1.1°C compared with the reference box room and the  $\phi$  for the reference and the composite PCM box room are 1h and 2.67h, respectively.

However, from Fig. 7-6(b) can be noted that the maximum indoor temperature of the composite PCM box room can be declined by 8.23 °C and the minimum temperature by 1.8 °C compared to the reference box room during the transition season, which is 4.93 °C higher than the peak summer temperature attenuation, suggesting that the thermal regulation effect of PCM on the transition season significantly better than that in summer. This is mainly due to the phase-transition temperature is lower (18-26°C) for summer, the outdoor temperature is higher than 26°C for about 80% of the time in the whole day (24h), so the PCM occur rapidly and keep the liquid state, which only to increase the wall thermal resistance, and its thermal regulation capacity is not given full play. As a result, shows the importance of choosing the suitable phase-transition temperature for different seasons or climates. When the PCM with relatively suitable phase change temperature is adopted in the transition season, the time for the indoor temperature to remain at 16-25 °C all day increases from 2.3h in the reference box to 7.3h. It shows that PCM can improve the indoor thermal comfort range of lightweight buildings through thermal regulation without mechanical equipment, which also further reflects the energy-saving effect of PCM. Furthermore, as can be noted from Fig. 7-6(c), the PCM reduces the indoor peak temperature by 6.9 °C in winter, while the minimum temperature is only increased by 0.7 °C. The main reason for this phenomenon is that the heat loss from the windows is higher due to the lower outdoor temperature in winter, which makes the PCM heat release basically complete before the outdoor temperature reaches the minimum temperature (higher release rate), resulting in the minimum indoor temperature not being remarkably improved. The indoor thermal comfort hours (16-25 °C) of the composite PCM box room is only 2h higher than the reference box room for the whole day (24h).

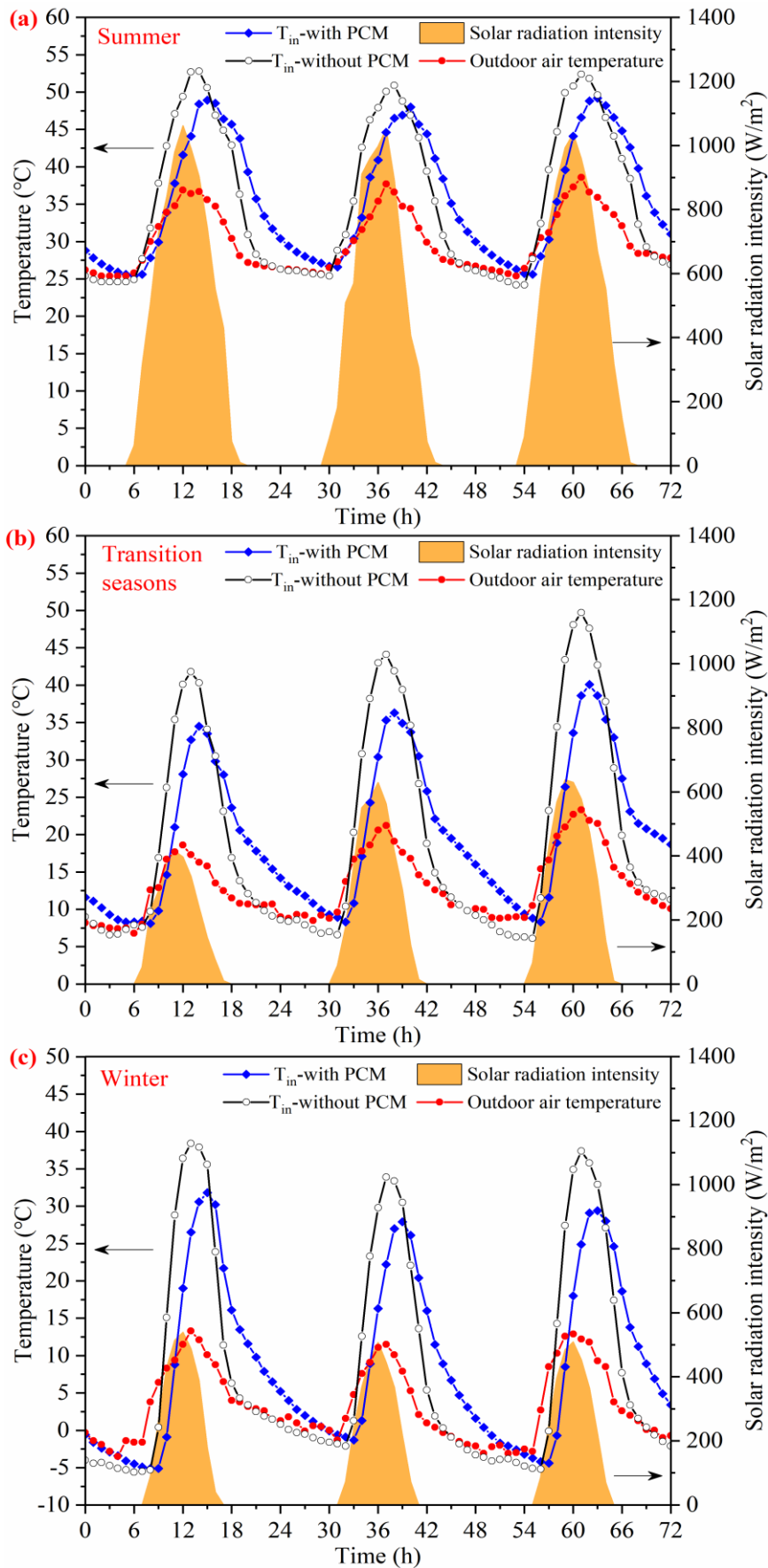
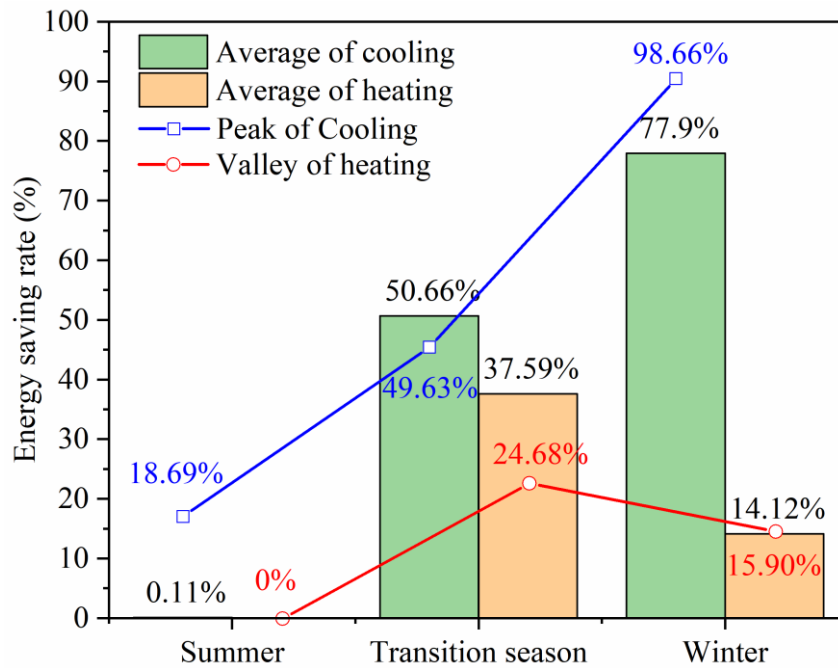


Fig. 7-6. Variation of indoor temperature in different seasons.

### 7.3.5 Energy saving potential analysis

To evaluate the impact of PCM on the energy saving of lightweight buildings, the energy-saving rate (ESR) method [17,20] is used in this paper to analysis preliminary the energy-saving potential of air conditioning and heating. However, it should be pointed out that the air conditioning and heating energy savings rates calculated in this paper are the relative levels generated by PCM, while the actual energy savings should be calculated in detail based on the annual operation. The set temperature of the air conditioner is 26°C, and the heating is 18°C (higher than 26°C for cooling, lower than 18°C for heating). Fig. 7-7 gives the energy-saving rate of cooling and heating loads in different seasons. It can be observed that the ESR of peak cooling load in summer is 18.69%, while the average is only 0.11%. The main reason is that although PCM can reduce the peak load by heat absorption, the average temperature is higher for the whole day due to the heat released. This further shows that PCM only through the heat storage and release capacity for thermal regulation but does not weaken the heat transfer effect of the wall.

Moreover, it can be more easily concluded from the transition season that the peak cooling load can be saved by 49.63% due to PCM can effectively suppress the overheating of indoor temperature under a relatively suitable phase-transition temperature. When the outdoor temperature is lower at night, the PCM can significantly increase the minimum temperature by releasing heat, which can diminish the heating load by 24.68%. The average ESR for the whole day (24h) is 50.66% for the cooling and 37.59% for the heating load. Which shows the great potential for energy savings by using appropriate PCM in different seasons. Finally, it can be drawn from the winter season that the overheating effect is shorter because of the lower outdoor temperature and solar radiation compared to the summer. The PCM can basically eliminate the overheating, and the ESR of peak cooling load can reach 98.66%, and the average can save 77.9%. Despite the higher heat loss from the windows, the PCM can still reduce the heat load by 15.9% at lower outdoor temperatures and the average ESR is 14.12%. Combining the above analysis, results can be obtained that lightweight buildings integrated PCM can not only improve the year-round indoor thermal comfort level but also obviously enhance its energy saving.



**Fig. 7-7. Energy-saving rate (ESR) for different loads in different seasons.**

#### 7.4 Summary

- (1) Lightweight building composite PCM can effectively suppress temperature fluctuation and rise under natural conditions in summer. Compared with the reference wall, the inner surface peak temperature and the attenuation rate ( $f$ ) can be reduced by 2.9°C and 18.08%, the delay time ( $\varphi$ ) is increased from 1.67h to 3.67h, the peak heat flux ( $q_{peak}$ ) can be lowered by 8.73%.
- (2) In the transitional season, the composite PCM is better than in summer for lightweight buildings, and its application can basically maintain the all-day temperature in a comfortable range. The peak and average temperature of the inner surface can be cut by 13.9 °C and 11.8 °C compared to the reference wall, and the  $f$  can be reduced by 42.9%, and the  $q_{peak}$  energy-saving rate can reach 50.47%.
- (3) When the outdoor temperature is lower in winter, the  $f$  of composite PCM is reduced by 29.39% and the  $\varphi$  is increased from 1h to 4h compared to the reference wall, and the thermal comfort hours are added to 27.8%. The maximum temperature decreased from 31.9 °C to 23.0 °C, and the minimum temperature improved by 1.9 °C.
- (4) The application effect of PCM is highly related to the outdoor thermal environment, and PCM with a more suitable phase-transition temperature should be selected in different seasons to maximize the effect. For indoor temperature, due to the high outdoor

temperature in summer, the lower phase-transition temperature basically causes the PCM to be in a liquid state, which only plays a certain thermal resistance. Its indoor peak temperature can be reduced by 3.3°C, while the whole day is still higher than 26°C for 91% of the time. However, the peak indoor temperature can be reduced by 8.23°C in the transition season, and the time that the indoor temperature remains at 16-25°C all day increases from 2.3h to 7.3h. In winter, the PCM releases heat quickly due to the lower outdoor temperature and high exterior window heat loss and its all-day indoor thermal comfort hours improve by only 2h.

- (5) Composite PCM has great energy-saving potential. The energy-saving rate (ESR) of peak cooling load in summer is 18.69%, and the average ESR is only 0.11% due to the high outdoor temperature. However, the peak cooling load can save 49.63% and the average is 50.66% in the transition season and the ESR of heating load can be improved by 24.68% in the lowest temperature period at night and the average raises 37.59%.
- (6) In winter, the time of overheating is shorter since outdoor and solar radiation is lower than that in summer. Using PCM can basically eliminate the peak overheating, and the ESR of peak and average cooling load can reach 98.66% and 77.9%. The valley of heating load can still reduce by 15.9% through PCM release heat despite the high heat loss from the windows at lower outdoor temperatures, with an average heat load savings of 14.12%.

## References

- [1] Neneth, B., Ujhidy, A., Toth, J., Gyenis, J. and Feczok T. (2021) Testing of microencapsulated phase-change heat storage in experimental model houses under winter weather conditions. *Building and Environment*. Vol. 49, pp. 108119.
- [2] Wang, C., Huang, X., Deng, S., Long, E. and Niu, J. (2018) An experimental study on applying PCMs to disaster-relief prefabricated temporary houses for improving internal thermal environment in summer. *Energy and Buildings*. Vol. 179, pp. 301-310.
- [3] Gracia, A., Navarro, L., Coma, J., Serrano, S., Romanı J., Perez, G. and Cabeza, L. F. (2018) Experimental set-up for testing active and passive systems for energy savings in buildings–lessons learnt, *Renewable and Sustainable Energy Reviews*. Vol. 82, pp. 1014-1026.
- [4] Chen, X., Ren, J., Xie, Z. and Dong, K. (2017) Temperature and Energy Consumption Simulation of Phase Change Materials Applied to Building Exterior Wall. *Building Energy Efficiency*. Vol. 45(4), pp. 56-62.
- [5] Soares, N., Gaspar, A. R., Santos, P. and Costa, J. J. (2014) Multi-dimensional optimization of the incorporation of PCM-drywalls in lightweight steel-framed residential buildings in different climates. *Energy and buildings*. Vol. 70, pp. 411-421.
- [6] Lei, J., Yang, J. and Yang, E. (2016) Energy performance of building envelopes integrated with phase change materials for cooling load reduction in tropical Singapore. *Applied Energy*. Vol. 162, pp. 207-217.
- [7] Long, X., Zhang, W., Li, Y. and Zheng, L. (2017) Thermal performance improvement of lightweight buildings integrated with phase change material: An experimental and simulation study. *Advances in Mechanical Engineering*. Vol. 9(6), pp. 1-8.
- [8] Gao, Y., He, F., Meng, X., Wang, Z. and Gao, W. (2020) Thermal behavior analysis of hollow bricks filled with phase-change material (PCM). *Journal of Building Engineering*. Vol. 31, pp. 101447.
- [9] Jia, C., Geng, X., Liu, F. and Gao, Y. (2021) Thermal behavior improvement of hollow sintered bricks integrated with both thermal insulation material (TIM) and Phase-Change Material (PCM). *Case Studies in Thermal Engineering*. Vol. 25, pp. 100938.
- [10] Li, Y., Long, E., Zhang, L., Dong, X. and Wang, S. (2021) Energy-saving potential of intermittent heating system: Influence of composite phase change wall and optimization strategy. *Energy Exploration & Exploitation*. Vol. 39(1), pp. 426-443.
- [11] Sari, A. (2016) Thermal energy storage characteristics of bentonite-based composite PCMs with enhanced thermal conductivity as novel thermal storage building materials. *Energy Conversion and Management*. Vol. 117, pp. 132-141.

- [12] Sun, X., Jovanovic, J., Zhang, Y., Fan, S., Chu, Y., Mo, Y. and Liao, S. (2019) Use of encapsulated phase change materials in lightweight building walls for annual thermal regulation. *Energy*. Vol. 180, pp. 858-872.
- [13] Sarri, A., Bechki, D., Bouguettaia, H., Al-Saadi, S. and Farid, M. M. (2021) Effect of using PCMs and shading devices on the thermal performance of buildings in different Algerian climates. A simulation-based optimization. *Solar Energy*. Vol. 217, pp. 375-389.
- [14] Sun, X., Zhu, Z., Fan, S. and Li, J. (2020) Thermal performance of a lightweight building with phase change material under a humid subtropical climate. *Energy and Built Environment*. Vol. 11, pp. 01-13.
- [15] Fateh, A., Borelli, D., Devia, F. and Weinlader, H. (2018) Summer thermal performances of PCM-integrated insulation layers for light-weight building walls: effect of orientation and melting point temperature. *Thermal Science and Engineering Progress*. Vol. 6, pp. 361-369.
- [16] Zwanzig, S. D., Lian, Y. and Brehob, E. G. (2013) Numerical simulation of phase change material composite wallboard in a multi-layered building envelope. *Energy Conversion and Management*. Vol. 69, pp. 27-40.
- [17] Xu, L., Gao, B., Zhao, H., Wang, J. and Long E. (2015) Study on Light Weight Building Envelope with Phase Change Material for Indoor Thermal Environment Adjustment in Winter. *Refrigeration & Air Conditioning*. Vol. 29(5), pp. 569-573.
- [18] Ministry of housing and urban-rural development. (2016) Code for Thermal Design of Civil Building (GB 50176-2016). China Architecture & Building Press, Beijing, China. Vol. 2016.
- [19] Liu, Z., Hou, J., Meng, X. and Dewancker, B. J. (2021) A numerical study on the effect of phase-change material (PCM) parameters on the thermal performance of lightweight building walls. *Case Studies in Construction Materials*. Vol. 15, pp. e00758.
- [20] Ministry of housing and urban-rural development. (2012) Design code for heating ventilation and air conditioning of civil buildings (GB50736-2012). China Architecture & Building Press, Beijing, China. Vol. 2012, pp. 46-50.
- [21] Wang, Z., Zhang, Z. and Kang L. (2002) Discussion of thermal comfort indices and design indoor temperature for winter heating. *Hv & Ac*. Vol. 32(2), pp. 26-28.

### Nomenclature

$t_m$	Phase-transition temperature, (°C)
$L_p$	Phase change latent heat, (kJ/kg)
$d$	Material thickness, (m)
$\lambda$	Thermal conductivity, [W/(m K)],Solid (Liquid)
$c$	Specific heat, [J/(kg K)]
$\rho$	Density, (kg/m <sup>3</sup> )
$T_{in}$	Indoor air temperature, (°C)
$T_{w,in}$	Inner surface temperature, (°C)
$T_{w,out}$	Outer surface temperature, (°C)
$T_{out}$	Outdoor air temperature, (°C)
$A_{w,in}$	Inner surface temperature amplitude, (°C)
$A_{out}$	Outdoor air temperature amplitude, (°C)
$Q$	Cooling or heating load, (W)
$F$	Heat transfer area of the envelope, (m <sup>2</sup> )
$T_{sa}$	Outdoor comprehensive temperature, (°C)
$q_{peak}$	Inner surface peak heat flux, (W/m <sup>2</sup> )
$t$	Time, (h)
$\varphi$	Delay time, (h)
$f$	Attenuation rate, (%)
$R_{wt}$	Thermal resistance of the original walls, [(m <sup>2</sup> K)/W]
$T_{cool/heat}$	Cooling (26°C) or heating (18°C) set temperature, (°C)
$t_{T,w,in,max}$	Time appeared of the inner surface peak temperature, (h)
$t_{T,out,max}$	Time appeared of the outdoor air peak temperature, (h)

### Abbreviations

LBW	Lightweight Building Walls
PCM	Phase-Change Materials
EPS	Expanded Polystyrene
ESR	Energy-Saving Rate

## ***Chapter 8. Impact and economic evaluation of the lightweight wall using PCM are used in building on reducing energy demands***

8.1	<i>Introduction.....</i>	8-1
8.2	<i>Methodology .....</i>	8-5
8.2.1	<i>Climate zones division and representative cities.....</i>	8-5
8.2.2	<i>Physical model and boundary conditions.....</i>	8-6
8.2.3	<i>Orthogonal experiment .....</i>	8-7
8.2.4	<i>Numerical simulation.....</i>	8-9
8.2.5	<i>Model validation.....</i>	8-11
8.3	<i>Analysis of energy simulation results.....</i>	8-13
8.3.1	<i>Energy simulation results for reference building in different climates/cities .....</i>	8-13
8.3.2	<i>Energy simulation results for each typical city based on orthogonal experiment .....</i>	8-14
8.4	<i>Optimal level and influence degree of each factor (parameter/configuration) under different climates/cities.....</i>	8-18
8.4.1	<i>Suitability level of each factor.....</i>	8-18
8.4.2	<i>Influence degree of each factor .....</i>	8-21
8.5	<i>PCM optimal configuration and energy-saving evaluation based on orthogonal experiment.....</i>	8-24
8.5.1	<i>Energy-saving and suitability of different PCM configurations (single and double layer).....</i>	8-24
8.5.2	<i>Energy-saving for different PCM amounts (thickness and utilization area) .....</i>	8-27
8.6	<i>Economic analysis of energy-saving strategies .....</i>	8-31
8.6.1	<i>Payback period based on PCM cost price.....</i>	8-31
8.6.2	<i>Acceptable cost price for PCM based on payback period.....</i>	8-34
8.7	<i>Summary .....</i>	8-36
	<i>Appendix .....</i>	8-38
	<i>References.....</i>	8-40
	<i>Nomenclature.....</i>	8-49



## 8.1 Introduction

With the rapid development of the global economy and the increasing demand for thermal comfort in buildings, the building industry is considered to be the largest single contributor to world energy consumption and greenhouse gas emissions [1,2]. According to statistics, 24% of total CO<sub>2</sub> emissions and 40% of total primary energy consumption worldwide are caused by the construction sector[3,4] and are still increasing. This alarming situation has prompted scholars to invest much effort in studying active and passive energy-saving strategies to ensure indoor thermal comfort while reducing building energy consumption [5-7]. However, many studies have found that active technologies in building energy saving usually face the problem of low energy efficiency of equipment [8], so passive energy-saving technologies are widely concerned [9]. The main includes adding Trombe walls [10,11], lightweight concrete walls [12], insulation materials [13], phase-change materials (PCM) [14,15], retro-reflective materials [16], and green roofs [17].

As a result, it is clear from the above energy-saving technologies that improve the thermal performance of the envelope is the primary measure to reduce building energy consumption. However, lightweight building envelopes lead to lower thermal comfort and higher energy consumption due to their lower thermal mass (thermal storage capacity) compared to conventional buildings [18]. So, to solve the above problem, phase-change energy storage materials have been developed [19-21], and their application and energy-saving potential have also been demonstrated in many studies. Among them, Sun [22] and Kalnæs et al. [23] found that PCM was more effective when applied to lightweight buildings than to heavy-structural buildings. Liu et al. [14,24] simulated the thermal performance of PCM integrated into lightweight walls and concluded that the delay time of inner surface temperature was added to 6.86 h and attenuation rate decreased by 90.45% under suitable PCM parameters compared to without PCM, and the peak heat flux and average heat flux was reduced by 66.52% and 33.39%. Subsequently, the contribution efficiency of PCM was found to be increased with the decrease of thermal resistance of the original wall. Rathore and Shukla [25] integrated PCM into the building envelope through an aluminum tube encapsulation technique and discovered that the temperature range of the phase-change room was reduced by 40.67% to 59.79%, and the cooling load was cut by 38.76%. Sun et al. [26] revealed through numerical simulations that lightweight buildings integrated with PCM could save energy by 2.6%-3.9% in summer under humid subtropical climate conditions. Soares et al. [27] concluded that applying PCM to lightweight buildings could reduce energy demand by 10-60% under different climatic conditions in Europe. In addition, Li et al. [28] concluded by using numerical simulations (EnergyPlus) that the integration of PCM into plain foam concrete walls could reduce the

heating load by 4.74% in the hot-summer and cold-winter zone (China).

Although it can be drawn based on previous studies [24-28] that PCM applied to lightweight buildings can significantly reduce energy consumption, the energy-saving potential of PCM can be found to be different in different climates and cities. To this end, Adilkhanova et al. [29] evaluated the energy-saving potential of PCM based on different climatic conditions using EnergyPlus. It was determined that PCM could effectively reduce indoor discomfort, but the energy-saving rate depended on the climatic conditions and the insulation properties of the envelope. Zwanzig et al. [30] also believed that PCM performance was highly correlated with weather and emphasized that PCMs with different thermal properties should be selected in different climatic regions. In the meantime, by numerical simulation, Liu et al. [31] analyzed the effect laws and applicability of PCM parameters on the thermal performance of lightweight walls with different orientations. The results showed that the application effects and suitable parameters of PCM in walls with different orientations were different. Furthermore, in addition to the fact that different outdoor climates affect the effectiveness of PCM applications, Biswas [32] and Kishore et al. [33] found that PCM parameters (PCM location, phase-transition temperature, thickness, latent heat, etc.) also greatly affected the energy saving potential of PCM. For this reason, many researchers have also studied the suitable parameters of PCM for different climatic zones, and the results are summarized in Table 1. It can be concluded that the following problems are still not well solved in the current study:

- When PCM is discussed to reduce energy demand, only a few research have traversed all key parameters of PCM, and most studies focus on some of them. However, other PCM parameters/configurations can also greatly affect the thermal performance of the wall and building energy consumption. Consequently, it is necessary to conduct a comprehensive analysis of different PCM parameters/configurations so as to utilize PCM better to reduce energy demands. As well, few studies have addressed the importance ranking of each PCM parameter/configuration in terms of energy saving, which reduces the information available for reference when PCM is selected to use.
- The effect of PCM applications and the appropriate PCM parameters/configurations are highly dependent on the surrounding thermal environment for buildings. For real buildings, the outdoor thermal environment of the wall in different orientations (especially the solar radiation intensity) is quite different due to the shading effect of the building (or itself). Furthermore, for PCM, the inherent phase-transition temperature may have satisfactory results in summer (winter) but may have unsatisfactory or negative consequences in winter (summer). However, although the suitability of PCM parameters/configurations has been studied before, it has mostly focused on specific climates or seasons. Finding the optimum

**Table 8-1** Summary of studies on suitable PCM parameters/configurations for different climates/cities.

Site	Season	Climate categories	PCM types <sup>1</sup>	Suitable PCM parameters/configurations						ESR	Ref.
				$T_p$	$\Delta T$	$d_p$	$H_p$	$P_L$	$P_D$		
Iraq	Summer	TDC	Paraffin wax	-	-	20	-	-	Roof	40%	[34,35]
Fukuoka	Summer	SC	TCM	22-32	-	10	175	Middle	-	66.52%	[22]
Fukuoka	Summer; Winter	SC	TCM	12-18;27-33	6	10 (5+5)	125	Middle	-	58.2%;36.4%	[36]
Boston	Annual	TCC	SS-PCM	25	-	-	-	-	Roof	29.6%	[37]
Iraq	Summer	TDC	RT-35/MC28	35	-	-	-	Outside	-	-	[38]
Santiago	Summer	MC	PCM23C	-	-	4/8	-	-	Ceiling+ wall	8.25%	[39]
Newcastle	Summer; Winter	TCC	PCM19-29	21;25	-	10	-	-	Roof+ wall	23%;12%	[40]
Qingdao	Summer	TMoC	PCM	20-30	-	-	125	Inside	-	57.6%	[19]
Anda/Lanzhou/ Kunming/ Wuhan/Xiamen	Annual	NTCSMC/TCC /SHMC/SMC/ SATMMC	Cetane/Heptadecane/ Octadecane/Gypsum board/Salt hydrate	16;20	-	10/20/30	350	Inside	Roof	14.51%- 67.47%	[41]
Baltimore	Annual	TCC	Organic fatty acids	-	1	19.1	200	Outside +Inside	Ceiling+ Floor+ Wall	10.8%	[42]
Kuwait	Summer	TDC	RT27/RT31/RT35HC/ Paraffin wax	35	-	40	-	-	-	40%	[43]
Chamb éy Phoenix/Las	Winter	TMaC	PCM board	18.1	-	10	150	-	-	10%	[44]
Vegas/Baltimor e/Denver/Billin gs	Summer; Winter	TCC	Fatty acids/glycerides	22;24	-	-	-	Middle	-	3.5%-47.2%; 0%-13.1%	[45]

Note:  $T_p$ : Phase-transition temperature, °C;  $\Delta T$ : Phase-transition temperature range, °C;  $d_p$ : PCM thickness, mm;  $H_p$ : PCM latent heat, kJ/kg;  $P_L$ : Location of PCM in the wall,-;  $P_D$ : PCM installation orientation,-; ESR: Energy-saving rate, %; 1: Specific PCM type can be found in the relevant references. TDC: Tropical desert climate; SC: subtropical climate; TCC: temperate continental climate; MC: Mediterranean-style climate; TMoC: temperate monsoon climate; NTCSMC: northern temperate continental semi-arid monsoon climate; SHMC: subtropical highland monsoon climate; SMC: subtropical monsoon climate; SHMC: subtropical highland monsoon climate; SATMMC: south Asian tropical maritime monsoon climate; TMaC: Temperate maritime climate.

PCM to reduce energy demands for lightweight buildings in different thermal environments (different climate zones, seasons, wall orientation) have not been well solved.

Hence, in order to better solve the problem of optimal configuration of PCM parameters under different climate characteristics, this study summarizes the key factors (parameters/configurations) affecting the use performance of PCM in previous studies [14,24, 31-33,42,46], including phase-transition temperature, phase-transition temperature range, PCM thickness, PCM latent heat, PCM installation location in the wall, PCM installation orientation, at the same time, different level taking values for above each factor was proposed. Obviously, optimizing the configuration of PCM multi-parameters for different climates and thermal comfort demands (cooling and heating) requires a multi-factor analysis. In this case, the following issues deserve to be considered:

- How do design fractional factorial experiments to cover the important features of the problem understudied?
- How to derive the most suitable parameters/configurations of PCM for different climatic conditions?
- How to determine the parameters that need to be prioritized when PCM is selected in different climates?

Based on the above problems, an efficient and important mathematical evaluation method was proposed for multiple levels under different factors, namely, orthogonal experiments, which can obtain more accurate and reliable optimization conclusions with a fewer number of experiments [47-50], and has been validated and applied in various fields [51-55]. Additionally, the economics of PCM is also the focus of current researchers and decision-makers due to its relatively high-cost price currently. Among them, Mi [56] and Ye et al. [57] pointed out that the payback period of PCM differs for different climates/cities even though suitable PCM was applied in buildings to reduce energy demands. The investment in some regions that were low in energy-saving effects could not be recovered at current PCM cost prices. Further, Hou et al. [58] suggested that it is necessary to select and develop a suitable PCM by sensitivity analysis of acceptable price. Overall, although many scholars have discussed the economics of PCM a lot, most of them have focused on the specific building structure and region. However, when PCM is selected for use, the PCM cost, energy-saving potential in different buildings (or energy demands) and energy price in different regions are also the key factors affecting its application value. Therefore, to better solve the above problems, orthogonal experiments and numerical simulations (EnergyPlus) are used in this study to explore the suitability and optimal solution of PCM parameters and configurations (single and double layer PCM) for lightweight buildings

to reduce energy demands in different climatic characteristics, and the influence degree of these parameters/configurations. Meanwhile, the economic applicability of different PCM usage (thickness and utilization area) are discussed based on different energy demands and energy prices. The research findings can maximize the application benefits of PCM, and provide a reference for decision-makers to weigh the selection and application of PCM from the perspective of energy saving and economy, as well as data support for the preparation of suitable PCM for lightweight buildings in the future.

## 8.2 Methodology

### 8.2.1 Climate zones division and representative cities

From previous studies, it can be easily found that lightweight buildings integrated with PCM can effectively reduce building energy consumption and improve indoor thermal comfort. However, climatic conditions are one of the main factors affecting the effectiveness of PCM in reducing energy demand [59]. China, as a country with diverse climate characteristics, it is divided into five climate zones according to the need for building thermal design [51], namely, severe cold zone (SCZ), cold zone (CZ), hot-summer and cold-winter zone (HSCW), hot-summer and warm-winter zone (HSWW), and moderate climate zone (MCZ), as shown in Fig. 8-1(a). The detailed information can refer [60,61]. As to Japan, according to the current energy efficiency standards and Heating Degree Day (HDD), the whole country can be divided into six zones (I-VI) as shown in Fig. 8-1(b) [59,62]. Meanwhile, the typical cities representing different climate zones in Japan and China have been marked in Fig. 8-1. In detail, the chosen cities ordered from northern to southern areas are Harbin (HRB), Beijing (BJ), Shanghai (SH), Kunming (KM) and Guangzhou (GZ) in China, as well as Sapporo (Sap.), Hachinohe (Hac.), Sendai (Sen.), Tokyo (Tok.), Kagoshima (Kag.) and Naha (Na.) in Japan. Detailed information of the chosen cities is presented in Appendix A [59].

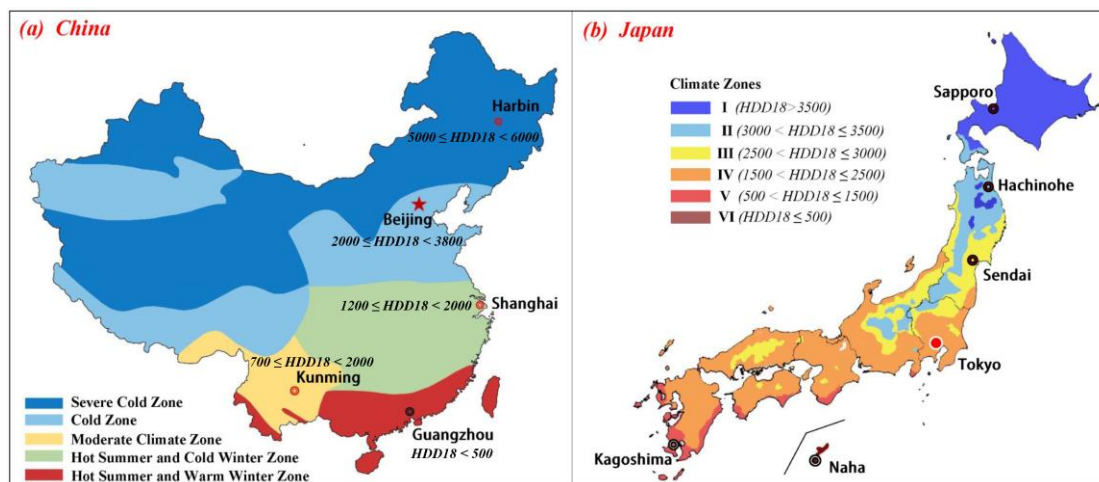


Fig. 8-1. Climatic zones of China and Japan and the location of the typical cities [60-62].

### 8.2.2 Physical model and boundary conditions

To compare and analyze the energy-saving effect of integrating PCM with different performances in lightweight buildings under different climates, a typical lightweight building and its walls/roof are built, and it is displayed in Fig. 8-2. Among them, Fig. 8-2(a) is a reference wall/roof (no PCM) with three layers, from outside to inside are exterior wallboard (12mm oriented strand board-OSB), insulation material ( $X_{ins}$ , mm), and interior wallboard (10mm gypsum board). Based on Fig. 8-2(a), Fig. 8-2(b)-(f) investigates the dynamic thermal behavior of the wall/roof by placing PCM in different locations of the reference wall ( $L_1, L_2, L_3, L_4, L_5$ ) to seek the ideal PCM parameters and locations. It should be stated that the total thickness of the wall/roof ( $\delta_{total}$ ) will change with the PCM thickness ( $d_p$ ), and the thickness of the insulation material (Glass wool,  $X_{ins}$ ) remains constant to ensure the same thermal resistance of the original wall ( $R_{wt}$ ) [14]. The relevant thermophysical parameters of materials are listed in Table 2. At the same time, in order to explore the variation of building cooling and heating loads in different climates, a typical lightweight building with 3800mm (length)  $\times$  5600mm (width)  $\times$  2700mm (height) is used in this study as a simulation model, and two 1700mm (length)  $\times$  1500mm (height) double hollow window (6mm+12A+6mm) are set on the north and south-facing of the room (the heat transfer coefficient (HTC) is 2.8 [W/(m<sup>2</sup> K)], and solar heat gain coefficient (SHGC) is 0.49), which is presented in Fig. 8-2(g).

Moreover, the “Ideal Loads Air System (ILAS)” [28] of EnergyPlus is utilized to simulate building cooling and heating load due to it returns precisely the energy that must be supplied to the room. Considering the residential behavior of the building, the personnel density of the room is set to 2 people whose activity is 72W/person (sitting and slight movement), the power used for indoor lighting is set to 2 W/m<sup>2</sup>, and other equipment (TV and refrigerator) is set to 15W/m<sup>2</sup> [11,63,64]. The ILAS has a constant heating setpoint of 20°C and a constant cooling setpoint of 26°C [65,66], and the indoor air change rate per hour was set to 1/hr. Meanwhile, considering the low thermal inertia [18] and poor indoor thermal comfort [66, 67] of lightweight buildings, the energy simulation time (ILAS running) of the building is set to the whole year (January 1 to December 31). In the process of energy simulation, the meteorological data are selected for the simulation with EPW format meteorological file, which comes from Typical Meteorological Year x (TMYx) [68-70], and it can be downloaded from the online repository [71]. TMYx files are typical meteorological files derived from ISD (US NOAA’s Integrated Surface Database [72]) with hourly data through 2021 using the TMY/ISO 15927-4:2005 methodologies [73]. Then it is constructed by choosing data for each month from different years so that the data for a given month is the most “typical” among the years present in the long-term data set [70]. The use of TMYx has gained wide consensus in the building simulation field

[74-76].

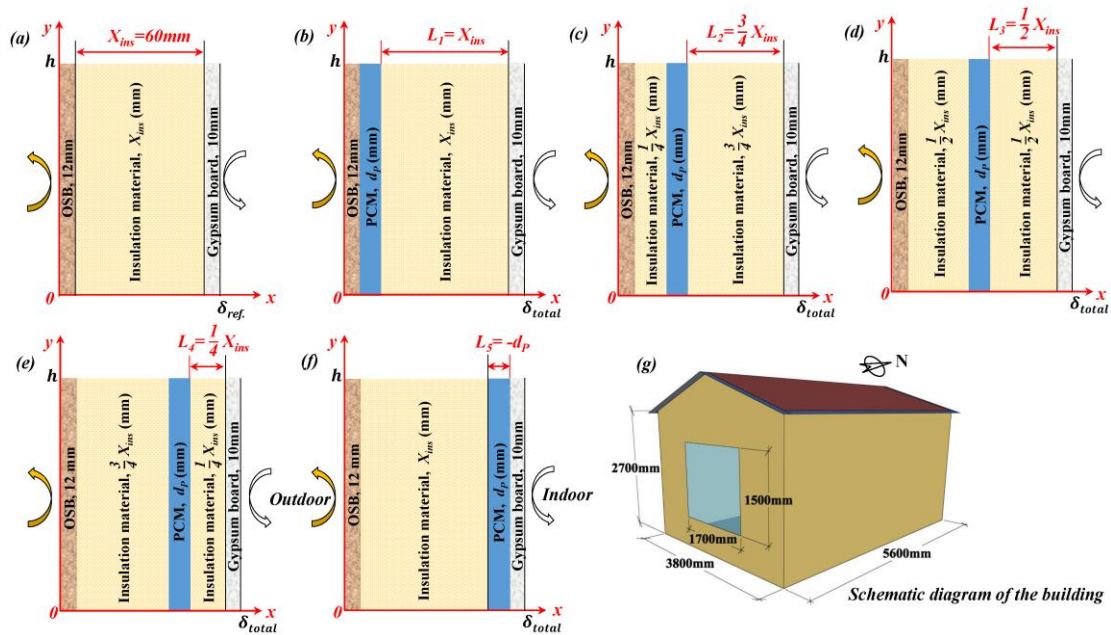


**Fig. 8-2.** (a)-(f) schematic diagram of the lightweight wall/roof and (g) typical lightweight building.

**Table 8-2** Thermo-physical parameters of wall materials [60,77].

Material	$T_p$ (°C)	$H_p$ (kJ/kg)	$d$ (mm)	$\lambda$ [W/(m K)]	$c_p$ [J/(kg K)]	$\rho$ (kg/m <sup>3</sup> )
PCM	16/20/24/28/ 32	25/75/125/175 /225	5/10/15/20/ 25	0.5(0.25)	1785	1300
OSB	-	-	12	0.105	1400	593
Glass wool	-	-	60	0.035	1220	40
Gypsum board	-	-	10	0.33	1050	1050

### 8.2.3 Orthogonal experiment

As mentioned earlier, orthogonal experimental design is an important mathematical method for the analysis of a specified target based on a multi-factor system, and it is designed to be based on tabular forms with random errors for interaction among multiple factors and indicators, which is an efficient, fast and economical arrangement for experimental factors [78]. The orthogonal experiment is used to arrange and test the performance of the proposed optimization strategies and further explore the feasible region of the energy optimization problem. In addition, the orthogonal table is the foundation of the orthogonal experimental design, and it can be found in related books [79], which forms as follows:

$$L_D(Q^M) \quad (8-1)$$

where  $L$  represents the symbol of the orthogonal experiment,  $D$  denotes the number of rows or

tests,  $Q$  indicates the number of levels, and  $M$  represents the number of columns or factors [48,80].

The results of the orthogonal experiment are usually analyzed by the average of experimental results ( $k_{i,m}$ ) and range analysis value ( $R_v$ ). Among them, the  $k_{i,m}$  is to determine the impact of different levels corresponding to each factor on the evaluation index by using the average of experimental results. The  $R_v$  aims to measure and demonstrate the influence degree of each factor using the difference between the maximum and minimum mean values of test results. In this study, to evaluate the optimal level (optimum combination) and influence degree of each factor selected, the  $k_{i,m}$  and  $R_v$  are calculated by Eqs. (8-2) and (8-3), where a larger  $R_v$  means a more considerable impact on the target, a lower  $k_{i,m}$  shows a smaller load and means the corresponding parameter level is optimal for the target [48,51].

$$k_{i,m} = K_{i,m} / s_{i,m} \quad (8-2)$$

$$R_v = \text{Max}\{k_1, k_2, \dots, k_i\} - \text{Min}\{k_1, k_2, \dots, k_i\} \quad (8-3)$$

where  $K_{i,m}$  is the sum of experimental results at level  $i$  of factor  $m$ , -;  $s_{i,m}$  represents the number of occurrences of level  $i$  of factor  $m$ , -.

Based on previous studies [14,24, 31-33,42,46], five PCM parameters and installation orientations are selected as six factors in this paper to explore the energy-saving effects of lightweight buildings integrated with different parameters/configurations of PCM. The six factors (parameters/configurations) are *A*-Phase-transition temperature ( $T_p$ , °C), *B*-Phase-transition temperature range ( $\Delta T$ , °C), *C*-Location of PCM in the wall ( $P_L$ , -), *D*-PCM thicknesses ( $d_p$ , mm), *E*-PCM latent heats ( $H_p$ , kJ/kg) and *F*-PCM installation orientation ( $P_D$ , -). Meanwhile, Each factor contains five levels (it is listed in Table 3), so the Orthogonal experiment table  $L_{25}(5^6)$  is used for the design (it can be seen in Table 5).

**Table 8-3 Five levels of each factor (parameter/configuration) designed.**

Levels	<i>A</i> ( $T_p$ , °C)	<i>B</i> ( $\Delta T$ , °C)	<i>C</i> ( $P_L$ , -)	<i>D</i> ( $d_p$ , mm)	<i>E</i> ( $H_p$ , kJ/kg)	<i>F</i> ( $P_D$ , -)
1	16	2	L <sub>1</sub>	5	25	East
2	20	4	L <sub>2</sub>	10	75	South
3	24	6	L <sub>3</sub>	15	125	West
4	28	8	L <sub>4</sub>	20	175	North
5	32	10	L <sub>5</sub>	25	225	Roof

### 8.2.4 Numerical simulation

The numerical software EnergyPlus v8.9 [81] is adopted to simulate the performance of PCM-integrated buildings. EnergyPlus is a building energy time-to-time simulation software developed by the U.S. Department of Energy (DOE) and Lawrence Berkeley National Laboratory (LBNL) based on BLAST and DOE-2, which applies an integrated and synchronized load/system/equipment simulation method [82]. The heat conduction of the envelope is usually calculated using the CTF (conduction transfer function) method in this software [83,84]. However, it is worth noting that the CTF is usually used for construction materials with constant properties [84]. For the more advanced materials, such as PCM or variable thermal conductivity, a more accurate method (conduction finite difference (CondFD) solution algorithm) is incorporated into EnergyPlus to model the heat transfer of PCM [85,86], which includes two different options for the specific scheme or formulation used for the finite difference model, namely, the fully implicit scheme and the Crank–Nicholson scheme [85,87]. In this study, the fully implicit scheme is employed. The algorithm applies the implicit finite difference scheme coupled with an enthalpy-temperature function to account for phase change energy [59,85], and it is described in Eq. (8-4).

$$C_p \rho \Delta x \frac{T_i^{j+1} - T_i^j}{\Delta t} = k_w \frac{(T_{i+1}^{j+1} - T_i^{j+1})}{\Delta x} + k_E \frac{(T_{i-1}^{j+1} - T_i^{j+1})}{\Delta x} \quad (8-4)$$

where  $C_p$  is the specific heat of the material, J/kg K;  $\rho$  is the density of the material, kg/m<sup>3</sup>;  $\Delta x$  is finite difference layer thickness, m;  $\Delta t$  is calculation time step, s;  $T$  is node temperature, °C;  $i$  stands for node being modeled;  $i+1$  stands for the adjacent node to the interior of construction;  $i-1$  stands for the adjacent node to the exterior of construction;  $j+1$  stands for new time step;  $j$  stands for the previous time step.  $k_w$  is thermal conductivity for interface between  $i$  node and  $i+1$  node, W/(m K);  $k_E$  is thermal conductivity for interface between  $i$  node and  $i-1$  node, W/(m K).

Further, it should be explained that EnergyPlus uses the following four types of nodes for the above schemes, as shown in Fig. 8-3. The grid for each material is established by specifying a half node for each edge of the material and equal size nodes for the rest of the material. Equations such as these are formed for all nodes in construction, and the formulation of all node types is also basically the same [85].

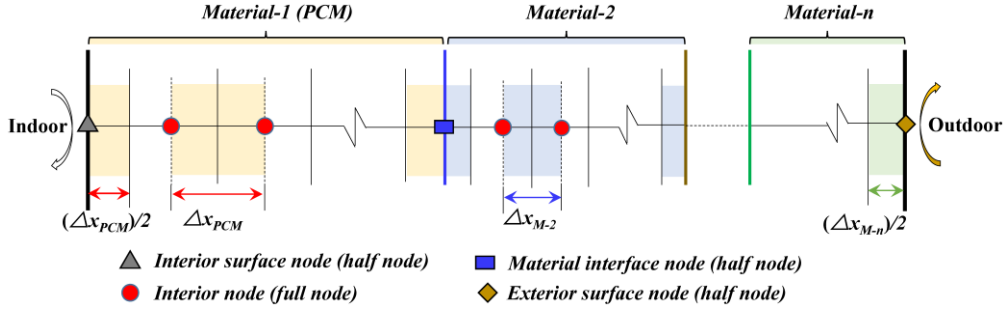


**Fig. 8-3. Node depiction for conduction finite difference model.**

Additionally, in the CondFD model, the surface discretization depends on the space discretization constant ( $\varepsilon$ ), the thermal diffusivity of the material ( $\alpha$ ,  $\text{m}^2/\text{s}$ ), time step ( $\Delta t$ , s), as shown in Eq. (8-5), and the default value of  $\varepsilon$  is 3 in the program [85].

$$\Delta x = \sqrt{\varepsilon \alpha \Delta t} \quad (8-5)$$

In addition, the indoor air temperature is not only affected by the heat transfer through the surface of the envelopes but also by the heat penetration from outdoor air and the heat gain from internal loads. The computational process of EnergyPlus is based on the integrated processing of multi-program modules [88,89] whose core is the basic heat balance principle. It can be simplified as Eq. (8-6) [9,48,90].

$$\sum_{i=1}^{N_{sl}} \dot{Q}_i + \sum_{i=1}^{N_{surfaces}} h_i A_i (T_{si} - T_z) + \sum_{i=1}^{N_{zones}} \dot{m}_i C_p (T_{zi} - T_z) + \dot{m}_{inf} C_p (T_{\infty} - T_z) + \dot{Q}_{sys} = 0 \quad (8-6)$$

In addition, the air heat balance in EnergyPlus can be formulated as Eqs. (8-7) and (8-8).

$$C_z \frac{dT_z}{dt} = \sum_{i=1}^{N_{sl}} \dot{Q}_i + \sum_{i=1}^{N_{surfaces}} h_i A_i (T_{si} - T_z) + \sum_{i=1}^{N_{zones}} \dot{m}_i C_p (T_{zi} - T_z) + \dot{m}_{inf} C_p (T_{\infty} - T_z) + \dot{Q}_{sys} \quad (8-7)$$

$$C_z = \rho_{air} C_p C_T \quad (8-8)$$

The heating and cooling loads of zones can be satisfied by air systems to provide hot or cold air. Thus the system energy provided to the zone,  $\dot{Q}_{sys}$  can be formulated from the difference between the enthalpy of supply air and that of air leaving the zone as Eq. (8-9):

$$\dot{Q}_{sys} = \dot{m}_{sys} C_p (T_{sup} - T_z) \quad (8-9)$$

If the air system has sufficient capacity (based on the desired zone air temperature) to meet

the zone conditioning requirements, i.e.,  $\dot{Q}_{sys} = \dot{Q}_{load}$ , so, the heating and cooling loads,  $\dot{Q}_{load}$ , can be expressed as Eq. (8-10) :

$$\dot{Q}_{load} = \sum_{i=1}^{N_{st}} \dot{Q}_i + \sum_{i=1}^{N_{surfaces}} h_i A_i (T_{si} - T_z) + \sum_{i=1}^{N_{zones}} \dot{m}_i C_p (T_{zi} - T_z) + \dot{m}_{inf} C_p (T_{\infty} - T_z) \quad (8-10)$$

Since the model in this paper has no adjacent rooms, the third term on the right-hand side of Eq. (8-9) can be deleted and written in Eq. (8-11).

$$\dot{Q}_{load} = \sum_{i=1}^{N_{st}} \dot{Q}_i + \sum_{i=1}^{N_{surfaces}} h_i A_i (T_{si} - T_z) + \dot{m}_{inf} C_p (T_{\infty} - T_z) \quad (8-11)$$

where  $\sum_{i=1}^{N_{st}} \dot{Q}_i$  represents the sum of the internal convective loads, J;  $\sum_{i=1}^{N_{surfaces}} h_i A_i (T_{si} - T_z)$  represents the convective heat transfer from the zone surfaces, W;  $\dot{m}_{inf} C_p (T_{\infty} - T_z)$  represents heat transfer due to infiltration of outside air, J/s;  $\sum_{i=1}^{N_{zones}} \dot{m}_i C_p (T_{zi} - T_z)$  represents heat transfer due to interzone air mixing, J/s;  $\dot{Q}_{sys}$  is air systems output, J;  $C_z \frac{dT_z}{dt}$  represents energy stored in zone air, J/kg;  $\rho_{air}$  is the zone air density, kg/m<sup>3</sup>;  $C_p$  is zone air specific heat, J/(kg K);  $C_r$  is sensible heat capacity multiplier, J/(kg K).

### 8.2.5 Model validation

The reliability and accuracy of EnergyPlus in predicting PCM performance have been verified by much research [27,57,91,92]. In this study, a small-scale lightweight building was manufactured and tested in Qingdao (China), which is presented in Fig. 8-4(a). The lightweight building (experimental system) is composed of a 1200mm (length) ×1000mm (width) ×1000mm (height) lightweight timber structure with walls are 12mm Plywood, 20mm EPS, 20mm PCM-2, and 5mm Plywood in order from the outside to the inside. Among them, the PCM-2 (TCM tube) used in the experiment is a new material that is easy to composite with the wall. It was developed by the Chavez Institute of Environmental Studies in Canada and the University of British Columbia [93]. The thermo-physical parameters of the above relevant materials are given in Table 4. In addition, the north and south directions of the lightweight building (experimental system) each have an 800mm (length) ×600mm (height) double hollow window (6mm+12A+6mm, Heat Transfer Coefficient (HTC) was 2.8 [W/(m<sup>2</sup> K)], and SHGC was 0.49). The experimental test site is located on the roof of a university building in Qingdao

with no shade around it. The test parameters mainly include indoor and outdoor air temperature, relative humidity, solar radiation intensity, outdoor wind speed, and so on. Among them, the indoor air temperature was measured using Testo-174H-Mini with a temperature range of -20-70 °C and an error of ±0.5 °C. The outdoor ambient parameters were measured by using JTR13-Multi-parameter Outdoor Weather Station within a range of temperature: -30°C-70°C (error: ±0.5 °C), relative humidity: 0-100%RH (error: ±3%), solar radiation intensity: 0-2000W/m<sup>2</sup> (error: ±2%) and wind speed: 0-30m/s (error: ±1m/s). The recording intervals were all set to 15 min. The experimental instruments were calibrated before the tests, and the tests were carried out from Jul. 15 to Jul. 25 (summer) to ensure the accuracy of the test data.

**Table 8-4 Thermo-physical parameters of wall materials [60,94].**

Material	$T_p$ (°C)	$L_p$ (kJ/kg)	$\lambda$ [W/(m K)], Solid (Liquid)	$c_p$ [J/(kg K)]	$\rho$ (kg/m <sup>3</sup> )
PCM-2	18-26	216	0.5(0.25)	1785	1300
Gypsum board	-	-	0.33	1050	1050
Plywood	-	-	0.17	2510	600
EPS	-	-	0.039	1380	20

Considering the stability of the experimental instruments, the data of July 22-24 (consecutive 72h) are selected for validation in this study, during which the measured outdoor meteorological data are taken as the boundary conditions [58]. Fig. 8-4(b) gives the comparison between the measured and simulated hourly air temperature in the test room. It is apparent that the trends of simulated values and measured values are basically similar. In order to assess the error more exactly, two metrics: root mean square error (RMSE) and coefficient of variation ( $CV_{(RMSE)}$ ) are employed [14,51], while RMSE measures the average spread of errors which provides a measure for the model's dispersion [94],  $CV_{(RMSE)}$  is the coefficient of variation in RMSE, as expressed by Eqs. (8-12) and (8-13), respectively, as follows:

$$RMSE = \sqrt{\frac{1}{n} \sum_{t=1}^n (M_t - S_t)^2} \quad (8-12)$$

$$CV_{(RMSE)} = \frac{RMSE}{M_t} \times 100\% \quad (8-13)$$

It is found by calculation compared to experimental results that the RMSE of the present numerical results and the  $CV_{(RMSE)}$  is only 1.66°C and 4.65%. These results meet the simulation requirements with the ASHRAE criterion of  $CV_{(RMSE)}$  less than 30% [95] and further indicate the reliability and accuracy of the CondFD solution algorithm and Phase-Change Hysteresis

module embedded in EnergyPlus for predicting the targets in this study.

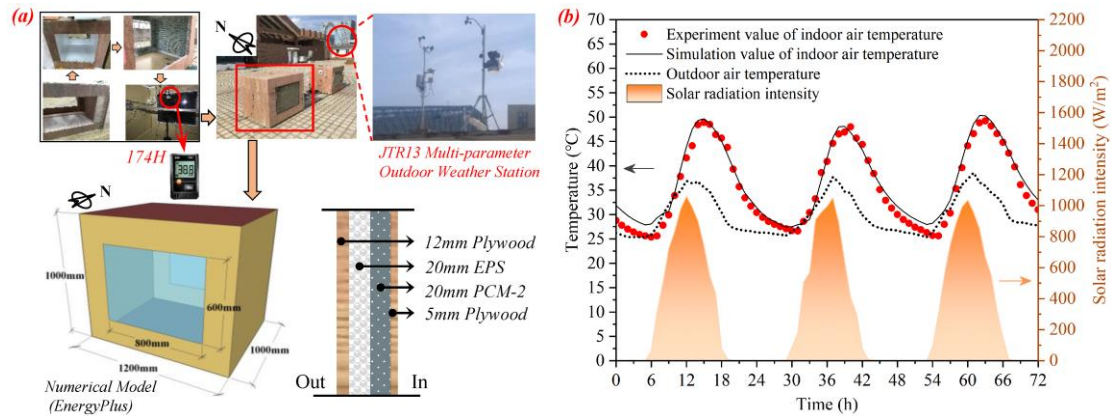


**Fig. 8-4. (a) Composition of the experimental system and (b) comparison of numerical indoor air temperature with experimental results.**

### 8.3 Analysis of energy simulation results

#### 8.3.1 Energy simulation results for reference building in different climates/cities

Different climatic conditions not only determine the local demand for cooling and heating loads in buildings but also further influence the building energy-saving optimization objectives [51]. Therefore, Fig. 8-5 presents the percentage of cooling and heating load demand for a typical lightweight building (no PCM) in different climates in China and Japan. It can be easily seen that the heating and cooling demand varies greatly between different climates/cities. For China, the heating demand in Harbin accounts for 73% of the annual total load. By contrast, the high heating demand is gradually replaced by the cooling with the increase of the annual average temperature increases (latitude approaching the equator) for different cities, and the heating load in Guangzhou only covers 0.96%. Simultaneously, a similar characteristic occurs in Japan, where the heating load in Naha with a high average annual temperature can be ignored (only 0.37kWh/m<sup>2</sup>). As a result, it is sufficient to demonstrate the importance of determining energy-saving design aim according to different climatic conditions and cooling and heating load requirements.

Moreover, the variability of different climates/cities in China is much higher than in Japan in terms of total annual load, where the demand in Kunming is the lowest by 65.09%, 52.18%, 48.08%, and 61.39%, respectively, compared to Harbin, Beijing, Shanghai, and Guangzhou. The main reason is that Kunming is a moderate climate, which is comfortable throughout the year. Nonetheless, there is still a demand for heating and cooling, especially cooling. It mainly relies on the fact that lightweight buildings usually have sizeable indoor temperature

fluctuations due to lower thermal mass. Specifically, the delay and attenuation of solar radiation heat irradiated on the exterior wall in summer are not obvious, resulting in high indoor temperatures [31]. It is also why lightweight buildings must focus on improving the indoor thermal environment compared to other heavy buildings. In comparison, the differences in total annual load demand in the other cities (different climate zones) except Naha are smaller in Japan, but it is also highly different in the proportion of heating and cooling demand due to different geographic locations and climatic characteristics. Such as Sapporo and Tokyo, whose total loads differ by only 1.12 kWh/m<sup>2</sup>, but Sapporo's heating demand (112.96 kWh/m<sup>2</sup>) is 234.60% higher than Tokyo's (33.76 kWh/m<sup>2</sup>), while the cooling load (Sapporo and Tokyo is 55.88 kWh/m<sup>2</sup> and 133.66 kWh/m<sup>2</sup>, respectively) is 58.19% lower. Furthermore, it is a noticeable feature that the difference in energy demand between China and Japan is larger even if the latitude (North latitude) is close (see Appendix A [59]). For example, the heating and cooling load in Beijing (N39°54') is 31.72% and 32.91% higher compared to Sendai (N38°15'). As a result, it further illustrates the differences in energy demand and energy-saving benefits between China and Japan. At the same time, the energy prices [13,96,97] in Japan are relatively high than in China. Consequently, discussing and comparing the energy-saving benefits of PCM in China and Japan can also better reflects the future application value and energy-saving potential of PCM.

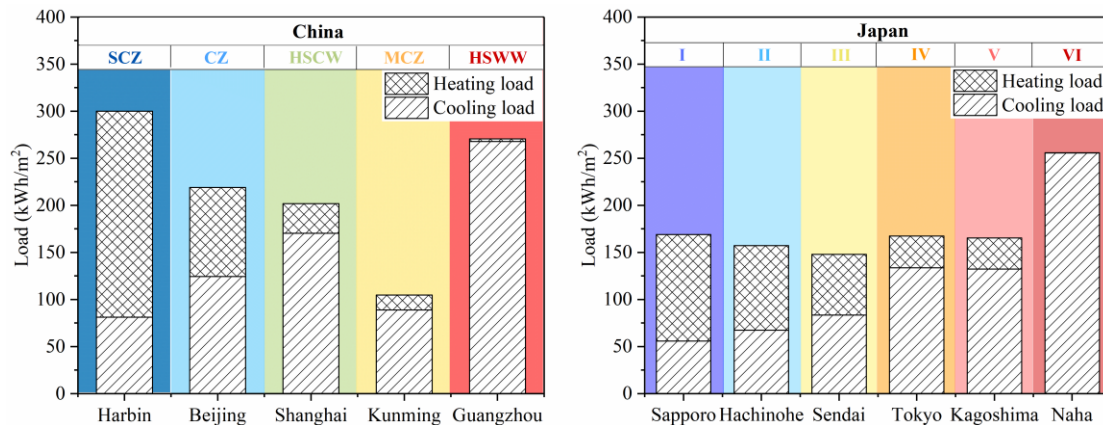


**Fig. 8-5. Energy simulation results for the reference building (no PCM) in different climates/cities.**

### 8.3.2 Energy simulation results for each typical city based on orthogonal experiment

In order to estimate the effect of different PCM thermo-physical properties on cooling and heating load in different climates/cities, the typical cities in China and Japan are compared based on an orthogonal experiment. Taking Harbin as an example, the result is given in Table 5, and it can be derived that the energy savings of PCM are highly correlated with its

parameters/configurations, different PCM parameters/configurations corresponding to different cooling and heating loads. Among them, E5 performed best in 25 orthogonal combinations and can save 12.2%, 5.08%, and 7.0% of the cooling load (CL), heating load (HL), and total load (TL), respectively, compared to the worst E1. In the meantime, it can save 12.31% of the cooling load, 5.05% of the heating load, and 7.01% of the total load compared with the reference building (no PCM). The above data demonstrate that appropriate PCM parameters/configurations can effectively improve building energy saving. However, a significant feature can be found to be that the worst combination E1, has an energy saving rate of 0.12% (cooling load), -0.04% (heating load), and 0.006% (total load) compared to the reference building. It shows that PCM is highly correlated with its parameters/configurations in reducing energy demand. Unsuitable PCM fails to achieve energy savings and also causes a negative result. For this reason, it is imperative to study the suitability of PCM parameters/configurations for different climates considering the cost of materials.

Likewise, Fig. 8-6 exhibits the cooling and heating load of each typical city in different regions of China and Japan with different PCM parameters/configurations (orthogonal combinations). A consistent result can be drawn that E5 still performs best. The result can be fully explained by the previous study [36] that PCM can function over a more extended period when the phase-change temperature range ( $\Delta T$ ) is wide. Meanwhile, the roof receives more heat than the walls, and the higher heat storage capacity (high thickness and latent heat) can be used to a greater extent. Nevertheless, a remarkable fact is that although E5 performs optimally, its energy savings vary considerably in different climates/cities. It is further evidenced that the climatic suitability of PCM parameters/configurations selected and applied should be given sufficient attention. As an example, in China, it can be found that the highest energy saving compared to the reference building (no PCM) is Kunming, whose cooling, heating, and total load can be saved by 18.13%, 63.16%, and 24.92%, respectively, which mainly because Kunming is a temperate region [51] with more comfortable throughout the year, the superior thermal regulation capability of PCM basically eliminates the impact of abnormal weather (high or low temperature). Then, it is observed that the energy savings of cooling load is decreased as the cooling demand is increased from Harbin to Guangzhou (except for Kunming) by 9.46% (Harbin), 6.81% (Beijing), 4.83% (Shanghai) and 2.83% (Guangzhou), respectively. In contrast, the energy-saving of the heating loads are improved from 5.91% to 89.23%. Comparable conclusions can be clearly drawn in Japan. It shows that there are climatic differences in the application of PCM in terms of energy reduction, which means that the possibility of PCM application has to be considered when the cost of PCM is highlighted (due to its high price currently).

In addition, comparing China and Japan reveals that there is also a notable difference in the energy-saving effect of PCM even though the latitude is basically the same. In the case of Harbin and Sapporo, the energy savings of Harbin is lower than that of Sapporo, with a difference of 3.3%, 5.5%, and 4.99% in cooling, heating, and total load, separately. This result is also related to their cooling and heating demand. Thus, it can also be concluded that the application potential of PCM is more popular in Japan when energy costs (higher in Japan than in China) are taken into account. In summary, considering that PCM is usually not replaced seasonally, the most suitable cities (ranking) for PCM installation in view of total load energy saving are Kunming (24.92%) > Beijing (10.97%) > Shanghai (8.58%) > Harbin (6.87%) > Guangzhou (3.66%) in China and Kagoshima (13.14%) > Sendai (12.60%) > Tokyo (12.16%) > Hachinohe (11.89%) > Sapporo (11.86%) > Naha (1.92%) in Japan.

**Table 8-5 Orthogonal experiment arrangements and results (take Harbin as an example).**

No.	Design Parameters						Evaluation index (Harbin)		
	<i>A</i> ( $T_p$ )	<i>B</i> ( $\Delta T$ )	<i>C</i> ( $P_L$ )	<i>D</i> ( $d_p$ )	<i>E</i> ( $H_p$ )	<i>F</i> ( $P_D$ )	CL	HL	TL
E1	1(16)	1(2)	1(L <sub>1</sub> )	1(5)	1(25)	1(East)	80.98	218.91	299.89
E2	1	2(4)	2(L <sub>2</sub> )	2(10)	2(75)	2(South)	79.71	216.56	296.27
E3	1	3(6)	3(L <sub>3</sub> )	3(15)	3(125)	3(West)	78.31	215.41	293.72
E4	1	4(8)	4(L <sub>4</sub> )	4(20)	4(175)	4(North)	79.28	216.54	295.82
<b>E5</b>	<b>1</b>	<b>5(10)</b>	<b>5(L<sub>5</sub>)</b>	<b>5(25)</b>	<b>5(225)</b>	<b>5(Roof)</b>	<b>71.1</b>	<b>207.79</b>	<b>278.89</b>
E6	2(20)	1	2	3	4	5	76.69	213.83	290.52
E7	2	2	3	4	5	1	78.21	215.57	293.78
E8	2	3	4	5	1	2	78.53	215.68	294.21
E9	2	4	5	1	2	3	77.67	214.55	292.22
E10	2	5	1	2	3	4	80.36	218.55	298.91
E11	3(24)	1	3	5	2	4	79.81	217.51	297.32
E12	3	2	4	1	3	5	76.03	215.8	291.83
E13	3	3	5	2	4	1	74.43	213.81	288.24
E14	3	4	1	3	5	2	79.51	216.89	296.4
E15	3	5	2	4	1	3	78.65	216.09	294.74
E16	4(28)	1	4	2	5	3	77.95	216.58	294.53
E17	4	2	5	3	1	4	78.96	217.18	296.14
E18	4	3	1	4	2	5	79.27	215.27	294.54
E19	4	4	2	5	3	1	79.15	216.67	295.82
E20	4	5	3	1	4	2	79.38	217.78	297.16
E21	5(32)	1	5	4	3	2	78.67	216.5	295.17
E22	5	2	1	5	4	3	79.33	216.41	295.74
E23	5	3	2	1	5	4	80.74	218.75	299.49
E24	5	4	3	2	1	5	78.1	215.66	293.76
E25	5	5	4	3	2	1	78.8	216.72	295.52

Note: CL= Cooling Load, kWh/m<sup>2</sup>; HL= Heating Load, kWh/m<sup>2</sup>; TL= Total Load, kWh/m<sup>2</sup>.

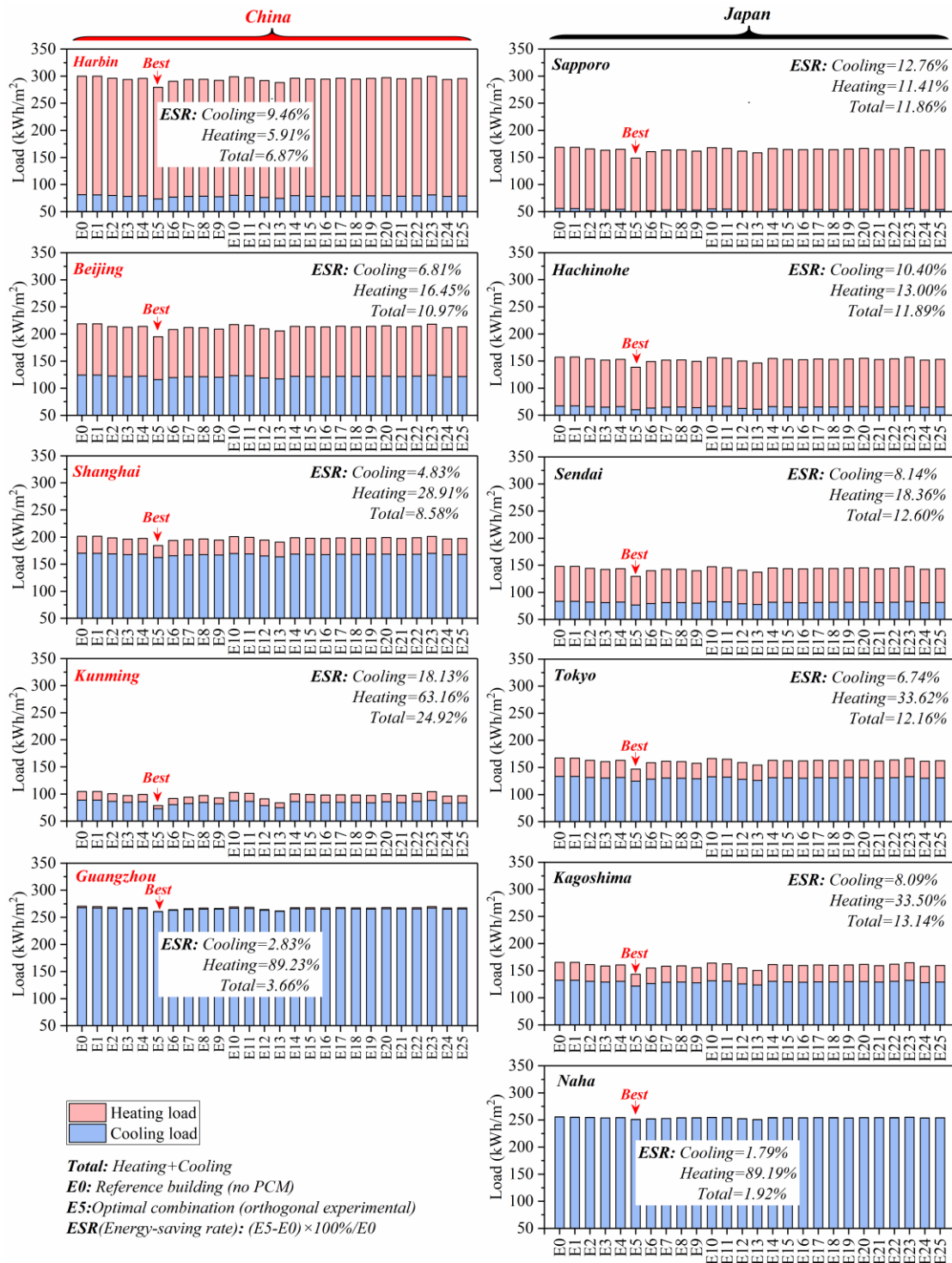


Fig. 8-6. Cooling/heating loads for typical cities under different climates and PCM parameters/configurations, based on orthogonal experiment.

## 8.4 Optimal level and influence degree of each factor (parameter/configuration) under different climates/cities

### 8.4.1 Suitability level of each factor

Based on the above orthogonal results, it is discovered that different PCM parameters/configurations have different effects on reducing energy demand in different climates/cities with large disparities. However, although the result on the optimal level of PCM parameters/configurations for different climates/cities can be intuitively derived from the orthogonal table for orthogonal experiments, it is not necessarily optimal for all possible level pairings ( $5^6=15625$ ). Accordingly, Fig. 8-7 gives the influence laws of each factor ( $m$ ) with different levels ( $i$ ) on loads (cooling, heating, and total) based on the average of experimental results at level  $i$  of factor  $m$  ( $k_{i,m}$ ) (the different PCM parameters/configurations are expressed as factors  $A-F$ , and the levels of each factor are expressed as 1-5, and the detail values are shown in Table 3). Taking factor  $A$  ( $T_p$ ) of Harbin as an example, the  $k_{i,m}$  of cooling load is shown in Fig. 8-7(a), and the corresponding five levels (1-5) are 77.88 kWh/m<sup>2</sup>, 78.29 kWh/m<sup>2</sup>, 77.69 kWh/m<sup>2</sup>, 78.94 kWh/m<sup>2</sup> and 79.13 kWh/m<sup>2</sup>, respectively. The data shows that the lowest cooling load is at Level 3, which means that  $A$  is more energy-saving for cooling load at level 3. In the same way, the optimal levels of factors  $B$ ,  $C$ ,  $D$ ,  $E$ , and  $F$  are Level 5, Level 5, Level 5, Level 5, Level 5, and Level 5, respectively. As a consequence, a new optimal combination represented by  $A_3B_5C_5D_5E_5F_5$  is generated. Similarly, the optimal combination of cooling load for the other cities can be derived by the above calculation. Yet, by comparison, the fact is revealed that there are climate/city differences in the optimal levels for the same factor. For example, factor  $E$  ( $H_p$ ) corresponds to an optimal level of  $E_5$  (225 kJ/kg) in Harbin and  $E_4$  (175 kJ/kg) in other cities. This is mainly because the higher latent heat of the PCM suppresses the heat transfer from daytime to indoors in summer, but it results in an increase in cooling load at night due to the exothermic behavior of the PCM. Conversely, the above phenomenon is often an advantage for winter (see Fig. 8-7(b)). Simultaneously, the comparison of Fig. 8-7 (a) and (b) shows that the optimal level is not the same at different cooling and heating demands. For instance,  $A_3$  (24 °C), the best performer in the energy saving of the cooling load for all cities, is not as good as  $A_1$  (16 °C) in heating load. In addition, this result (the energy saving of heating) does not hold for Guangzhou and Naha, with a similar climate characteristic, whose optimal level is  $A_2$  (20 °C).

Furthermore, for factor  $B$  ( $\Delta T$ ), it can be noticed from Fig. 8-7 (a) and (b) that although  $B_5$  ( $\Delta T = 10$  °C) is optimal, its variation is not linear in energy saving for both cooling and heating loads regardless of the city. The energy-saving advantage of  $B_3$  ( $\Delta T = 6$  °C) gradually

approaches B5 with the enhancement of the annual cooling demand (annual heating demand decreases), and it is the optimal choice in Guangzhou (heating) and Naha (cooling and heating). This result is sufficient to explain that the wider  $\Delta T$  is not better in cities with high cooling demand., The wider  $\Delta T$  is, the better its ability to adapt to the environment, but it is worse to suppress temperature fluctuations,  $\Delta T = 6\text{ }^{\circ}\text{C}$  is relatively optimal, which has been demonstrated in previous studies [36]. Further, the optimal level is C5 ( $L_5$ ) in both China and Japan for factor C ( $L_P$ ), and C1 ( $L_1$ ) performs worst, which is different from the previous study [24] (optimal location in the middle), it mainly related to the outdoor boundary condition action period. The boundary condition used by seven consecutive days in the summer high-temperature period for the literature [24], while the outdoor boundary condition of 8760h (whole year) is utilized in this study. This difference in boundary conditions results in different energy-saving effects, which in turn will have different effects on the optimal location of PCM [31]. It further illustrates the necessity to analyze the application effects of PCM from a year-round perspective. Concurrently, it is found that the cooling and heating load are reduced by 0.73-3.25 kWh/m<sup>2</sup> (average: 1.65 kWh/m<sup>2</sup>) and 0.068-1.68 kWh/m<sup>2</sup> (average: 1.21 kWh/m<sup>2</sup>) as the level changed from C1 ( $L_1$ ) to C4 ( $L_4$ ), respectively. However, as a comparison, the cooling and heating load are reduced by 0.78-3.67 kWh/m<sup>2</sup> (average: 1.79 kWh/m<sup>2</sup>) and 0.07-3.37 kWh/m<sup>2</sup> (average: 2.19 kWh/m<sup>2</sup>) from C4 to C5. The data show that the advantage of PCM being installed in the interior ( $L_5$ ) of the wall is much higher than in other locations. Additionally, the cooling and heating loads are reduced by 0.59%-7.98% and 1.49%-42.81% when the level changes from C1 to C5, respectively, indicating that the change in location has a higher impact on the heating load than the cooling load under the appropriate PCM parameters/configurations.

In addition, a common result for the factor D ( $d_P$ ) in China and Japan is that the best performance is D5 (25 mm) followed by D2 (10 mm) in reducing cooling load (Figure 7(a)). However, a remarkable feature is that the cooling load shows an enhancement as D2 (10 mm) is increased to D4 (20 mm), continuing to increase to D5 (25 mm) the minimum value occurs. The phenomenon is produced because the thicker PCM increases the thermal resistance of the wall, and the latent heat effect of the PCM is gradually replaced by the thermal resistance, which has been found in the previous study [14]. It also further explains why D5 is the optimal value in the heating load (Fig. 8-7(b)). In parallel, factor E ( $H_P$ ) has a similar conclusion to factor D. That is, the increase in wall thermal storage capacity does not produce higher energy savings for limited outdoor heat [24,36]. The E4 (175kJ/kg) is the best for cooling loads (except for Harbin is 225kJ/kg), and E5 (225kJ/kg) is for heating loads in all cities. Afterward, the factor F ( $D_P$ ) has the same conclusion on the optimal level of cooling load in both China and Japan, namely, F5 (Roof) is the preferred choice for the PCM installation orientation (largest energy

savings contribution), followed by F1 (East), F3 (West), F2 (South) and F4 (North), which is consistent with the previous study [31]. In contrast, the roof (F5) is still the most energy-saving in heating load, but there are notable distinctions in the ranking for other orientations in different cities. Most cities are F1 (East) > F3 (West) > F2 (South) > F4 (North), Harbin and Beijing show F3 > F1 > F2 > F4 and F2 > F3 > F1 > F4. In the meantime, the above-mentioned is more obvious in Japan and also very different from China, where Sapporo, Hachinohe, and Sendai are F3 > F1 > F2 > F4, whereas Tokyo, Kagoshima, and Naha are F3 > F2 > F1 > F4, F1 > F3 > F2 > F4 and F1 > F2 > F3 > F4, respectively. It shows that this difference of factor F is not only related to the cooling and heating demand but also to the altitude, solar radiation intensity, and sunshine hours of different climates/cities.

Additionally, Fig. 8-7(c) presents the total annual load at different levels of each factor, yielding that the phase-transition temperature of 16 °C (A1) is more suitable for cities with a higher annual heating load demand while 24 °C (A3) shows the best energy saving effect in Kunming, Guangzhou and Naha (high annual cooling load). As for factor B, B5 ( $\Delta T = 10$  °C) perform optimally in both China and Japan (except Naha is B3), but it can still be observed that the advantage of B3 ( $\Delta T = 6$  °C) becomes prominent as the proportion of cooling load demand is increased in different cities (the difference between B3 and B5 is weakened). It is mainly caused by the small effect of the  $\Delta T$  on the cooling load in summer for the cities with high heating demand based on an annual standpoint [36]. Also, PCM installed in the interior (C5,  $L_5$ ) of the wall is still the best choice for all cities, and it is also found that the differences in energy saving for PCM installed in different locations of the interior ( $L_2, L_3, L_4$ ) of the wall are smaller, but all show the characteristic of more energy saving the further inside the house. Factor D still shows the best with D5 (25 mm), followed by D2 (10 mm). However, for E, except for Guangzhou and Naha, where E4 (175 kJ/kg) is preferred, the larger the latent heat of other cities contributes to energy savings, but this energy-saving effect is gradually weakened, which has been proved in the literature [24]. Apart from that, the best order of factor F ( $D_p$ ) is F1 > F3 > F2 > F4, except F5 is optimum for reducing the total load, but it is found that the difference in energy savings between F1 and F5 is reduced as the cooling load demand is boosted. For example, the difference is 4.74 kWh/m<sup>2</sup> for Harbin and 1.70 kWh/m<sup>2</sup> for Guangzhou, which has similar findings in Japan. It shows that for cities with a high percentage of cooling demand, the energy saving in east-facing walls is not negligible in addition to roofs as a priority choice, especially in Guangzhou and Naha. In summary, the differences for different climates/cities in the selection of the parameters and configurations of PCM to maximize the benefits of PCM applications should be taken seriously.

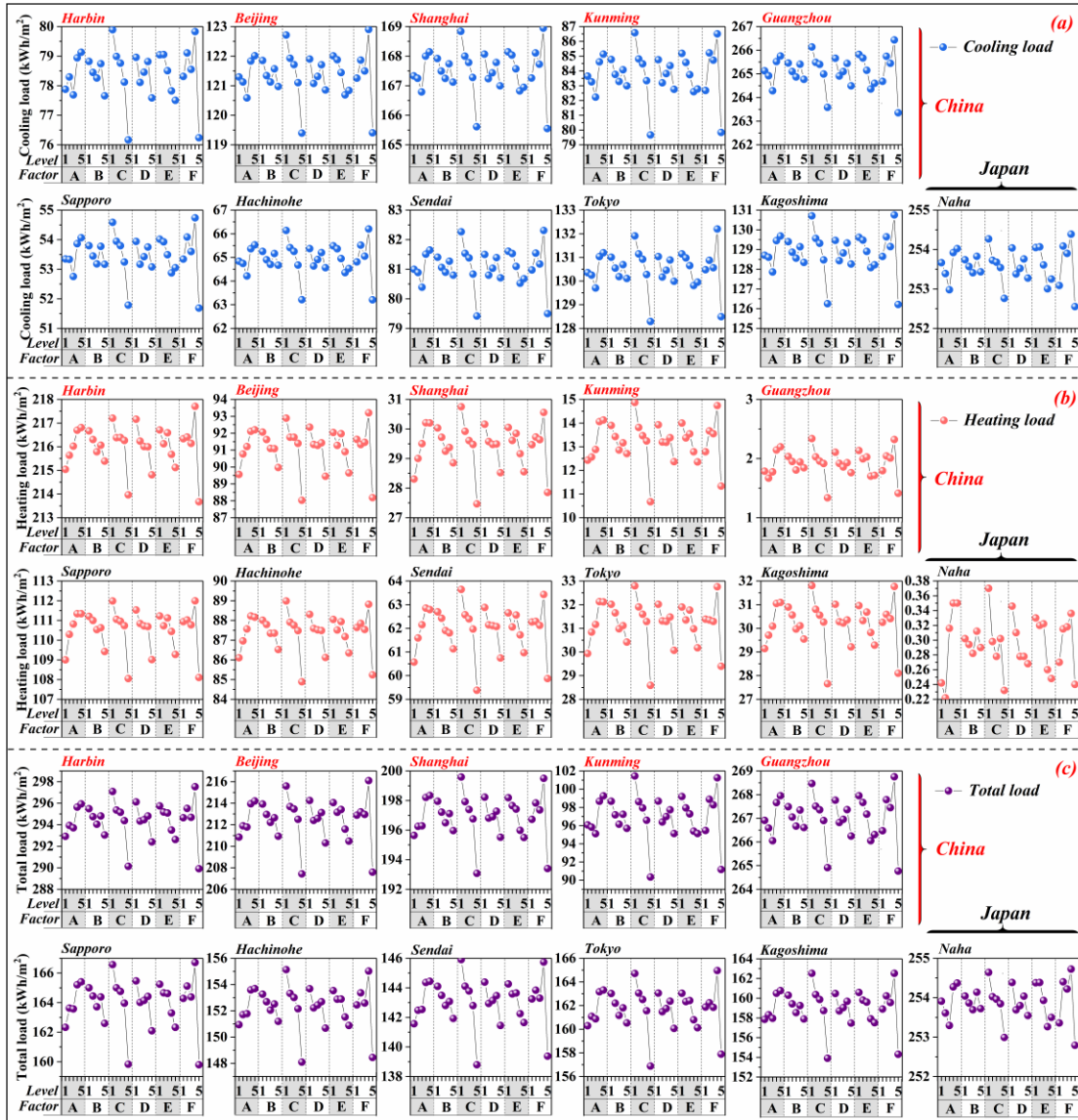


Fig. 8-7. Suitability level ( $k_{i,m}$ ) of each PCM factor (parameter/configuration) on (a) cooling load, (b) heating load and (c) total load in different climates/cities.

### 8.4.2 Influence degree of each factor

Based on the above result, it is obtained that there is a noticeable distinction in the energy saving rate of the different cities for both heating and cooling loads by increasing the level of different factors from 1 to 5. Particularly, factor C ( $L_P$ ) has a markedly higher change rate than the other factors, further indicating those parameters/configurations that should be the primary focus when choosing a PCM to apply. Therefore, the influence degree ( $R_v$ ) of each factor on the evaluation index (cooling and heating load) is expressed in Fig. 8-8. It can be discovered that the importance ranking of each factor on the influence of cooling, heating, and total load varies considerably among which factors C ( $L_P$ ) and F ( $D_P$ ) have the highest degree of influence. It means that the installation location (factor C) and orientation (factor F) of PCM are the key

considerations for energy saving. Despite this, it can be viewed from Fig. 8-8(a) that the factors C and F still have some importance ordering in terms of cooling load energy saving, except for Harbin, Kunming and Sendai, where  $C > F$ , the other cities are  $F > C$ . Meanwhile, most of the cities show consistency in the importance ranking of other factors, that is,  $A (T_p) > E (H_p) > D (d_p) > B (\Delta T)$ . Harbin is  $E > A > D > B$ . The results show that the phase-transition temperature (factor A) is the most important parameter to be considered after determining the installation location (factors C and F) to reduce cooling load, while the phase-transition temperature range (factor B) is the least important.

Nonetheless, the above results are dissimilar in the heating load, as shown in Fig. 8-8(b). It can be found that factor F, which has the greatest impact on cooling load, is less important than C in terms of heating load in most cities, that is,  $C > F$  (except Harbin and Beijing for  $F > C$ ), and the factor B is still not a priority. Furthermore, for the factor D with a low influence on the cooling load, the influence on the heating load cannot be neglected, especially in Harbin, Beijing of China, and Sapporo, Hachinohe of Japan, where it is second only to F and C, with  $F > C > D > A > E > B$  (Harbin and Beijing) and  $C > F > D > A > E > B$  (Sapporo and Hachinohe), respectively. This is mainly related to the low thermal conductivity of PCM, and the thickness of PCM is increased to provide more advantages in thermal insulation and thus greatly reduces the heating load. On the contrary, the influence degree of factor D gradually decreases for different cities as the average annual temperature increases (annual cooling load demand is raised), whereas the importance of A is enhanced, for Shanghai in China and Sendai, Tokyo, Kagoshima in Japan are  $C > F > A > D > E > B$ . Guangzhou and Kunming are  $C > F > A > E > D > B$ . Factor A is more influential than F in Naha, which is  $C > A > F > E > D > B$ . As a result, it suggests that the priorities of paying attention to the parameters/configurations of PCM are different when choosing to apply it in areas with different heating and cooling demands. For example, areas with higher annual heating demand should pay more attention to factor D and areas with higher cooling demand should focus on factor A. At the same time, factor E is found to be more important in summer than in winter. Moreover, regarding the different thermal zones between China and Japan (see Appendix A), the importance of each PCM parameter/configuration is also substantially different. For instance, in terms of heating load reduction, most of the thermal zones (III, IV, V) in Japan are  $F > C > A > E > D > B$ , while only HSCW in China shows this performance. Thus, it can be concluded that there are not only seasonal (summer and winter) but also regional differences in the importance degree of each PCM factor and that the appropriate PCM should be selected according to different cooling and heating requirements and climate characteristics to maximize its performance.

Considering the inherent thermal properties (not changing with the season) of PCM and

its effectiveness, Fig. 8-8(c) provides the influence degree of each factor based on the total annual load. It can be shown that the importance of factors C and F are still maximum and B minimum, which means that determining the appropriate PCM installation location/orientation can dramatically improve the building energy saving under other relatively suitable PCM parameters. Then, factor A is more influential (after C and F) in most cities of China (Shanghai, Kunming, and Guangzhou), with  $C > F > A > D > E > B$  (Shanghai),  $C > F > A > E > D > B$  (Kunming) and  $F > C > A > E > D > B$  (Guangzhou), respectively. In contrast, factor A is more important in the Japanese region only in Tokyo. Meanwhile, in the northern regions of China (higher heating load), such as Harbin, Beijing, and in Sapporo, Hachinohe, and Sendai of Japan, the influence of factor D on the total annual load is higher than A, with  $F > C > D > A > E > B$  (Harbin, Sapporo),  $F > C > D > E > A > B$  (Beijing) and  $C > F > D > A > E > B$  (Hachinohe and Sendai), respectively. In addition, it is found that the influence degree of factor E is rather low (only higher than B) in Harbin and most cities in Japan (except Kagoshima and Naha). It is further concluded that PCM latent heat plays a limited role in the energy saving of total annual loads in areas with high annual heating requirements. In the above case, the application of PCM may not be superior to insulation material when the cost of PCM is considered, and the PCM economic applicability should be considered more. In comparison, the importance of factors A and E is heightened in Guangzhou (China) and Naha (Japan), which is  $F > C > A > E > D > B$  (Guangzhou) and  $F > C > E > A > D > B$  (Naha). This result is sufficient to show that PCM is more suitable for areas with higher temperatures throughout the year (higher cooling demand) or in summer. Notwithstanding, the importance of factor E is found to be ranked after A in Guangzhou and before A in Naha, indicating that there are still regional or microclimatic differences in the priority of the PCM thermal parameters to be considered when selecting a PCM. In general, it is especially necessary to determine PCM according to the influence degree of parameters/configurations to maximize the effectiveness of PCM applications.

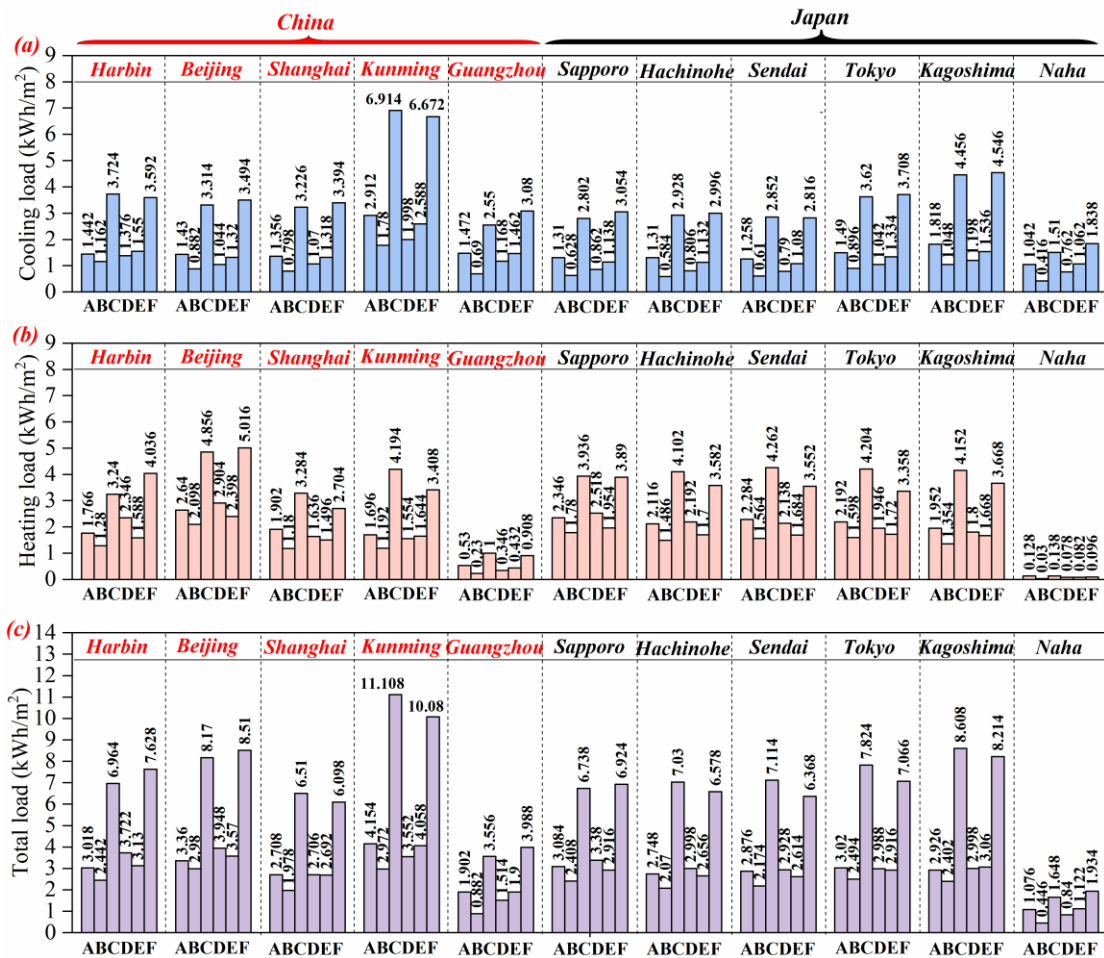


Fig. 8-8. Influence degree ( $R_v$ ) of each PCM factor (parameter/configuration) on the (a) cooling load, (b) heating load and (c) total load in different climates/cities.

## 8.5 PCM optimal configuration and energy-saving evaluation based on orthogonal experiment

### 8.5.1 Energy-saving and suitability of different PCM configurations (single and double layer)

Based on the above orthogonal results, Table 6 gives the optimized combination scheme, importance ranking, and energy-saving effect of PCM parameters/configurations under different climates/cities. It can be drawn that when only summer or winter energy savings are considered choosing the appropriate PCM parameters/configurations between different climates/cities can save 4.11%-21.52% (China) and 3.25%-16.20% (Japan) for the cooling load, the heating load reductions are 5.91%-96.54% (China) and 11.41%-100% (Japan), and the total annual load energy savings 5.02%-28.58% (China) and 3.40%-13.14% (Japan). It shows that a suitable PCM can not only improve indoor thermal comfort (reduce indoor temperature fluctuations [14,24,31,36]) but also dramatically reduce energy consumption, especially in

areas with low heating load demand, where choosing a suitable PCM can make the heating load reach nearly zero energy consumption (NZE). Moreover, the inherent thermal properties of PCM do not meet the optimal requirements for energy savings in both seasons (summer and winter) simultaneously. PCM configurations that are superior in reducing the cooling load (optimal combination) are different in heating load, especially in PCM phase-transition temperature. As well, the optimal PCM configuration selected, even in terms of total annual load, is only biased towards the side with high cooling or heating demand, which means that the energy-saving potential of PCM is weakened for annual energy savings (PCM only works in one season for thermal regulation).

As a result, a double-layer PCM configuration is proposed in this study based on the above results, taking Harbin as an example, as shown in Fig. 8-9. Each layer is determined by the optimal PCM parameters/configurations for summer and winter, respectively, and the thickness is 1/2 of the single-layer PCM to ensure the total amount of PCM. Table 7 shows the cooling and heating loads and total annual load for the optimal configuration of the double-layer PCM, which can be obtained that although the energy-saving of double-layer PCM is less than single-layer PCM in terms of cooling or heating load, it is superior for the total annual load. In the case of Harbin, the energy savings of single-layer PCM for cooling and heating loads are 12.31% and 5.91%, respectively, compared to 11.95% and 5.81% for double-layer PCM, which are 0.36% and 0.1% higher, but the total annual load savings is 0.6% lower. Considering that PCM is not replaced intermittently due to seasonal differences when applied to building walls, double-layer PCM is a more advantageous option, which was also mentioned in a previous study [36]. Conversely, the above conclusions cannot be justified in areas with higher and moderate temperatures throughout the year. For example, in Guangzhou, the cooling and heating load of double-layer PCM under the optimal configuration can be saved by 3.86% and 98.08%, and single-layer PCM is 4.11% and 96.54%, respectively. As an outcome, although the double-layer PCM can further reduce the heating load by 1.54% compared with the single-layer, the double-layer PCM is 0.26% lower than the single-layer PCM for the energy-saving of total annual load due to the large difference in the percentage of its cooling and heating load (the cooling load accounts for 99.04% of the total load). Hence, it can be drawn that the double-layer PCM is not applicable in areas where the heating demand is close to zero (Guangzhou and Naha) or mild year-round (Kunming), and the single-layer PCM is better for their energy savings.

**Table 8-6 Optimal strategies/configurations and order of influencing factors of single- layer PCM for different cities in summer/winter and the whole year based on orthogonal design.**

Country	City	Summer			Winter			Whole year		
		Optimal Strategy (Single)	Factor Impact Degree	Cooling (kWh/m <sup>2</sup> )	Optimal Strategy (Single)	Factor Impact Degree	Heating (kWh/m <sup>2</sup> )	Optimal Strategy (Single)	Factor Impact Degree	Total (kWh/m <sup>2</sup> )
China	Harbin	A <sub>3</sub> B <sub>5</sub> C <sub>5</sub> D <sub>5</sub> E <sub>5</sub> F <sub>5</sub>	C>F>E>A>D>B	71.10(12.31%)	A <sub>1</sub> B <sub>5</sub> C <sub>5</sub> D <sub>5</sub> E <sub>5</sub> F <sub>5</sub>	F>C>D>A>E>B	205.90(5.91%)	A <sub>1</sub> B <sub>5</sub> C <sub>5</sub> D <sub>5</sub> E <sub>5</sub> F <sub>5</sub>	F>C>D>A>E>B	279.31(6.87%)
	Beijing	A <sub>3</sub> B <sub>5</sub> C <sub>5</sub> D <sub>5</sub> E <sub>4</sub> F <sub>5</sub>	F>C>A>E>D>B	114.26(8.14%)	A <sub>1</sub> B <sub>5</sub> C <sub>5</sub> D <sub>5</sub> E <sub>5</sub> F <sub>5</sub>	F>C>D>A>E>B	79.00(16.45%)	A <sub>1</sub> B <sub>5</sub> C <sub>5</sub> D <sub>5</sub> E <sub>5</sub> F <sub>5</sub>	F>C>D>E>A>B	194.91(10.97%)
	Shanghai	A <sub>3</sub> B <sub>5</sub> C <sub>5</sub> D <sub>5</sub> E <sub>4</sub> F <sub>5</sub>	F>C>A>E>D>B	159.82(6.13%)	A <sub>1</sub> B <sub>5</sub> C <sub>5</sub> D <sub>5</sub> E <sub>5</sub> F <sub>5</sub>	C>F>A>D>E>B	22.33(28.92%)	A <sub>1</sub> B <sub>5</sub> C <sub>5</sub> D <sub>5</sub> E <sub>5</sub> F <sub>5</sub>	C>F>A>D>E>B	184.37(8.58%)
	Kunming	A <sub>3</sub> B <sub>5</sub> C <sub>5</sub> D <sub>5</sub> E <sub>4</sub> F <sub>5</sub>	C>F>A>E>D>B	69.79(21.52%)	A <sub>1</sub> B <sub>5</sub> C <sub>5</sub> D <sub>5</sub> E <sub>5</sub> F <sub>5</sub>	C>F>A>E>D>B	5.81(63.16%)	A <sub>3</sub> B <sub>5</sub> C <sub>5</sub> D <sub>5</sub> E <sub>5</sub> F <sub>5</sub>	C>F>A>E>D>B	74.77(28.58%)
	Guangzhou	A <sub>3</sub> B <sub>5</sub> C <sub>5</sub> D <sub>5</sub> E <sub>4</sub> F <sub>5</sub>	F>C>A>E>D>B	256.89(4.11%)	A <sub>2</sub> B <sub>3</sub> C <sub>5</sub> D <sub>5</sub> E <sub>4</sub> F <sub>5</sub>	C>F>A>E>D>B	0.09(96.54%)	A <sub>3</sub> B <sub>5</sub> C <sub>5</sub> D <sub>5</sub> E <sub>4</sub> F <sub>5</sub>	F>C>A>E>D>B	256.92(5.02%)
	Sapporo	A <sub>3</sub> B <sub>5</sub> C <sub>5</sub> D <sub>5</sub> E <sub>4</sub> F <sub>5</sub>	F>C>A>E>D>B	46.83(16.2%)	A <sub>1</sub> B <sub>5</sub> C <sub>5</sub> D <sub>5</sub> E <sub>5</sub> F <sub>5</sub>	C>F>D>A>E>B	100.07(11.41%)	A <sub>1</sub> B <sub>5</sub> C <sub>5</sub> D <sub>5</sub> E <sub>5</sub> F <sub>5</sub>	F>C>D>A>E>B	148.82(11.86%)
Japan	Hachinohe	A <sub>3</sub> B <sub>5</sub> C <sub>5</sub> D <sub>5</sub> E <sub>4</sub> F <sub>5</sub>	F>C>A>E>D>B	58.26(13.47%)	A <sub>1</sub> B <sub>5</sub> C <sub>5</sub> D <sub>5</sub> E <sub>5</sub> F <sub>5</sub>	C>F>D>A>E>B	78.20(13.01%)	A <sub>1</sub> B <sub>5</sub> C <sub>5</sub> D <sub>5</sub> E <sub>5</sub> F <sub>5</sub>	C>F>D>A>E>B	138.53(11.89%)
	Sendai	A <sub>3</sub> B <sub>5</sub> C <sub>5</sub> D <sub>5</sub> E <sub>4</sub> F <sub>5</sub>	C>F>A>E>D>B	75.06(10.06%)	A <sub>1</sub> B <sub>5</sub> C <sub>5</sub> D <sub>5</sub> E <sub>5</sub> F <sub>5</sub>	C>F>A>D>E>B	52.71(18.36%)	A <sub>1</sub> B <sub>5</sub> C <sub>5</sub> D <sub>5</sub> E <sub>5</sub> F <sub>5</sub>	C>F>D>A>E>B	129.37(12.6%)
	Tokyo	A <sub>3</sub> B <sub>5</sub> C <sub>5</sub> D <sub>5</sub> E <sub>4</sub> F <sub>5</sub>	F>C>A>E>D>B	123.00(7.97%)	A <sub>1</sub> B <sub>5</sub> C <sub>5</sub> D <sub>5</sub> E <sub>5</sub> F <sub>5</sub>	C>F>A>D>E>B	22.41(33.62%)	A <sub>1</sub> B <sub>5</sub> C <sub>5</sub> D <sub>5</sub> E <sub>5</sub> F <sub>5</sub>	C>F>A>D>E>B	147.06(12.16%)
	Kagoshima	A <sub>3</sub> B <sub>5</sub> C <sub>5</sub> D <sub>5</sub> E <sub>4</sub> F <sub>5</sub>	F>C>A>E>D>B	119.57(9.69%)	A <sub>1</sub> B <sub>5</sub> C <sub>5</sub> D <sub>5</sub> E <sub>5</sub> F <sub>5</sub>	C>F>A>D>E>B	21.86(33.5%)	A <sub>1</sub> B <sub>5</sub> C <sub>5</sub> D <sub>5</sub> E <sub>5</sub> F <sub>5</sub>	C>F>E>D>A>B	143.56(13.14%)
	Naha	A <sub>3</sub> B <sub>3</sub> C <sub>5</sub> D <sub>5</sub> E <sub>4</sub> F <sub>5</sub>	F>C>A>E>D>B	247.22(3.25%)	A <sub>2</sub> B <sub>3</sub> C <sub>5</sub> D <sub>5</sub> E <sub>5</sub> F <sub>5</sub>	C>A>F>E>D>B	0.00(100%)	A <sub>3</sub> B <sub>3</sub> C <sub>5</sub> D <sub>5</sub> E <sub>4</sub> F <sub>5</sub>	F>C>E>A>D>B	247.22(3.40%)

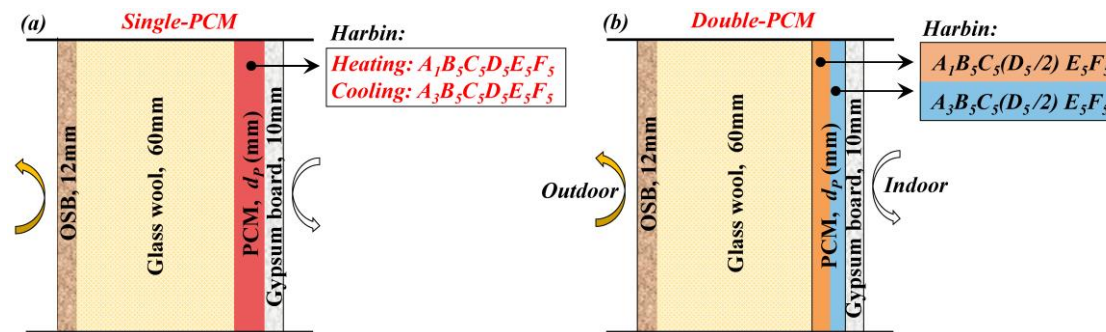


**Fig. 8-9. Double-layer PCM optimization strategy/configuration based on orthogonal experiment (Take Harbin as an example).**

**Table 8-7 Cooling/heating and total load for different cities under the double-layer PCM optimization strategy/configuration.**

Country	City	Optimal Strategy (Double-PCM)	Cooling (kWh/m <sup>2</sup> )	Heating (kWh/m <sup>2</sup> )	Total (kWh/m <sup>2</sup> )
China	HB	(A <sub>1</sub> +A <sub>3</sub> )B <sub>5</sub> C <sub>5</sub> (D <sub>5</sub> /2+D <sub>5</sub> /2)E <sub>5</sub> F <sub>5</sub>	71.39(11.95%)	206.11(5.81%)	277.50(7.47%)
	BJ	(A <sub>1</sub> +A <sub>3</sub> )B <sub>5</sub> C <sub>5</sub> (D <sub>5</sub> /2+D <sub>5</sub> /2)(E <sub>5</sub> +E <sub>4</sub> )F <sub>5</sub>	114.39(8.03%)	79.48(15.94%)	193.87(11.45%)
	SH	(A <sub>1</sub> +A <sub>3</sub> )B <sub>5</sub> C <sub>5</sub> (D <sub>5</sub> /2+D <sub>5</sub> /2)(E <sub>5</sub> +E <sub>4</sub> )F <sub>5</sub>	160.28(5.86%)	22.25(29.17%)	182.53(9.49%)
	KM	(A <sub>1</sub> +A <sub>3</sub> )B <sub>5</sub> C <sub>5</sub> (D <sub>5</sub> /2+D <sub>5</sub> /2)(E <sub>5</sub> +E <sub>4</sub> )F <sub>5</sub>	70.00(21.28%)	5.52(65.00%)	75.52(27.87%)
	GZ	(A <sub>2</sub> +A <sub>3</sub> )(B <sub>3</sub> +B <sub>5</sub> )C <sub>5</sub> (D <sub>5</sub> /2+D <sub>5</sub> /2)E <sub>4</sub> F <sub>5</sub>	257.57(3.86%)	0.05(98.08%)	257.62(4.76%)
	Sap.	(A <sub>1</sub> +A <sub>3</sub> )B <sub>5</sub> C <sub>5</sub> (D <sub>5</sub> /2+D <sub>5</sub> /2)(E <sub>5</sub> +E <sub>4</sub> )F <sub>5</sub>	47.08(15.75%)	100.74(10.82%)	147.82(12.45%)
Japan	Hac.	(A <sub>1</sub> +A <sub>3</sub> )B <sub>5</sub> C <sub>5</sub> (D <sub>5</sub> /2+D <sub>5</sub> /2)(E <sub>5</sub> +E <sub>4</sub> )F <sub>5</sub>	58.62(12.93%)	78.55(12.62%)	137.17(12.75%)
	Sen.	(A <sub>1</sub> +A <sub>3</sub> )B <sub>5</sub> C <sub>5</sub> (D <sub>5</sub> /2+D <sub>5</sub> /2)(E <sub>5</sub> +E <sub>4</sub> )F <sub>5</sub>	75.32(9.75%)	53.04(17.85%)	128.36(13.28%)
	Tok.	(A <sub>1</sub> +A <sub>3</sub> )B <sub>5</sub> C <sub>5</sub> (D <sub>5</sub> /2+D <sub>5</sub> /2)(E <sub>5</sub> +E <sub>4</sub> )F <sub>5</sub>	122.93(8.03%)	22.10(34.54%)	145.03(13.37%)
	Kag.	(A <sub>1</sub> +A <sub>3</sub> )B <sub>5</sub> C <sub>5</sub> (D <sub>5</sub> /2+D <sub>5</sub> /2)(E <sub>5</sub> +E <sub>4</sub> )F <sub>5</sub>	119.74(9.57%)	21.71(33.95%)	141.45(14.42%)
	Na.	(A <sub>2</sub> +A <sub>3</sub> )B <sub>3</sub> C <sub>5</sub> (D <sub>5</sub> /2+D <sub>5</sub> /2)(E <sub>5</sub> +E <sub>4</sub> )F <sub>5</sub>	247.90(2.99%)	0.00(100%)	247.90(3.13%)

### 8.5.2 Energy-saving for different PCM amounts (thickness and utilization area)

For PCM, when the PCM parameters and installation location are determined, the amount (thickness and utilization area) of PCM directly affects the total heat storage and release capacity of the wall, indoor thermal environment, and energy saving. Thereby, the total annual load for different thicknesses and installation orientations (utilization area) based on the above derived optimal parameters/configurations are obtained in this study, as shown in Fig. 8-10. A common feature is that the thicker the PCM, the higher the energy saving rate. Take Harbin as an example, and the total load is reduced by 15.77 kWh/m<sup>2</sup> (5.27%), 19.56 kWh/m<sup>2</sup> (6.52%), 20.82 kWh/m<sup>2</sup> (6.94%), 21.68 kWh/m<sup>2</sup> (7.23%), and 22.41 kWh/m<sup>2</sup> (7.47%) for every 5 mm increase in PCM from 0 mm to 25 mm compared to 0 mm (no PCM) when the PCM is installed in Roof only. However, an apparent result from the above data is that the energy saving rate of the total load is decreased by 5.27%, 1.52%, 0.42%, 0.29%, and 0.24% for every 5mm is increased based on 0mm. It is demonstrated that the energy-saving effect gradually is weakened as the thickness of PCM is increased, which is consistent with previous studies [24,36]. Considering the cost of PCM [58], thicker PCM may have a negative impact on building energy saving, which is a similar conclusion to the continuous increase of insulation materials [13,90]. Furthermore, the energy savings vary greatly with the same thickness of PCM in different climates/cities. For example, 25mm PCM installed on Roof, for China, the best performance is Kunming (28.42%), followed by Beijing (11.45%) and Shanghai (9.49%), and the worst is Guangzhou (5.02%). In contrast, for Japan, the difference in energy savings is slight (12.45%-14.42%) except for Naha (3.40%), and the most favorable is in Kagoshima (14.42%). The results illustrate that there are regional differences in the applicability of PCM when energy

saving is being taken as an essential evaluation indicator. Guangzhou (China) and Naha (Japan), where PCM is not recommended by comparison, mainly because the percentage of heating demand in Guangzhou and Naha is close to zero. Although the appropriate PCM parameters/configurations are chosen, the effectiveness of PCM is only applicable to the higher temperature period in summer due to their inherent thermal properties, which is a relatively low energy-saving contribution compared to the whole year. It also means that economic analysis becomes particularly necessary when PCM is applied to buildings due to the current expensive PCM [58].

In addition, the priority order of PCM installation with different orientations obtained through the above results ( $k_{i,m}$ ) is Roof, East, West, South, and North, respectively. For that, this study installed PCM in Roof (R), Roof + East (RE), Roof + East + West (REW), Roof + East + West + South (REWS), and Roof + East + West + South + North (REWSN) for energy saving analysis, and the results are shown in Fig. 8-10. It can be observed that the energy saving laws are similar to those installed only in Roof with the thickness of PCM is added, which both show a downward trend and gradually stabilize. When 25mm PCM is installed in REWSN, the highest energy saving rate is 38.06% in Kunming, and the lowest is in Guangzhou and Naha, but still, 7.3% and 5.17% can be saved. Other than that, the energy savings in other typical cities of China ranged from 14.49% to 16.88% and from 18.25% to 20.37% in Japan. However, it should be noted that the total load is suddenly reduced at 25 mm and 20 mm when PCM is installed in REWS and REWSN in Harbin compared to other cities, which can be explained by the fact that the total thermal resistance of the wall caused by the lower thermal conductivity of PCM is enhanced under the PCM thickness is increased further leading to a higher contribution rate of the thermal conductivity to energy saving than the latent heat of PCM, the additional latent heat of PCM will not be fully utilized beyond a certain thickness, as confirmed in a previous study [14]. Again, when the PCM thickness is determined, all cities show the same tendencies that the contribution rate of energy saving to continue installing in other orientations to PCM on the basis of Roof increases but gradually stabilizes. Using 5 mm for Harbin as an example, the total load is reduced by 15.81 kWh/m<sup>2</sup> (5.27%), 20.92 kWh/m<sup>2</sup> (6.98%), 26.29 kWh/m<sup>2</sup> (8.77%), 29.39 kWh/m<sup>2</sup> (9.80%) and 29.40 kWh/m<sup>2</sup> (9.80%) respectively compared to the reference building (no PCM) by installing PCM in R, RE, REW, REWS, and REWSN respectively. Despite this, the energy savings of REWSN compared to REWS, REW, RE, and R are only improved by 0%, 1.03%, 2.82%, and 4.53%, correspondingly. As a consequence, installing PCM in all directions is not the best choice, and the RE or REW is recommended, but whether it is the optimal choice or not needs to be further determined by economic analysis. In addition, a significant result is found that although PCM installed on Roof has a higher energy-

saving priority, it does not mean that it brings a higher energy-saving benefit under the same volume ( $V_{PCM}$ ) compared to evenly distributed on all orientations (by installation priority). Taking Harbin as an instance, installing 25mm PCM in Roof ( $V_{PCM}=0.562m^3$ ) reduces the total load by 22.41 kWh/m<sup>2</sup> (7.47%), while installing 5mm PCM in REWSN ( $V_{PCM}=0.356m^3$ ) is dropped by 46.11 kWh/m<sup>2</sup> (15.37%). To sum up, as a result, it is more important to analyze the economics for different amounts (thickness and utilization area) of PCM in different climates to apply based on the cost of PCM.

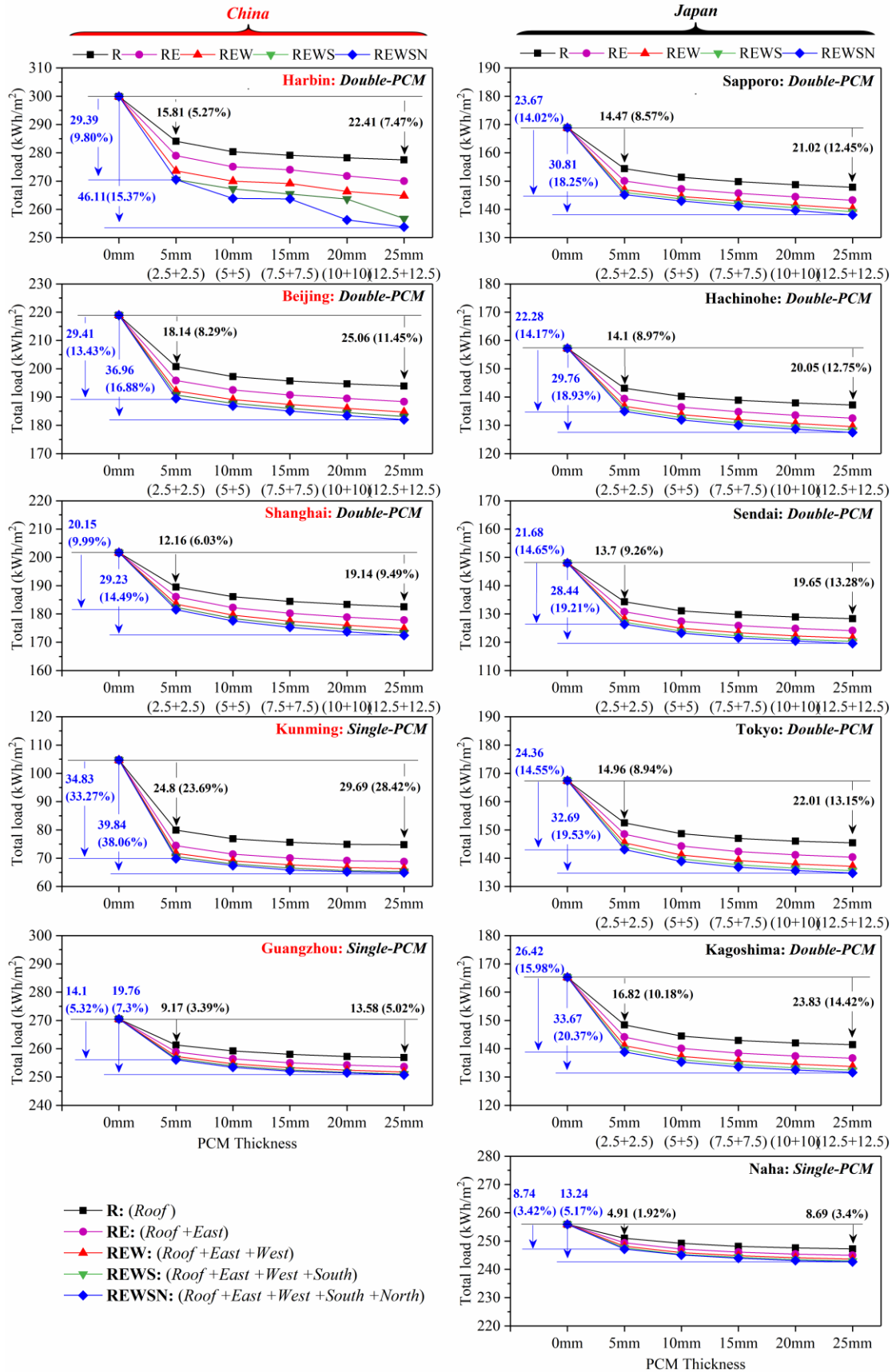


Fig. 8-10. The relationship between the annual total load and PCM thicknesses under different building orientations integrated with PCM.

## 8.6 Economic analysis of energy-saving strategies

### 8.6.1 Payback period based on PCM cost price

The cost of PCM is a crucial consideration for PCM applications. Higher amounts (thickness and utilization area) mean higher initial investment for PCM [98]. Therefore, the static payback period (SPP) is used in this study to explore the economics of PCM for different amounts (thickness and utilization area) to apply. The SPP was widely used in many techno-economic analyses due to its simplicity of calculation [56,99,100], and it is expressed by Eq. (8-14) [56]. Additionally, it should be pointed out that there is no uniform price in the market for the cost of PCM, so the current prices of PCM were counted in this study through the relevant literature and listed in Appendix B, and the average (4.6 \$/kg) is utilized to analyze. At the same time, considering the energy profitability, the price of electricity obtained by the relevant official websites and literature is 0.18 \$/kWh [96,97] in Japan and 0.07 \$/kWh in China [13] (1 \$ = 7.24 CNY, 1 \$ = 147.69 JPY [101]).

$$SPP = \frac{C_{PCM}}{S} \quad (8-14)$$

where  $SPP$  is a static payback period, year;  $C_{PCM}$  is the initial investment of PCM, \$/kg;  $S$  is the income generated from energy savings, \$.

Further, it is worth mentioning that although the dynamic payback period (DPP) is often closer to the actual energy management cost based on the time value of money [56,58], this study focuses mainly on the economic applicability of PCM. The results obtained by DPP will be more unsatisfactory if SPP does not meet the demand because the DPP is often greater than SPP. Hence, only SPP is calculated in this study, and the results are shown in Fig. 8-11. It can be deduced that the payback period of all cities in China is more than 100 years when 25 mm PCM is installed on REWSN. In the meanwhile, although most cities are below 100 years in Japan (Naha is above 100 years), all are high than 80 years (82.6-93.4 years). However, the service life is basically around 50 years [102] for most buildings, which represents an inability to recover the cost. Also, it is noticed that the payback period in Japan is lower than that in China for the same installation orientation when the PCM thickness is defined. Taking the 5 mm PCM installed on the Roof as an example, the payback period of cities in different climates of China ranged is 18.2-49.2 years, and it is 10.4-35.8 years in Japan. The longest payback period is in Guangzhou (49.2 years) and Naha (35.8 years). Meanwhile, a noteworthy difference is that the average payback period in other cities of China is 27.2 years (except for Guangzhou), while in Japan, it is only 11.9 years (except for Naha). This situation is partly influenced by the

energy saving of the load, but more importantly, the higher energy prices (in Japan are about 2.5 times higher than in China) in Japan lead to a relatively short payback period under little difference in energy savings. As a result, it further indicates that the rising trend of energy prices will contribute more positively to the economic benefits of PCM applications in buildings under the same energy savings per year.

Another, it can be seen when the payback period is set to 20 years that for China, only Kunming's 5 mm PCM installed on Roof meets the requirement. Comparatively, the amount of PCM that meets the requirement for all cities in Japan (except Naha) is 5 mm PCM installed on R, RE and REW for Sapporo, Hachinohe, Tokyo and Kagoshima, 5 mm PCM installed on R and RE for Sendai, 5 mm PCM installed on REWS for Kagoshima, as well as 10 mm PCM installed on R for Sapporo, Tokyo, and Kagoshima. The results reveal that the PCM thickness exceeding 10mm is not the optimal solution based on the current PCM cost, even though it can reduce the energy demand to a certain extent. Moreover, if 50 years is set as the payback period, Harbin, Beijing, and Kunming in China are recommended for 5mm PCM installed on REWSN, and Shanghai for 5mm installed on RE, as this can bring higher energy saving and longer indoor thermal comfort at the same volume of PCM and Guangzhou does not suggest the installing PCM. By contrast, for the same payback period, more options are available in Japan, but it is still recommended to install at most 10mm PCM on REWSN. Naha is only recommended to install 5 mm PCM on RE. Nevertheless, as a conclusion, it is to be emphasized that the energy price and PCM cost are assumed to remain unchanged in this study, which means that if the results of the economic analysis of PCM applications are positive, then higher energy prices and lower PCM costs will bring higher energy saving benefits to actual projects in the future.

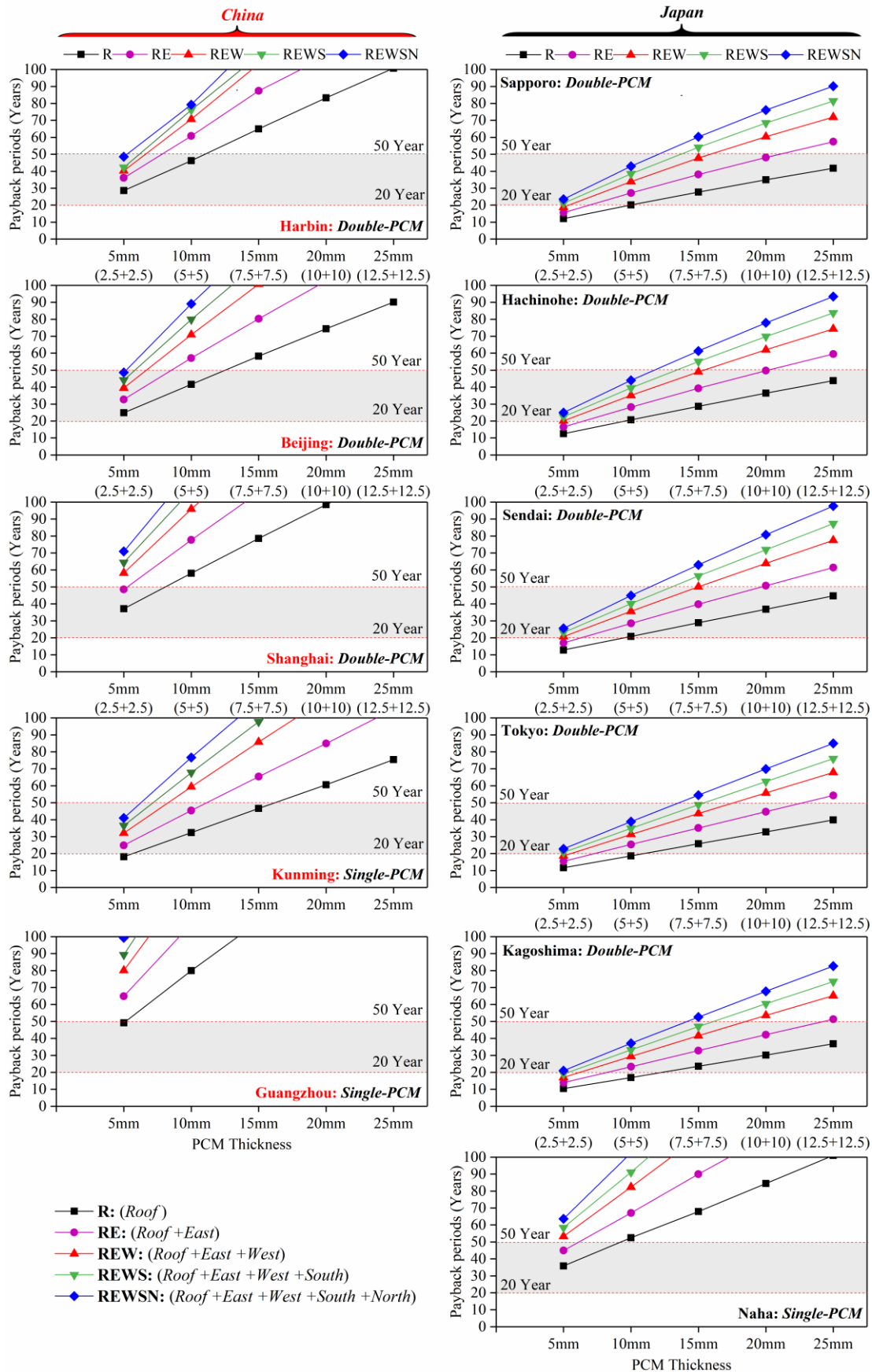


Fig. 8-11. Payback period for different PCM thickness integrated into different orientations under certain PCM cost price.

### 8.6.2 Acceptable cost price for PCM based on payback period

Based on the above results, it is found that the payback period is highly correlated with the PCM amount for a particular PCM cost. Similarly, PCM applicability is highly correlated with PCM cost when the payback period is determined, and higher PCM cost may not positively impact on energy-saving benefits. Accordingly, the acceptable maximum PCM cost prices are discussed in this study for different PCM amounts in different climates/cities using 20 years as the payback period, and the results are shown in Fig. 8-12. It can be seen that the acceptable PCM price varies significantly due to the different energy-saving of PCM in different regions. For example, the acceptable PCM price for 5mm PCM installed on Roof is 3.22 \$/kg in Harbin and 1.87 \$/kg in Guangzhou. In contrast, the price for PCM in Japan is more relaxed. The acceptable price is 7.18-8.81 \$/kg, except for Naha (2.57 \$/kg). Furthermore, taking Harbin and Sapporo with lower annual average temperatures as examples, it can be found that only 5 mm PCM installed on the Roof meets the requirement in Harbin, assuming a maximum acceptable price of 3.22 \$/kg. However, there are more options in Sapporo, such as 5 mm PCM can be installed on R to REWSN, 10 mm PCM can be installed on R and RE, and 15 mm PCM can be installed on R. It means that Japan is more suitable for PCM applications than China in terms of current energy prices and PCM cost. Furthermore, a consistent trend is found that the required PCM price, although lower with the PCM amount (thickness and utilization area) is added, its difference is gradually narrowed. For instance, in Harbin, the acceptable PCM price reduction for each additional 5mm in the base of 5mm (3.22 \$/kg) is 1.23 \$/kg, 0.58 \$/kg, 0.31 \$/kg and 0.19 \$/kg, respectively, when PCM is installed on Roof only. As well, the corresponding prices are 3.22 \$/kg, 2.55 \$/kg, 2.29 \$/kg, 2.17 \$/kg, and 1.89 \$/kg when 5mm PCM is installed on R, RE, REW, REWS and REWSN accordingly, with the reductions of 0.67 \$/kg, 0.26 \$/kg, 0.12 \$/kg, and 0.28 \$/kg, separately. This result is mainly due to the more aggressive energy demand reduction with the increased PCM amount. It also further illustrates that increasing the PCM usage (thickness and utilization area) will also become a favorable option when the PCM cost is reduced to an acceptable price range considering the higher indoor comfort brought by PCM.

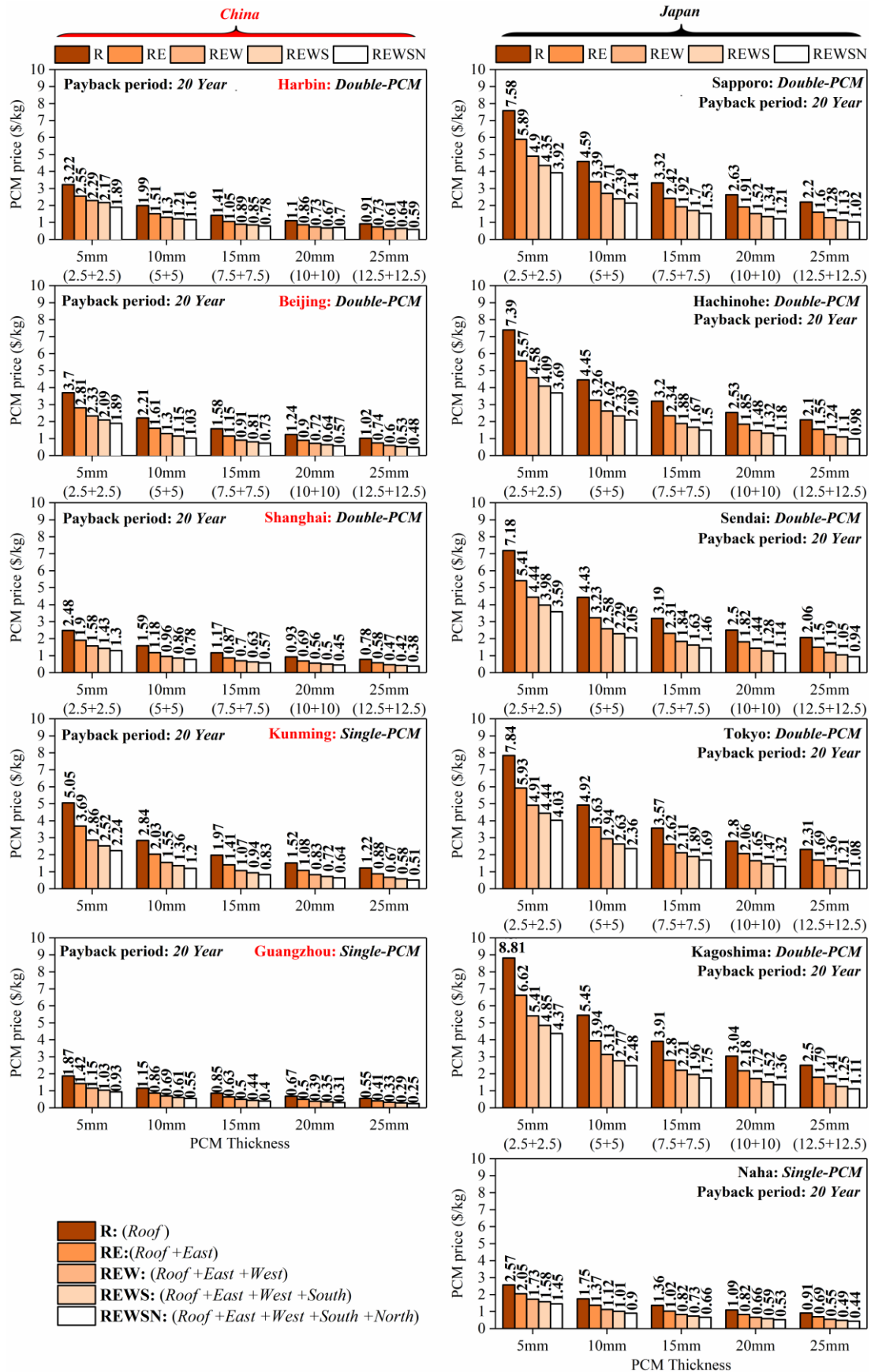


Fig. 8-12. Acceptable maximum PCM cost price for different PCM thickness integrated into different orientations under fixed payback period (20 years).

## 8.7 Summary

The suitable parameters and configurations for PCM to reduce the energy demand in lightweight buildings in typical cities (with different climatic characteristics and energy prices) of China and Japan were discussed in this study by numerical simulation and orthogonal experiment, and the selection priorities (order of importance) and optimal levels of each parameter/configuration ( $A-T_P$ ,  $B-\Delta T$ ,  $C-P_L$ ,  $D-d_P$ ,  $E-H_P$ ,  $F-P_D$ ) were obtained. Meanwhile, the economic applicability of PCM in different climates/cities and the maximum acceptable PCM cost price for a given payback period were further evaluated based on the optimal parameters/configurations. The main conclusions are gained as follows:

(1) PCM is highly correlated with its parameters/configurations in reducing energy demand. In the meanwhile, the difference in energy demand leads to different optimal PCM parameters/configurations.

(2) Factors  $C (P_L)$  and  $F (P_D)$  have the highest impact on energy savings, while  $B (\Delta T)$  is the lowest among the PCM parameters/configurations. The importance ordering (influence degree) of each factor is  $F > C > A (T_P) > E (H_P) > D (d_P) > B$  for reducing the cooling load in most cities. In contrast, the energy-saving for the heating load is shown as  $C > F$ , and the other factors vary considerably in different climates/cities. Among them, the influence degree of factor  $D$  is diminished with the heating demand decreased (the cooling load is increased), and the importance of  $A$  is enhanced. In addition, factor  $E$  is more important to energy-saving in the cooling load than in the heating load. Meanwhile, the optimal order of factor  $F$  is  $F_5$  (Roof)  $> F_1$  (East)  $> F_3$  (West)  $> F_2$  (South)  $> F_4$  (North) from the perspective of energy saving in total annual load.

(3) Double-layer PCM on energy-saving is low than single-layer PCM for cooling or heating loads, but it is superior in total annual load. Nonetheless, single-layer PCM is the optimal choice in Guangzhou, Naha, and Kunming.

(4) 25mm PCM installed on REWSN (Roof + East + West + South + North) can save up to 7.3%-38.06% (China) and 5.17%-20.37% (Japan) of the total load under the optimal parameters/configurations compared to the reference building (no PCM). The lowest energy savings are in Guangzhou and Naha, and the highest in Kunming and Kagoshima.

(5) Although installing PCM on the Roof has a higher energy-saving priority, the same volume of PCM ( $V_{PCM}$ ) evenly distributed on all orientations (by priority: Roof  $>$  East  $>$  West  $>$  South  $>$  North) can bring higher energy-saving benefits.

(6) The payback period is shorter for the same PCM amount applied in Japan than in China

regarding the current PCM cost price. Meanwhile, the payback period for 5mm PCM installed on Roof recommended is 18.2-37.1 years for China (Guangzhou is not recommended) and 10.4-35.8 years for Japan. Additionally, the maximum acceptable PCM cost price is currently 5.05 \$/kg in China and 8.81 \$/kg in Japan under 20 years as the payback period.

The cities selected in this study represent the climatic characteristics of different regions in China and Japan, and the proposed PCM parameters and configurations accurately indicate the factors that need to be considered in the application of PCM. The research results can provide data references for the optimal application of PCM in lightweight buildings for energy-saving under different climates.

## Appendix

### Appendix A. Detail information of the chosen cities [59].

Country	City	Coordinates	Annual average temperature	Climate Characteristics	Climate categories
China	Harbin	E126°40' N45°48'	5.6°C	Long cold winter and short hot summer	TMoC
	Beijing	E116°23' N39°54'	12.6°C	Hot and rainy summer and cold and dry winter	WTSSMC
	Shanghai	E121°30' N31°14'	15.6°C	Hot summer and cold winter	SMC
	Kunming	E102°41' N25°04'	15°C	Four seasons like spring	SHMC
	Guangzhou	E113°20' N23°10'	22.3°C	Hot summer and warm winter	SMC
Japan	Sapporo	E141°21' N43°04'	8.9°C	Cool summer and icy winter	TMoC
	Hachinohe	E141°30' N40°30'	10.8°C	Cool summer and dry winter	POOC
	Sendai	E140°53' N38°15'	12.4°C	Moderate humid summer and cold winter	SMC
	Tokyo	E139°76' N35°68'	16.1°C	Hot summer and generally mild winter	SMMC
	Kagoshima	E130°11' N31°21'	19.2°C	Hot humid summer and relatively mild winter	SC
	Naha	E127°40' N26°12'	23.1°C	Hot humid summer and warm winter	HTRSTC

Note: TMoC, temperate monsoon climate; WTSSMC, warm temperate semi-humid semi-arid monsoon climate; SMC, subtropical monsoon climate; SHMC, subtropical highland monsoon climate; POOC, pacific ocean oceanic climate; SMMC, subtropical maritime monsoon climate; SC, subtropical climate; HTRSTC, high temperature and rainfall subtropical type climate.

**Appendix B.** Cost of some phase-change materials.

Material	Cost (\$/kg)	Ref.
paraffin-based PCM	5.11	[26]
Paraffin Wax (organic)	1.94	[103]
Eicosane-technical grade (organic)	7.04	[103]
Oleic acid (fatty acid)	1.71	[103]
Biodiesel crude glicerine (fatty acid)	0.25	[103]
PCM Energy P. Ltd (min)( salt hydrates)	3.07	[103,104]
PCM Energy P. Ltd (max) ( salt hydrates)	4.94	[103,104]
PCM products	6.63	[104]
Fatty acid PCM product	3.23	[105,106]
Stearic acid (fatty acid)	1.49	[106]
M-27 (commercially available fatty acid)	14.26	[106]
M-51 (commercially available fatty acid)	11.13	[106]
Calcium chloride (inorganic-salt hydrates)	0.20	[104,106]
Latest™29T (commercially available salt hydrates)	4.95	[104,106]
CaCl <sub>2</sub> 6H <sub>2</sub> O	2	[107]
PCM	1.2	[108]
Rubitherm (RT20)	16.31	[109]
Rubitherm (RT 23,25,27)	0.68	[110]
BioPCM	1.30	[111]

## References

- [1] X Cao, X Dai, J Liu, Building energy-consumption status worldwide and the state-of-the-art technologies for zero-energy buildings during the past decade, *Energy and buildings* 128 (2016) 198-213.
- [2] A. Allouhi, Y. E. Fouih, T. Kousksou, A. Jamil, Y. Zeraoui, Y. Mourad, Energy consumption and efficiency in buildings: current status and future trends, *Journal of Cleaner Production* 109 (2015) 118-130.
- [3] Q. Al-Yasiri, M. Szabó, Incorporation of phase change materials into building envelope for thermal comfort and energy saving: A comprehensive analysis, *Journal of Building engineering* 36 (2021) 102122.
- [4] Y. M'hamdi, K. Baba, M. Tajayouti, A. Nounah, Energy, environmental, and economic analysis of different buildings envelope integrated with phase change materials in different climates, *Solar Energy* 243 (2022) 91-102.
- [5] Q. Li, Z. Ju, Z. Wang, L. Ma, W. Jiang, D. Li, J. Jia, Thermal performance and economy of PCM foamed cement walls for buildings in different climate zones, *Energy and Buildings* 277 (2022) 112470.
- [6] K. Guo, L. Zhang, T. Wang, Optimal scheme in energy performance contracting under uncertainty: a real option perspective, *Journal of cleaner production* 231(2019) 240-253.
- [7] L. Zhang, Y. Li, R. Stephenson, B. Ashuri, Valuation of energy efficient certificates in buildings, *Energy and buildings* 158 (2018) 1226-1240.
- [8] F. Harkouss, F. Fardoun, P. H. Biwole, Passive design optimization of low energy buildings in different climates, *Energy* 165 (2018) 591-613.
- [9] J. Hou, T. Zhang, Z. Liu, L. Zhang, H. Fukuda, Application evaluation of passive energy-saving strategies in exterior envelopes for rural traditional dwellings in northeast of Sichuan hills, China, *International Journal of Low-Carbon Technologies* 17 (2022) 342-355.
- [10] K. Sergei, C. Shen, Y. Jiang, A review of the current work potential of a trombe wall, *Renewable and Sustainable Energy Reviews* 130 (2020) 109947.
- [11] L. Zhang, Y. Hou, Z. Liu, J. Du, L. Xu, G. Zhang, L. Shi, Trombe wall for a residential building in Sichuan-Tibet alpine valley—A case study, *Renewable Energy* 156 (2020) 31-46.
- [12] J. Shi, B. Liu, Z. He, Y. Liu, J. Jiang, T. Xiong, J. Shi, A green ultra-lightweight chemically foamed concrete for building exterior: A feasibility study, *Journal of Cleaner Production* 288 (2021) 125085.
- [13] L. Zhang, Z. Liu, C. Hou, J. Hou, D. Wei, Y. Hou, Optimization analysis of thermal

- insulation layer attributes of building envelope exterior wall based on DeST and life cycle economic evaluation, *Case Studies in Thermal Engineering* 14 (2019) 100410.
- [14] Z. Liu, J. Hou, Y. Huang, J. Zhang, X. Meng, B. J. Dewancker, Influence of phase change material (PCM) parameters on the thermal performance of lightweight building walls with different thermal resistances, *Case Studies in Thermal Engineering* 31 (2022) 101844.
- [15] Y. Li, E. Long, P. Ding, S. Guo, Characteristics optimization of composite phase-change wall during intermittent heating process, *Science and Technology for the Built Environment* 26(4) (2020) 541-551.
- [16] J. Wang, S. Liu, X. Meng, W. Gao, J. Yuan, Application of retro-reflective materials in urban buildings: a comprehensive review, *Energy and Buildings* 247 (2021) 111137.
- [17] J. Dong, M. Lin, J. Zuo, T. Lin, J. Liu, C. Sun, J. Luo, Quantitative study on the cooling effect of green roofs in a high-density urban Area—A case study of Xiamen, China, *Journal of Cleaner Production* 255 (2020) 120152.
- [18] B. Nemeth, A. Ujhidy, J. Toth, J. Gyenis, T. Feczko, Testing of microencapsulated phase-change heat storage in experimental model houses under winter weather conditions, *Building and Environment* 204 (2021) 108119.
- [19] Y. Gao, F. He, X. Meng, Z. Wang, M. Zhang, H. Yu, W. Gao, Thermal behavior analysis of hollow bricks filled with phase-change material (PCM), *Journal of Building Engineering* 31 (2020) 101447.
- [20] L. Yang, X. Jin, Y. Zhang, K. Du, Recent development on heat transfer and various applications of phase-change materials, *Journal of Cleaner Production* 287 (2021) 124432.
- [21] F. He, R. Bo, C. Hu, X. Meng, W. Gao, Employing spiral fins to improve the thermal performance of phase-change materials in shell-tube latent heat storage units, *Renewable Energy* 203 (2023) 518-528.
- [22] Y. Sun, S. Wang, F. Xiao, D. Gao, Peak load shifting control using different cold thermal energy storage facilities in commercial buildings: A review, *Energy conversion and management* 71 (2013) 101-114.
- [23] S. E. Kalnæs, B. P. Jelle, Phase change materials and products for building applications: A state-of-the-art review and future research opportunities, *Energy and Buildings* 94 (2015) 150-176.
- [24] Z. Liu, J. Hou, X. Meng, B. J. Dewancker, A numerical study on the effect of phase-change material (PCM) parameters on the thermal performance of lightweight building walls, *Case Studies in Construction Materials* 15 (2021) e00758.
- [25] P. K. S. Rathore, S. K. Shukla, An experimental evaluation of thermal behavior of the building envelope using macroencapsulated PCM for energy savings, *Renewable Energy*

- 149 (2020) 1300-1313.
- [26] X. Sun, Z. Zhu, S. Fan, J. Li, Thermal performance of a lightweight building with phase change material under a humid subtropical climate, *Energy and Built Environment* 3(1) (2022) 73-85.
- [27] N. Soares, A. R. Gaspar, P. Santos, J. J. Costa, Multi-dimensional optimization of the incorporation of PCM-drywalls in lightweight steel-framed residential buildings in different climates, *Energy and buildings* 70 (2014) 411-421.
- [28] Y. Li, E. Long, L. Zhang, X. Dong, S. Wang, Energy-saving potential of intermittent heating system: Influence of composite phase change wall and optimization strategy, *Energy Exploration & Exploitation* 39(1) (2021) 426-443.
- [29] I. Adilkhanova, S. A. Memon, J. Kim, A. Sheriyev, A novel approach to investigate the thermal comfort of the lightweight relocatable building integrated with PCM in different climates of Kazakhstan during summertime, *Energy* 217 (2021) 119390.
- [30] S. D. Zwanzig, Y. Lian, E. G. Brehob, Numerical simulation of phase change material composite wallboard in a multi-layered building envelope, *Energy Conversion and Management* 69 (2013) 27-40.
- [31] Z. Liu, J. Hou, D. Wei, X. Meng, B. J. Dewancker, Thermal performance analysis of lightweight building walls in different directions integrated with phase change materials (PCM), *Case Studies in Thermal Engineering* 40 (2022) 102536.
- [32] K. Biswas, Y. Shukla, A. Desjarlais, R. Rawal, Thermal characterization of full-scale PCM products and numerical simulations, including hysteresis, to evaluate energy impacts in an envelope application, *Applied Thermal Engineering* 138 (2018) 501-512.
- [33] R. A. Kishore, M. V. A. Bianchi, C. Booten, J. Vidal, R. Jackson, Parametric and sensitivity analysis of a PCM-integrated wall for optimal thermal load modulation in lightweight buildings, *Applied Thermal Engineering* 187 (2021) 116568.
- [34] Q. Al-Yasiri, M. Szabo, Case study on the optimal thickness of phase change material incorporated composite roof under hot climate conditions, *Case Studies in Construction Materials* 14 (2021) e00522.
- [35] Q. Al-Yasiri, M. Szabó, Experimental study of PCM-enhanced building envelope towards energy-saving and decarbonisation in a severe hot climate, *Energy and Buildings* 279 (2023) 112680.
- [36] Z. A. Liu, J. Hou, Y. Chen, Z. Liu, T. Zhang, Q. Zeng, B. J. Dewancker, X. Meng, G. Jiang, Effectiveness assessment of different kinds/configurations of phase-change materials (PCM) for improving the thermal performance of lightweight building walls in summer and winter, *Renewable Energy* 202 (2023) 721-735.

- [37] Z. Xiao, P. Mishra, A.M. Nejad, M. Tao, S. Granados-Focil, S. V. Dessel, Thermal optimization of a novel thermo-optically responsive SS-PCM coatings for building enclosures, *Energy and Buildings* 247 (2021) 111129.
- [38] A. H. N. Al-mudhafar, M. T. Hamzah, A. L. Tarish, Potential of integrating PCMs in residential building envelope to reduce cooling energy consumption, *Case Studies in Thermal Engineering* 27 (2021) 101360.
- [39] J. Bohórquez-Órdenes, A. Tapia-Calderón, D. A. Vasco, O. Estuardo-Flores, A. N. Haddad, Methodology to reduce cooling energy consumption by incorporating PCM envelopes: a case study of a dwelling in Chile, *Building and Environment* 206 (2021) 108373.
- [40] E. Mohseni, W. Tang, Parametric analysis and optimisation of energy efficiency of a lightweight building integrated with different configurations and types of PCM, *Renewable Energy* 168 (2021) 865-877.
- [41] J. Jia, B. Liu, L. Ma, H. Wang, D. Li, Y. Wang, Energy saving performance optimization and regional adaptability of prefabricated buildings with PCM in different climates, *Case Studies in Thermal Engineering* 26 (2021) 101164.
- [42] S. Wijesuriya, C. Booten, M. V. A. Bianchi, R. A. Kishore, Building energy efficiency and load flexibility optimization using phase change materials under futuristic grid scenario, *Journal of Cleaner Production* 339 (2022) 130561.
- [43] N. Elawady, M. Bekheit, A. A. Sultan, A. Radwan, Energy assessment of a roof-integrated phase change materials, long-term numerical analysis with experimental validation, *Applied Thermal Engineering* 202 (2022) 117773.
- [44] F. Kuznik, J. P. A. Lopez, D. Baillis, K. Johannes, Phase change material wall optimization for heating using metamodeling, *Energy and Buildings* 106 (2015) 216-224.
- [45] R. A. Kishore, M. V. A. Bianchi, C. Booten, J. Vidal, R. Jackson, Optimizing PCM-integrated walls for potential energy savings in U.S. Buildings, *Energy and Buildings* 226 (2020) 110355.
- [46] R. A. Kishore, C. Booten, M. V. A. Bianchi, J. Vidal, R. Jackson, Evaluating cascaded and tunable phase change materials for enhanced thermal energy storage utilization and effectiveness in building envelopes, *Energy and Buildings* 260 (2022) 111937.
- [47] Q. Li, H. Hu, L. Ma, Z. Wang, M. Arıcı, D. Li, D. Luo, J. Jia, W. Jiang, H. Qi, Evaluation of energy-saving retrofits for sunspace of rural residential buildings based on orthogonal experiment and entropy weight method, *Energy for Sustainable Development* 70 (2022) 569-580.
- [48] H. X. Li, Y. Li, B. Jiang, L. Zhang, X. Wu, J. Lin, Energy performance optimisation of building envelope retrofit through integrated orthogonal arrays with data envelopment

- analysis, *Renewable energy* 149 (2020) 1414-1423.
- [49] L. Zhang, H. Liu, D. Wei, F. Liu, Y. Li, H. Li, Z. Dong, J. Cheng, L. Tian, G. Zhang, L. Shi, Impacts of spatial components on outdoor thermal comfort in traditional Linpan settlements, *International Journal of Environmental Research and Public Health* 19(11) (2022) 6421.
- [50] W. Zuo, E. Jiaqiang, X. Liu, Q. Peng, Y. Deng, H. Zhu, Orthogonal experimental design and fuzzy grey relational analysis for emitter efficiency of the micro-cylindrical combustor with a step, *Applied Thermal Engineering* 103 (2016) 945-951.
- [51] Z. Liu, J. Hou, L. Zhang, B. J. Dewancker, X. Meng, C. Hou, Research on energy-saving factors adaptability of exterior envelopes of university teaching-office buildings under different climates (China) based on orthogonal design and EnergyPlus, *Heliyon* 8(8) (2022) e10056.
- [52] Y. Xiong, Y. Pan, L. Wu, B. Liu, Effective weight-reduction-and crashworthiness-analysis of a vehicle's battery-pack system via orthogonal experimental design and response surface methodology, *Engineering Failure Analysis* 128 (2021) 105635.
- [53] L. Fang, X. Liao, Q. Zhang, L. Shi, L. Zhou, H. Zhao, W. Kong, An orthogonal experimental design and QuEChERS based UFLC-MS/MS for multi-pesticides and human exposure risk assessment in Honeysuckle. *Industrial Crops and Products* 164 (2021) 113384.
- [54] Y. Sun, C. Li, J. You, C. Bu, L. Yu, Z. Yan, X. Liu, Y. Zhang, X. Chen, An Investigation of the Properties of Expanded Polystyrene Concrete with Fibers Based on an Orthogonal Experimental Design, *Materials* 15(3) (2022) 1228.
- [55] B. Liu, L. Sha, K. Huang, W. Zhang, A topology optimization method for collaborative robot lightweight design based on orthogonal experiment and its applications, *International Journal of Advanced Robotic Systems* 19(1) (2022) 17298814211056143.
- [56] X. Mi, R. Liu, H. Cui, S. A. Memon, F. Xing, Y. Lo, Energy and economic analysis of building integrated with PCM in different cities of China, *Applied Energy* 175 (2016) 324-336.
- [57] R. Ye, R. Huang, X. Fang, Z. Zhang, Simulative optimization on energy saving performance of phase change panels with different phase transition temperatures, *Sustainable Cities and Society* 52 (2020) 101833.
- [58] J. Hou, Z. Liu, L. Zhang, T. Zhang, C. Hou, H. Fukuda, Parametric and economic analysis of incorporating phase change material (PCM) into exterior walls to reduce energy demand for traditional dwellings in northeast of Sichuan hills, China, *Applied Thermal Engineering* 223 (2023) 119982.

- [59] Q. Wu, H. Ren, W. Gao, J. Ren, Multi-criteria assessment of building combined heat and power systems located in different climate zones: Japan–China comparison, *Energy* 103 (2016) 502-512.
- [60] Ministry of housing and urban-rural development, Code for Thermal Design of Civil Building (GB 50176-2016), China Architecture & Building Press, Beijing, China, 2016.
- [61] D. Wei, L. Yang, Z. Bao, Y. Lu, H. Yang, Variations in outdoor thermal comfort in an urban park in the hot-summer and cold-winter region of China, *Sustainable Cities and Society* 77 (2022) 103535.
- [62] N Enteria, H Yoshino, R Takaki, A Mochida, A Satake, S. Baba, H. Ishihara, R. Yoshie, Case analysis of utilizing alternative energy sources and technologies for the single family detached house, *Solar energy* 105 (2014) 243-263.
- [63] ASHRAE, ASHRAE Handbook Fundamentals, American society of heating, Refrigerating and Air-Conditioning Engineers Inc., Atlanta, GA, 2013.
- [64] ASHRAE, ANSI/ASHRAE standard 55-2013, in: Thermal Environmental Conditions for Human Occupancy, 2013.
- [65] Ministry of housing and urban-rural development of the People’s Republic of China, Design code for heating ventilation and air conditioning of civil buildings (GB 50736-2012), China Architecture & Building Press, Beijing, China, 2012.
- [66] R. Wang, H. Hu, C. Zhao, Y. Qiu, Study on thermal comfort of indoor environment about typical residential air conditioning room, *Chinese Journal of Ergonomics* 24 (6) (2018) 11–16.
- [67] W. Xu, Research and Comparison on International Building Energy Codes & Standards, China Architecture & Building Press, 2012, pp. 235–280.
- [68] F. Bre, L. K. Lawrie, D. B. Crawley, R. Lamberts, Assessment of solar radiation data quality in typical meteorological years and its influence on the building performance simulation, *Energy and Buildings* 250 (2021) 111251.
- [69] D. D'Agostino, D. Parker, I. Epifani, D. Crawley, L. Lawrie, How will future climate impact the design and performance of nearly zero energy buildings (NZEBS)?, *Energy* 240 (2022) 122479.
- [70] T. Huld, E. Paietta, P. Zangheri, I. P. Pascua, Assembling typical meteorological year data sets for building energy performance using reanalysis and satellite-based data, *Atmosphere* 9(2) (2018) 53.
- [71] Files, Asia Weather. [https://climate.onebuilding.org/WMO\\_Region\\_2\\_Asia/](https://climate.onebuilding.org/WMO_Region_2_Asia/), (Accessed 6 August 2022).
- [72] National Centers for Environmental Information. <https://www.ncei.noaa.gov/>, (Accessed

6 August 2022).

- [73] A. Moradi, Impact of Typical-year and Multi-year Weather Data on The Energy Performance of The Residential and Commercial Buildings, University of Ottawa, Master thesis, 2022.
- [74] L. Yang, J. C. Lam, J. Liu, C. L. Tsang, Building energy simulation using multi-years and typical meteorological years in different climates, *Energy conversion and management* 49(1) (2008) 113-124.
- [75] V. Costanzo, G. Evola, M. Infantone, L. Marletta, Updated typical weather years for the energy simulation of buildings in mediterranean climate. A case study for sicily, *Energies* 13(16) (2020) 4115.
- [76] G. Evola, V. Costanzo, M. Infantone, L. Marletta, Typical-year and multi-year building energy simulation approaches: A critical comparison, *Energy* 219 (2021) 119591.
- [77] L. Xu, H. Wang, Y. Gao, J. Wang, E. Long, R. Zhao, Study on Performance of Composite PCM (Phase-change Material)'s Adjusting Indoor Thermal Environment of Light Weight Enclosure Buildings, *Building Science* 029(012) (2013) 45-49,107.
- [78] L. Pan, Q. Xu, Y. Nie, T. Qiu, Analysis of climate adaptive energy-saving technology approaches to residential building envelope in Shanghai, *Journal of Building Engineering* 19 (2018) 266–272.
- [79] K. Chen, *Design and Analysis of Experiments*, second ed., Tsinghua University Press, Beijing, China, 2005.
- [80] J. Tang, G. Gong, H. Su, F. Wu, C. Herman, Performance evaluation of a novel method of frost prevention and retardation for air source heat pumps using the orthogonal experiment design method, *Applied Energy* 169 (2016) 696–708.
- [81] P. C. Tabares-Velasco, C. Christensen, M. Bianchi, Verification and validation of EnergyPlus phase change material model for opaque wall assemblies, *Building and Environment* 54 (2012) 186-196.
- [82] Y. Pan, *Building Energy Simulation Handbook*, China Architecture & Building Press, Beijing, China, 2013, pp. 55-60.
- [83] M. K. Urbikain, M. G. Davies, A frequency domain estimation of wall conduction transfer function coefficients, *Energy and Buildings* 51 (2012) 191-202.
- [84] U.S. Department of Energy, EnergyPlus™ Version 22.1.0 Documentation Input Output Reference, 2022.
- [85] U.S. Department of Energy, EnergyPlus™ Version 22.1.0 Documentation Engineering Reference, 2022.
- [86] Y. Qu, D. Zhou, F. Xue, L. Cui, Multi-factor analysis on thermal comfort and energy saving

- potential for PCM-integrated buildings in summer, *Energy and Buildings* 241 (2021) 110966.
- [87] R. Ye, X. Fang, Z. Zhang, Numerical Study on Energy-Saving Performance of a New Type of Phase Change Material Room, *Energies* 14(13) (2021) 3874.
- [88] D. B. Crawley, L. K. Lawrie, F. C. Winkelmann, W. F. Buhl, Y. J. Huang, C. O. Pedersen, R. K. Strand, R. J. Liesen, D. E. Fisher, M. J. Witte, J. Glazer, EnergyPlus: creating a new-generation building energy simulation program, *Energy and buildings* 33(4) (2001) 319-331.
- [89] EnergyPlus 8.5 Manual, Lawrence Berkeley National Laboratory, USA, 2016.
- [90] J. Hou, T. Zhang, Z. Liu, C. Hou, H. Fukuda, A study on influencing factors of optimum insulation thickness of exterior walls for rural traditional dwellings in northeast of Sichuan hills, China, *Case Studies in Construction Materials* 16 (2022) e01033.
- [91] Y. Li, N. Nord, Q. Xiao, T. Tereshchenko, Building heating applications with phase change material: A comprehensive review, *Journal of Energy Storage*. 31 (2020) 101634.
- [92] K. Saafi, N. Daouas, Energy and cost efficiency of phase change materials integrated in building envelopes under Tunisia Mediterranean climate, *Energy* 187 (2019) 115987.
- [93] Canada's High-Tech Co. Ltd (Tri-Y Enterprises Ltd) Kelowna Branch. <http://tcm-energysaver.com>, (Accessed 8 April 2022).
- [94] C. Wang, S. Deng, J. Niu, E. Long, A numerical study on optimizing the designs of applying PCMs to a disaster-relief prefabricated temporary-house (PTH) to improve its summer daytime indoor thermal environment, *Energy* 181 (2019) 239–249.
- [95] ASHRAE, Guideline 14-2014: Measurement of Energy and Demand Savings, Atlanta, 2014, pp. 17-20.
- [96] Calculation of Electricity Rate in Japan. <https://www.denkikeisan.com/>, (Accessed 20 October 2022)
- [97] J. Yuan, C. Farnham, K. Emura, M. A. Alam, Proposal for optimum combination of reflectivity and insulation thickness of building exterior walls for annual thermal load in Japan, *Building and Environment* 103 (2016) 228-237.
- [98] H. Wang, W. Lu, Z. Wu, G. Zhang, Parametric analysis of applying PCM wallboards for energy saving in high-rise lightweight buildings in Shanghai, *Renewable Energy* 145 (2020) 52-64.
- [99] X. Kong, S. Lu, Y. Li, J. Huang, S. Liu, Numerical study on the thermal performance of building wall and roof incorporating phase change material panel for passive cooling application, *Energy and Buildings* 81 (2014) 404-415.
- [100] SM Sajjadian, J Lewis, S Sharples. The potential of phase change materials to reduce

- domestic cooling energy loads for current and future UK climates, *Energy and Buildings* 93 (2015) 83-89.
- [101] OANDA SMARTER TRADING. <https://www.oanda.com/currency-converter/>, (Accessed 20 October 2022).
- [102] Ministry of housing and urban-rural development of the People's Republic of China, Unified standard for reliability design of building structures (GB50068-2018), China Architecture & Building Press, Beijing, China, 2018.
- [103] J. Kosny, N. Shukla, A. Fallahi, Cost analysis of simple phase change material enhanced building envelopes in southern U.S. climates. Tech. rep. Fraunhofer CSE: U. S. Department of Energy, 2013.
- [104] Y. Cascone, A. Capozzoli, M. Perino, Optimisation analysis of PCM-enhanced opaque building envelope components for the energy retrofitting of office buildings in Mediterranean climates, *Applied Energy* 211 (2018) 929-953.
- [105] PCM Products. [http://www.pcmproducts.net/Phase\\_Change\\_Material\\_Products.htm](http://www.pcmproducts.net/Phase_Change_Material_Products.htm), (Accessed 15 October 2022).
- [106] F. Souayfane, P. H. Biwole, F. Fardoun, P. Achard, Energy performance and economic analysis of a TIM-PCM wall under different climates, *Energy* 169 (2019) 1274-1291.
- [107] H. Benli, A. Durmuş, Performance analysis of a latent heat storage system with phase change material for new designed solar collectors in greenhouse heating, *Solar energy* 83(12) (2009) 2109-2119.
- [108] D. A. El-Raheim, A. Mohamed, M. Fatouh, H. Abou-Ziyan, Comfort and economic aspects of phase change materials integrated with heavy-structure buildings in hot climates, *Applied Thermal Engineering* 213 (2022) 118785.
- [109] N. Chaiyat, Energy and economic analysis of a building air-conditioner with a phase change material (PCM), *Energy conversion and Management*, 2015, 94: 150-158.
- [110] M. Saffari, A. D. Gracia, S. Ushak, L. F. Cabeza, Economic impact of integrating PCM as passive system in buildings using Fanger comfort model, *Energy and Buildings* 112 (2016) 159-172.
- [111] A. Baniassadi, B. Sajadi, M. Amidpour, N. Noori, Economic optimization of PCM and insulation layer thickness in residential buildings, *Sustainable Energy Technologies and Assessments* 14 (2016) 92-99.

## Nomenclature

$T_p$	Phase-transition temperature, (°C)
$H_p$	Phase change latent heat, (kJ/kg)
$d$	Material thickness, (m)
$\lambda$	Thermal conductivity, [W/(m K)],Solid (Liquid)
$c_p$	Specific heat, [J/(kg K)]
$\rho$	Density, (kg/m <sup>3</sup> )
$\Delta T$	Phase-transition temperature ranges, (°C)
$L$	Symbol of orthogonal experiment,-
$D$	the number of rows or tests,-
$Q$	the number of levels,-
$M$	the number of columns or factors,-
$K_{i,m}$	Sum of experimental results at level $i$ of factor $m$ ,-
$k_{i,m}$	Average of experimental results at level $i$ of factor $m$ ,-
$s_{i,m}$	The number of occurrences of level $i$ of factor $m$ ,-
$R_v$	The difference (range-value) between the max and min of $k_{i,m}$ ,-
$h_i$	Inside surface coefficient of heat transfer, [W/(m <sup>2</sup> K)]
$C_z$	Heat capacity of zone air and internal thermal mass, [J/(kg K)]
$k$	Heat transfer coefficient, [W/(m <sup>2</sup> K)]
$P_L$	Location of PCM in the wall,-
$P_D$	PCM installation orientation,-
$T_o$	Temperature of Outdoor air, (°C)
$T_{zi}$	Inter zone air temperature, (°C)
$T_{si}$	Inside surface temperature, (°C)
$T_z$	Zone air temperature, (°C)
$\dot{Q}_i$	Convective internal loads, (J)
$C_p$	Zone air specific heat, [J/(kg K)]
$C_T$	Heat capacity multiplier, [J/(kg K)]
$\dot{m}_{inf}$	Zone infiltration mass flow rate, (kg/s)
$A_i$	Zone surface area, (m <sup>2</sup> )
$\dot{Q}_{sys}$	Total building systems load, (J)
$\rho_{air}$	Air density, (kg/m <sup>3</sup> )
$M_t$	Measured temperatures at each hour, (°C)

$S_t$	Simulated temperatures at each hour, (°C)
$\overline{M}_t$	Average of the measured data values, (°C)
$C_{pcm}$	Initial investment cost of PCM, (\$/kg)
$S$	Income generated from energy savings,( \$)

***Abbreviations***

PCM	Phase-Change Material
OSB	Oriented Strand Board
TMY	Typical Meteorological Year
SCZ	Severe cold zone
CZ	Cold zone
HSCW	Hot summer and cold winter zone
HSWW	Hot summer and warm winter zone
MCZ	Moderate climate zone
ANOVA	Analysis of variance
RMSE	Root Mean Square Error
$CV_{(RMSE)}$	Coefficient of Variation of the Root Mean Square Error
SPP	Static Payback Period

## ***Chapter 9. Conclusions***

<i>9.1 Conclusions</i> .....	<i>9-1</i>
------------------------------	------------



## 9.1 Conclusions

Phase-change material (PCM) integrated into walls has been extensively studied and optimized, proving its effectiveness in thermal performance improvement of the wall. Among them, it can be drawn that the heat storage and release of PCM are affected by various factors, such as PCM thermo-physical parameters, application objects, installation locations, and climatic conditions, which are complex and non-linear. However, the current research mostly focuses on a specific factor, which makes the existing conclusions, rules, and interrelationships between the obtained influencing factors too absolute and flawed. Therefore, the typical unit lightweight walls (mainly thermal insulation materials) were taken as the research object to ascertain the basic scientific problem of the influence laws and suitability of different PCM thermo-physical parameters of the thermal performance of lightweight walls under different thermal boundaries through theoretical analysis, numerical simulation, and experiment. Meanwhile, evaluate the energy-saving potential (cooling and heating) of lightweight walls using PCM applied to buildings and determined economic feasibility in different climates/cities. The main findings are as follows:

**In Chapter 1, research on background, review and purpose.** The current status of building energy consumption, energy-saving technologies, indoor thermal environment characteristics of lightweight buildings and PCM characteristics are introduced. Then, the effectiveness of PCM application in different structural forms is reviewed through a large number of previous studies, and the difference in the contribution benefits of PCM to reducing energy demand under different climatic conditions are obtained. Meanwhile, the thermo-physical parameters of PCM affecting its application effect and the appropriate values are summarized. Eventually, the problems existing in the application of PCM in buildings are deeply analyzed based on a large number of literature reviews, and the research contents and purposes of this paper are clarified.

**In Chapter 2, the causes of the indoor thermal environment of lightweight buildings are analyzed, and the mathematical heat transfer model of lightweight wall using PCM are established. In addition, the solution method are determined and the evaluation indexes for the effect of PCM on the thermal performance of lightweight wall are proposed.** It is found that: (1) the difference between indoor and outdoor air temperature is directly related to the initial temperature of the lightweight building and is positively related to solar radiation, and is negatively correlated with outdoor air temperature and long-wave radiation; (2) Lightweight buildings are prone to indoor temperatures much higher than outdoor in summer, which is directly related to the thermal resistance and thermal inertia index of

lightweight walls being too small; (3) The enthalpy method model is determined to be used to solve the heat storage and release process of the phase-change composite wall, and it is validated; (4) The delay time ( $\varphi$ ) and attenuation rate ( $f$ ) of the inner surface temperature, and the peak heat flux ( $q_{peak}$ ) and average heat flux ( $q_{ave}$ ) of the inner surface are proposed to evaluate the thermal performance improvement of lightweight walls integrated with different PCM thermo-physical parameters.

**In Chapter 3, the influence rules of PCM thermo-physical parameters on the thermal performance of lightweight walls are systematically evaluated.** It is found that: (1) The thickness, latent heat and density of PCM have a positive correlation with the delay time ( $\varphi$ ) and a negative correlation with the attenuation rate ( $f$ ) and peak heat flux ( $q_{peak}$ ); (2) The influence begins to be weakened when each parameter of PCM exceeds a particular value, that is, it has a relative optimal value; (3) The specific heat of PCM has basically no effect on thermal performance; (4) PCM installed in the middle of the lightweight wall is better than the outside or inside at a suitable phase-transition temperature.

**In Chapter 4, the influence laws and contribution efficiency of different PCM thermo-physical parameters on the thermal performance of lightweight walls with different thermal resistance are assessed.** The results show that: (1) The suitable phase-transition temperature of PCM is more correlated with PCM location and less correlated with the thermal resistance of the original walls ( $R_{wt}$ ), but the greater the  $R_{wt}$ , the lower the degree of phase-change of the PCM; (2) Under a suitable phase-transition temperature, the difference between PCM installation on the inside and outside is small and the suitable PCM location is almost independent of  $R_{wt}$ ; (3) The optimal thickness exists in PCM applications, and its value shows a certain correlation with the  $R_{wt}$ . The optimum thickness is 10 mm when the  $R_{wt}$  is  $2.0(\text{m}^2 \cdot \text{K})/\text{W}$ , while no more than 5 mm is recommended when the  $R_{wt}$  is enhanced to  $5.0(\text{m}^2 \cdot \text{K})/\text{W}$  or higher. (4) The optimal value and contribution efficiency of PCM are diminished and gradually converge with the  $R_{wt}$  is boosted.

**In Chapter 5, the difference, applicability and appropriate parameters for the application effect of PCM integrated into different directions of walls are determined.** The results show that: (1) The application effects and suitable parameters of PCM in walls in different directions are different. PCM location (phase-transition temperature) is adapted to the middle (20–30 °C) for the east and south-facing wall, while the inside (18–28 °C) and outside (24–34 °C) is optimal for the west and north-facing wall; (2) The thermal performance improvement with the most noticeable in the east and west-facing walls at suitable PCM parameters and their peak and average heat flux can be reduced by 62.8–66.4% and 28.2–29.5%,

and delay time increased by 5–5.34h compared to reference wall.

**In Chapter 6, the effectiveness of different kinds/configurations of PCM on the thermal performance of lightweight walls in winter and summer are assessed, and suitable PCM kinds/configurations for both seasons are proposed.** The results show that: (1) Double-layer PCM applications exhibit superior thermal regulation ability in both summer and winter under the same PCM thickness; (2) The effectiveness of double-layer PCM is closely related to the temperature difference between indoor and outdoor (comprehensive outdoor temperature), which is better in summer than in winter; (3) The effectiveness of double-layer PCM reaches saturation when thickness and latent heat exceed 10 mm (5 mm+5 mm) and 125 kJ/kg, respectively. Nevertheless, the difference in application effect due to different total thermal resistance of the wall caused by another layer of PCM in different seasons (or different phase states) is diminished by enhancing the thermal storage capacity of the PCM.

**In Chapter 7, the regulation ability of PCM on the thermal performance of lightweight walls and indoor thermal environments in different seasons under a natural environment (no mechanical equipment) is discussed by experimental tests.** The results show that: (1) Under natural conditions, the contribution efficiency of PCM for improving the thermal performance of lightweight buildings varies in different seasons. In the transitional season, PCM application can basically maintain the all-day temperature in a comfortable range; (2) The attenuation rate of the internal surface temperature in different seasons can be reduced by 18.08%-42.90%, the delay time can be improved to 2.67-4h compared with the reference wall; (3) Composite PCM can reduce the maximum indoor temperature by 4.9-12.0 °C, and increase by 1.1-2.8 °C when the outdoor temperature is lower.

**In Chapter 8, the energy-saving potential (cooling and heating) of lightweight walls using PCM applied to buildings is evaluated by using EnergyPlus, and the economic feasibility in different climates/cities are determined by static payback period (SPP).** The results show that: (1) PCM is highly correlated with its parameters/configurations in reducing energy demands; (2) different PCM parameters/configurations are required for different climates and energy demands; (3) higher energy saving benefits can be achieved by evenly distributing to all orientations (priority: Roof > East > West > South > North) under the same PCM volume ( $V_{PCM}$ ) compared to installing only on the Roof; (4) PCM can save up to 7.3%-38.06% (China) and 5.17%-20.37% (Japan) for the total loads based on the optimal PCM parameters/configurations; (5) the maximum acceptable PCM cost is currently 5.05 \$/kg in China and 8.81 \$/kg in Japan based on a payback period of 20 years.

**In Chapter 9, the research findings of the each chapters are summarized.** The research

results can provide a systematic evaluation method for effect of PCM applied to opaque envelopes under different thermal boundaries at the theoretical significance. Meanwhile, the research results can also provide reference for decision-makers to select suitable PCM products in lightweight wall or building in terms of energy-saving and economics, as well as provide data support for manufacturers to develop innovative energy-saving lightweight wall products using PCM.